The Effect of Temperature and Salt Contamination on Corrosion of Reinforcing Steel in OPC and Blended Cement Concretes

by

C. N. Sadath Ali Khan

A Thesis Presented to the

FACULTY OF THE COLLEGE OF GRADUATE STUDIES

KING FAHD UNIVERSITY OF PETROLEUM & MINERALS

DHAHRAN, SAUDI ARABIA

In Partial Fulfillment of the
Requirements for the Degree of

MASTER OF SCIENCE

In

CIVIL ENGINEERING

August, 1993

Order Number 1355315

The effect of temperature and salt contamination on corrosion of reinforcing steel in OPC and blended cement concretes

Khan, C. N. Sadath Ali, M.S.

King Fahd University of Petroleum and Minerals (Saudi Arabia), 1993

U·M·I
300 N. Zeeb Rd.
Ann Arbor, MI 48106

THE EFFECT OF TEMPERATURE AND SALT CONTAMINATION ON CORROSION OF REINFORCING STEEL IN OPC AND BLENDED CEMENT CONCRETES

BY

C.N. SADATH ALI KHAN

A Thesis Presented to the

FACULTY OF THE COLLEGE OF GRADUATE STUDIES

KING FAHD UNIVERSITY OF PETROLEUM & MINERALS

DHAHRAN, SAUDI ARABIA

In Partial Fulfillment of the
Requirements for the Degree of

MASTER OF SCIENCE

In

CIVIL ENGINEERING

AUGUST, 1993

KING FAHD UNIVERSITY OF PETROLEUM AND MINERALS
DHAHRAN 31261, SAUDI ARABIA

COLLEGE OF GRADUATE STUDIES

This thesis, written by

SADATH ALI KHAN C.N.

under the direction of his thesis advisor and approved by his thesis committee, has been presented to and accepted by the Dean of the College of Graduate Studies, in partial fulfillment of the requirements for the degree of ***MASTER OF SCIENCE IN CIVIL ENGINEERING*** **(Structures)**

Thesis Committee

Chairman (Dr. Islem .A . Basunbul)

Co-Chairman (Prof. A. J. Al - Tayyib) A. J. Tayyib 22/9/93

Member (Dr. G. J. Al - Sulaimani)

Member (Dr. Al - Farabi Sharif)

Dr. Al-Farabi Sharif
Department Chairman

Dr. Ala H. Al-Rabeh
Dean, College of Graduate Studies

Date: Sep. 27th, 1993

Dedicated To My Beloved Parents

And to that Personality, Who Was a Constant Source of Inspiration and Guidance

ACKNOWLEDGMENTS

All thanks to ***Allah*** Subhanahu Watala for having made it possible for me to complete this work. I am grateful to King Fahd University of Petroleum and Minerals (KFUPM) for the financial support extended to me during the course of the MS program.

I thank my advisor Dr. I. A. Basunbul and Co-advisor Prof. A. J. Al-Tayyib, for their guidance and support, and the other committee members Dr. G. J. Al- Sulaimani, and Dr. Al-Farabi Sharif, for their constant help.

My special thanks are due to Mr. Mohammed Maslehuddin who helped me in the various stages of this work. I appreciate the help rendered by Dr. O.S.B. Al-Amoudi. I would also like to thank Mr. Ibrahim Asi, Mr. Mohammed Al-Nahash, Mr. Tony, Mr. Omar Ahmed, Mr. Hassan Zakaria and Mr. Mumtaz Ali Khan and other staff of the Civil Engineering Department for their assistance.

Thanks are also due to Dr. Hassan Al-Ahmadi for extending the PC laboratory facilities. Special thanks are due to my friends Mr. C. M. Navaz and Mr. Shaikh Ilyas Ahmed for their help.

Lastly, but not the least, I would like to extend my gratitude to all my colleagues and friends who made my stay at KFUPM worth remembering.

TABLE OF CONTENTS

LIST OF TABLES

LIST OF FIGURES

LIST OF PLATES

THESIS ABSTRACT

NAME OF STUDENT C. N. SADATH ALI KHAN

TITLE OF STUDY THE EFFECT OF TEMPERATURE AND SALT CONTAMINATION ON CORROSION OF REINFORCING STEEL IN OPC AND BLENDED CEMENT CONCRETES

MAJOR FIELD CIVIL ENGINEERING

DATE OF DEGREE JUNE, 1993

This study was conducted to investigate the effect of relatively high temperatures (25 to 70 °C) and chloride and sulfate contamination on the reinforcement corrosion in ordinary portland cement (OPC) and blended cement concretes. To achieve the objectives of this research study, more than 500 concrete specimens were cast and tested. The effect of temperature and chloride and sulfate contamination on the compressive strength, porosity, electrical resistivity, alkalinity, water soluble chloride and sulfate concentration, and corrosion of reinforcing steel was evaluated.

Results indicated that both the temperature and chloride-sulfate contamination influence the compressive strength of OPC and blended cement concrete specimens. The compressive strength in OPC and blended cement concrete specimens was observed to decrease with increasing exposure temperature. Addition of chloride and chloride plus sulfate ions resulted in a decrease in the strength of OPC specimens, while an increase in the strength of the blended cement concrete specimens was indicated due to the addition of these salts. The cumulative pore volume in the OPC paste specimens was observed to increase with increasing exposure temperature. This trend was also observed in blended cements.

The Cl^-/OH^- ratio was also observed to increase with the exposure temperature. The effect of temperature on Cl^-/OH^- ratio was more pronounced for exposure temperatures of more than 40 °C.

The reinforcement corrosion activity, as measured by the corrosion current density on steel, in both the OPC and blended cement concrete specimens was observed to be higher in specimens contaminated with both chloride and sulfate salts as against those contaminated with only chloride salts. This indicates that the presence of both chloride and sulfate ions increases the rate of corrosion. At 70 °C exposure temperature, and chloride-sulfate contamination, the performance of all the blended cements investigated, except ASTM C 618 Class C fly ash, was not better than that of plain cements. This indicates that the technological benefit of using supplementary cementing materials like fly ash, silica fume and blast furnace slag can be utilized only when the chloride and/or sulfate contamination contributed by the mix constituents are minimized.

THESIS ABSTRACT

NAME OF STUDENT C. N. SADATH ALI KHAN

TITLE OF STUDY THE EFFECT OF TEMPERATURE AND SALT CONTAMINATION ON CORROSION OF REINFORCING STEEL IN OPC AND BLENDED CEMENT CONCRETES

MAJOR FIELD CIVIL ENGINEERING

DATE OF DEGREE AUGUST, 1993

This study was conducted to investigate the effect of relatively high temperatures (25 to 70 °C) and chloride and sulfate contamination on the reinforcement corrosion in ordinary portland cement (OPC) and blended cement concretes. To achieve the objectives of this research study, more than 500 concrete specimens were cast and tested. The effect of temperature and chloride and sulfate contamination on the compressive strength, porosity, electrical resistivity, alkalinity, water soluble chloride and sulfate concentration, and corrosion of reinforcing steel was evaluated.

Results indicated that both the temperature and chloride-sulfate contamination influence the compressive strength of OPC and blended cement concrete specimens. The compressive strength in OPC and blended cement concrete specimens was observed to decrease with increasing exposure temperature. Addition of chloride and chloride plus sulfate ions resulted in a decrease in the strength of OPC specimens, while an increase in the strength of the blended cement concrete specimens was indicated due to the addition of these salts. The cumulative pore volume in the OPC paste specimens was observed to increase with increasing exposure temperature. This trend was also observed in blended cements.

The Cl^-/OH^- ratio was also observed to increase with the exposure temperature. The effect of temperature on Cl^-/OH^- ratio was more pronounced for exposure temperatures of more than 40 °C.

The reinforcement corrosion activity, as measured by the corrosion current density on steel, in both the OPC and blended cement concrete specimens was observed to be higher in specimens contaminated with both chloride and sulfate salts as against those contaminated with only chloride salts. This indicates that the presence of both chloride and sulfate ions increases the rate of corrosion. At 70 °C exposure temperature, and chloride-sulfate contamination, the performance of all the blended cements investigated, except ASTM C 618 Class C fly ash, was not better than that of plain cements. This indicates that the technological benefit of using supplementary cementing materials like fly ash, silica fume and blast furnace slag can be utilized only when the chloride and/or sulfate contamination contributed by the mix constituents are minimized.

الملخص

أجريت هذه الدراسه لبحث تأثير الحراره المرتفعه نوعاً ما (من ٢٥ إلى ٧٠°م) والتلوّث بالكلور والكبريتات على صدأ الحديد في خرسانة الإسمنت العاديه وخرسانة إسمنت المواد المضافه . ولذلك ، تم صبّ وإختبار أكثر من ٥٠٠ عيّنة خرسانيه لتحقيق أهداف هذه الدراسه . كما تم تقويم تأثير درجة الحراره والتلوّث بالكلور والكبريتات على قوة الضغط ، المساميه ، المقاومِيّه الكهربائيه ، القلويّه ، تركيز الكلور والكبريتات الذائبه في الماء وصدأ حديد التسليح .

دلّت نتائج هذه الدراسه بأنّ درجة الحراره والتلوّث بالكلور والكبريتات يؤثران على قوة ضغط الخرسانه العاديه وخرسانة المواد المضافه ، ولوحظ أن قوة ضغط الخرسانه لهاذين النوعين تنقص بإزدياد درجة حرارة التعريض . كما إنّ إضافة الكلور والكلور والكبريتات معاً تتسبّب في نقص قوة ضغط الخرسانه العاديه بينما تزداد قوة خرسانة المواد المضافه بإضافة هذه الأملاح . ولوحظ أنّ حجم الفراغات التراكمي في عيّنات العجينه الإسمنتيه العاديه يزداد بإزدياد درجة الحراره ، كما لوحظ ذلك أيضاً في إسمنت المواد المضافه .

كما أنّ نسبة الكلور إلى الهيدروكسيل تزداد بزيادة درجة حرارة التعريض . وأنّ تأثير درجة الحراره على هذه النسبه كان أكثر وضوحاً عندما كانت درجة حرارة التعريض أكثر من ٤٠°م .أنّ نشاط حديد التسليح ، والذي تم قياسه بكثافة تيار الصدأ على الحديد ، في عيّنات خرسانة الإسمنت العاديه وإسمنت المواد المضافه يزداد في العيّنات الملوّثه بالكلور والكبريتات معاً مقارنةً مع العيّنات الملوّثه بالكلور فقط . ودلّ ذلك على أنّ وجود أيونات الكلور والكبريتات معاً يزيد من مُعدّل الصدأ .كان أداء جميع أنواع إسمنت المواد المضافه ، ماعدا الرماد المتطاير نوع C (معيار ASTM C 618) . ليس أفضل من الإسمنت العادي عندما كانت درجة حرارة التعريض ٧٠°م وعند التلوّث بالكلور والكبريتات . مما يدل على أن الفائده التكنولوجيه المرجوه من إستخدام إسمنت المواد المضافه مثل الرماد المتطاير ، غبار السيليكون وخبث الفرن العادي ، لا تتحقق إلاّ عندما تكون مكونات الخلطه الخرسانيه غير ملوثه بالكلور أو بالكلور والكبريتات معاً .

CHAPTER 1

INTRODUCTION

1.1 PERFORMANCE OF CONCRETE IN AGGRESSIVE ENVIRONMENTS

Portland cement concrete is extensively used to build the infrastructure needed for the modern development all over the world. The reasons for its extensive use are : (a) its economic superiority over other construction materials, (b) ease of molding, (c) nominal maintenance requirements, (d) availability of the constituent materials, etc.

It was assumed that concrete produced by mixing of cement, aggregate and water can withstand all types of weather and exposure conditions. Concrete was thought of as a maintenance-free material, until durability problems were reported from various parts of the world. Notable among the case histories, where concrete was blamed for its failure as a maintenance-free material, are the deterioration of bridge decks in USA and Europe, and the deterioration of reinforced concrete structures in the coastal areas of the Arabian Gulf [1,2,8]. It is estimated that more than $ 20 billions are needed for the repair and rehabilitation of highway structures in the USA, and £ 600 million for road bridges in the UK [1]. The cost of repair and rehabilitation of reinforced concrete structures in the Arabian Gulf is not well documented. But undoubtedly, considerable amount of resources have to be allocated towards restoring the useful service-life of structures serving in this environment. The deterioration of concrete structures, mainly due to reinforcement corrosion, in the temperate climatic conditions of North America and Europe are caused due to the use of chloride salts, which are used as deicer salts [1]. The reduction in the useful service life of concrete structures in the coastal areas of the Arabian Gulf is attributed to an interplay of geomorphic and environmental factors characterized by (i) environment charged with high concentrations of chloride and sulfate, (ii) high ambient temperature and humidity, (iii) daily and seasonal variations in the temperature and humidity, (iv) contaminated ground water at very shallow depths

and (v) contaminated and absorptive aggregates.

The major forms of deterioration observed in the Arabian Gulf conditions are reinforcement corrosion, sulfate attack and salt weathering. But, wide occurrence of deterioration due to reinforcement corrosion overshadows all other forms of concrete failure [2]. It may not be out of place to mention that to meet the growing demand for infrastructure, specifications borrowed from other parts of the world were in judiciously used by the construction industry in this part of the world. The inadequacy of the imported specifications, for the local conditions was realized only after failures were observed within a short span of about 10 to 15 years [2].

The failure of concrete to act as a durable material in this aggressive geomorphic and environmental conditions, is attributable to the unrealistic evaluation of the severity of the service conditions. The environmental and geomorphic conditions in the coastal areas of Arabian Gulf constitute a very hostile environment for concrete structures. The geomorphic conditions are characterized by contaminated aggregates, soil and ground water. The soil, and ground water which are contaminated with chloride and sulfate salts form an aggressive environment for structural components placed below grade. Environmental conditions characterized by the daily and seasonal variations in the temperature and the humidity regimes influence the performance of concrete components above grade.

Results of field studies carried out at King Fahd University of Petroleum and Minerals (KFUPM) indicated reinforcement corrosion to be the major form of deterioration [2]. Initiation and propagation of reinforcement corrosion was hitherto attributed mainly to chlorides which are present in the concrete as contribution from the mix constituents or by permeating to the steel-concrete interface from the service-environment. However, premature deterioration of concrete, mainly due to reinforcement corrosion, indicates the need to evaluate other factors affecting the mechanism of reinforcement corrosion, other than chloride. In this direction, the other

factors which seem to influence the mechanisms of reinforcement corrosion in concrete are elevated temperature and humidity conditions, and the sulfate ions contamination of concrete either through the mix ingredients and/or permeation from the environment.

Studies [3] carried out by Holden, et al. on the pore solution composition of pastes made with chlorides and sulfates, indicate an increase in the OH^- ion concentration due to inclusion of sulfates as compared to the alkalinity of pore solution of cement pastes contaminated with only chloride salts. Their results also showed a substantial decrease in the chloride binding capacity of cements in which sodium chloride and sodium sulfate were mixed. These results reflect the tendency of sulfate ions to react preferentially with the tricalcium aluminate (C_3A) phase, thus inhibiting the formation of calcium chloroaluminate. Al-Tayyib et al [4] reported seven fold increase in corrosion activity in mild steel exposed to sulfate containing calcium hydroxide solutions over those containing chloride salts. In another study carried out at KFUPM [5], sulfate ions permeating into hardened concrete from the external environment were observed to significantly influence the rate of reinforcement corrosion. The results of the studies cited above have an important bearing on the durability performance of concrete structures in this region, as ground water, aggregates and environment are heavily contaminated with both chloride and sulfate salts. These salts may be inducted into the concrete either through the mix water, and aggregates or penetrate the hardened concrete from the external environment. Further, the ground water table being shallow, the concrete components inadvertently get contaminated with the chloride and sulfate salts.

Environmental conditions in the coastal areas of the Arabian Gulf are characterized by the daily and seasonal variations in the temperature and humidity regimes. The variations in the humidity and temperature regimes accentuate the deterioration processes. The ambient temperatures in the Arabian Gulf area are relatively high (25 to 45 °C) compared to USA or Europe (10 to 20 °C). The direct solar radiation effect

raises the surface temperature of concrete to as high as 70 to 75 °C. This thermal effect influences the over all mechanisms of the corrosion of steel reinforcement in concrete; both induced by chloride ingress and carbonation. Higher rates of carbonation were observed in structures exposed to hot weather conditions [6]. Chloride diffusion is also known to increase with increasing temperature [7]. Thus, there is a need to elucidate the mechanisms of reinforcement corrosion under elevated temperature conditions as is the case in the coastal areas of the Arabian Gulf. Since superstructures in the Arabian Gulf area are exposed to elevated temperatures and chloride and sulfate salts, the concomitant effect of elevated temperature and sulfate-chloride contamination on the mechanisms of reinforcement corrosion need also to be investigated.

Since the durability characteristics of concrete are extremely permeability oriented, mineral admixtures like pozzolans, and industrial by-products such as fly ash, blast furnace slag and silica fume are being used to produce dense and impermeable concrete. The use of these materials reportedly reduces heat of hydration as well as cracking and degradation due to sulfate attack, alkali-aggregate reaction and corrosion of reinforcement [8]. However, the addition of a wide range of blending materials of differing chemical composition introduces significant diversity into the cement system. While a variety of blending materials have been extensively used in other countries, meager data are available on the performance of cements incorporating these supplementary cementing materials in the Arabian Gulf region. Whatever data available on the performance of blended cement concretes were developed through laboratory studies and are mainly concentrated on the chloride induced corrosion of steel in these concretes. Since pozzolans combine with $Ca(OH)_2$ to form secondary calcium silicate hydrates, it would seem reasonable to think that this can cause a reduction in the pH level within the concrete. Studies conducted at KFUPM [6] indicated higher depths of carbonation in concretes incorporating about 40% fly ash as replacement of cement. Incorporation of silica fume in concrete is known to decrease the pH of the pore solution. The chloride binding capacity of such concretes is also

known to be lower than in other concretes. As such, the mechanism of reinforcement corrosion in blended cements, particularly under the influence of **elevated temperatures** such as in the Arabian Gulf, and in the presence of chloride and sulfate salts introduced as contamination needs to be investigated.

1.2 RESEARCH OBJECTIVES

This study was conducted to investigate the effect of relatively high temperatures (25 to 70 °C) and chloride and sulfate contamination's on the reinforcement corrosion in plain and blended cement concretes. The specific objectives of this study were:

(i) to evaluate the effect of temperature and sulfate contamination on the water soluble chloride and sulfate concentration in the plain and blended cements,

(ii) to study the effect of chloride and sulfate contamination on the alkalinity of cement,

(iii) to investigate the effect of chloride and sulfate contamination on the electrical resistivity of concrete, and

(iv) to ascertain the synergistic effect of relatively high temperatures and chloride and sulfate contamination's on reinforcement corrosion.

The data developed through this study will be helpful in planning strategies for producing durable concrete to withstand the aggressive service conditions of the Arabian Gulf.

1.3 RESEARCH PROGRAM

To achieve the objectives of this research study, extensive laboratory investigations were carried out. The laboratory work was divided into five series. The salient features of the work performed in each of these series is discussed in the following paragraphs,

while the details of the experimental techniques used are discussed in Chapter 3.

1.3.1 Series I: Effect of Temperature and Salt Contamination's on the Compressive Strength of Concrete

In this series, the effect of relatively high temperatures, and chloride and sulfate contamination's on the compressive strength of plain and blended cement concretes was investigated. The details of the materials, test conditions and experimental techniques used in this series are shown in Fig. 1.1.

1.3.2 Series II: Effect of Temperature and Salt Contamination on the Concrete Porosity

In this series the effect of relatively high temperatures and chloride and sulfate contamination's on the pore size distribution in plain and blended cements was evaluated. The details of the materials, test conditions, and experimental techniques used in this series are shown in Fig. 1.2.

1.3.3 Series III: Effect of Temperature, and Salt Contamination on the Electrical Resistivity of Concrete.

In this series the effect of relatively high temperatures and chloride and sulfate contamination on the electrical resistivity of plain and blended cement concretes was investigated. The details of the materials, test conditions, and experimental techniques used in this series are shown in Fig. 1.3.

1.3.4 Series IV: Effect of Temperature and Salt Contamination on the Chloride Binding Capacity of Cements

In this series the synergistic effect of relatively high temperature and chloride and sulfate contamination on the OH^-, Cl^- and SO_4^{--} ion concentrations in plain and blended cements was investigated. The details of the materials, test conditions, and

experimental techniques used in this series are shown in Fig. 1.4.

1.3.5 Series V: Effect of Temperature and Salt Contamination on Reinforcement Corrosion

In this series the effect of relatively high temperatures and chloride and sulfate contamination's on the reinforcement corrosion in plain and blended cements was investigated. The details of the materials, test conditions, and experimental techniques used in this series are shown in Fig. 1.5.

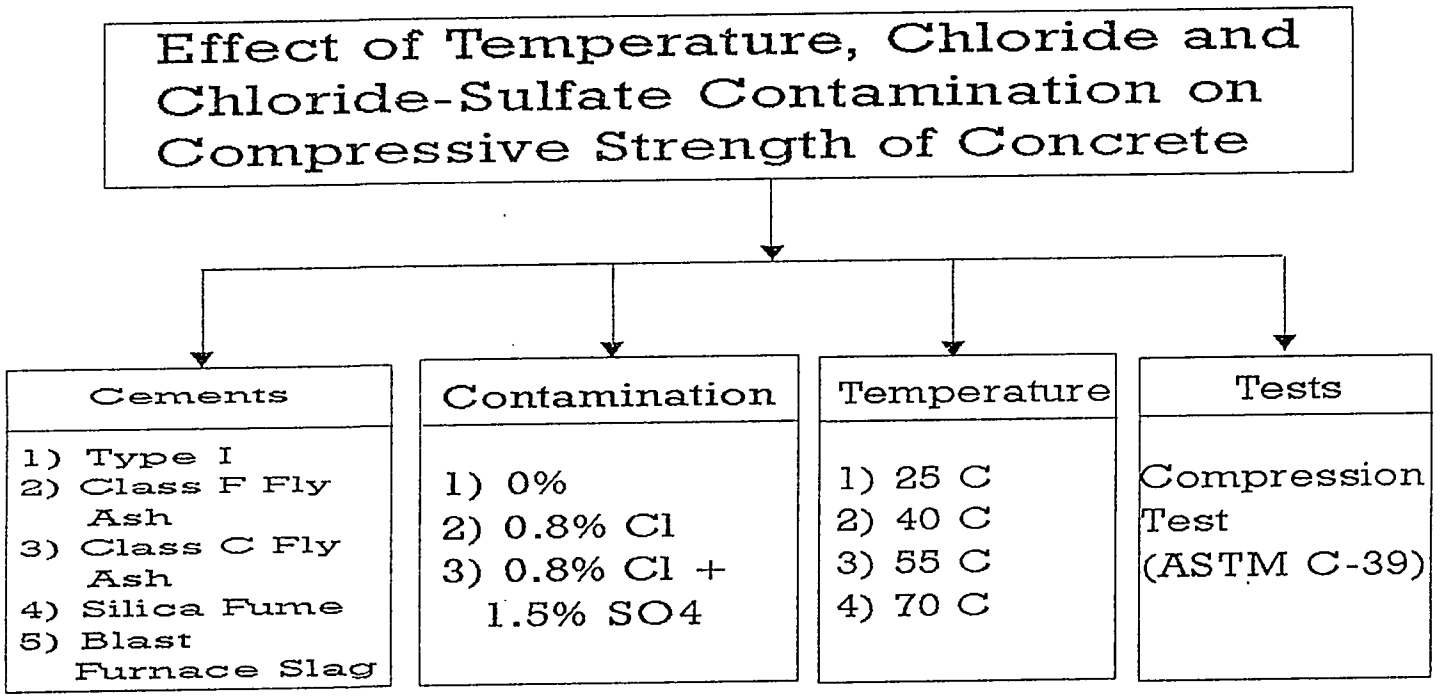

Fig.1.1 Experimental Program For Series I Specimens

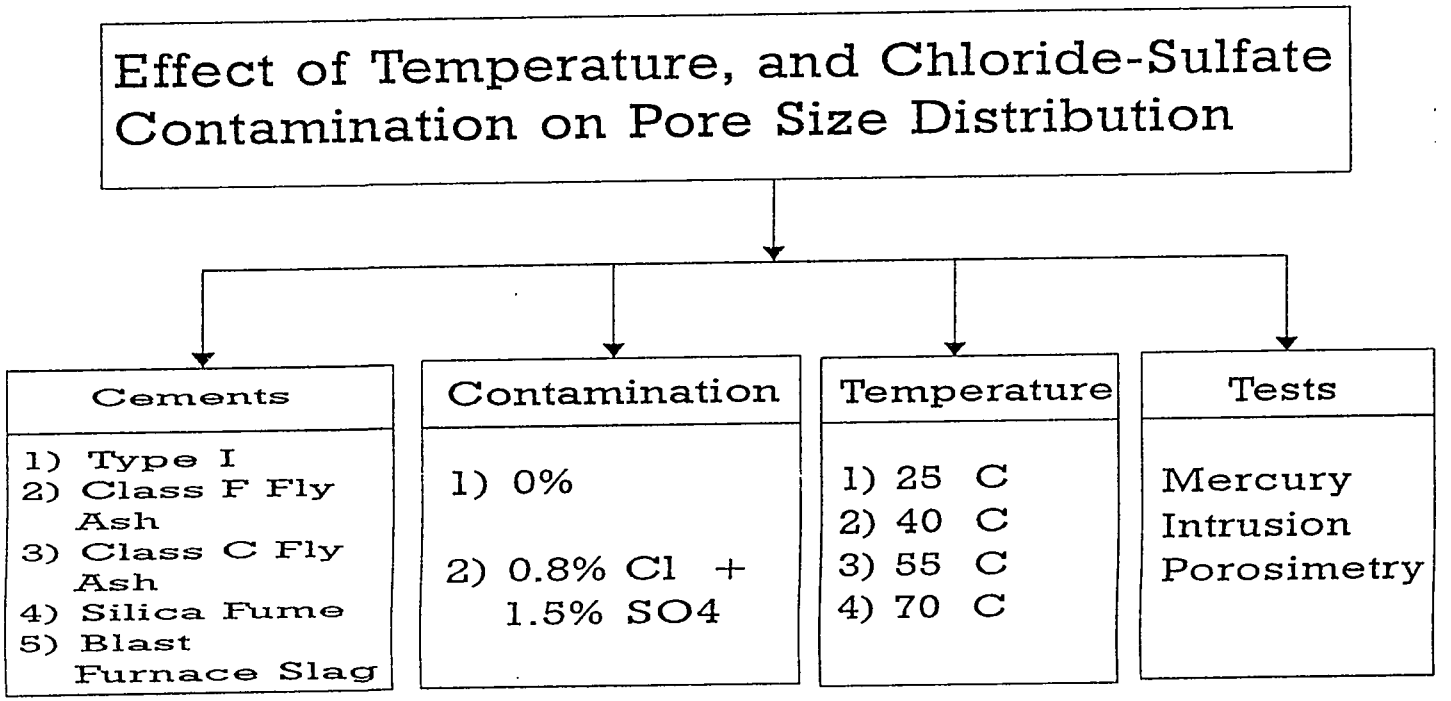

Fig.1.2 Experimental Program For Series II Specimens

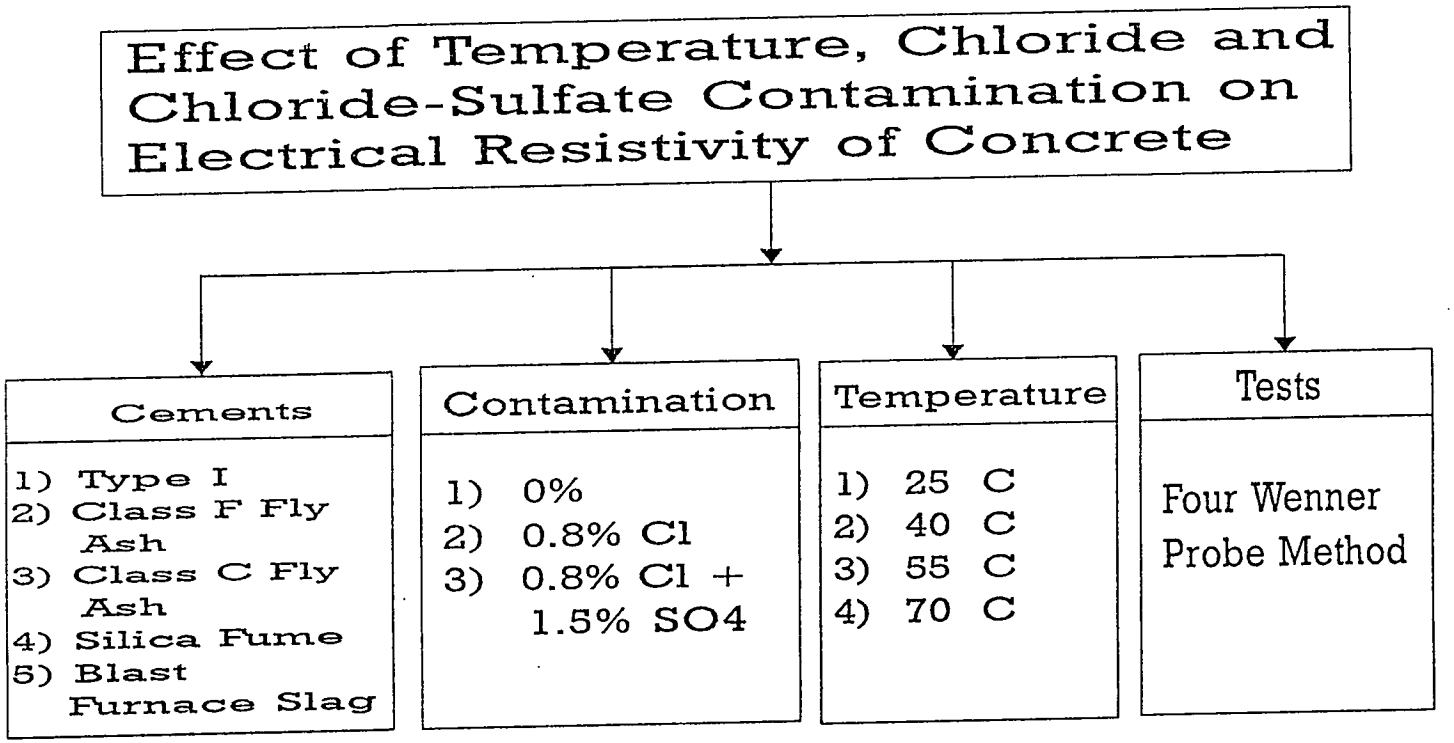

Fig. 1.3 Experimental Program For Series III Specimens

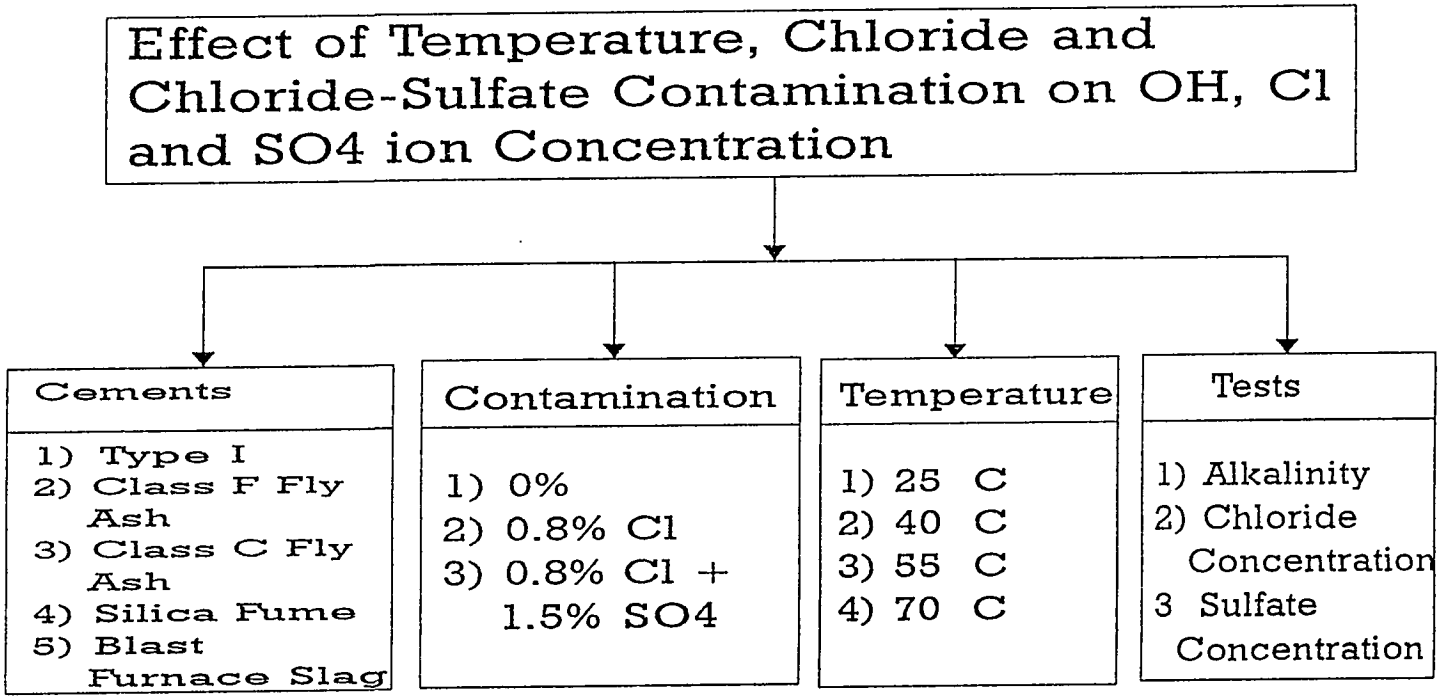

Fig. 1.4 Experimental Program For Series IV Specimens

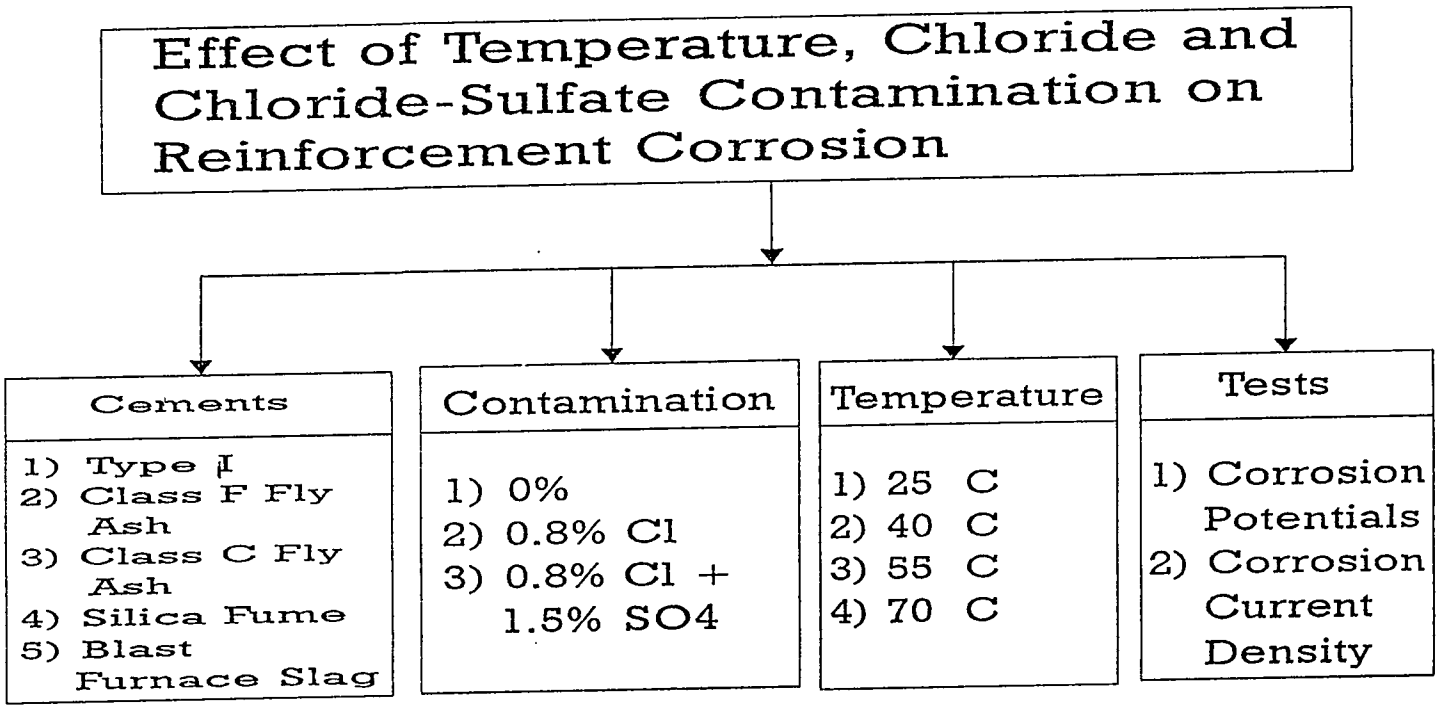

Fig. 1.5 Experimental Program For Series V Specimens

CHAPTER 2

LITERATURE REVIEW ON CONCRETE DURABILITY

2.1 COMPOSITION OF PORTLAND CEMENT CONCRETE

Portland cement concrete essentially consists of coarse and fine aggregate, cement, and water. Other admixtures, such as pozzolans, and chemical admixtures, such as water reducers, air entraining agents, maybe used to obtain desired properties. Since aggregates are considered inert the durability performance of portland cement concrete is predominantly governed by the chemical composition of the cement. The strength of portland cement concrete is a function of the physical and chemical properties of cement, properties of coarse and fine aggregate, cement to aggregate ratio and the water to cementitious material ratio. Because portland cement concrete is weak in tension, concrete structural members are reinforced with steel bars. Concrete incorporating steel reinforcement is called reinforced concrete. Since the durability performance of concrete is predominantly governed by the properties of cement[11], a discussion of cement chemistry will be worthwhile.

Portland cement essentially consists of clayey and siliceous materials burnt at around 1600 °C. The chemical composition of unhydrated cement is normally denoted by the following notation[8].

C_3S - Tricalcium silicate

C_2S - Dicalcium silicate

C_3A - Tricalcium aluminate

C_4A - Tetra calcium aluminoferrite

Normally, 3-5% of gypsum is added to cement to regulate the time of set. When cement is mixed with water, it forms a gel called calcium silicate hydrate (CSH), which binds the coarse and fine aggregate. The reaction of water with calcium and silica in cement is primarily responsible for the production of the CSH gel. Calcium hydroxide ($Ca(OH)_2$) is produced as a byproduct of cement hydration. The quantum of $Ca(OH)_2$ liberated is dependent on C_3S/C_2S ratio. However, the quantum of $Ca(OH)_2$ produced due to hydration reaction is more than 30% by weight of cement [9]. The $Ca(OH)_2$ produced by the hydration reaction significantly influences the durability performance of portland cement concrete. On one hand it increases the alkalinity of the pore solution which is helpful in providing electrochemical protection to steel, while on the other hand it forms an essential component for deterioration of portland cement concrete due to sulfate attack. The deleterious and beneficial role of $Ca(OH)_2$ on the performance of portland cement concrete will be elucidated in the following sections. The other compound of cement which controls its durability performance is tricalcium aluminate (C_3A). The susceptibility of portland cement concrete to sulfate attack increases with increasing quantum of C_3A, whereas a higher C_3A content is beneficial from reinforcement corrosion view point [8].

2.2 DETERIORATION OF CONCRETE

ACI Committee 201 [10] defines durable concrete as that which can resist weathering action, chemical attack, abrasion, or any other process of deterioration. The concrete deterioration processes are generally classified into physical and chemical [8]. Physical deterioration processes includes abrasion, erosion, cavitation, crystallization of salts in pores, frost action, scaling, fire, early thermal contraction, long-term drying shrinkage, crazing etc. While Chemical deterioration process generally include reinforcement corrosion, sulfate attack, alkali-aggregate reaction, carbonation etc. These types of deterioration are triggered by the chemical reaction, between one or more of the cement constituents, with the aggressive species present within the concrete

or contributed by the external environment. However, once concrete is chemically attacked, physical effects may accelerate the deterioration process, and they are intermingled with each other, and the separation of the main cause is difficult at advanced stage of deterioration.

Published reports and papers [1,2,11,12] indicate that concrete cracking and spalling due to corrosion of reinforcing steel, and cracking and loss of strength due to sulfate attack are the major form of deterioration of concrete structures in almost all parts of the world. These forms of concrete deterioration are caused by the presence of sulfate and/or chloride ions in concrete. Other forms of concrete deterioration, which manifests in the form of crazing and map cracking and is attributed to the reaction of cement with certain reactive components in aggregates, such as silica and carbonates, has also been reported [13]. However, deterioration of concrete due to sulfate attack and reinforcement corrosion is more pronounced than that due to alkali-aggregate reaction, particularly in the Arabian Gulf [2]. As such, this literature review will be restricted to concrete deterioration due to corrosion of reinforcement and sulfate attack.

2.2.1 Sulfate Attack

Deterioration of concrete due to sulfate attack is caused by reaction of certain cement constituents namely $Ca(OH)_2$ and C_3A with sulfate ions. This type of deterioration was identified as early as 1918, by Thorvaldson and his co-workers[9]. Sulfate attack is manifested in sulfate bearing soils and ground waters. Soil and ground water contain dissolved sulfates in the form of $MgSO_4.7H_2O$ (Epsom), $Na_2SO_4.10H_2O$ (Merablite), or $Ca_2SO_4.2H_2O$ (gypsum or Glauber's salt). Sulfate attack takes place only when these salts are in solution. Since the solubility of Ca_2SO_4 is very low, sulfate attack is predominantly attributed to the reaction of cement with Na_2SO_4 and $MgSO_4$ [8].

Sulfate attack in concrete is primarily characterized by the reactions of sulfate ions

from the various sources and gypsum with hydrated calcium aluminate or hydrated mono sulfo aluminate (AF_m) which is unstable and exists as a hydration product in cements with high C_3A content. These reactions are shown in following equations [8].

$$Ca(OH)_2 + Na_2SO_4 + 2\,H_2O \rightarrow 2CaSO_4.H_2O + 2NaOH \qquad (2.1)$$

$$Ca(OH)_2 + K_2SO_4 + 2\,H_2O \rightarrow CaSO_4.2H_2O + 2KOH \qquad (2.2)$$

$$2C_3A + C_3ACS\,H_{18} \rightarrow 3C_3A.\,CS\,H_{18}\,(AF_m) \qquad (2.3)$$

The reaction of AF_m with sulfate ions, either from the external sources or internal sources, results in the formation of ettringite ($3CaO.Al_2O_3.3CaSO_4.3H_2O$) some times referred as AF_t. Reaction products are expansive in nature and has a volume 6 to 7 times that of the original cement. The reaction is shown in the equation below. This results in the cracking of concrete.

$$C_3A\,C\,S\,H_{18} + 2CH + 2\,\bar{S} + 12H \rightarrow C_3A\,.3C\bar{S}\,H_{32} + CH \qquad (2.4)$$

Another type of sulfate attack is portlandite ($Ca(OH_2)$) based on the reaction with the sulfate ions. This type of deterioration generally occurs in low C_3A, sulfate resistant, cements. C_3S and C_2S produce more than 20% of $Ca(OH)_2$ as by products of hydration. $Ca(OH)_2$ has great affinity towards sulfate ions and is soluble in water. This results in the formation of gypsum causing production of AF_m. This type of attack is manifested by an eating away or softening of the cement matrix which leaves the aggregate standing out from the eroded concrete. The effect of cement chemistry on the two types of sulfate deterioration are presented graphically in Fig. 2.1 and 2.2, respectively [9].

Another type of sulfate attack, which is more deleterious compared to the two types discussed earlier, is the reaction between the cement compounds, especially $Ca(OH)_2$,

and the magnesium sulfate. In this type of sulfate attack reaction between Mg_2SO_4 and $Ca(OH)_2$, gypsum and $Mg(OH)_2$ are formed. This reaction lowers the pH of the cement pore solution to about 10.4 due to low solubility of $Mg(OH)_2$. Thus CSH gel liberates lime to maintain the required pH of 12.5. This reaction converts part of CSH gel into a non-binding lime less, silica gel, and accelerates the degradation process [8].

$$MgSO_4 + Ca(OH)_2 + 2H_2O \rightarrow CaSO_4\ 2H_2O + Mg(OH)_2 \quad (2.5)$$

$$3CaO\ 2SiO_2 + 3MgSO_4\ 7H_2O \rightarrow CaSO_4\ 2H_2O + 3Mg(OH)_2 + 2\ SiO_2 \quad (2.6)$$

As shown in the above equation the main constituent of cement that reacts with Mg_2SO_4 is $Ca(OH)_2$. In the absence of $Ca(OH)_2$, such as in the blended cements; in which it is consumed by the pozzolonic reaction, the Mg ion reacts with the CSH gel thus accelerating the deterioration process [14] .

Preventive measures to mitigate sulfate attack include (1) minimizing the sulfate contamination of the constituent materials (ii) using a dense and impermeable concrete through use of low water cement ratio and (iii) use of cement type compatible with the service environment.

Type V cement was hitherto used when concrete is placed in sulfate bearing soils and ground waters. But due to its susceptibility to portlandite based sulfate attack that is characterized by high C_3S/C_2S ratio, pozzolanic cements are normally used. Blending of properly characterized pozzolans reduces the quantity of $Ca(OH)_2$, and decreases the permeability of sulfate ions, thereby retarding deterioration of concrete [9].

2.2.2 Corrosion of Reinforcement

The corrosion of reinforcing steel in concrete is the single most important cause of poor durability of structural concrete. It has received increasing attention in recent years because it was first observed in marine structures and chemical manufacturing plants. More recently numerous reports of its occurrence in bridge decks, parking structures, pipes, buildings, piles, pre-stressed concrete, and other structures exposed to chlorides have made the problem particularly prominent.

Metals are formed or manufactured at elevated energies from their ores. These metals tend to revert to their native state, either in the form of oxides chlorides or sulfides. This process is called **corrosion**. Steel corrodes because the corrosion products are thermodynamically more stable than the metals themselves. It may occur by direct oxidation such as burning, or by acid attack, but these are of little concern to reinforcement in concrete. Corrosion of steel in concrete due to stress corrosion, hydrogen embrittlement, stray electrical current etc. have rarely been reported as possible causes of distress. Therefore, it is believed that nearly all of the corrosion of concrete reinforcement that occurs are essentially due to electrochemical reaction [17].

The corrosion of reinforcement in concrete is an electrochemical process involving a galvanic cell wherein chemical energy is converted to electrical energy. When steel is embedded in concrete, potential difference at various parts of the rebar [17] are produced due to complex and heterogeneous nature of concrete. This potential may be either due to differences in metal composition itself (metal defects or impurities) or much more readily due to differences in the physical and / or chemical environments of the highly heterogeneous concrete. The latter may be due to differences in alkalinity, chloride concentrations, oxygen availability, segregation, compaction, bleeding, permeability, and exposure conditions. When conditions are favorable, corrosion of steel occurs through the dissolution of metal ions into the electrolyte leaving the electrons. This is defined as an anodic reaction and the point at which this reaction

occurs is known as an anode. The electrons which are released at the anodic site react with moisture and oxygen forming OH^- ions (oxygen reduction). This reaction is known as the cathodic reaction and its location is known as cathode. The OH^- ions flow back to the anode to complete the circuit, and reacts with Fe^{++} to form $Fe(OH)_2$ which is an indirect oxidation resulting from dissimilar environments, or dissimilar potentials around the rebar. In general, electrochemical corrosion requires four primary elements, an anode, a cathode, an electrolyte and a circuit [17].

Passivation of Steel in Concrete

All metals, including steel are naturally protected from corroding by a phenomena called passivation. The passive film is formed due its reaction with the environment. When steel is first exposed to the environment, it reacts with air to form ferric oxide Fe_2O_3, blue colored layer, which protects steel from corrosion. The high alkalinity of the pore solution in the concrete results in the formation of a tightly adhering sub microscopically thin film of -ferric oxide which passivates the steel and protects it from corrosion [15,16]. Further, the dense and impermeable structure of concrete which retards the ingress of aggressive species like moisture, oxygen, and carbon dioxide, into its interior provides physical protection to steel.

Loss of Passivation

The passive film on the steel surface is disrupted by the reduction of pH of the pore solution either due to carbonation or due to the penetration of aggressive ions like chlorides, to the steel concrete interface. The chlorides may be induced into the concrete through the mix constituents namely aggregates, water and admixtures. Although they may penetrate the hardened concrete from the service environment [1,8].

The damage to concrete resulting from corrosion of embedded steel manifests in the form of expansion, cracking and eventually spalling of the cover. Additionally, a reinforced concrete member may suffer structural damage due to loss of bond between

steel and concrete. The loss of rebar cross sectional area sometimes leads to the structural failure [17].

Mechanisms of Corrosion of Steel in Concrete

Corrosion of steel in concrete is an electrochemical process. At the anode, metallic ions of iron go into solution by oxidation i.e. loss of electrons.

$$Fe \rightarrow Fe^{++} + 2e^{-} \qquad (2.7)$$

At the cathode, dissolved oxygen in the pore water which has diffused to the steel surface is reduced by electrons supplied by the anodic reaction to form hydroxyl ions in the presence of moisture as follows:

$$O_2 + 2H_2O + 4e^{-} \rightarrow 4(OH^{-}) \qquad (2.8)$$

The current completes the circuit back to the anode through the concrete in the form of negative hydroxyl ions. The rate of this transfer depends on the **temperature**, moisture content, **ionic** concentration, and **electrical resistivity**. This is an ionic diffusion process, but it can be modeled by Ohm's law relating the potential, current and resistance of the electrolyte [42]. The OH^{-} ions at the anode then combine with Fe^{++} cation to form ferrous hydroxide as follows:

$$Fe^{++} + 2OH^{-} \rightarrow Fe(OH)_2 \qquad (2.9)$$

Given sufficient time and oxygen, ferrous hydroxide can be further oxidized to form insoluble hydrated red rust which is accompanied by large increase in volume up to ten times that of the original metal (Fig. 2.3 and Fig. 2.4).

Factors Affecting the Corrosion of Reinforcing Steel

Corrosion of reinforcement in concrete is a heterogeneous complex electrochemical reaction involving various parameters.

The most significant active parameters affecting the reinforcement corrosion are [10]:

(i) *Concrete mix variables*: affect the alkalinity (pH), the quantity of uptake and transmission of water, oxygen and chlorides. These factors significantly affect the magnitude and rate of corrosion. The concrete mixture variables that affect the corrosion process are: w/c ratio, aggregates, cement and admixtures.

(ii) *Construction variables*: influence the condition that facilitate the movement of water, chlorides, and oxygen to the steel concrete interface. Some of these variables like concrete cover over reinforcement steel, degree of consolidation, and curving of concrete have profound effect on the corrosion processes.

(iii) *Temperature and humidity*: are also known to influence the kinetics of hydration, setting and hardening of concrete and initiation and propagation of corrosion of reinforcement. The factors affecting reinforcement corrosion in concrete are schematically shown in Fig. 2.5.

2.2.3 Effect of Chloride Ions on Reinforcement Corrosion

Presence of chloride ions at or near the steel concrete interface has a uniquely damaging effect on the degree of protection afforded by concrete to the embedded steel. It is now acknowledged that chloride ions are primarily responsible for the overwhelming majority of the reported cases of corrosion of steel in concrete. Almost all researchers agree that the chloride ion acts as an essential catalyst in the corrosion reaction. The precise role which the chloride ion plays in the corrosion processes, however, is not agreed upon. Most researchers believe that the chloride ion initiates the corrosion reaction by depassivating the protective oxide film on the steel surface allowing the iron to dissolve into solution. However, the depassivation does not necessarily occur through a direct reduction of alkalinity in the electrolyte by the chloride-induced reaction. Some researchers now believe that the chloride ion also

reacts directly by migrating through the film, as first proposed by Hoar [19]. The actual mechanism of migration, however, is not well understood or agreed upon. Ogura and Ohama [20] recently suggested that nucleation sites are related to microscopic inclusions and grain boundaries on the metal surface. Other theories include the effects of chloride ion concentration [21-24] and localized concentrations resulting in the lowering of pH at the film-electrolyte interface due to reduction of the iron oxide film.

Chloride ions also cause a shift of potential of the steel. Non-uniform penetration of chloride ions to the level of the steel produces differences in potential and leads to the formation of "Macro" corrosion cells. This is a general occurrence, and results from such factors as variations in concrete cover and local differences in concrete quality. On reaching the steel substrate, the chloride ion acts as a catalyst for the oxidation of steel by taking an active part in the anodic reaction. According to Uhlig [21] it oxidizes the steel to form $FeCl_3$ and draws its unstable ferrous ion into solution, where it reacts with the available hydroxyl ions to form $Fe(OH)_2$. This releases the Cl^- ions back into solution and consumes hydroxyl ions, as seen in the following reactions:

$$2\,Fe^{+} + 6\,Cl^{-} \rightarrow 2FeCl_3 + 4e^{-} \qquad (2.10)$$

$$1/2\,O_2 + H_2O + 4\,e^{-} \rightarrow 2\,OH^{-} \qquad (2.11)$$

$$FeCl_3 + 2\,OH^{-} \rightarrow Fe(OH)_2 + 3\,Cl^{-} \qquad (2.12)$$

The electrons released in the oxidation reaction flow through the steel to the cathode. This process results in an increase in the concentration of chloride ions and a reduction of the pH at the points of corrosion initiation, probably accounting for the process of pitting corrosion. The lowered pH at these sites contributes to the continual breakdown of the passive oxide film [25]. The last equation shows that three molecules of chloride are released as a byproduct, indicating that once the chloride ion reaches the metal surface, no further chlorides are required and depending on the

electrical resistivity of concrete either general or local corrosion proceeds.

It is reported [26-28] that chloride ions react with hydrated tricalcium aluminate phase in cement to form calcium chloroaluminate ($C_3A.CaCl_2.10H_2O$). Because of this reaction with tricalcium aluminate, a threshold concentration of chloride ions in the concrete mass must be present above which localized chloride concentrations can be effective in destroying the passive film surface. The American Concrete Institute Building Code Requirements (ACI 318-85) [29] limit water soluble chlorides to 0.15% by weight of cement, while the BS CP 8110 [30] allows a maximum of 0.4% acid soluble chlorides by weight of cement. According to Hausmann [31] corrosion initiates when the Cl^-/OH^- is above 0.6 (Fig. 2.6). Lambert et al [32] investigated the relationship between Cl^-/OH^- and corrosion current density in various cements. Their investigations indicated that passive condition of steel in concrete characterized by corrosion current density (I_{corr}) values substantially lower than 100 mA/cm^2 are maintained until a threshold Cl^-/OH^- ratio of approximately 3 was exceeded. There was a considerable scatter in the values of I_{corr} recorded at Cl^-/OH^- ratios in excess of 3 and, even at Cl^-/OH^- ratios as high as 15 to 20, there were instances where reinforcing bars did not show significant corrosion.

Gouda [33], based on tests conducted in $Ca(OH)_2$ solutions of pH in the range of 11.8 to 13.95, indicated that the threshold Cl^-/OH^- ratio is 0.30. Diamond [34] has also supported this value.

Also, there are conflicting data on the extent of chloride that combines chemically with C_3A. Clear [35] reported that when the total chloride content is near corrosion threshold level only 15 to 50 percent of the chloride will combine, the balance remains as free or uncombined chloride. Research carried out by Monfore and Verbeck [36] indicated that as much as 75 to 90 percent of the chloride ions combined with the cement to form chloroaluminate compound and only the remaining existed in the uncombined or free soluble chloride.

Effect of Carbonation on Reinforcement Corrosion

Carbonation involves the reaction of carbon dioxide with calcium hydroxide in the cement to form insoluble calcium carbonate and water. This reaction results in a significant reduction in pH of the electrolyte due to removal of hydroxyl ions from the pore water resulting in the decrease of pore pH of pore solution to about 8.5 [37]. At this low pH, the steel is no longer passive and corrosion can occur if other conditions are satisfied. Factors influencing the carbonation of concrete and the subsequent corrosion of embedded steel include concrete mix design, depth of reinforcement cover, curing, moisture conditions, **temperature** and the presence of chlorides. For a high quality, dry or water saturated concrete, carbonation is normally not a problem. Although carbonation is normally not a significant concern because it proceeds at a very slow rate. However significant corrosion damage resulting from carbonation of light weight concrete has been reported [38]. Also, the importance of carbonation, which is a slow process, under natural conditions has grown in recent years owing to the increased atmospheric pollution and the aging of the concrete structures.

Effect Sulfate Contamination on Reinforcement Corrosion

While much is known about the role of sulfate ion on concrete deterioration, very little data exist on the effect of sulfate ions on chloride-induced reinforcement corrosion. Stratfull [39] investigated the individual effect of sodium sulfate and sodium chloride on reinforcement corrosion. In his studies, corrosion of reinforcing steel in concrete was observed only in specimens subjected to sodium chloride solution, while no reinforcement corrosion was observed in specimens treated with sodium sulfate within the duration of the tests (214 days). The effect of sodium chloride as well as sodium sulfate, added to the cement paste specimens, on the pore solution chemistry of plain and blended cements was investigated by Holden et al. [3]. The chloride ion concentration in the specimens contaminated with chloride and sulfate salts was observed to be more than that in specimens contaminated with only chlorides. This

effect was attributed to the preferential reaction of the C_3A of the cement with the sulfate ions, thus inhibiting the binding capacity of chlorides with C_3A and formation of calcium chloroaluminate (Friedel's salt). An increase in the hydroxyl ion concentration was also observed with sulfate addition because the hydroxyl ions tend to enter the pore solution to balance the anions removed in the form of insoluble complex salts. However, the net effect of sulfate and chloride was found to increase the Cl^-/OH^- ratio when compared to the effect chlorides existed alone in cement for the five types of cement pastes investigated [3]. Treadaway et al. [40] have confirmed the results of the aforesaid laboratory studies by conducting long-term exposure trials. Al-Tayyib et al. [4] reported 7 fold increase in the corrosion activity in mild steel exposed to sulfate containing calcium hydroxide solutions over that exposed to chloride salts.

The role of sulfate ions on chloride-induced reinforcement corrosion when the sulfate and chloride ions permeate hardened concrete from the external environment is also not clear. However, since the diffusion rate of chloride ions is much higher than that of sulfate ions, Friedel's salt is initially formed. At a later stage, when the sulfate ions penetrate the hardened concrete, they react with Friedel's salt leading to the liberation of chlorides ions. Studies carried out by Al-Amoudi and Maslehuddin [41] on the interactive effect of chlorides and sulfates on corrosion of steel in cement paste specimens indicated that while sulfate ions are hardly able to induce reinforcement corrosion, considerable reinforcement corrosion was observed in specimens immersed in the chloride-sulfate solutions. The concentrations of free sulfate beyond 0.55% and above and associated with 15.7% chloride ions were found to be necessary to accelerate the corrosion process. An extension of this study [42] to plain and blended cement concrete specimens indicated a similar trend. However, the effect of sulfate concentration was found to be more pronounced on the rate of corrosion, while no systematic effect was observed on the time to initiation of corrosion.

In the Arabian Gulf, concrete is contaminated with both chloride and sulfate ions

and is exposed to relatively elevated temperature conditions. The concomitant effect of these factors needs to be fully elucidated.

2.3 BLENDED CEMENTS

Pozzolonic and cementitious by products, such as fly ash, blast furnace slag and silica fume, are being strongly suggested as additives to improve the properties of concrete in general and durability, in particular. When such materials used as a partial replacement or addition to the cement, they modify both the physical structure and chemical composition of the hydrated cement. The advantages of incorporating these materials to the cement include, improved resistance to sulfate and dilute acid attack, reduction in amounts and rate of heat evolution which is beneficial in the casting of thick sections of concrete, reduction in the alkali level of the cementitious component in order to minimize the risk of alkali silica reaction, improvements in the characteristics of fresh concrete, continuing strength development and decrease in the permeability to water and other aggressive species.

The cementitious and pozzolanic properties of blended cements depend on the chemical composition, source of origin, particle-shape, size and distribution, and mineralogical composition. Siliceous and pozzolanic byproducts are classified into five categories by Mehta [43] and adopted by the RILEM Technical Committee on the Use of Siliceous By Products in Concrete. Mehta's classification of the pozzolanic material is shown in Table 2.1. Fig. 2.7 shows classification of blended cements on CaO-Al_2O_3-SiO_2 trinary system.

2.3.1 Pozzolanic Reaction in Blended Cements

Pozzolans are defined as siliceous or aluminous siliceous materials with little or no cementitious property which react with $Ca(OH)_2$, a byproduct of hydration of cement, and forming a relatively stable low strength CSH gel in the presence of moisture [8].

This secondary CSH gel, although less dense than the primary CSH gel, effectively fills up the large capillary space, thus improving the strength and impermeability of the hardened cement. The resulting structure is likely to be dense with a refined and discontinuous pore structure [8]. The pozzolanic action has three features, first the reaction is slow, second the lime is consumed, third the pore structure refined.

Among the pozzolanic materials, blast furnace slag efficiently fills up the large capillary voids, due to hydration of particles of blast furnace slag itself with water. This produces highly impermeable concrete. Fly ash particles do not react with water [9] and leaves some space as shown in the Fig. 2.8 This increases the permeability, in comparison with blast furnace slag and ordinary portland cement.

2.3.2 Durability of Blended Cement Concretes

Compared to ordinary portland cement, blended portland cements indicate superior durability performance when the properly characterized pozzolans are used in appropriate proportions, mixed and cured. Since deterioration process, such as expansion and cracking of concrete due to sulfate attack, alkali aggregate reaction, freezing and thawing, corrosion of embedded steel etc., are mainly dependent on the permeability of concrete, blended cements have an advantage over plain cements. Since micro cracks and continuous pores in concrete are the principle source of permeability, pozzolanic materials show improved performance compared to plain cements due to a reduction in the permeability and discontinuous pore structure [43].

Permeability

Water is usually involved in most processes of concrete deterioration; therefore, it is the permeability of concrete to water which generally controls the rate of deterioration. Since micro cracks in concrete are the principal source of permeability, by reducing the micro cracks caused by a variety of physical and chemical factors,

incorporation of supplementary cementing materials in concrete the mineral admixtures can have a beneficial effect on general durability of concrete [11].

Quantitative data from water permeability tests on concrete are generally not reliable because of experimental problems, such as the difficulty to achieve a steady state of flow. However, Berry and Malhotra [44] cited studies dated as far back as 1950's to show that well-cured (age 6 months) concrete pipe containing 30 or 50% fly ash, as replacement of cement were approximately five times as impermeable as the corresponding concrete without the fly ash. Douglas [45] cited Kondo et al. and Bakker's work on cement mortars to show that, with curing age, the diffusion coefficient in slag cement mortars diminished faster than the diffusion coefficient in ordinary portland cement mortar. The slag cement mortars were 10 to 100 times less permeable to water than portland cement mortar. Bakker [46] has reported extensive data on diffusion coefficients of Na^+, K^+, and Cl^- ions in 0.50 to 0.65 w/c mortars made with blended Portland cement, containing 60 or 75% slag.

Condensed silica fume being highly pozzolanic, compared to fly ash or slag, it decreases the concrete permeability rapidly. Results from studies by Markestad [47] and Gjorv [48] on water permeability of concretes in which the cement content varied from 100 to 500 kg/m^3 showed that a lean concrete mixture incorporating 100 kg/m^3 cement and only 10% condensed silica fume had its permeability decreased to about 4 x 10^{-10} m/sec, compared to 1.6 10^{-7} m/sec without the silica fume. The permeability of concrete containing 100 kg/m^3 cement and 20% silica fume was similar to the one containing 250 kg/m^3 cement and no silica fume. At high cement contents, the degree of effectiveness of silica fume in reducing the permeability of concrete was diminished.

Sulfate Attack

Sulfate resistance of fly ash blended cements was investigated by various researchers [49-52]. Due to a wide variation in physical properties and chemical

composition of different fly ashes their performance in terms of sulfate attack is also variable. Dunstan [49] from his study, conducted on 13 concrete mixes made with lignite or sub-bituminous coal sources, established an empirical sulfate resistance factor, R, related to the chemical oxide analysis of the ash. R was reported to be directly proportional to sulfate resistance. If R is less than 1.5, the sulfate resistance of the fly ash blended cement was improved. However, when R is more than 3, the sulfate resistance was reduced. Mehta (50) based on his experimental data showed that even fly ashes having an R factor less than 1.5 reduced the sulfate resistance. He suggested that rather than the chemical composition, or R factor of fly ash, it is the mineralogical composition of cement and fly ash interaction product that controls the sulfate resistance. When hydrated cement-fly ash mixtures contained the mono sulfate hydrate or (AF_m) or calcium aluminate hydrates, sulfate immersion showed expansion and strength loss associated with ettringite formation. However, when fly ash cement, contained ettringite prior to immersion in sulfate it performed satisfactorily. Whether a hydrated cement fly ash system will form a AFm, calcium aluminum hydrates or ettringite depends on its alumina to sulfate ratio.

As with fly ash, use of blast furnace slag leads to reduction in concrete permeability and the calcium hydroxide content and hence they enhance the sulfate resisting characteristics of concrete. From various studies [53-56] it has been shown that higher levels of slag content, greater than 60%, are most effective in inhibiting the deterioration due to sulfate attack.

Results of tests conduced at KFUPM [57], and others [58,59] show that silica fume addition to Portland cement improves the resistance to sodium sulfate attack. However incorporation of silica fume can impair resistance of hardened concrete to magnesium sulfate attack. Rasheeduzzafar et al. [57] observed that the pozzolanic reaction between calcium hydroxide and silica fume removed most of the calcium hydroxide from the hydrated cement, as confirmed by X-ray diffraction analysis.

Apart from decreasing the vulnerability to formation of gypsum, the reduction in calcium hydroxide concentration increases the solubility of hydrated calcium aluminates thereby causing the sulfate reaction to occur through solution and thereby without expansion. Mehta [59] has hypothesized that in the absence of calcium hydroxide the ettringite produced is in the form of large lath-like crystals which are not expansive. It is only in the presence of calcium hydroxide that micro-crystalline ettringite is formed which is capable of absorbing the large amounts of water on its surface causing considerable expansion.

Reinforcement Corrosion

The reinforcing steel in concrete remains covered with a passive iron oxide film, which must be destroyed before the electrochemical reactions resulting in steel corrosion can begin. The depassivation of steel can occur in the presence of chlorides or when the pH of concrete is reduced to <11 by acid attack such as by carbonation. Once the steel has been depassivated, the progress of corrosion would be controlled by the rates of oxygen and moisture flow to the steel and the electrical resistivity of concrete. Furthermore, the spalling of concrete cover is dependent on the tensile strength of concrete.

When supplementary cementing materials are used in ordinary portland cement, the hardened concrete is dense and impermeable [8]. Also the electrical resistivity and the flexural strength of blended cement concretes is higher than that of ordinary portland cement concrete [11]. The increase in impermeability and attendant favorable changes in the flexural strength and electrical resistivity extends the time to initiation of corrosion and reduces the rate of corrosion [111].

Due to lower amounts of calcium hydroxide available in concretes containing mineral admixtures, there is a concern about their carbonation behavior. From a review of several publications, Berry and Malhotra [60] concluded that well-compacted and

properly cured concretes, with low w/c ratio, appear to be sufficiently impermeable to resist the advance of atmospheric carbonation beyond the first few millimeters. The authors cited a study by Ho and Lewis, in which an inverse relationship was found between the concrete strength and depth of carbonation. At strength levels lower than 30 MPa the fly ash cement concrete was more readily carbonated than the reference concrete without fly ash. This happened when the concretes were exposed to carbonation at a given age, rather than at an equivalent strength. The fly ash concretes cured to 90 days before carbonation, showed a lower rate of carbonation compared to the reference concrete. In conclusion, compared to normal concrete, a fly ash concrete increases the corrosion protection of reinforcing steel provided it is adequately proportioned, mixed and cured prior to environmental exposure.

In concrete made with a cement containing a relatively large amount of slag (50 to 75 wt. %), greater carbonation depths compared to control concrete were reported by some researchers. For instance, Litvan and Meyer [62] found that the long-term depths of carbonation were greater in a slag concrete. This was attributed to the coarsening of the pore size distribution as a consequence of carbonation of the slag-cement paste. On the contrary, due probably to calcium carbonate formation by chemical reaction between $Ca(OH)_2$ and CO_2 subsequent sealing of large pores, the reference concrete containing portland cement showed a decreasing carbonation rate with age. Evidently, as Berry and Malhotra [60] concluded, the solution lies in using a low w/c ratio, high cement content, and adequate consolidation and curing of concrete so that carbonation can be stopped at the concrete surface.

With regards to silica fume concretes, Vennesland and Gjorv [61] and Gjorv [63] reported the results of 10 or 20% silica fume incorporation on the rate of oxygen transport, carbonation, and electrical resistivity. Although, as a result of silica fume incorporation, the rate of oxygen transport through water-saturated concrete as well as the depth of carbonation were only slightly reduced in lean concrete mixes [low cement

contents and high W/(C+SF) ratios], the electrical resistivity was significantly enhanced. In a high-strength concrete mixture with 400 kg/m^3 cement content, 20% silica fume, and 0.38 W/(C+SF), the electrical resistivity increased from about 9 to about 127 K-Ω.cm due to silica fume addition. This, obviously, would have a dramatic effect on reducing the corrosion potential of steel in concrete containing condensed silica fume.

2.4 EFFECT OF TEMPERATURE ON CORROSION OF REINFORCEMENT

In arid and semi-arid regions concrete is exposed to relatively high temperatures of 40 to 45 °C. Concrete surface temperatures reaches to 70 to 75 °C due to solar radiation's. It is well known that increase in temperature increases the kinetics of the corrosion reaction and respective factors. These effects are confirmed by Mehta and Gerwick [64]. The concrete used in beams of San Mateo Bridge over San Francis Bay is high quantity 375 kg/m^3 cement with w/c of 0.45. All beams were exposed to same environment. After 17 years, the steam cured beams had to be repaired because of corrosion damage. But the naturally cured beams showed no damage. They believe that micro cracking due to temperature gradients in the steam cured beams made them more permeable to chlorides and oxygen thus accelerating the corrosion process.

It was observed that increase in temperature decreases the viscosity [65] of water thus allowing more flow of dangerous species and hence accelerating the corrosion process. The increase of kinetics of corrosion reaction at elevated temperatures is in good agreement with Arrhenius Equation [66].

As this is the case, very little performance data is available on the corrosion behavior of reinforced concrete at relatively high temperatures. It was stated that [67] for the adopted mix details the initiation time for the corrosion of reinforcement at 30 °C is approximately one third of that at 10 °C.

TABLE 2.1 Classification of Pozzolanic Materials (after Mehta [43])

Classification	Chemical and Mineralogical Composition	Particle Characteristics
I. Cementitious		
Rapidly-cooled blast furnace slag	Mostly silicate glass containing calcium, magnesium, and aluminum. Crystalline compounds of melilite group and merwinite may be present in small quantities.	Unprocessed material is granular or pelletized and contains 5 to 15% moisture. Before use it is dried and ground to particles mostly less than 45 μm (400 to 500 m^2/kg Blaine). Particles have rough texture.
II. Cementitious and Pozzolanic		
High-calcium fly ash (> 10% CaO)	Mostly silicate glass+ containing calcium, magnesium, and aluminum. The small quantity of crystalline matter present generally consists of quartz, and C_3A; free lime and periclase may be present; $C\bar{S}$ and $C_4A_3\bar{S}$ may be present in the case of high-sulfur coals. Unburnt carbon is usually less than 2%.	Powder corresponding to 10-15% particles larger than 45 μm (usually 300-400 m^2/kg Blaine). Most particles are solid and spheroidal with less than 20 μm diameter. Particle surface is generally smooth but not as clean as in low-calcium fly ash.
III. Highly Pozzolanic		
a. Condensed silica fume	Consist essentially of silica in non-crystalline form.	Extremely fine powder consisting of solid and spheroidal particles mostly less than 0.1 μm diameter (about 20000 m^2/kg surface area by nitrogen adsorption).
b. Rice husk ash produced by controlled incineration	Consist essentially of silica in noncrystalline form.	Particles are generally less than 45 μm but they are highly cellular (about 60000 m^2/kg surface area by nitrogen absorption).
IV. Normal Pozzolanic		
Low-calcium fly ash (< 10% CaO)	Mostly silicate glass containing aluminum, and iron. The small quantity of crystalline matter present consists generally of quartz, mullite, hematite, and magnetite. Unburnt carbon is usually less than 5% but at times may be up to 10%.	Powder corresponding to 15-30% particles larger than 45 μm (usually 250-350 m^2/kg Blaine). Most particles are solid and spheroidal with average 20 μm diameter. Cenospheres and plerospheres may be present.
V. Others		
a. Slowly-cooled blast furnace slag	Consist essentially of crystalline silicate minerals, and relatively small amount of noncrystalline matter.	The materials must be pulverized to very fine particle size in order to develop satisfactory cementitious or pozzolanic activity. Ground particles are rough in texture.
b. bottom ash, boiler slag, field-burnt rice husk ash.		

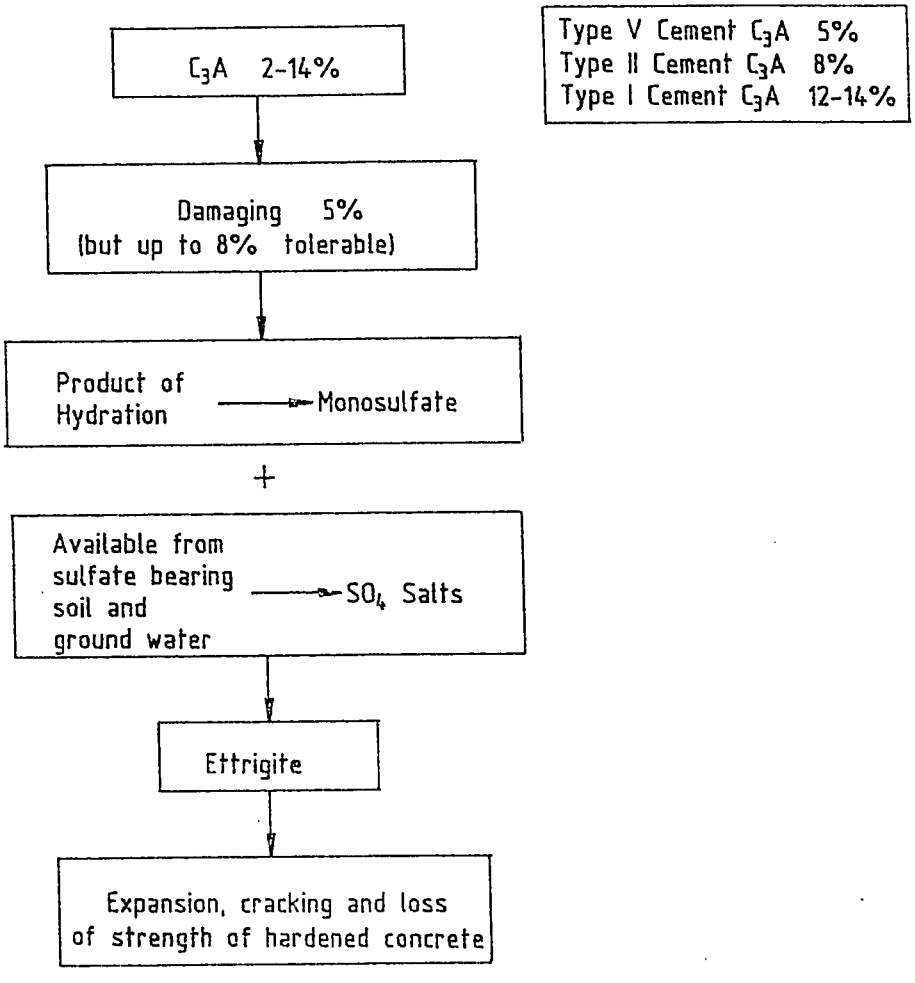

Fig. 2.1 C_3A Oriented Sulfate Attack (after Rasheeduzzafar[9])

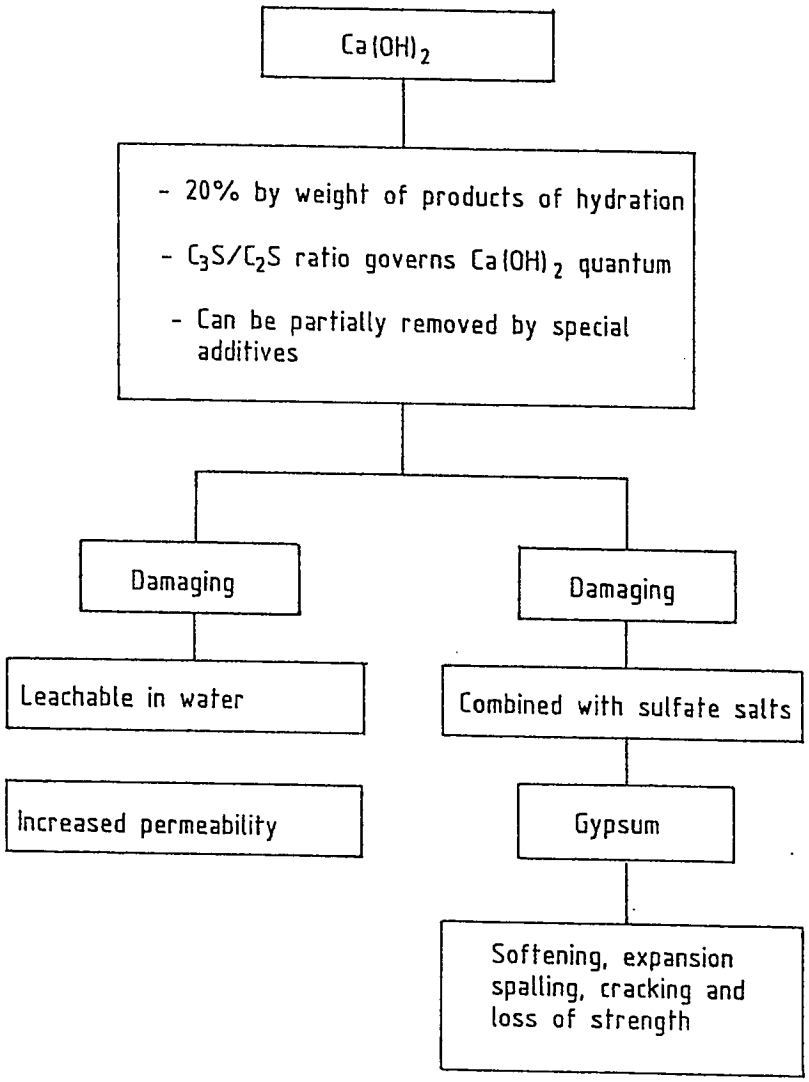

Fig. 2.2 Portlandite Oriented Sulfate Attack (after Rasheeduzzafar[9])

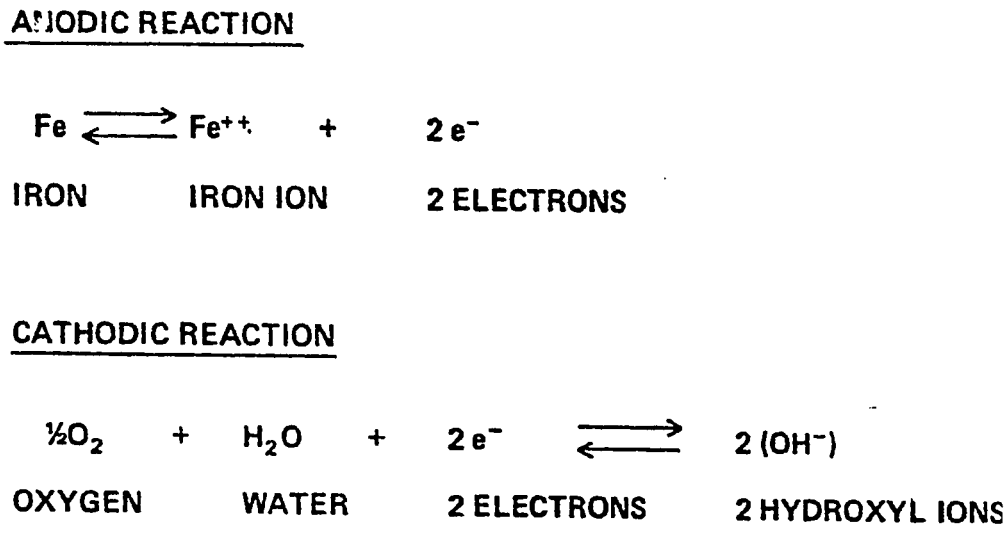

Fig. 2.3 Anodic and Cathodic Reactions (after Bernard and Verbeck[17])

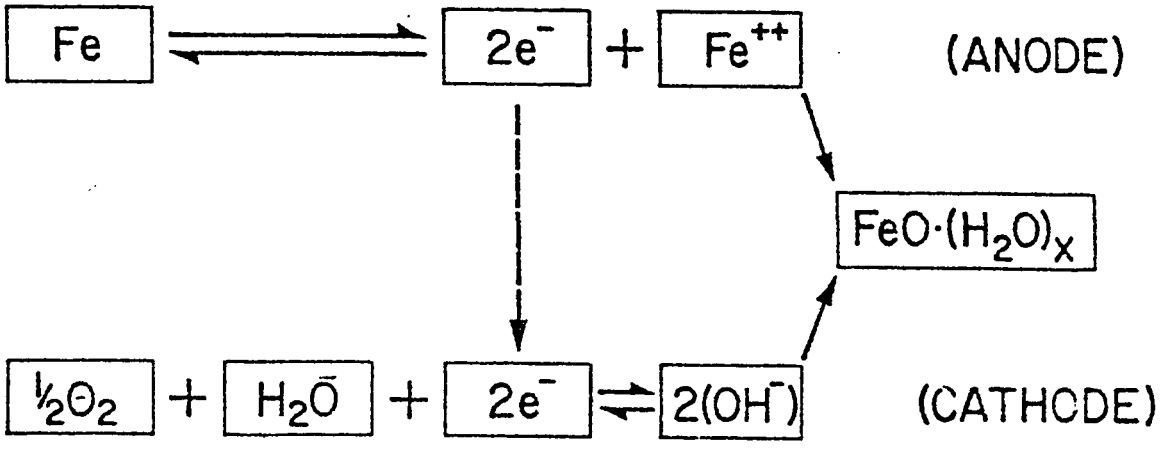

Fig. 2.4 Flow Diagram Depicting the Corrosion Process (after Bernard and Verbeck [17])

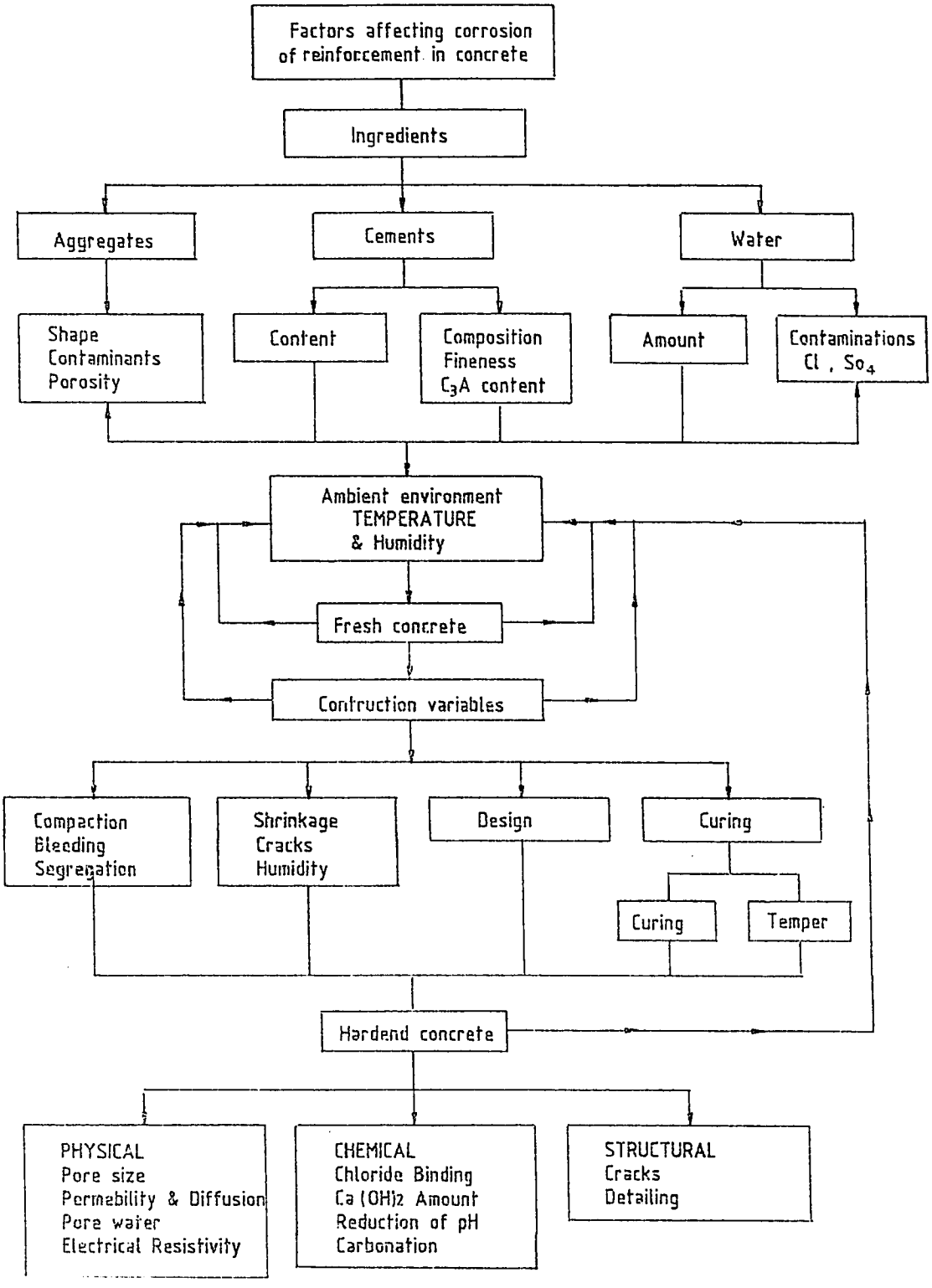

Fig. 2.5 Schematic Representation of Factors Affecting the Corrosion of Reinforcing Steel in Concrete

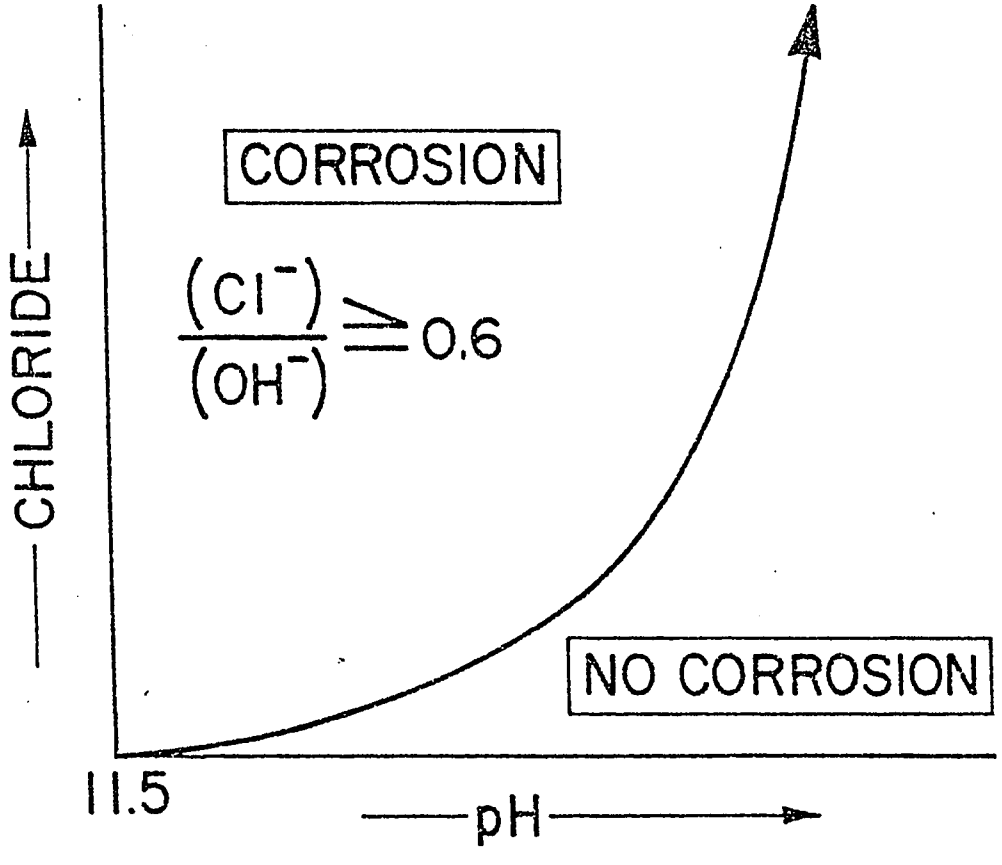

Fig. 2.6 Relation Between Cl^- and OH^- on Corrosion of Steel (After Hausmann [31])

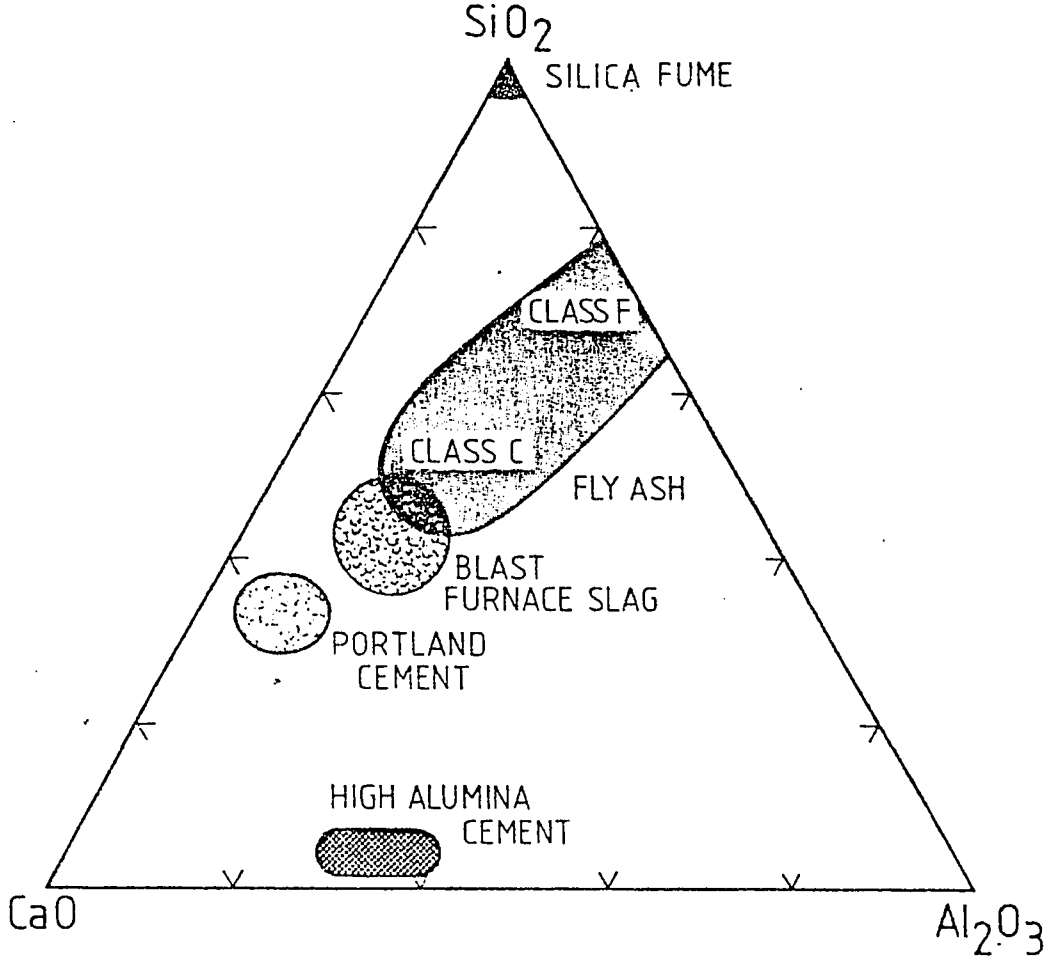

Fig. 2.7 Classification of Blended Cements on Ternary CaO-Al_2O_3-SiO_2 System Composition (After Mehta [43])

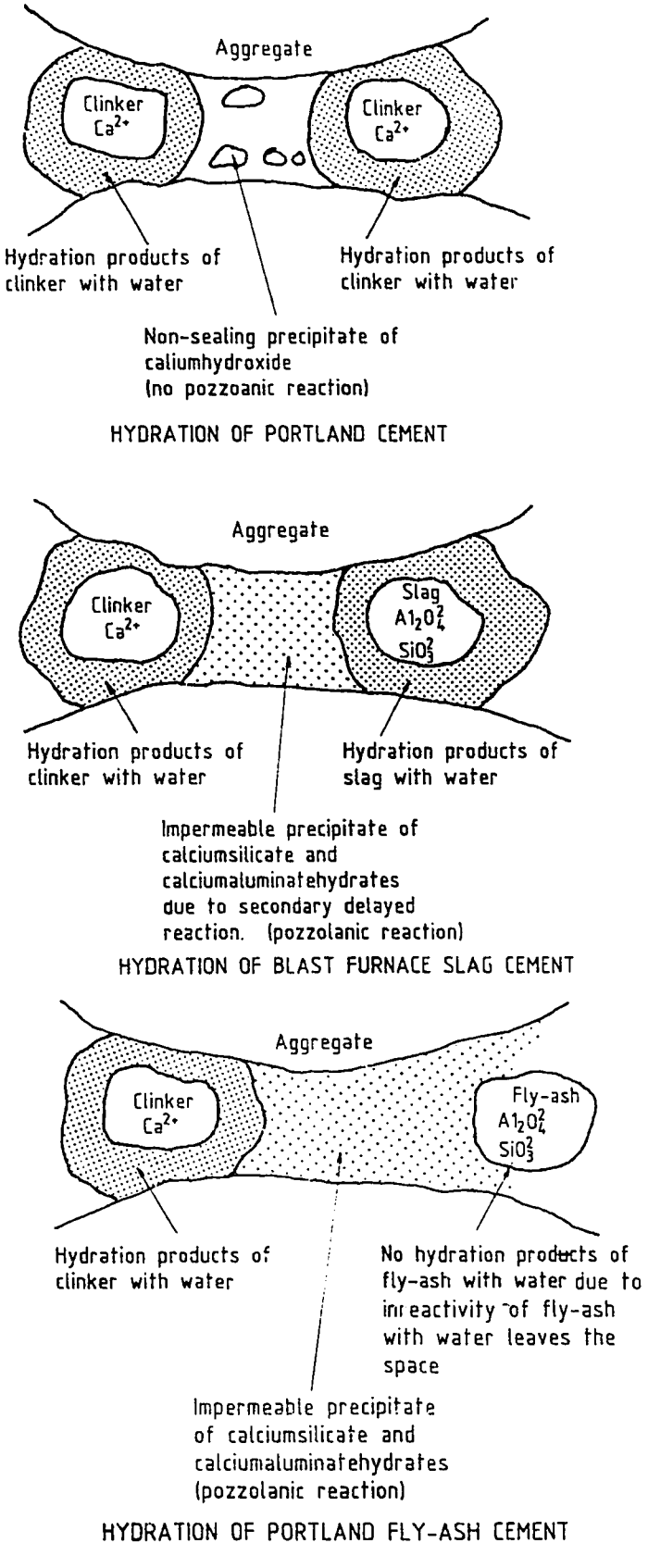

Fig. 2.8 Hydration of Ordinary and Blended Portland Cements (As Quoted in Ref. 9)

CHAPTER 3

METHODOLOGY OF RESEARCH

This chapter outlines the type and number of specimens, materials and techniques used to carry out the experimental program in this study. Whenever possible ASTM or BS methods have been used for the testing carried out in this study. Any deviation from the standard methods have been described in this chapter.

3.1 SPECIMENS

Concrete and cement paste specimens were used in the experimental program. Concrete specimens were used to evaluate the compressive strength, electrical resistivity and reinforcement corrosion. The cement paste specimens were used to determine the alkalinity, chloride and sulfate ion concentration. These specimens were also used to evaluate the porosity and micro structure. The details of the specimen geometry and number used for each test are shown in the Table 3.1.

3.2 CONCRETE MIX DESIGN

Plain and blended cement concrete mixes were designed using absolute volume method. The following factors were kept invariant in all the concrete mixes:

- Cementitious material: **350 kg/m^3**
- Effective water cementitious material ratio: **0.50**
- coarse to the fine aggregate ratio: **1.63**

The weights of ingredients used in the plain and blended cement concrete mixes are shown in Table 3.2.

3.3. MATERIALS

3.3.1 Cementitious Materials

In the plain cement concrete and cement paste specimens, ASTM C150 Type I cement was used. The chemical composition of cement is shown in Table 3.3. Four pozzolans were used in the preparation of blended cement concrete and cement paste specimens. The pozzolans used in the preparation of blended cements were:

1. ASTM C618 Class F Fly ash
2. ASTM C618 Class C Fly ash
3. Blast Furnace Slag
4. Silica Fume.

The chemical composition of the pozzolans used is shown in the Table 3.3. The chemical compositions of cements were determined in the laboratory. In fly ash blended cement concrete and paste specimens 20% cement was replaced. In silica fume blended cement concrete and paste specimens 10% silica fume was used as a replacement of cement. Blast furnace slag blended concrete and paste specimens contained 70% blast furnace slag and 30% Type I cement.

3.3.2 Aggregates

The coarse aggregate used in the concrete mixes were crushed limestone procured from quarries in Riyadh. The specific gravity and absorption of coarse aggregates were determined in accordance with ASTM C 127. Data on the specific gravity and absorption of coarse aggregates are shown in Table 3.4. The Coarse aggregates grading was selected in accordance with ASTM C 33. The chosen grading curve lies between the lower and upper limits of curves for 12.5 mm maximum size. The coarse aggregates grading used in all the mixes is shown in Table 3.5.

Beach sand was used as fine aggregates in all the concrete and cement paste specimens. The specific gravity, and absorption of the fine aggregates are shown in Table 3.6. Typical sieve analysis of the sand used is plotted in Fig. 3.1.

Portable water was used in the preparation of concrete and cement paste specimens.

3.3.3 Mixing and Casting of Concrete and Paste Specimens

The concrete constituents were mixed in a revolving drum type mixer. The constituents were mixed for approximately 3 to 5 minutes till the concrete was uniform. Additional mixing time of two minutes was provided for concrete mixes containing silica fume. In contaminated cement concrete mixes the salts, sodium chloride and sodium sulfate, were mixed thoroughly in the water, before it was introduced in the mixer. Further, a water reducing admixture, Conplast 430, was added in the silica fume cement concrete mixes at a dosage of 0.9 % by weight of the cementitious material to increase the workability. After mixing, the concrete was placed in the molds in two layers and vibrated on a vibrating table, till complete consolidation was achieved. After casting the surface of the specimen was leveled and then covered with plastic sheets to minimize the loss of moisture. The cement paste specimens used for the determination of chloride, alkalinity and sulfate concentration and porosity determination were made with a water to cementitious material ratio as in the concrete specimens. The cement paste, was mixed in a laboratory blender till a uniform color was obtained. The cement paste was also placed in the molds in two layers and consolidated by slow speed vibration till all the entrapped air was eliminated. In blended cement paste specimens the cementitious material, was first mixed in the blender and then water added in installments till a uniform color was observed.

3.3.4 Specimen Curing and Exposure

After casting the concrete and cement paste specimens were cured under plastic sheet at laboratory conditions for one day. After this period, the specimens were then

demolded and cured under 100% Relative Humidity for a further period of 27 days before they were placed in the exposure chamber.

To evaluate the effect of temperature on the durability performance of plain and blended cement concrete and paste specimens, plain and contaminated, were placed in humidity-temperature chambers. Four such chambers were used to maintain the temperature at 25, 40, 55 and 70 °C. The relative humidity in these chambers was maintained invariant in the range of 85-90%. Plates 3.1 and 3.2 show the chambers used for exposure of specimens at 40, 55 and 70 °C. The specimens were retrieved at predetermined intervals from the chambers for testing.

3.4 EXPERIMENTAL TECHNIQUES

3.4.1 Reinforcement corrosion

Ordinary portland and blended cement reinforced concrete specimens, 200 x 200 x 75 mm, made with two 12 mm bars were used to evaluate the reinforcement corrosion due to salt contamination and temperature. Electrical wires were soldered to the bars, and the wire steel interface was coated with epoxy paint. Part of the bars and their ends were also coated with epoxy paint to prevent crevice corrosion. Rebars were placed in the molds using plastic spacers which provided the bars an overall cover of 37.5 mm. Two bars were used in each specimen to facilitate corrosion measurements. One bar was used as working electrode while the other was used as the counter electrode. The details of the reinforced concrete specimens are shown in plate 3.3 through 3.9.

Reinforcement corrosion was monitored at periodic intervals by measuring corrosion potentials and corrosion current density. The corrosion potentials were measured by connecting the negative terminal of a high impedance voltmeter to the rebar. The positive terminal of the voltmeter was connected to a saturated calomel electrode (SCE) placed on the surface of the concrete specimen. The corrosion current density was measured using a Potentiostat/Galvanostat and linear polarization

resistance method. In this technique the working electrode is polarized by applying a potential of ±10 mV of the corrosion potential against the reference electrode and the resulting current between the working and the counter electrode is measured for each potential increment. The corrosion current density, I_{corr} is then calculated using the following relationship proposed by Stern and Gearey [68].

$$I_{corr} = B / R_p$$

where $$B = \beta_a . \beta_c / (2.3.(\beta_a+\beta_c))$$

β_a and β_c are the anodic and cathodic Tafel constants.

R_p is the slope of the potential current curve.

A typical linear polarization potential current plot obtained using this technique is shown in Fig. 3.2.

The Tafel constants can be determined by polarizing steel to ±250 mV of the rest potential or corrosion potential. In the absence of sufficient data on Tafel constants, a value of 100 mV is normally used for steel in highly resistive media [69]. Gonzalez et al [70] have observed a good correlation between weight-loss determined by gravimetric method and LPRM techniques by using values of B equal to 26 mV for steel in active condition and 52 mV for steel in passive condition. Al-Tayyib et al [71] also observed good relation between weight-loss determined by gravimetric method and LPRM technique. In the present study $\beta_a=\beta_c=120$ mV was used for all the specimens. An Amel Potentiostat/Galvanostat with IR compensation was used to polarize the steel. Plate 3.10 shows the test set up. As scan rate of 0.1 mV/sec was used in all the determinations. A data acquisition system connected to a computer was used to collect and analyze the data.

3.4.2 Chemical Analysis

Ordinary portland and blended cement paste specimens were used to evaluate the effect of salt contamination and temperature on OH^-, Cl^-, SO_4^{--} ion concentrations. After designated exposure periods, these specimens were retrieved from the temperature-humidity chamber and finely crushed to pass ASTM # 100 sieve. Five grams of the crushed powder was mixed with 25 ml of distilled water and the solution stirred using a magnetic stirrer for 30 minutes. The beaker containing the cement slurry was securely sealed to avoid carbonation. After stirring, the solution was stored in an air tight chamber for 24 hours. After this period the cement slurry was filtered through a medium and fine filter paper and the filtrate collected and stored in air tight test tubes. Further, the volume of the filtrate adjusted to 100 ml. This filtrate was analyzed to determine the alkalinity, chloride and sulfate ion concentration.

Alkalinity

To determine alkalinity the cement paste extract was titrated against 0.01 M Nitric acid using phenolphthalein as an indicator. The OH^- ion concentration, by weight of cement was calculated using the volume of the filtrate and weight of cement. The pH of the extract was also calculated from the measured OH^- ion concentration using the following relationship:

$$pH = 14 + \log_{10}[0H^-]$$

where OH^- ion concentration is in Moles/Liter.

Water Soluble Chloride Ion Concentration

The water soluble chloride ion concentration was determined using the spectrophotometric method [72]. 0.2 ml of the cement extract was diluted to 10 ml using de ionized water. To this dilute solution 2 ml of saturated mercuric thyocyanate and 2 ml of 0.25 M ferric ammonium sulfate was added. The solution was lightly

stirred and then kept undisturbed for half an hour. The absorbency of this solution was then measured against de ionized water at a wave length of 460 nm. The chloride concentration of the solution was then evaluated from a calibration curve prepared using a similar procedure. The chloride ion concentration was then calculated as percent by weight of cement.

Water Soluble Sulfate Ion Concentration

The sulfate ion concentration was also measured using the spectrophotometric method [73]. 0.2 ml of the cement paste extract was diluted to 10 ml using de ionized water. To this solution 2 ml of a conditioning agent and approximately 4 to 5 grams of Analar grade barium chloride was added and stirred for 60±15 seconds. After stirring, the solution is placed in the test tube and absorption measured after 5±1/2 minutes against distilled water on a spectrophotometer at a wave length of 420 nm. The sulfate ion concentration of the paste extract is calculated from a calibration curve prepared following a similar procedure. The sulfate ion concentration was also expressed ass percent by weight of cement

3.4.3 Electrical Resistivity

Electrical resistivity measurements were conducted on 75 mm x 150 mm cylindrical concrete specimens(Plate 3.11). Two copper rods were inserted in the specimen 75 mm apart, and fixed with a cement paste of similar water to cementitious material ratio as the parent concrete. The specimens were fixed in a prefabricated steel frame. The fixing plates of this frame are made of copper and are covered with wet cloth, wetted with copper sulfate solution. The copper plate wet cloth combination was used to ensure uniform distribution of current across the cross section of the specimen. Plate 3.12 shows the frame with specimen.

The resistance meter applies a DC. current of known magnitude across the length of the specimen and the potential drop over a known distance of 75 mm for the

specimens used in this study, is measured. The resistance is then displayed by comparing with known built in circuit. The electrical resistivity instrument used was a Hippotronics model D4500 ground resistance meter. This is shown in Plate 3.13 Plate 3.14 shows the experimental set up. The electrical resistivity was calculated using the following relationship

$$\rho = \frac{R\,A}{L}$$

where

ρ= resistivity in Ω.cm.

R = resistance in Ω

A = cross sectional area of the specimen

L = length between the measuring pins

3.4.4 Compressive Strength Measurements

Compressive strength of concrete specimens, in 75 x 150 mm cylinders, (plate 3.15) was determined at an age of 90 days. Initially the specimens were cured for 28 days in the curing chamber at room temperature. After 28 days, they were exposed to designated temperature in the temperature humidity chambers. The specimens were then taken out from exposure chambers and capped with sulfur and tested according to ASTM C 39, using a hydraulically operated digital compression testing machine of ±0.1 kN accuracy. Three cylinders were tested and the average values are reported.

3.4.5 Pore Size Distribution

The effect of temperature on pore size distribution was evaluated by mercury intrusion porosimetry (MIP). The hardened cement paste (HCP) is made up of solids, voids and water. Solids consist of CSH gel, $Ca(OH)_2$, Calcium sulfo aluminate and

unhydrated clinker constitute the solid portion. Voids consist of inter layer space in CSH gel or gel space, irregular shaped capillary voids and regular shaped air voids. Water present in HCP is classified based on ease with which it can be removed, as capillary water, adsorbed water, interlayer water, chemically combined water. The presence of capillary voids will lead to the porosity of the HCP. Porosity is the volume property and represents the contents of the pores which are not necessarily interconnected. Thus porosity is the inherent property which results from the hydration process of cement. Mercury intrusion porosimetry, helium porosimetry and gas adsorption/desorption techniques are some of the widely used techniques for measurement of porosity.

In the Mercury intrusion porosimetry, mercury, a non-wetting liquid is forced into the pores of the material at a high pressure. Pore size and volume quantification are accomplished by submerging the sample under a confined quantity of mercury and then increasing the pressure of the mercury hydraulically. As the applied pressure is increased the radius of the pores which can be filled with mercury decreases and consequently the total amount of mercury intruded increases. The data obtained give the pore volume distribution directly and with the aid of pore physical model, the pore size distribution can be ascertained.

In this study, the pore size distribution of the selected samples was carried out using Carlo Erba Model 2000 high pressure mercury intrusion porosimeter. This is an automatic instrument for the determination of the pore size and pore volume distribution in the range of 3.7 to 7500 nm radius. The operating pressure ranges from 0.1 Mpa to 200 Mpa. According to Wash Burn equation of capillary suction or depression, the radius of the cylindrical pore which will be reached by a pressure p is given by:

$$r_1 = 2\, r \cos\theta / P$$

where r is surface tension, θ is the contact angle. If r and are constant for a certain material, r is inversely proportional to p. In this study a value of r equal to 480 dynes and equal to 141.3° was used. Then r (nm) = 750/p Mpa. This means that pore sizes of 3.75 nm to 7500 nm can be detected.

Representative cement paste specimen, approximately 1 gram, was used for pore size distribution. The pressure in the pressure vessel of the porosimeter was increased from 0.1 to 200 Mpa slowly. This slow increase of pressure prevented the mercury from heating up during the test. The measurements of the pressure and the introduced volume of mercury were recorded and used to draw the pore volume against the radius.

TABLE 3.1 Specimen Description

Test Description	Specimen		
	Type	Size	Number
Reinforcement Corrosion	Concrete	200x200x75 mm	60
Electrical Resistivity	Concrete	75x150 mm	180
Compressive Strength	Concrete	75x150 mm	180
Chemical Analysis	Cement Paste	25x25x25 mm	60
Pore size Distribution	Cement Paste	25x25x25 mm	40

TABLE 3.2 Weights of Constituent Materials per Cubic Meter of Concrete

Constituents	Weight (Kg/ m^3)				
	Ordinary portland Cement	Blast Furnace Slag	Fly Ash Class F	Fly Ash Class C	Silica Fume
Cement	350	105	280	280	315
Pozzolan	----	245	70	70	35
Coarse Aggregate	1159	1159	1159	1159	1159
Fine Aggregate	710	710	710	710	710
Water	175	175	175	175	175

TABLE 3.3 Chemical Composition of Type I Cement and Pozzolanic Materials

Constituents (Wt. %)	Ordinary Portland Cement	Blast Furnace Slag	Fly Ash Class C	Fly Ash Class F	Silica Fume
CaO	64.19	43.70	2.0	0.48	0.50
SiO_2	22.59	35.40	51.30	47.15	92.50
Al_2O_3	4.61	7.80	24.10	45.12	0.40
Fe_2O_3	2.71	0.52	12.60	1.38	0.40
SO_3	2.22	1.13	0.84	0.20	0.50
Na_2O	--	0.39	0.32	0.08	1.10
K_2O	--	0.11	3.06	0.05	0.40
Alkalinity	0.27	0.46	2.33	--	--
C_3S	50.95	--	--	--	--
C_2S	26.33	--	--	--	--
C_3A	7.63	--	--	--	--
C_4AF	8.25	--	--	--	--

TABLE 3.4 Specific Gravity and Absorption of Coarse Aggregates

Sieve	Absorption (%)	Bulk Specific Gravity	Specific Gravity (SSD)	App. Specific Gravity
# 10	2.336	2.53	2.589	2.688
#4	1.785	2.569	2.615	2.693
3/8"	1.414	2.599	2.635	2.698
1/2"	1.10	2.62	2.649	2.697
Overall Grading	4.417	2.596	2.633	2.695

TABLE 3.5 Grading of Coarse Aggregates

Sieve Opening (mm)	Percentage Retained	Cum. Percentage Retained	Percentage Passing
12.5	55	55	45
9.5	5	60	40
4.75	35	95	5
2.36	5	100	0

TABLE 3.6 Specific Gravity and Absorption of Fine Aggregates

Absorption %	Bulk Specific Gravity
0.227	2.70

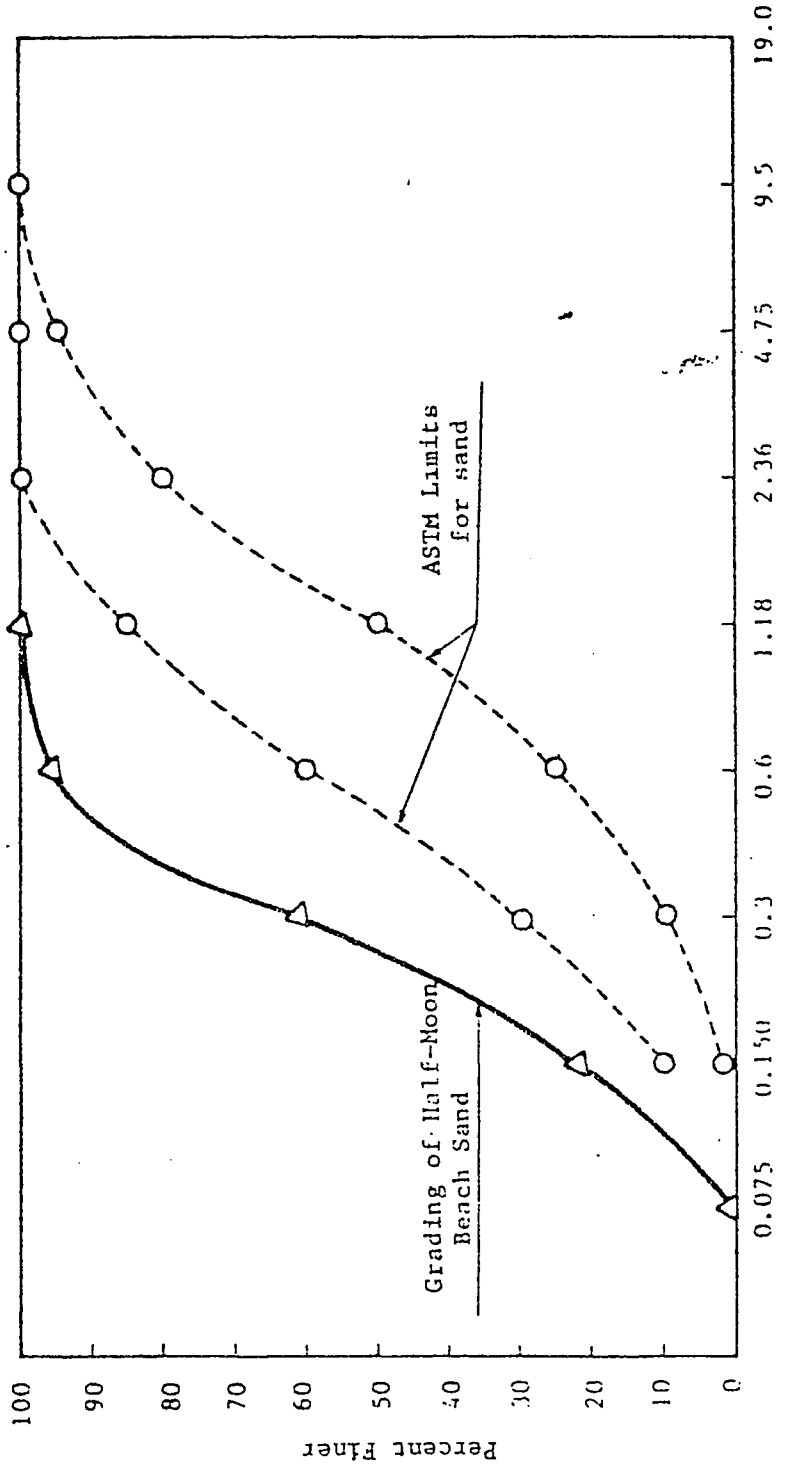

Fig. 3.1 Sieve Analysis of the Fine Aggregate (Sand)

Current mA	Potentials mV	Regression Fit Y=2.2093X−269.59
−5.42	−280.40	−281.57
−2.83	−275.80	−275.84
−1.43	−273.00	−272.74
0.03	−270.10	−269.53
1.32	−267.30	−266.67
2.57	−264.50	−263.92
3.72	−261.90	−261.37
4.77	−259.30	−259.06
5.77	−256.70	−256.83
6.76	−254.10	−254.65
7.73	−251.60	−252.51

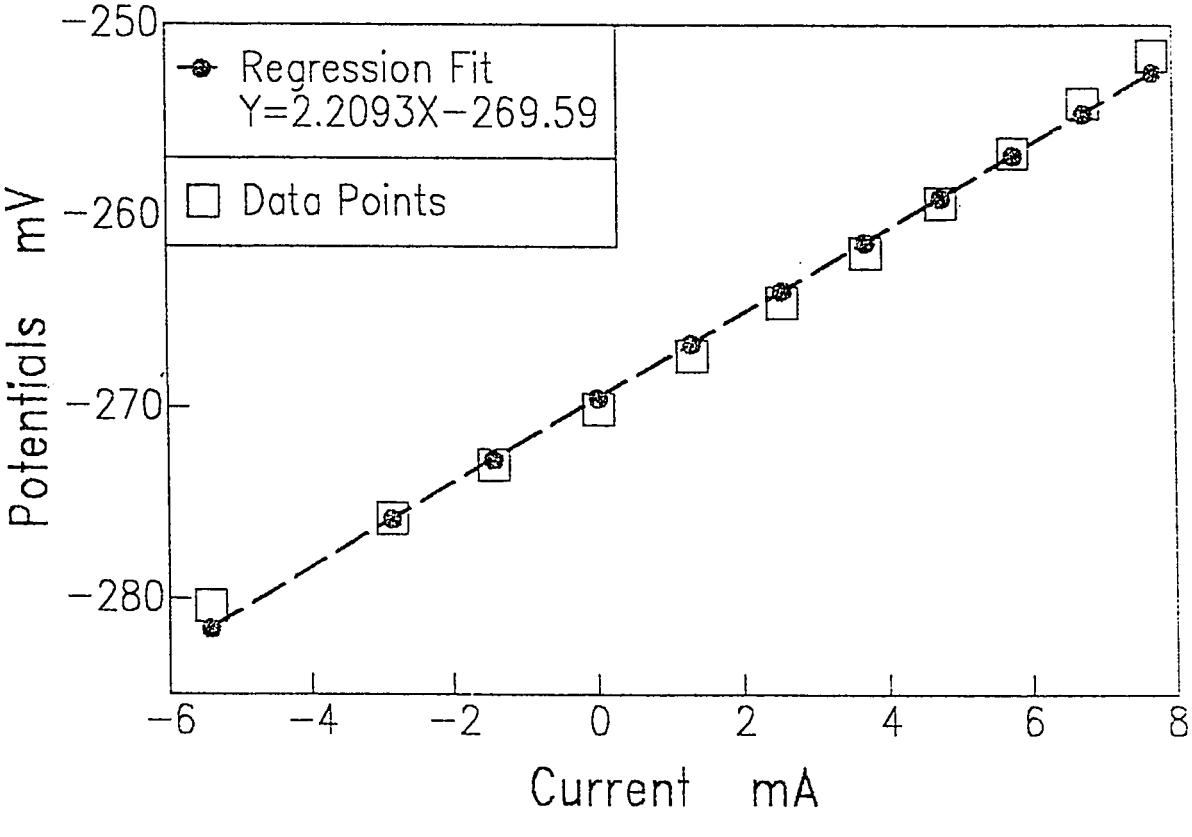

Fig. 3.2 A Typical Linear Polarization Plot

Plate 3.1 Temperature and Humidity Chambers used for Exposure of Specimens at 40 and 55 °C

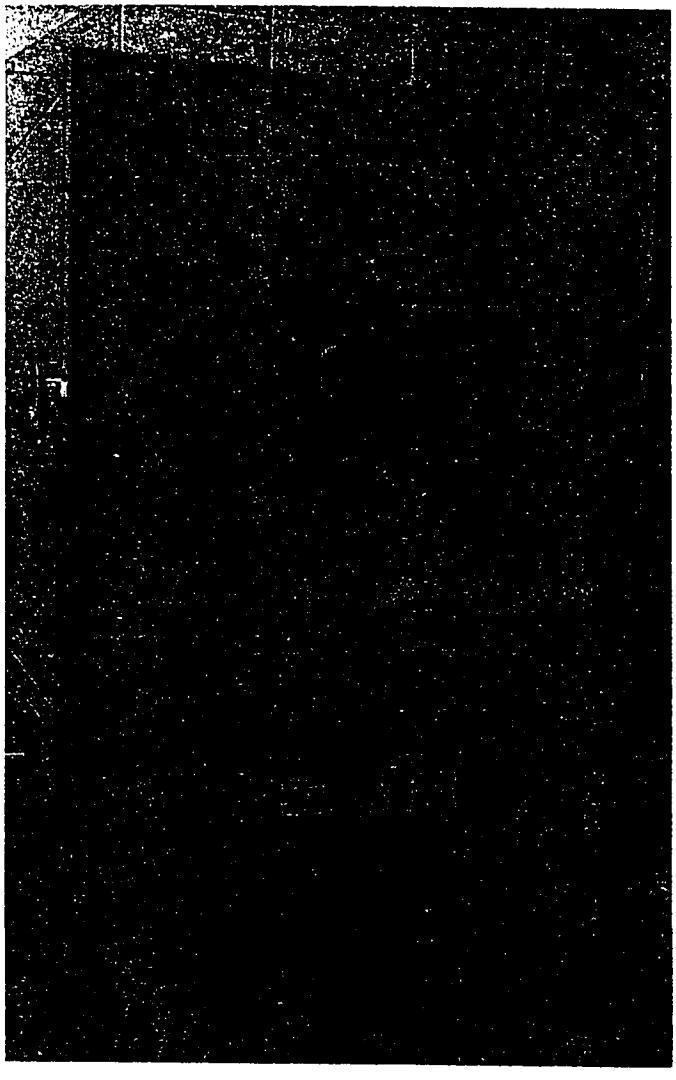

Plate 3.2 Temperature and Humidity Chamber used for Exposure of Specimens at 70 °C

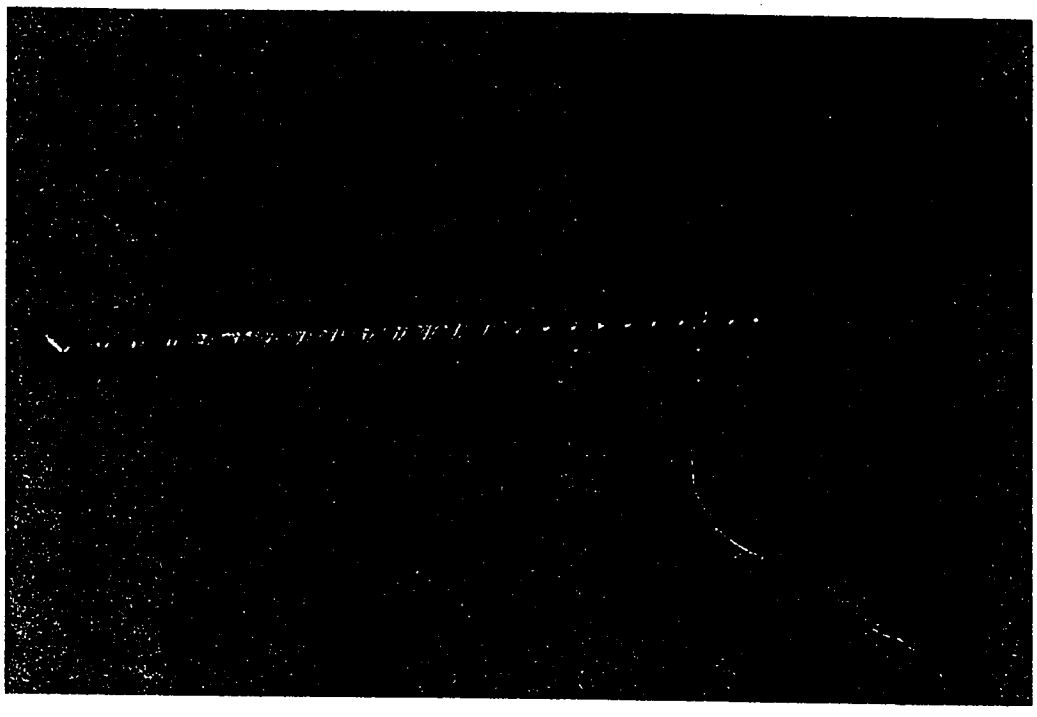

Plate 3.3 Rebar used for Corrosion Monitoring in Concrete

Plate 3.4 Rebar with Spacers

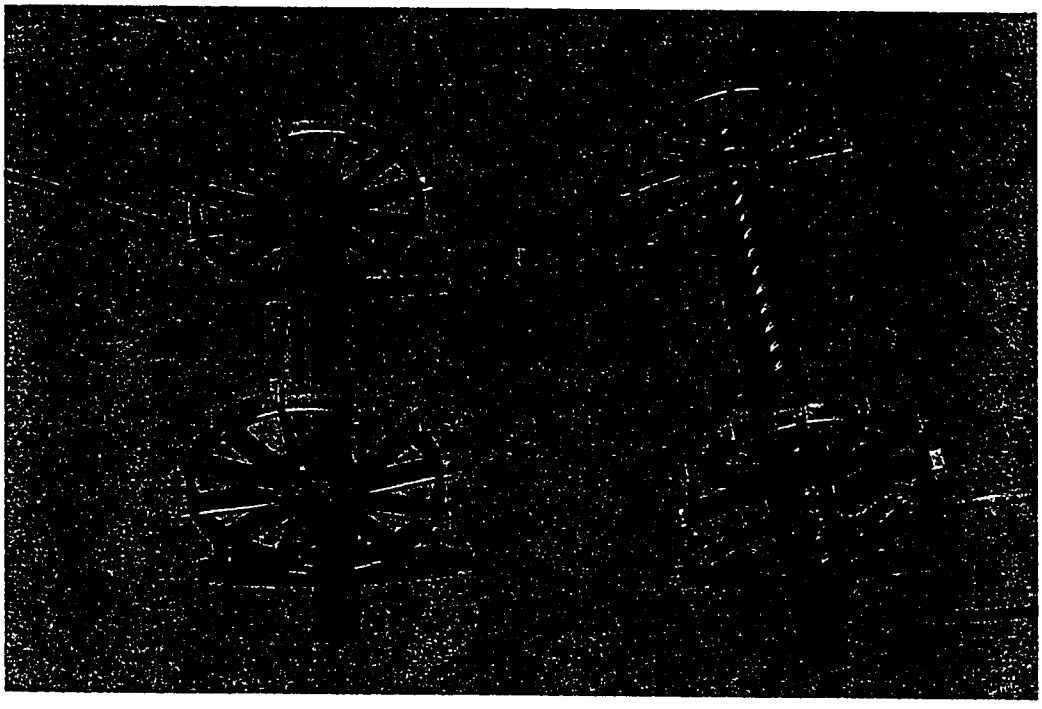

Plate 3.5 Rebars with Spacers

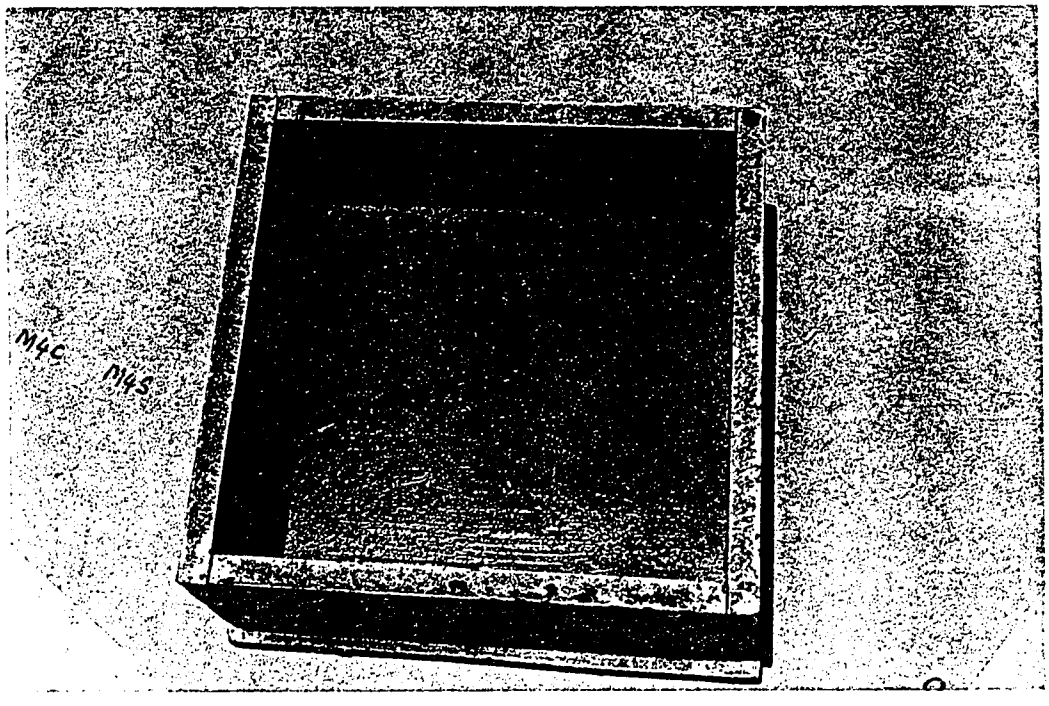

Plate 3.6 Mold used for Preparation of Corrosion Specimens

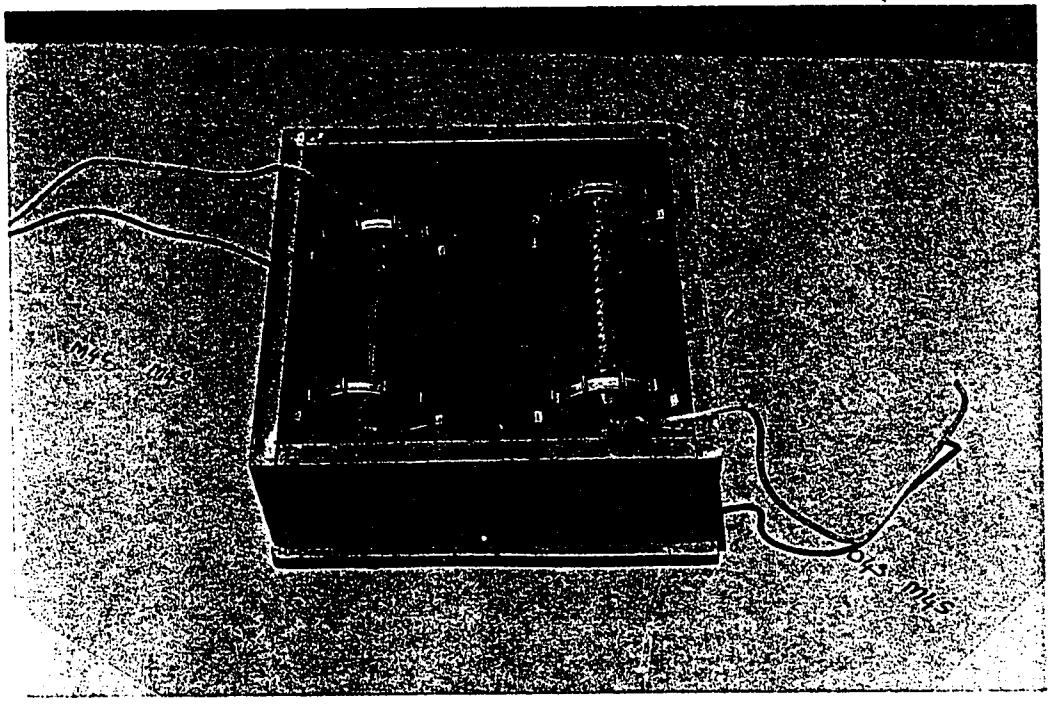

Plate 3.7 Mold with Rebars

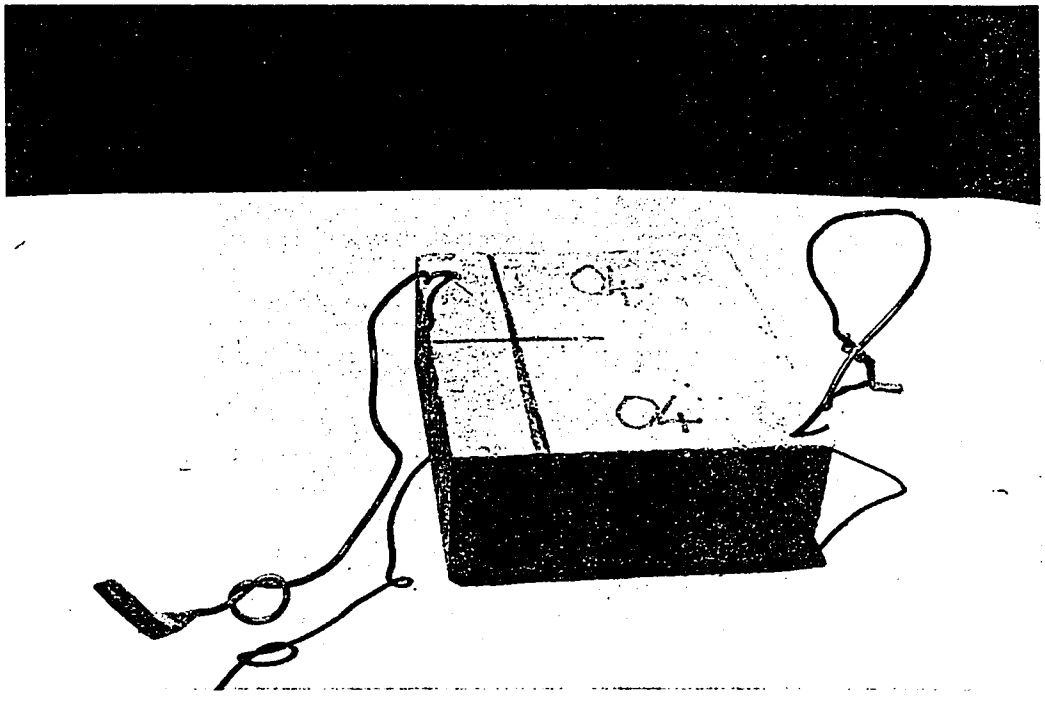

Plate 3.8 Reinforced Concrete Corrosion Specimen used for Corrosion Monitoring

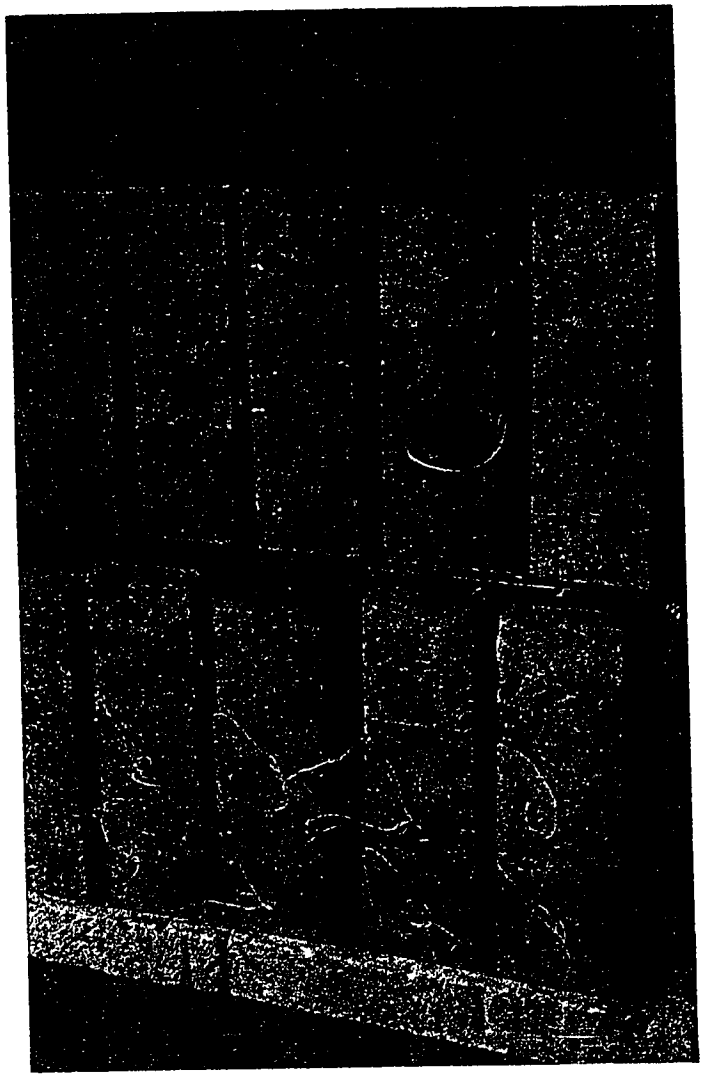

Plate 3.9 Some of the Concrete Samples Used for Corrosion Monitoring

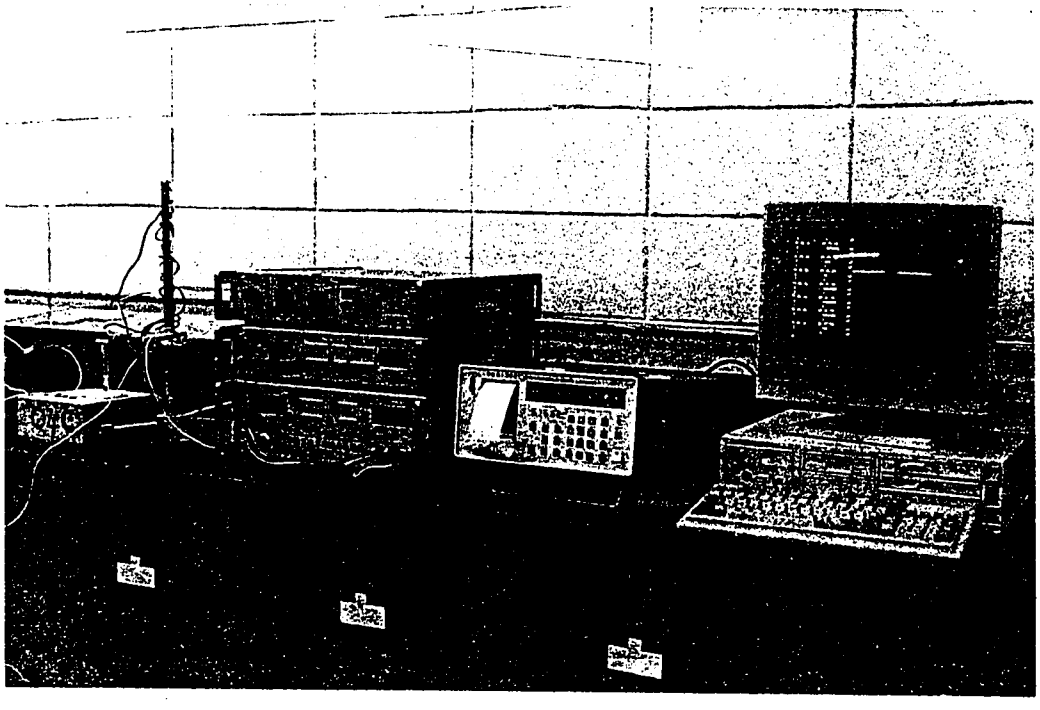

Plate 3.10 Test Setup for Corrosion Monitoring

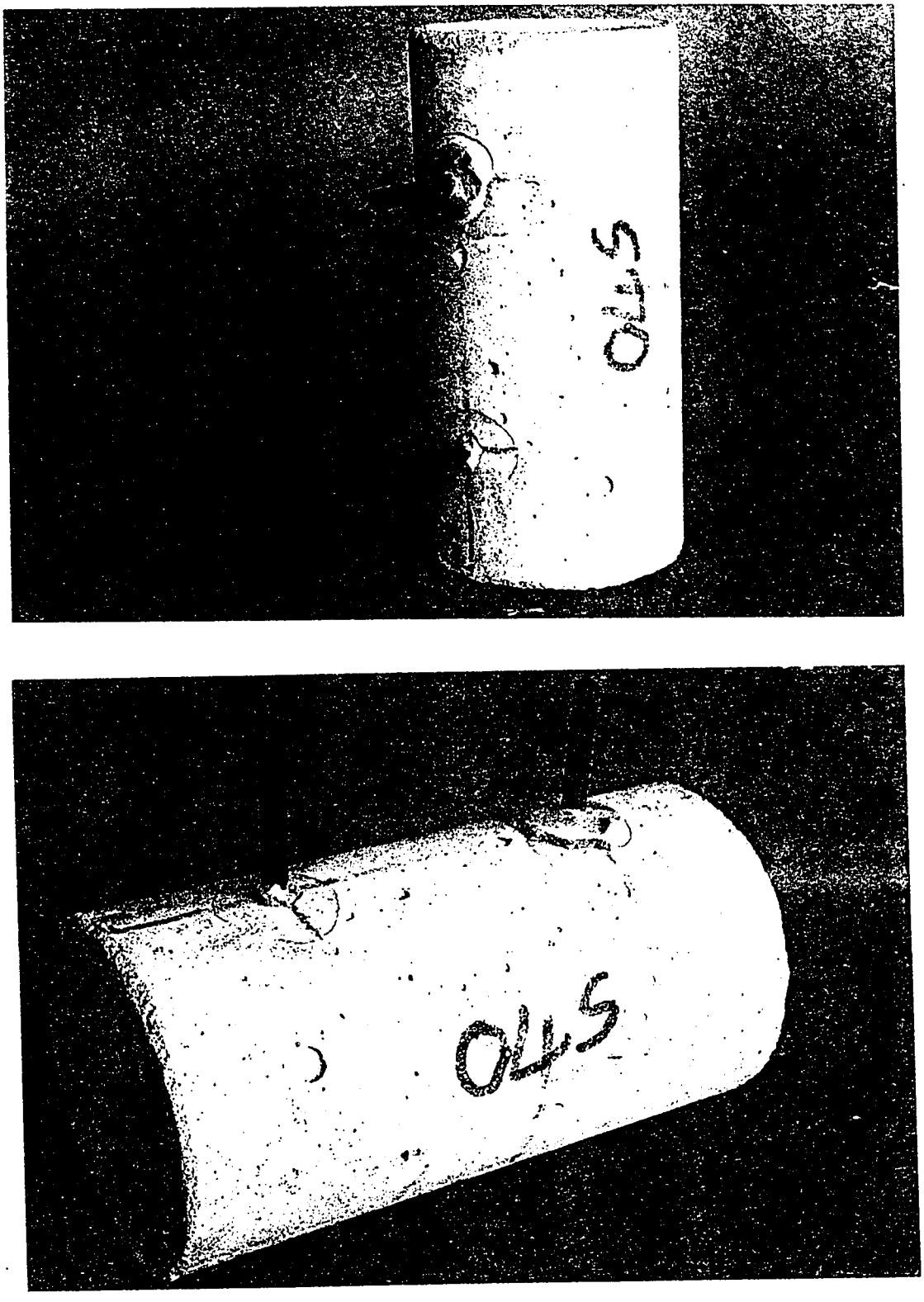

Plate 3.11 Concrete Specimen used for Electrical Resistivity Measurement

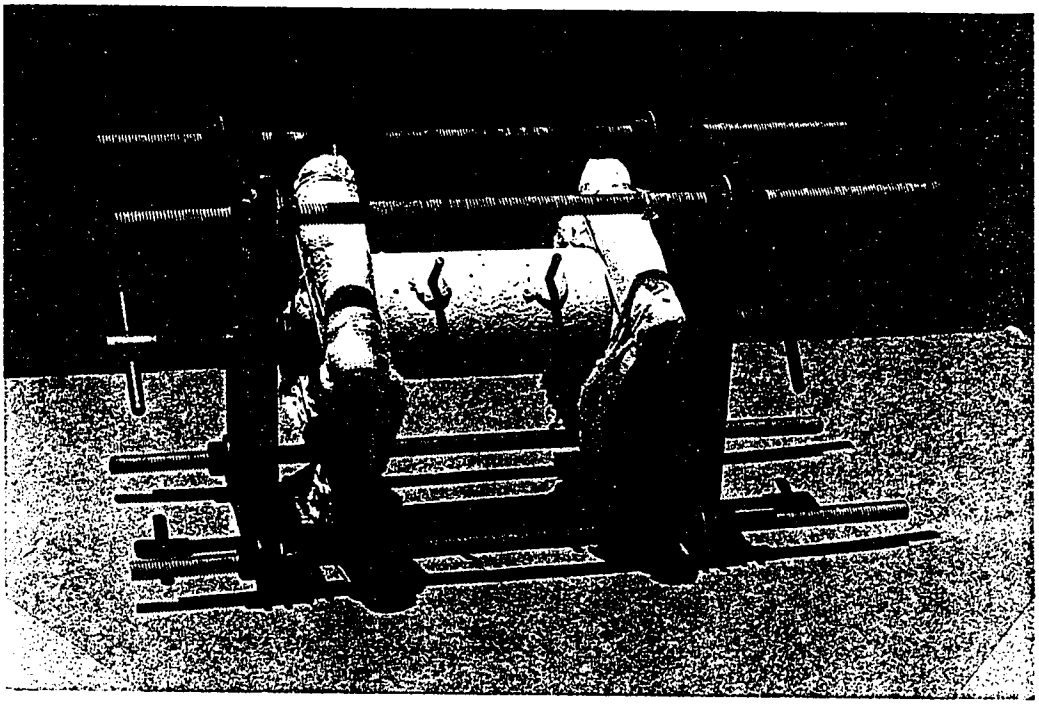

Plate 3.12 Prefabricated Frame with Specimen used for Electrical Resistivity Measurements

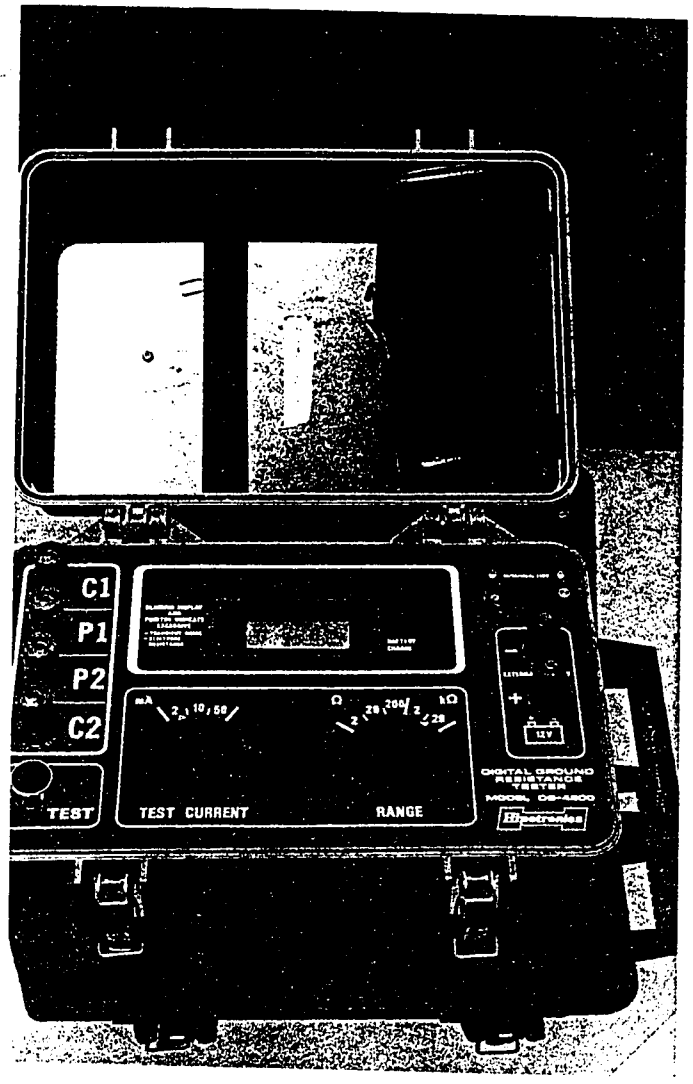

Plate 3.13 Hippotronics Model 2000 Ground Resistance Meter

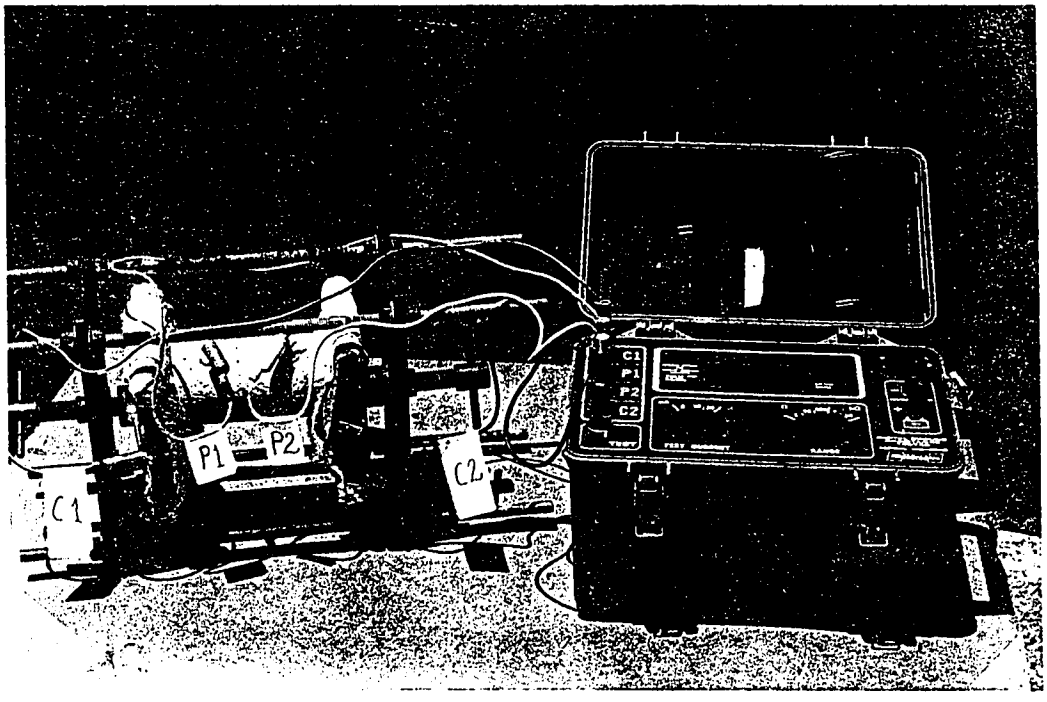

Plate 3.14 Experimental Setup used for Electrical Resistivity Measurements

Plate 3.15 Some of the Concrete Specimens used for Compressive Strength

CHAPTER 4

RESULTS AND DISCUSSIONS

4.1 EFFECT OF TEMPERATURE AND SALT CONTAMINATION ON COMPRESSIVE STRENGTH OF PLAIN AND BLENDED CEMENTS

The compressive strength of contaminated and uncontaminated OPC, BFS, SF and Class C and Class F fly ash concrete specimens exposed to 25 to 70 °C are presented in Fig. 4.1 through 4.5. The compressive strength was found to decrease with an increase in the exposure temperature in both plain and blended cements. Fig. 4.1 shows the effect of temperature on the compressive strength of OPC concrete specimens. Further, an increase in temperature showed a reduction in the compressive strength in both contaminated and uncontaminated specimens. The compressive strength of contaminated specimens was lower than that of the uncontaminated specimens.

Chloride bearing concretes showed a negligible reduction in strength compared to the uncontaminated concretes at 25 °C . The reduction in strength was on an average about 9.7% at all temperatures, with a maximum of 28.63% at 40 °C. Addition of chloride and sulfate salts reduces the strength at all levels of exposure temperatures. An average of 15.2% strength reduction was observed in sulfate-chloride bearing concrete over plain concrete. The reduction in compressive strength of concrete at various curing or exposure temperatures in OPC without any contamination was reported by many researchers[74-78].

As a conclusion to their review of the rates and mechanisms of the hydration of C_3S and C_2S at 5°, 25° and 50 °C, Braunauer and Kantro [74] indicated that in the early stages of hydration, both the reactions have normal temperature coefficients. This indicates that the rate determining step is a chemical reaction, diffusion takes over the control of the rate when the gel coating around the hydrating cement particle is so thick that the diffusion of water through it is slower than the slowest step in the chemical

reaction. The experimental data [74] indicated that the composition of the CSH gel varies with temperature. The gel coating formed at higher temperatures appears to be less pervious than the one at lower temperatures. This is in good agreement with earlier observations [75,76] . Concrete strength increased with increase in the initial and curing temperatures of the concrete. At later ages, however the specimens cast and cured at higher temperatures had lower strengths than those made and cured at lower temperatures. Verbeck and Helmuth [77] also showed that uniform distribution of the gel provides optimum strength, whereas the strength is reduced due to non-uniform distribution caused by the higher initial rate of hydration at higher temperatures. Collepardi [78] reported that cement pastes hydrated at 40°, 60° and 90 °C were morphologically similar to those at room temperatures.

The reduction in compressive strength of concrete specimens at elevated temperatures in the present study may be attributed to:

(i) the difference in coefficient of linear expansion of aggregates and hardened cement paste,

(ii) the diffusion of moisture from concrete and dehydration of mineral components of hardened cement paste. This diffusion of moisture from concrete creates integrative volume deformations thus decreasing the compressive strength of the concrete [79], and

(iii) at elevated temperatures, cement hydration proceeds more rapidly, because of their low solubility and diffusiblity, and hence hydration products cannot diffuse to significant distance from the cement grain in the time allowed by rapid hydration. This results in a non-uniform distribution of the hydration products and corresponding reduction in strength [77]. This view was supported by Skalny and Odler [80] Who found that elevated curing temperatures cause a coarsening of the

hydration products.

The reduction of strength due to chloride addition at all temperatures may be attributed due to the leaching of gypsum and calcium sulphoaluminate. Gypsum, which is an admixture, and calcium sulphoaluminate, which is the product of hydration of cement, are more soluble in chloride solution and are thus leached out leading to strength reduction [96,98].

The reduction of strength due to addition of chloride and sulfate salts is mainly attributable to the sulfate attack phenomenon as described in Section 2.2.1. The sulfates added will react with AF_m or monosulfate phase, resulting in the formation of ettringite, which is expansive in nature and causes the reduction of strength [8,17,41].

Fig. 4.2 shows the effect of temperature on the strength in BFS cement concrete specimens. These data also indicate a decrease in strength with increasing in temperature. However, due to addition of chlorides, strength enhancement was observed in BFS cement concrete specimens. The sulfate-chloride bearing specimens indicated lower compressive strength than that of the chloride bearing concrete specimens. However the compressive strength of these specimens was higher than that of uncontaminated concrete specimens. The compressive strength of concrete specimens exposed at 70 °C was 43% of those exposed at 25 °C. At 70 °C, chloride contaminated and chloride-sulfate contaminated specimens showed around 42% reduction in strength.

The compressive strength of BFS cement concrete specimens was less than that of OPC concrete specimens at all temperatures and at all contamination levels. Similar results have been reported by Chern and Chan [81]. According to them, the reduction in strength in 70% BFS cement concrete when compared to OPC is due to inadequate supply of reactive materials, which reacts together and forms secondary CSH gel, which reduces the pores and increases the strength. It is also reported that alkali

hydroxides needed for the pozzolanic reaction of slag has greater solubility with increasing temperature, therefore it promotes the early reactions of slag and results in higher early strengths.

As seen in the Fig. 4.2, concrete specimens exposed at lower temperature indicated higher ultimate compressive strength. This is may be attributed to the fact that with low temperature curing, the micro structure will be more uniform which accounts for higher ultimate strength. Hwang and Lin [82] reported that the strength of BFS cement concrete specimens cured at 80 °C was lower than that cured at 50 °C.

The increase in strength of BFS cement concrete specimens with chloride addition is attributable to lower amount of ettringite and higher rate of hydration [103]. These results are in good agreement with those reported by Tashrio and Yoshimoto [103] at 25 °C . They also observed that Na_2SO_4 addition reduced the rate of hydration, increased the ettringite formation thus reducing the strength than chloride addition only.

Fig. 4.3 shows the effect of temperature on the compressive strength of silica fume cement concrete specimens, with and without contamination. These data also show a trend similar to that indicated by BFS cement concrete specimens. Chloride addition enhances the compressive strength where as sulfate-chloride addition reduces the compressive strength. The strength results of non-contaminated concrete specimens are in good agreement with the data reported by Yamato et al [83]. They observed a reduction in strength for 20% and 30% of silica fume blended cement concrete when exposed to 30 °C.

Fig. 4.4 shows the effect of temperature on the compressive strength of Class F fly ash cement concrete specimens made with and without salt contamination. These data also show a trend similar to that indicated by other blended cements. Incorporation of sulfate and chlorides reduced the strength at all temperatures. About 19%, to 35% reduction was observed in specimens exposed to 70 °C as compared to those exposed

to 25 °C. These values are lower than in the Class C fly ash cement concrete specimens (Fig. 4.5). This may be attributed to the differences in chemical composition, mainly the CaO content, of these two fly ashes.

The effect of temperature on the compressive strength reduction in uncontaminated fly ash concrete specimens observed in the present study are in good agreement with that reported by Ravina [84]. While working on fly ash concrete under hot weather, with temperatures in the range of 20 °C to 40 °C, he reported that the increase in temperature reduces the strength. The enhancement of strength in fly ash concrete over plain concrete at higher temperature may be attributed to higher quantum of $Ca(OH)_2$ liberated which results in formation of more secondary CSH gel.

The decrease in strength of OPC, fly ash and silica fume concretes specimens with the addition of chloride and chloride-sulfate at room temperature has also been reported by Hughes [85]. He observed a decrease in the strength in OPC mortars, which were immersed in sodium sulfate solution and magnesium chloride solutions. This reduction in strength was correlated to the expansion due to sulfate attack. The Na_2SO_4 addition as contamination in concrete produces a conversion of $Ca(OH)_2$ to NaOH; thus making the pore water as a saturated solution with pH of 10.5 . At this low pH, CSH gel is unstable and loss of strength may be expected. Inclusion of pozzolanic materials in concrete modifies the hydration process, such that CSH exhibits a lower Ca/Si ratio compared to neat OPC concrete [85].

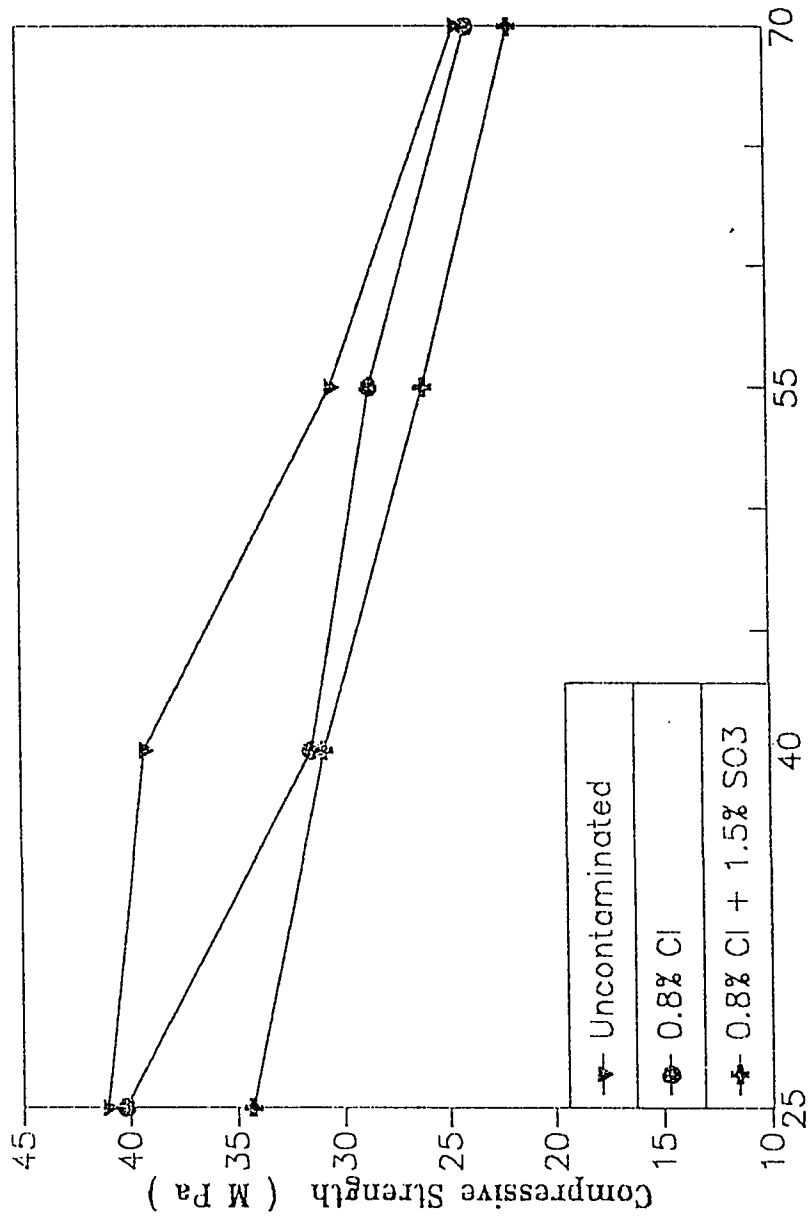

Fig. 4.1 Effect of Temperature on the Compressive Strength of Contaminated and Uncontaminated OPC Concrete Specimens

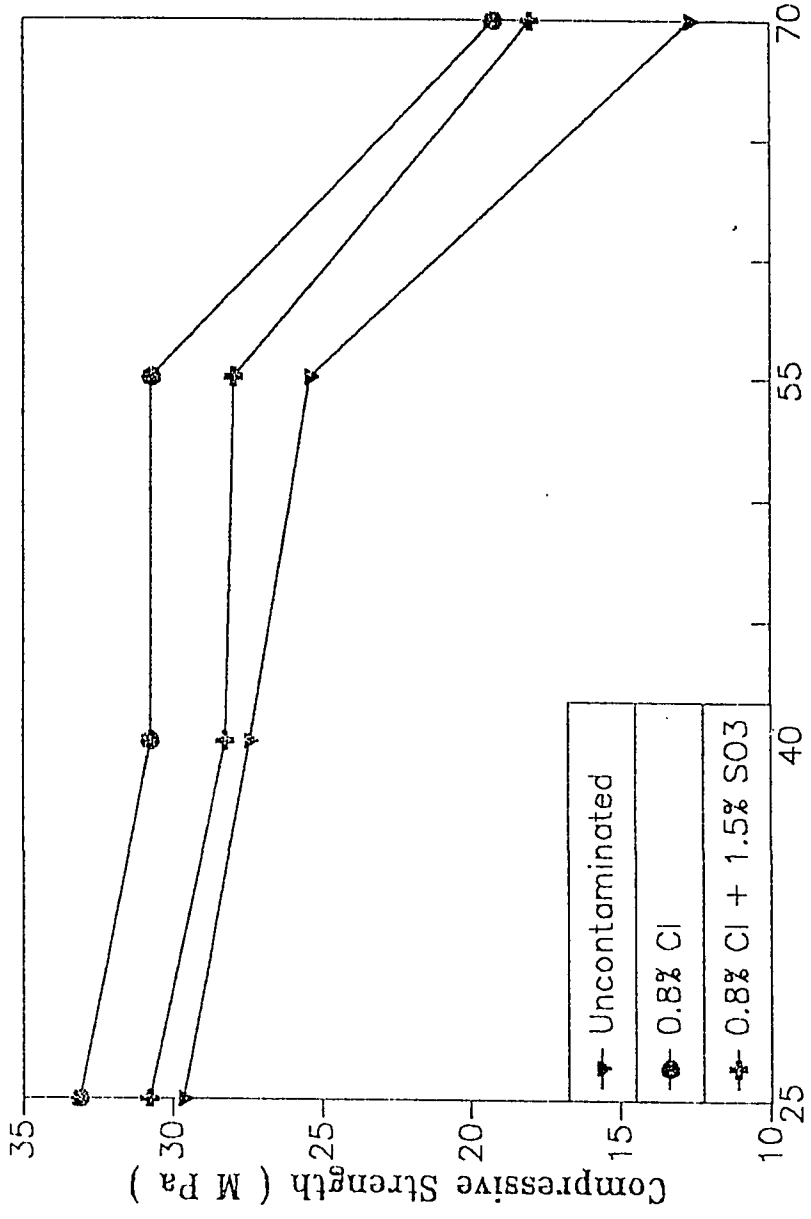

Fig. 4.2 Effect of Temperature on the Compressive Strength of Contaminated and Uncontaminated BFS Cement Concrete Specimens

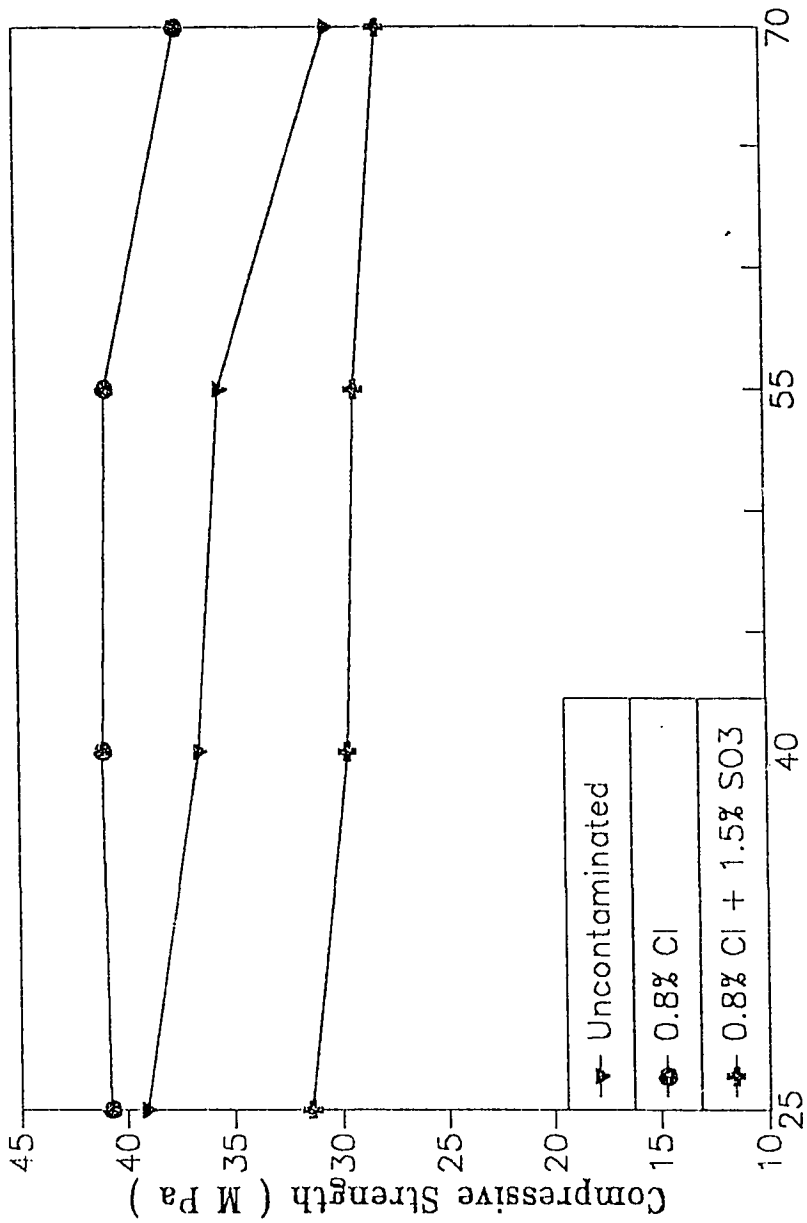

Fig. 4.3 Effect of Temperature on the Compressive Strength of Contaminated and Uncontaminated SF Cement Concrete Specimens

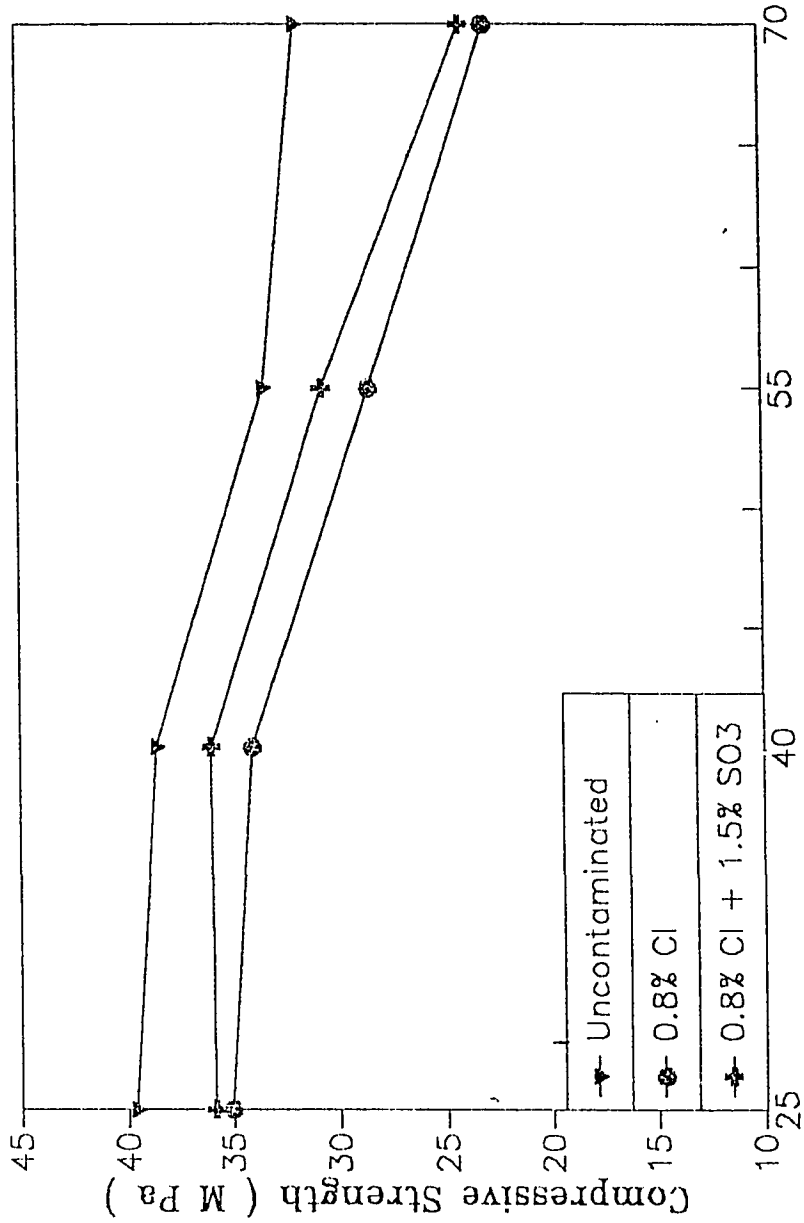

Fig. 4.4 Effect of Temperature on the Compressive Strength of Contaminated and Uncontaminated Class F FA Cement Concrete Specimens

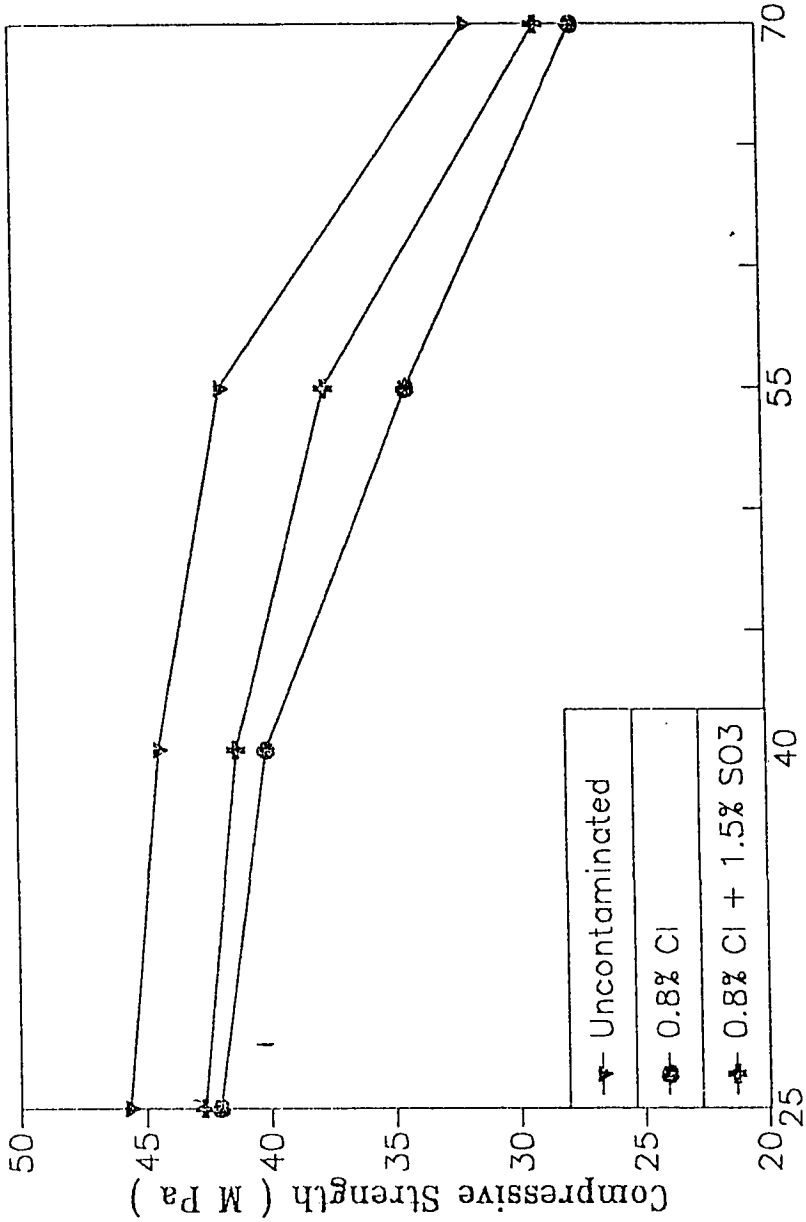

Fig. 4.5 Effect of Temperature on the Compressive Strength of Contaminated and Uncontaminated Class C FA Cement Concrete Specimens

4.2 EFFECT OF TEMPERATURE AND SALT CONTAMINATION ON PORE SIZE DISTRIBUTION IN ORDINARY PORTLAND AND BLENDED CEMENTS

The effect of temperature and salt contamination on the pore size distribution in plain and blended cement paste specimens is shown in Fig. 4.6 through 4.15. An increase in the pore volume was observed in all the cements, both with and without salt contamination, with increasing exposure temperature. The increase in the pore volume was particularly significant in smaller pores. The pore size distribution in the contaminated cement paste specimens was not similar to that in the non contaminated cement specimens. The effect of the two parameters, namely temperature and salt contamination on the pore size distribution, in each of the cements investigated is discussed in the following paragraphs.

Fig. 4.6 and 4.7 show the pore size distribution in the uncontaminated and chloride-sulfate contaminated ordinary portland cement paste specimens, respectively. The cumulative pore volume increased with increasing exposure temperature. The increase in pore volume at elevated temperatures was reported by Verbeck and Helmuth [77]. They stated that at low temperatures the hydration product has sufficient time to diffuse throughout the cement paste matrix and precipitates uniformly. However, at higher temperatures the rate of reaction is much faster than the rate of diffusion, due to which the hydration product remains near the cement grains, leaving the interstitial space relatively open. The increase in the total pore volume as the exposure temperature was raised from 55 to 70 °C was negligible. The total pore volume at 25, 40, 55 and 70 °C was 61.63, 123.83, 184.12, and 179.61 mm^3/g respectively. The results also show that the temperature has a greater effect on the finer pores, in that the effect of temperature seems to be negligible on pore sizes greater than 10^4 Å. These results are in good agreement with the data reported by Mangat and El-Khatib [86]. They reported that higher temperature of curing has a detrimental effect on the pore volume of silica fume

blended cement paste specimens. Knut et al [87] studied pore structure of plain cement pastes hydrated at 5, 20 and 50 °C, using mercury intrusion porosimetry (MIP) and back scattered electron microscopy. They observed that an increase in the curing temperature resulted in increased porosity, particularly for pore radius in the range of 200-1000 Å. They compared these results with back scattered electron images and found that increase in temperature resulted in increased porosity particularly for the pores of the radius 2500-12,500 Å. They attributed this difference to the ink bottle effect inherent in the mercury intrusion porosimetry technique. Sleeved [88] also found that steam curing (97 °C) resulted in a coarser pore structure. Goo and [89] found that total porosity of the pastes hydrated at 60 °C was greater than that of pastes hydrated at 27 °C. They attribute this difference in porosity of cement pastes largely due to the difference in volume of pores of radius 750-2300 Å.

Villadsen [90] used low temperature colorimeter as an indirect measure of porosity for cement pastes cured at different temperatures. As the curing temperature increased the amount of pore water frozen at -4 °C also increased, again indicating the coarser pore structure due to elevated curing temperatures. Marsh et al [91] found that for plain cement pastes elevated curing temperatures resulted in increased permeability. This result also indicates the formation of larger pores at elevated temperatures and has significant implication on the concrete durability. Mehta and Manmohan [92] propose a pore diameter of 1000 Å as measured by IMP as a somewhat arbitrary dividing point between large pores which contribute most to permeability, and "small" pores which are much less significant.

Fig. 4.7 shows the effect of temperature on pore size distribution in the ordinary portland cement paste specimens contaminated with chloride and sulfate salts. The presence of salts increased the cumulative pore volume as compared to uncontaminated specimens. The cumulative pore volume in the contaminated paste specimens exposed to 25, 40, 55 and 70 °C was 79.81, 154.22, 152.85 and 207.53 mm^3/g, respectively.

The pore volume at 1000 $\mathring{A}$ was higher in specimens cured at 55 and 70 °C where as pore volume at this radius in specimens exposed to 25 and 40 °C was not that different.

No data are available on the effect of temperature and salt contamination on the pore size distribution. However, it was observed that [93] concentrated solutions altered the physical structure of the hardened cement paste by lowering the evaporable water content due to osmotic pressure with a concomitant increase in strength, and additionally by chemical change in which the calcium chloro aluminate hydrate C_3A $CaCl_2$ .10 H_2O is formed.

Richartz [94] reported that during the hydration of portland cement in the presence of chlorides, ettringite is always formed first, until all the gypsum is used up. Then the calcium mono chloro aluminate is formed. Regourd et al [95] found that when chloride ions penetrate hardened cement paste the initially fibrous CSH gel is changed to a reticulated morphology. Midglay and Illston [96] found that penetrating chloride ions reduces the permeability, thus reducing the smaller pores. They concluded that either the chlorides are reacting to form extra material such as $CaCl_2$ or the surface binding of chloride ions on to the CSH surface fill in the pores. It is also possible that chloride affects the rate of formation of CSH or its morphology to reduce the inter-solid pores. Finally, they suggested from experimental studies that the reduction in pore size is due to the formation of $CaCl_2$ on the surface of the CSH gel.

Fig. 4.8 shows the effect of temperature on the pore size distribution in silica fume blended cement paste specimens. The cumulative pore volume was observed to increase with increasing temperature. Further, at 70 °C exposure, the pore structure was finer than the specimens exposed to other temperatures. The cumulative pore volume for exposure temperatures of 70, 55, 40 and 25 °C was 200.38, 147.14, 119 and 88 mm^3/g, respectively. The effect of temperature, up to 55 °C, was not significant on the pore volume for pore radii above 1000 $\mathring{A}$. The relationship between pore radius

and pore volume for pore radius of 1000 Å and below is influenced by the exposure temperature. This indicates that silica fume cement paste specimens may have large number of coarser pores, particularly at higher temperatures. This is shown in the Plates 4.1 and 4.2. Plate 4.1 shows the silica fume and OPC specimens at 70°C with no contamination. Plate 4.2 shows the silica fume and OPC specimens exposed at 70 °C with chloride-sulfate contamination. In both cases silica fume cement specimens show a more open structure compared to OPC paste specimens.

These results are in good agreement with those reported by Mangat and El-Khatib [86]. They concluded that higher temperature of curing has a detrimental effect on the pore volume of silica fume cement paste specimens. Reinhardt and Gaber [97] also showed that at ordinary temperatures, silica fume blended cements have a greater tendency to form coarser pores.

The higher pore volume observed in silica fume cements may also be related to the measuring technique used. The pore structure in blended cements is sensitive to the pressure applied in the mercury intrusion porosimetry. It has been observed that porosity values of blended cements determined by MIP were greater than those obtained by helium and methanol pycnometry. The increase in pore volume was attributed to the destruction of the pore structure by the high differential pressures of the mercury during intrusion.

Fig. 4.9 shows the effect of temperature on the pore size distribution in sulfate-chloride bearing silica fume blended cement paste specimens. The pore structure of specimens exposed to 55 and 70 °C was coarser than those cured at 25 and 40 °C.

Fig. 4.10 shows the effect of temperature on the pore size distribution in the uncontaminated blast furnace slag cements. The cumulative pore volume for specimens exposed to 25, 40, 55 and 70 °C was 43.30, 70.91, 99.0 and 100.81 mm^3/g respectively, indicating a denser pore structure compared to ordinary portland cement

paste specimens. The pore structure, however, is much finer than that of OPC paste specimens. BFS cement paste specimens exposed to 70 °C exhibited a much finer pore structure as compared to those exposed to other temperatures.

A similar trend was observed [86] for 40% BFS cement specimens exposed to 45 °C and 20 °C. The intruded pore volume was 32% less in air-cured BFS cement compared to plain cement. The results at 25 °C are in good agreement with the data reported by Page et al [98], who indicated that addition of BFS reduced the cumulative pore volume. It was also observed that, at room temperature [97], BFS cement is known to have a finer pore structure when properly cured, whereas a coarser pore structure results when it is not properly cured.

The pore size distribution curves for BFS cement paste specimens contaminated with chloride and sulfate ions and exposed to temperatures in the range of 25 to 70 °C are shown in Fig. 4.11. These curves indicate a very negligible effect of temperature on the pore size distribution and cumulative pore volume in these specimens. The cumulative pore volume was 161.54, 162.03, 185.8 and 195.6 mm^3/g for exposure temperatures of 25, 40, 55 and 70 °C, respectively. Further, all the specimens exhibited a very fine pore structure. The reasons for the production of a very fine structure even at lower temperatures of 25 to 40 °C need further elucidation.

Fig. 4.12 and 4.13 show the effect of temperature and chloride-sulfate contamination on pore size distribution in fly ash cement paste specimens. The pore size distribution in uncontaminated specimens exposed to 40 °C was more or less similar to those exposed to 25 °C. However, when the exposure temperature was raised to 55 °C, a distinct change in the pore structure was observed. The cumulative pore volume in specimens exposed to 25, 40, 55 and 70 °C was 79.36, 94.35, 176.82 and 220.45 mm^3/g, respectively.

Addition of chloride and sulfate ions to fly ash cement paste specimens reduced the

pore size and altered the pore structure, particularly in specimens exposed to 25 and 40 °C. There was pore refinement in the contaminated fly ash cement paste specimens. Up to 800 Å radii, there was no appreciable change in coarser pore structure at 25, 40, and 55 °C. Beyond 55 °C, large pores, and higher pore volumes were observed. The cumulative pore volume was 175, 160, 99 and 48 mm^3/g, respectively, for specimens exposed to 70, 55, 40 and 25 °C.

The pore size distribution curves for Class C fly ash also exhibited a trend similar to that observed in Class F fly ash in uncontaminated pastes (Fig. 4.14), but the contaminated specimens showed a different situation (Fig. 4.15).

No appreciable change in coarser pore size up to 800 nm radii was observed for temperatures of less than 40 °C. However, for temperatures of 55 and 70 °C, a much finer pore structure and higher cumulative pore volume was indicated. Also, the pore volume intruded, at lower radii, was similar to or slightly lower than that in specimens exposed to 70 °C. The conversion of the bigger pores to a finer structure, due to pozzolanic reaction in blended cements have been reported by several investigators at lower temperatures [91 to 96, 99]. The increase in finer pore structure in fly ash cement paste specimens with increase in temperature is mainly attributable to the reduction in $Ca(OH)_2$ content and degree of C_3S hydration. This has been shown in the Fig. 4.16 and 4.17.

4.3 EFFECT OF TEMPERATURE AND SALT CONTAMINATION ON THE ELECTRICAL RESISTIVITY OF ORDINARY PORTLAND AND BLENDED CEMENT CONCRETES

Fig. 4.18 to 4.22 show the effect of temperature and salt contamination on the electrical resistivity (ER) of plain and blended cement concrete specimens. The electrical resistivity in all the cements investigated was observed to increase with increasing exposure temperature. The electrical resistivity, in contaminated specimens was, however, lower than that in the uncontaminated specimens at all the exposure

temperatures. The electrical resistivity in specimens contaminated with chloride and sulfate salts was lower than those contaminated with only chloride salts.

Fig. 4.18 shows the electrical resistivity in plain cement concrete specimens exposed to temperatures in the range of 25 to 70 °C. The electrical resistivity in both uncontaminated and contaminated specimens was observed to increase with increasing temperature. However, the increase in the resistivity when the temperature was raised to 70 °C was very significant. The electrical resistivity at 70 °C was 17.3, 25 and 4.5 times that at 25 °C in the uncontaminated, chloride contaminated and chloride-sulfate contaminated concrete specimens. The electrical resistivity, was, however, observed to decrease with chloride and chloride-sulfate contamination. At 70 °C, the electrical resistivity of uncontaminated concrete specimens was approximately 1.5 times that of chloride contaminated specimens. The electrical resistivity of specimens contaminated with chloride-sulfate was 1/6 of that in uncontaminated specimens.

The electrical resistivity of concrete is important from reinforcement corrosion point of view, since it controls the flow of corrosion current from the anode to the cathode and vice versa. The decrease in the electrical resistivity due to chloride and chloride-sulfate salts indicates the risk of corrosion in underground structures. In contaminated specimens, ions such as Na^{+}, K^{+}, Ca^{++} Cl^{-}, OH^{-}, SO_4^{--} etc. contribute to the conductance of current. The conductivity of course is also a function of the moisture content of concrete. The increase in electrical resistivity due to increase in temperature, therefore, may be attributed to the decrease in the moisture content in concrete. A drastic increase in the electrical resistivity at 70 °C indicates a drastic reduction in the moisture content. Similar results projecting the drastic reduction in the electrical resistivity in dry concrete has been reported by several investigators [100-102].

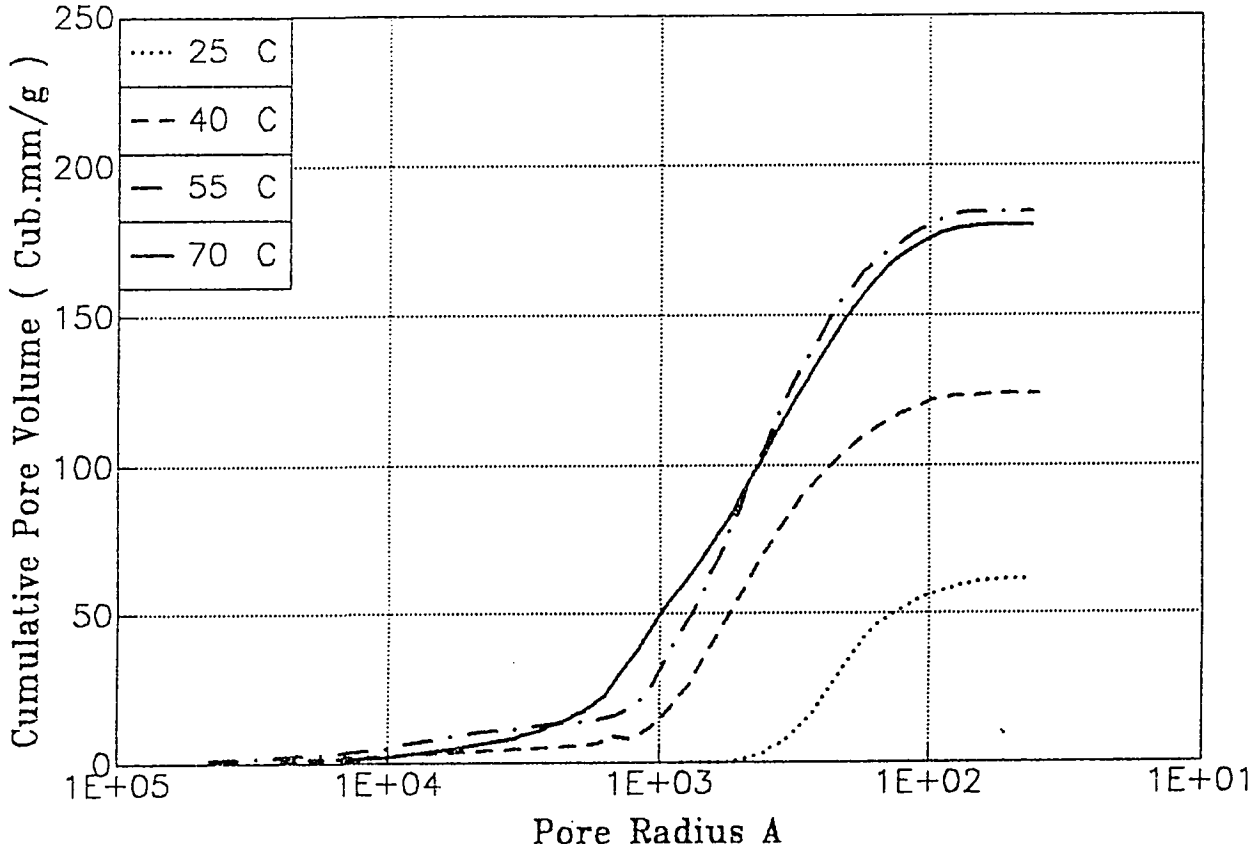

Fig. 4.6 Effect of Temperature on the Pore Size Distribution in Uncontaminated OPC Paste Specimens.

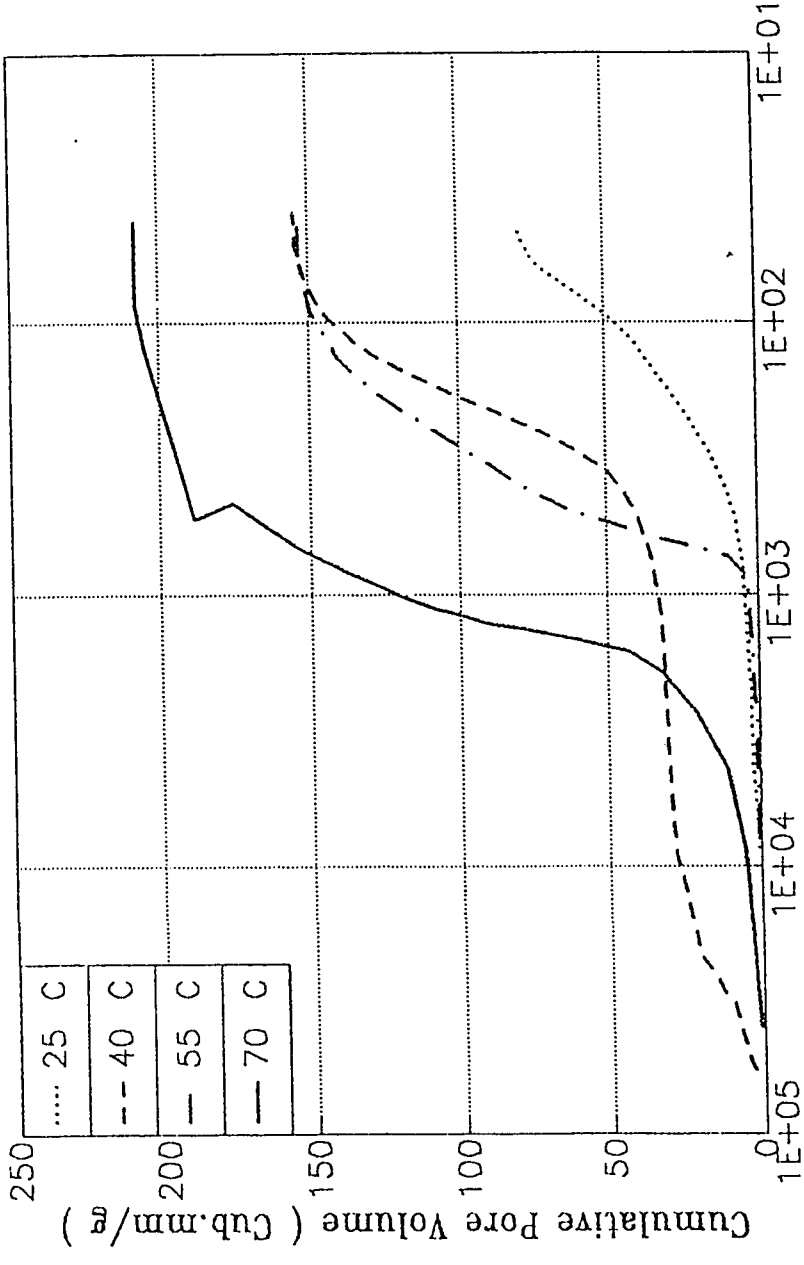

Fig. 4.7 Effect of Temperature on the Pore Size Distribution in the Contaminated OPC Paste Specimens.

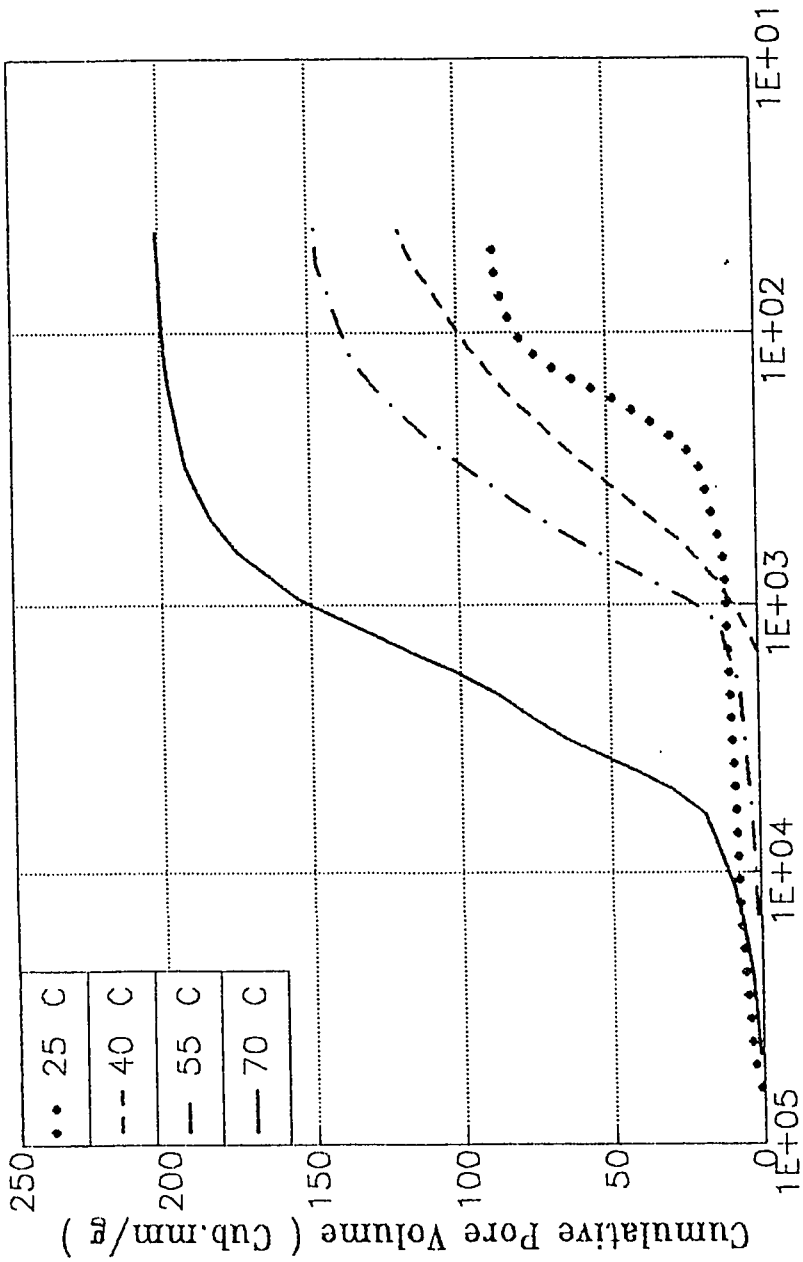

Fig. 4.8 Effect of Temperature on the Pore Size Distribution in Uncontaminated SF Cement Paste Specimens

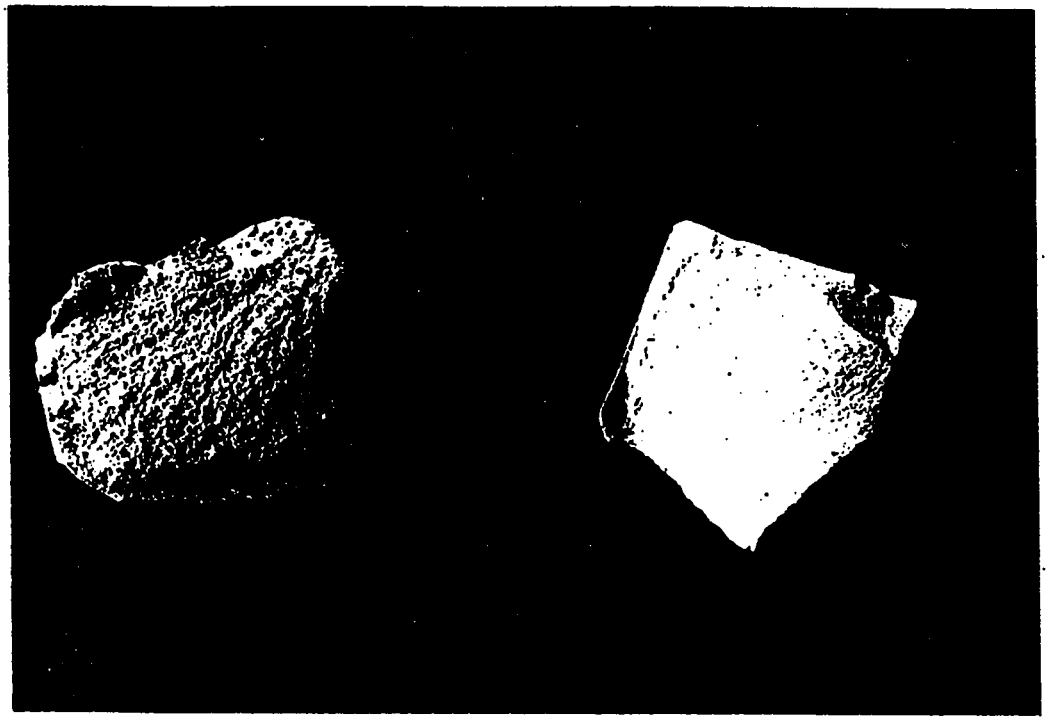

Plate 4.1 Silica fume and OPC Paste Specimens at 70 °C without Contamination

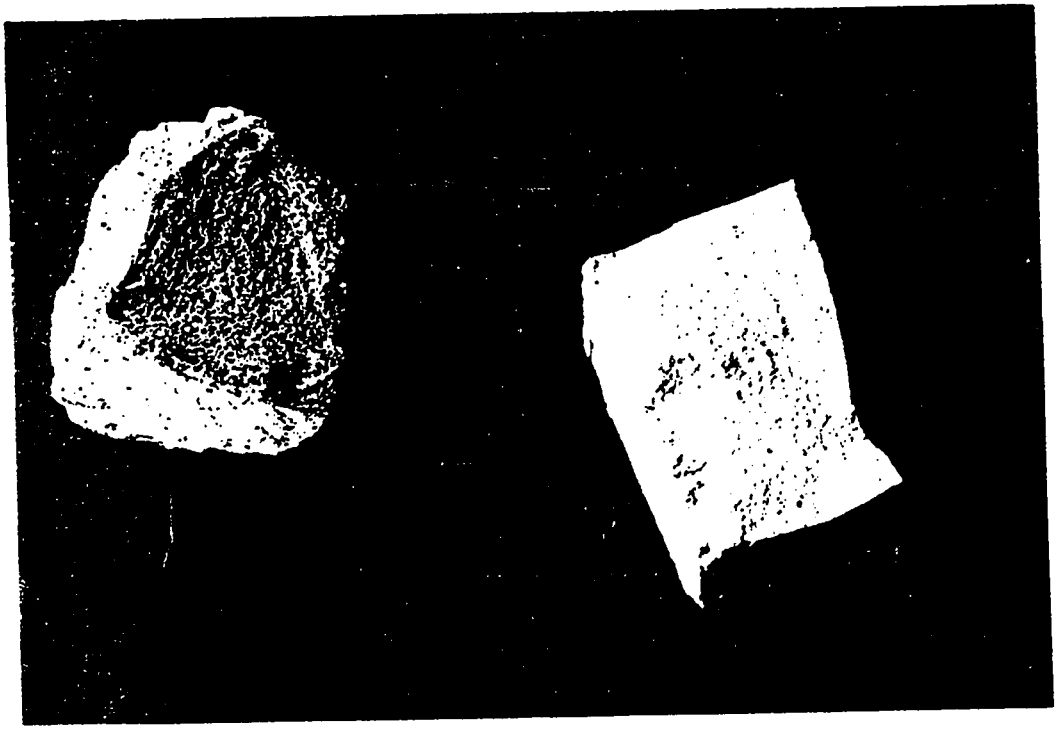

Plate 4.2 Silica fume and OPC Paste Specimens at 70 °C with Chloride and Sulfate Contamination

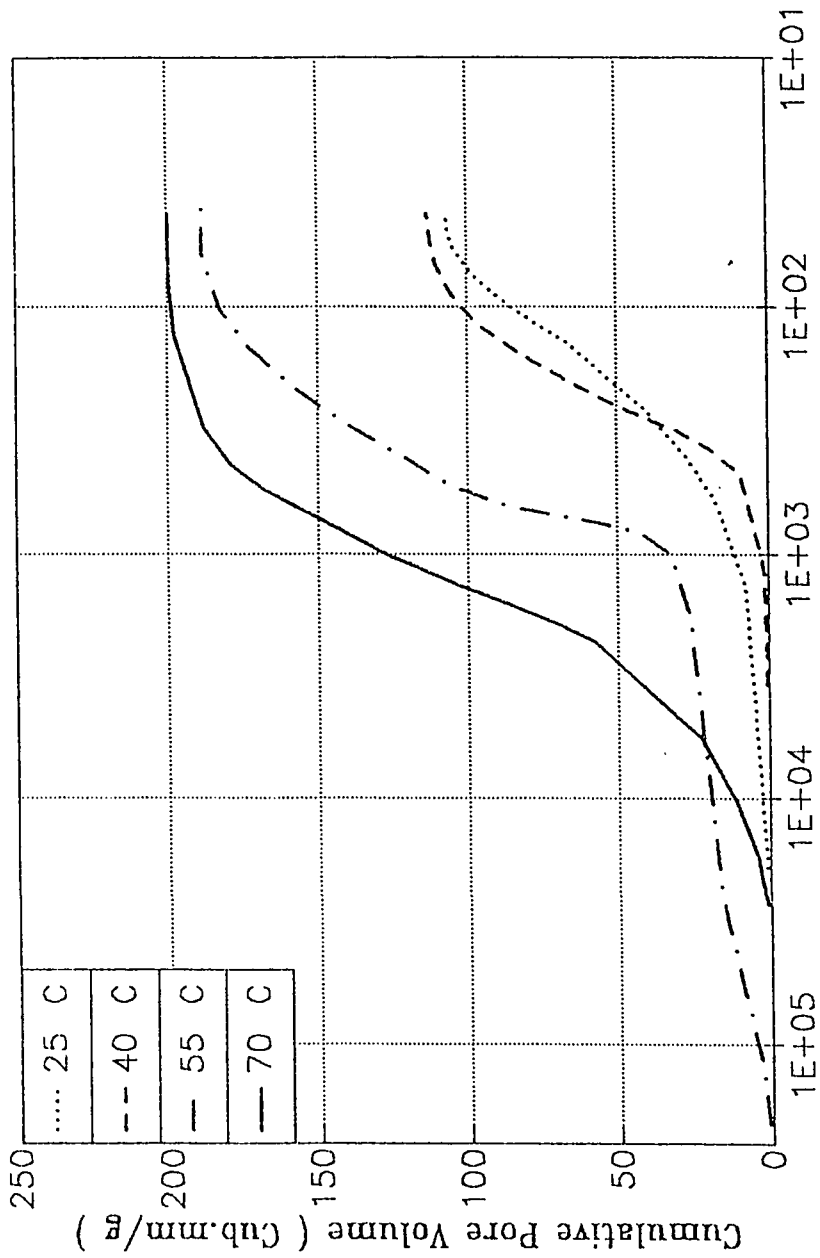

Fig. 4.9 Effect of Temperature on the Pore Size Distribution in the Contaminated SF Cement Paste Specimens

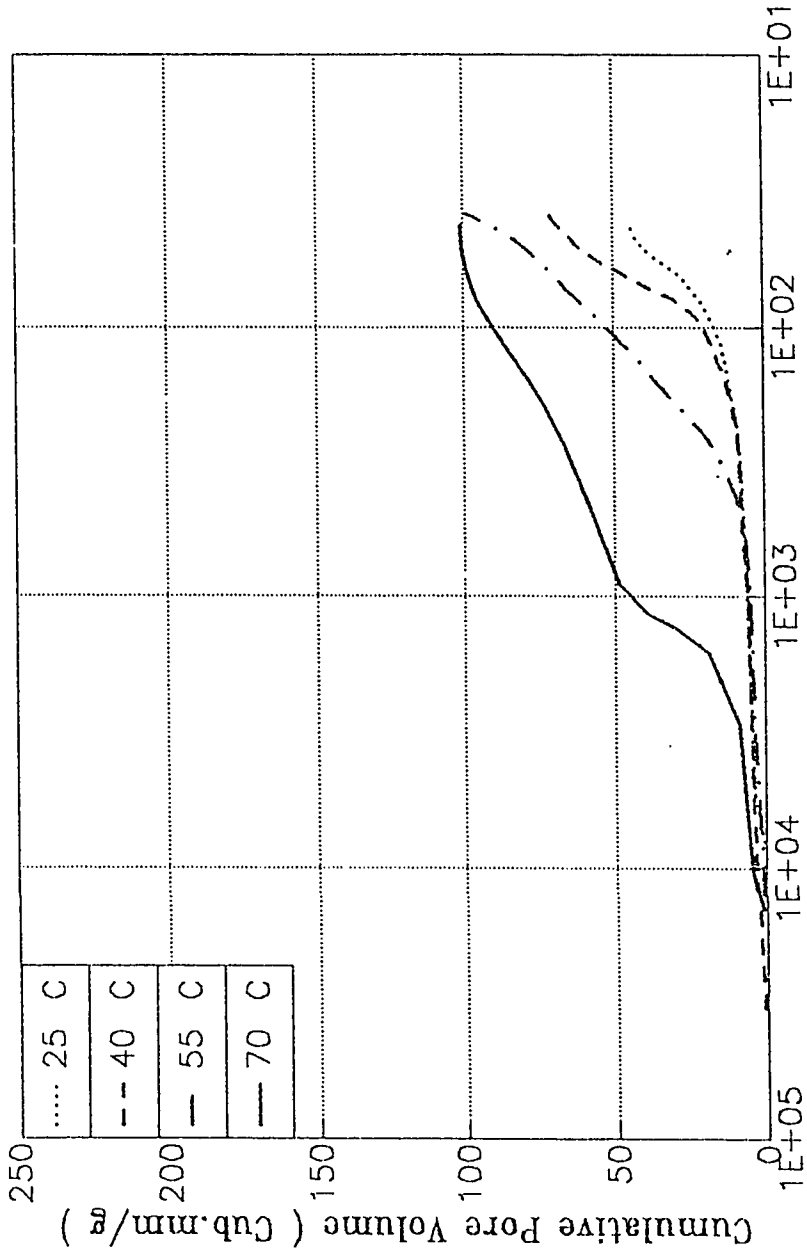

Fig. 4.10 Effect of Temperature on the Pore Size Distribution in Uncontaminated BFS Cement Paste Specimens

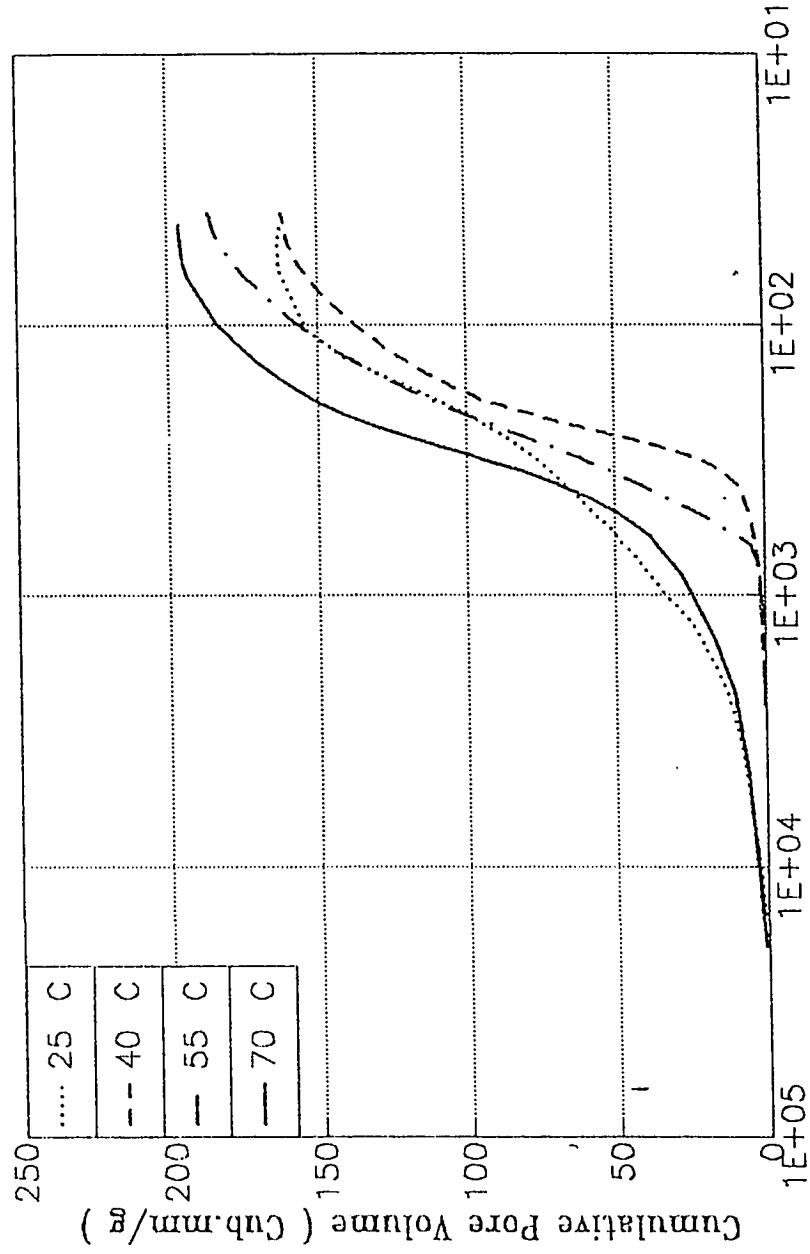

Fig. 4.11 Effect of Temperature on the Pore Size Distribution in the Contaminated BFS Cement Paste Specimens

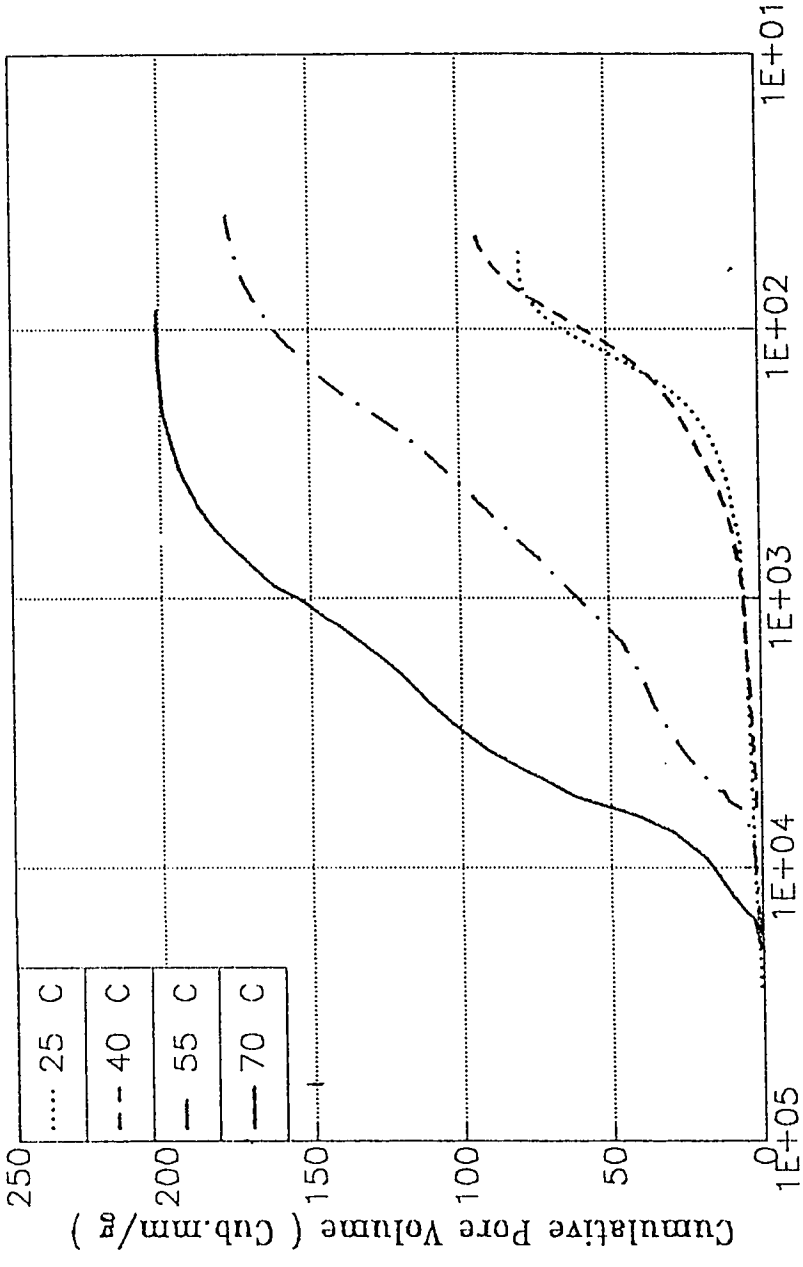

Fig. 4.12 Effect of Temperature on the Pore Size Distribution in Uncontaminated Class F FA Cement Paste Specimens

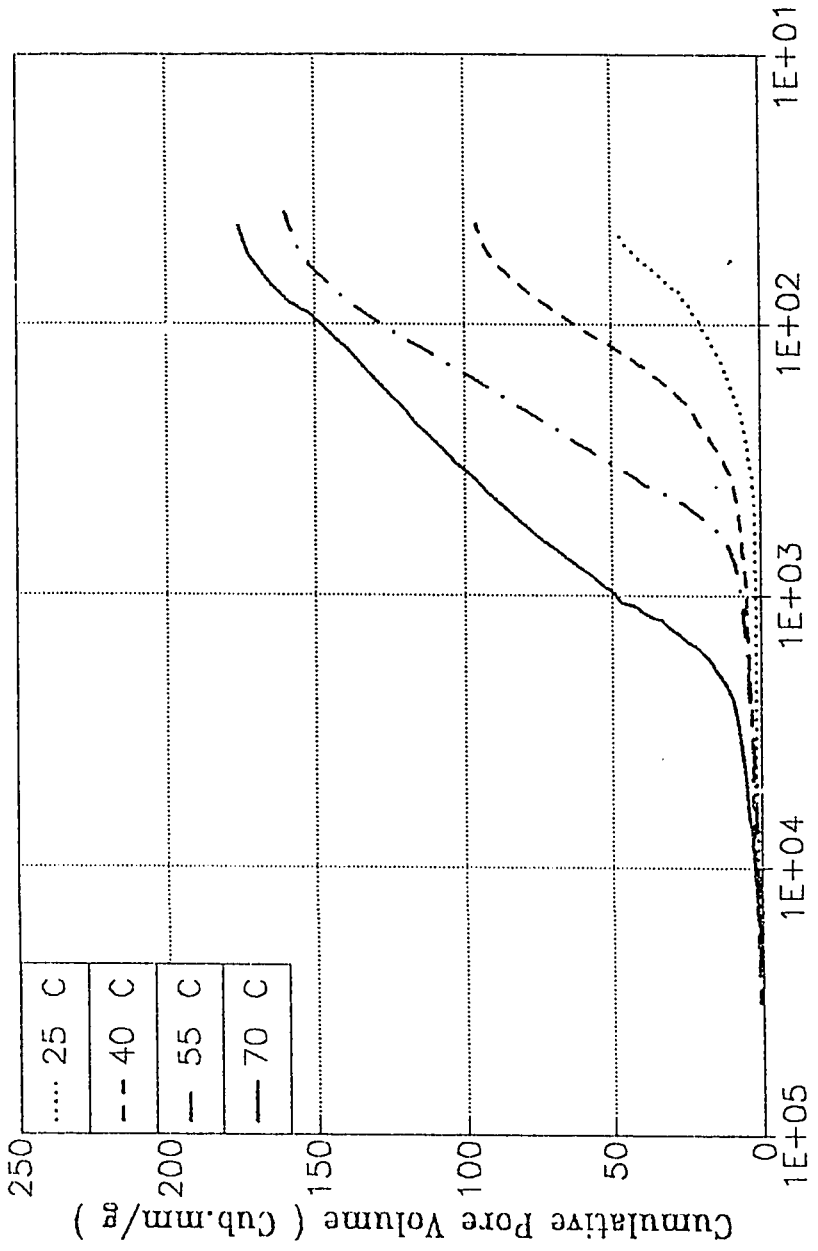

Fig. 4.13 Effect of Temperature on the Pore Size Distribution in the Contaminated Class F FA Cement Paste Specimens

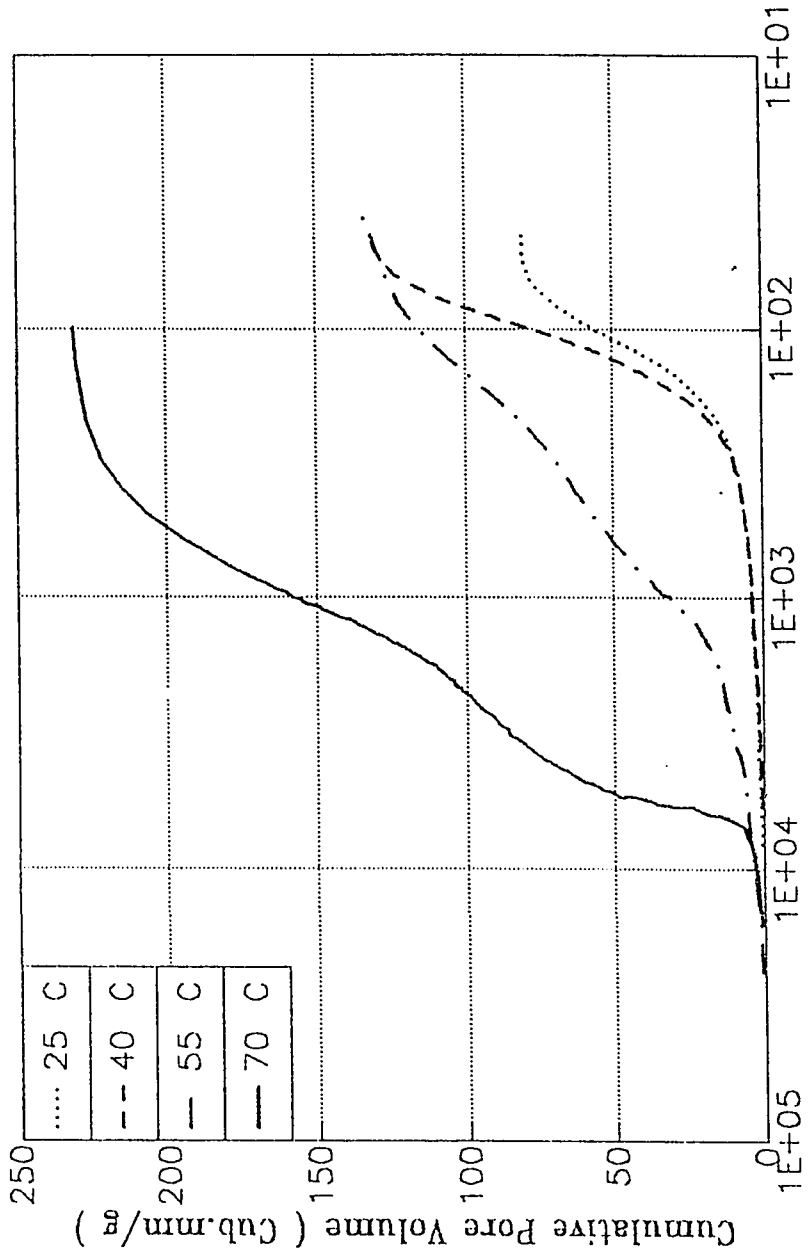

Fig. 4.14 Effect of Temperature on the Pore Size Distribution in Uncontaminated Class C FA Cement Paste Specimens

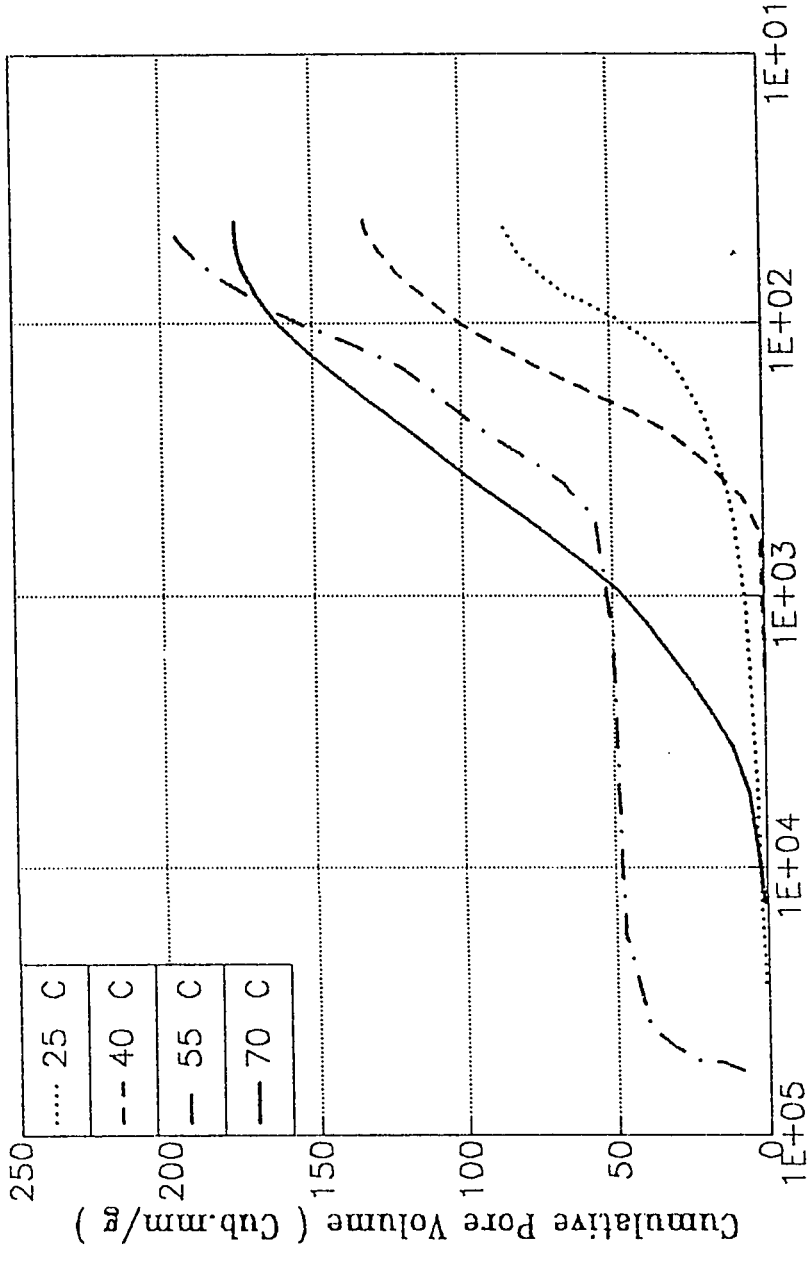

Fig. 4.15 Effect of Temperature on the Pore Size Distribution in the Contaminated Class C FA Cement Paste Specimens

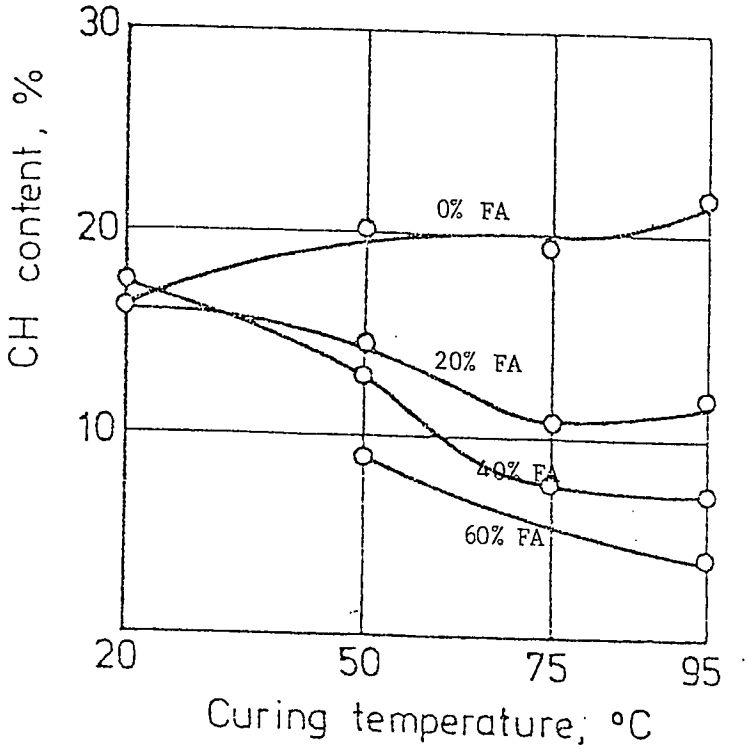

Fig. 4.16 Effect of Curing Temperature on $Ca(OH)_2$ in Fly Ash Cement Pastes (After Shiyuan [91])

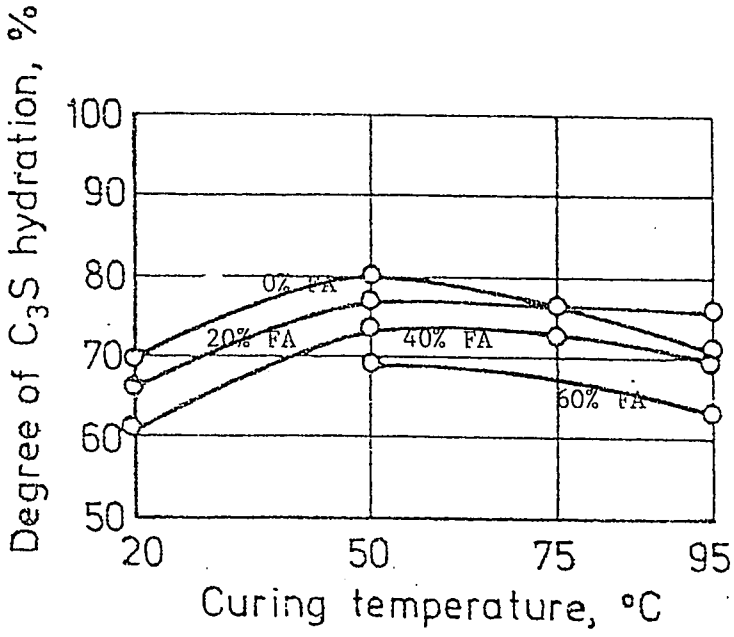

Fig. 4.17 Effect of Curing Temperature on Degree of C_3S Hydration of Fly Ash Cement and Pure Cement Pastes (After Shiyuan.; [91])

The greater influence of temperatures over changes in moisture content was confirmed by resistivity studies in UK over a 12 month period. The oven dry concrete has a resistivity which is many orders of magnitude higher than that of saturated concrete [100].

Lewis and Copenhagen [101] have reported that in coastal atmosphere where sea salt and moisture can penetrate the concrete, resistivities as low as 100 Ω.cm have been observed.

Fig. 4.19 shows the electrical resistivity of silica fume cement concrete specimens. These data show a trend similar to that observed in plain cement concrete specimens, in that the resistivity increased with increasing temperature and decreased with salt contamination. The electrical resistivity of silica fume cement concrete specimens was, however, much higher than that in plain cement concrete specimens. At 70 °C the electrical resistivity of silica fume cement concrete specimens was on an average 1.5 times that in ordinary portland cement concrete specimens. Similar increase in electrical resistivity due to silica fume blending of ordinary portland cement was also observed at 25 °C [100].

Fig. 4.20 shows the relationship between temperature and electrical resistivity in contaminated and uncontaminated blast furnace slag cement concrete specimens. These data also show a trend similar to that indicated by silica fume cement concrete specimens. At all temperatures the electrical resistivity of blast furnace slag cement concrete specimens was higher than that in ordinary portland cement concrete specimens. At 25 °C, the electrical resistivity in blast furnace slag cement concrete specimens was 1.8, 2.2 and 1.4 times that in ordinary portland cement concrete specimens. At 70 °C, the electrical resistivity was 17.5, 113.5 and 3.6 times that at 25 °C in non-contaminated, chloride contaminated and chloride-sulfate contaminated concrete specimens.

The electrical resistivity of concrete specimens blended with Class F fly ash and Class C fly ash are plotted in Fig. 4.21 and 4.22, respectively. These data show a trend similar to that indicated by other blended cements concrete specimens. The increased electrical resistivity in blended cements is attributed to the pozzolanic reaction which produces a dense and impermeable concrete. Similar results were obtained at room temperature in fly ash cement paste specimens [102].

TABLE 4.1 Effect of Temperature and Chloride-Sulfate Contamination on the Electrical Resisivity of OPC Concrete Specimens

Exposure Temperature °C	Electrical Resistivity k.Ω.cm		
	Uncontaminated	Chloride	Chloride + Sulfate
25	18.01	7.97	11.41
40	26.02	25.91	7.79
55	38.99	38.26	5.49
70	311.13	198.43	50.99

TABLE 4.2 Effect of Temperature and Chloride-Sulfate Contamination on the Electrical Resistivity of SF Concrete Specimens

Exposure Temperature °C	Electrical Resistivity k.Ω. cm		
	Uncontaminated	Chloride	Chloride+ Sulfate
25	30.43	18.62	18.52
40	38.20	22.92	12.81
55	45.53	32.49	8.98
70	447.80	341.79	79.78

TABLE 4.3 Effect of Temperature and Chloride-Sulfate Contamination on the Electrical Resistivity of BFS Concrete Specimens

Exposure Temperature °C	Electrical Resistivity k.Ω.cm		
	Uncontaminated	Chloride	Chloride + Sulfate
25	32.30	17.40	15.37
40	49.01	22.84	17.88
55	66.71	36.27	19.06
70	560.35	236.09	54.27

TABLE 4.4: Effect of Temperature and Chloride-Sulfate Contamination on the Electrical Resistivity of Class F FA Cement Concrete Specimens

Exposure Temperature °C	Electrical Resistivity k.Ω.cm		
	Uncontaminated	Chloride	Chloride+ Sulfate
25	355.90	137.20	127.68
40	371.68	210.80	113.50
55	381.90	363.83	135.701
70	4566.30	2487.79	532.551

TABLE 4.5 Effect of Temperature and Chloride-Sulfate Contamination on the Electrical Resistivity of Class C FA Cement Concrete Specimens

Exposure Temperature °C	Electrical Resistivity k.Ω. cm		
	Uncontaminated	Chloride	Chloride+ Sulfate
25	41.22	22.74	16.36
40	50.46	33.96	16.88
55	80.18	41.28	17.02
70	399.38	297.93	63.40

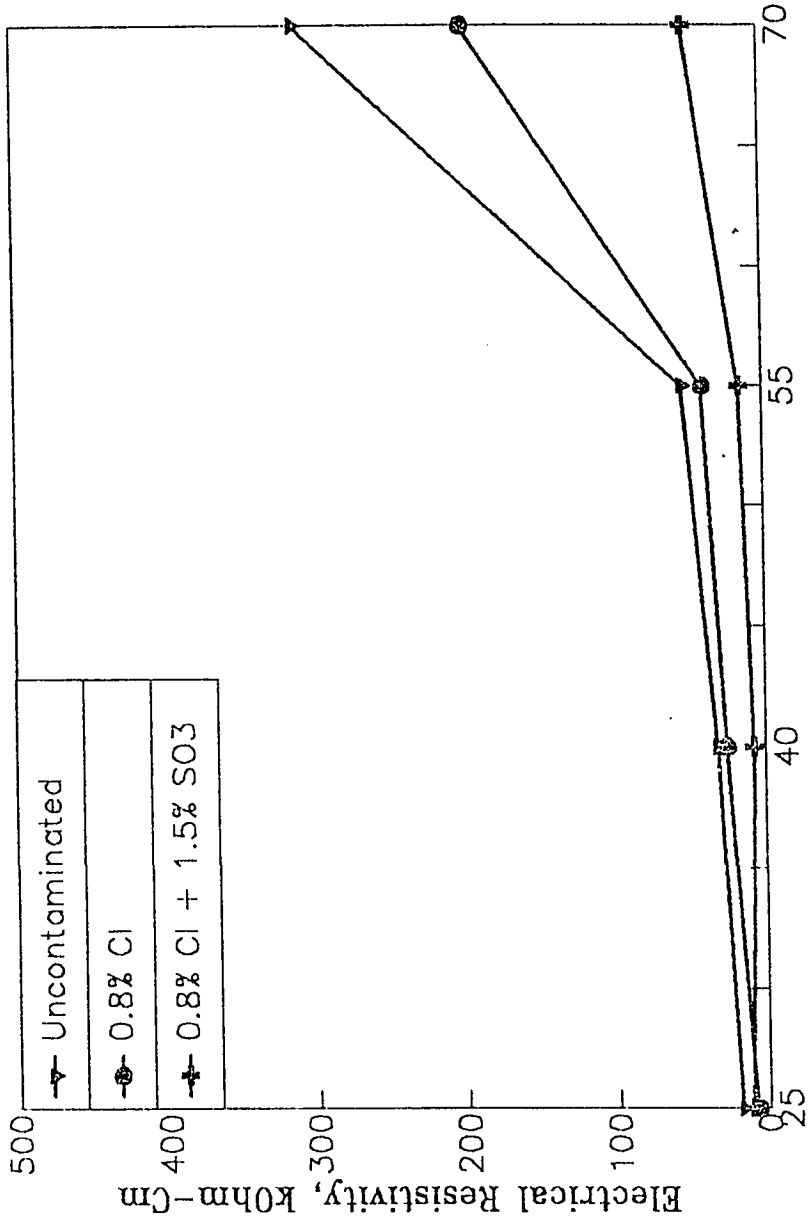

Fig. 4.18 Effect of Temperature and Chloride-Sulfate Contamination on the Electrical Resistivity of OPC Concrete Specimens

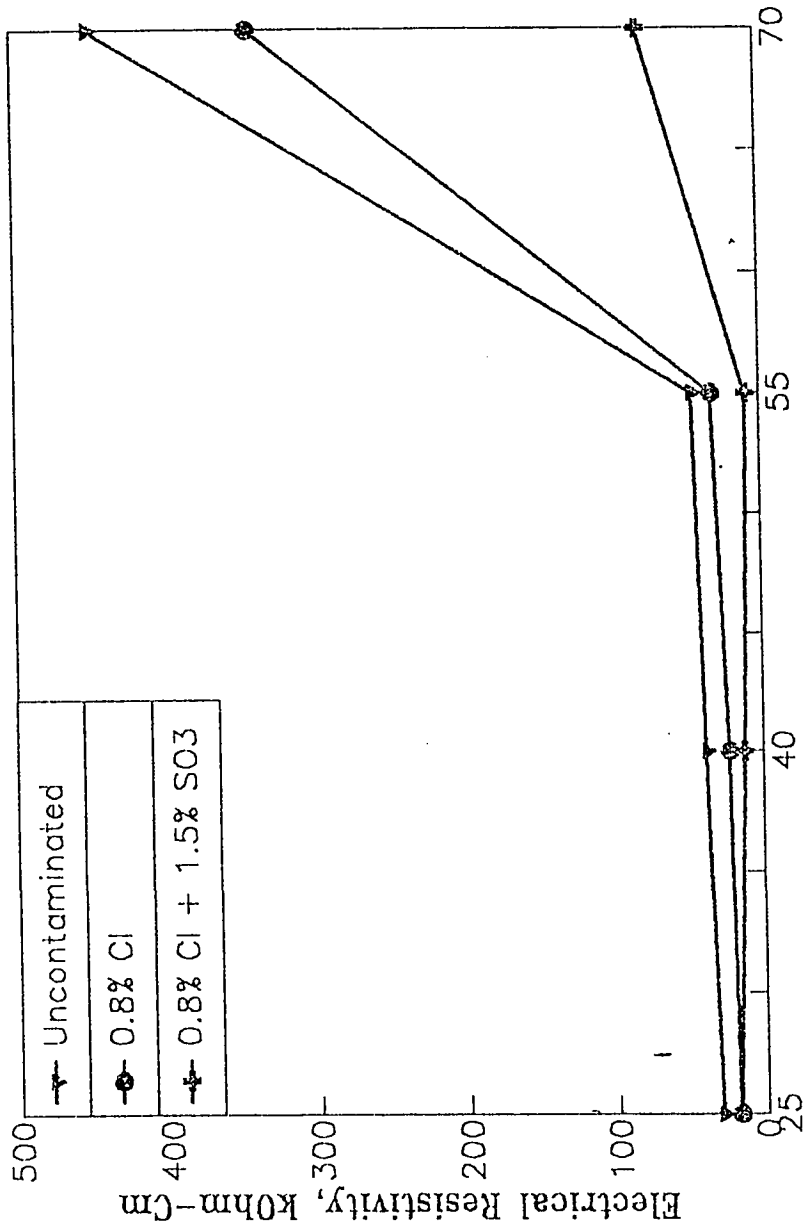

Fig. 4.19 Effect of Temperature and Chloride-Sulfate Contamination on the Electrical Resistivity of SF Cement Concrete Specimens

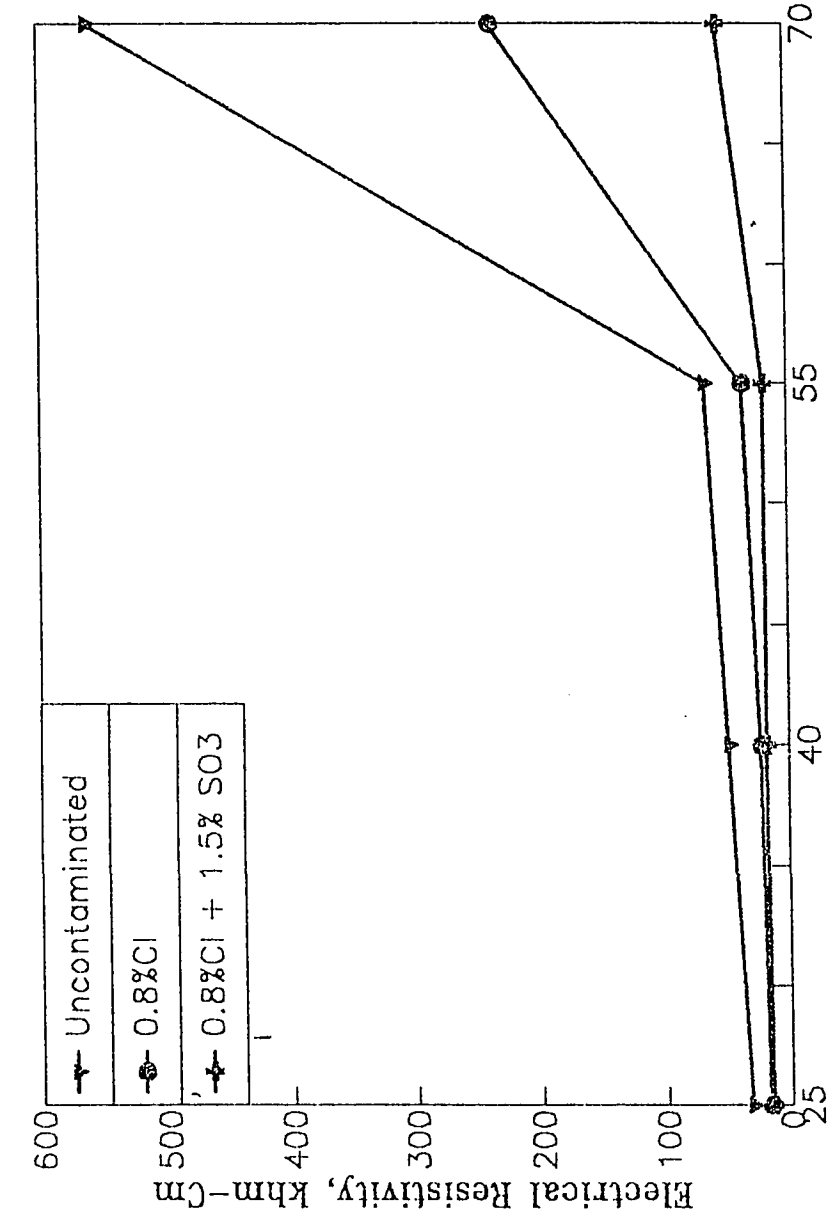

Fig. 4.20 Effect of Temperature and Chloride-Sulfate Contamination on the Electrical Resistivity of BFS Cement Concrete Specimens

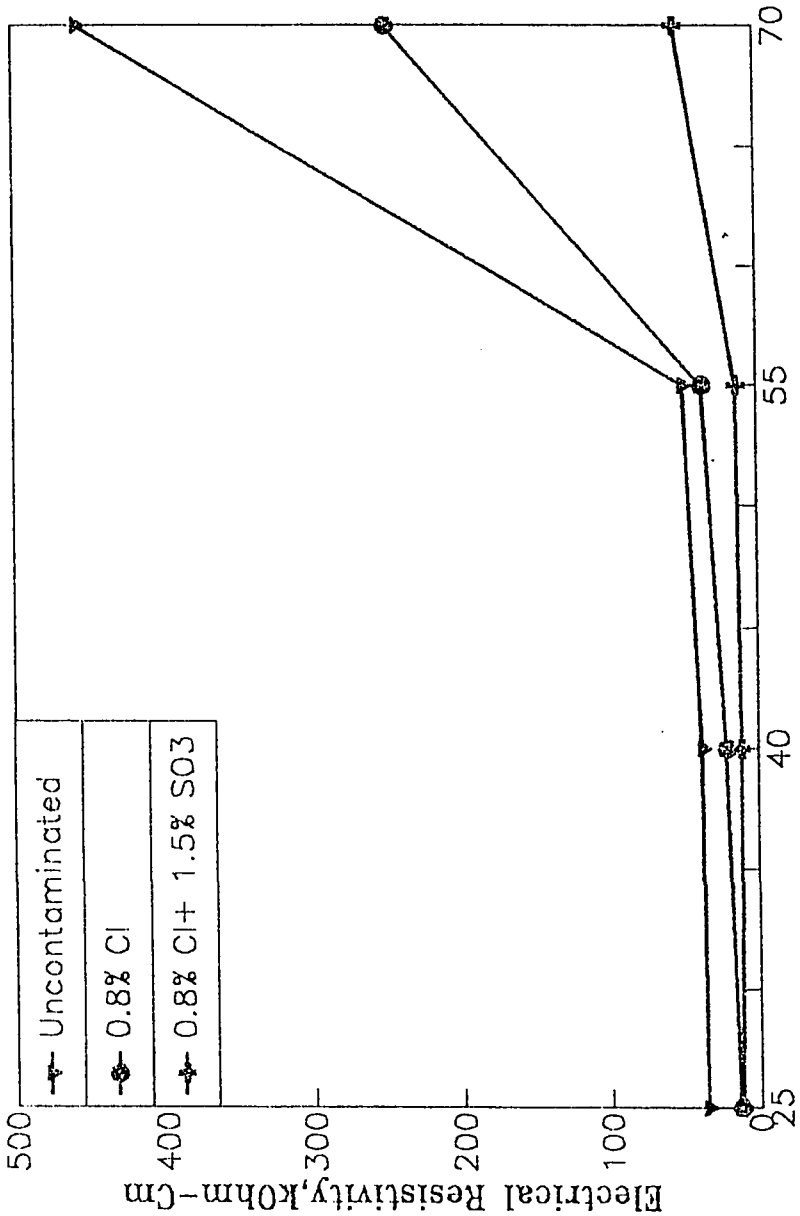

Fig. 4.21 Effect of Temperature and Chloride-Sulfate Contamination on the Electrical Resistivity of Class F FA Cement Concrete Specimens

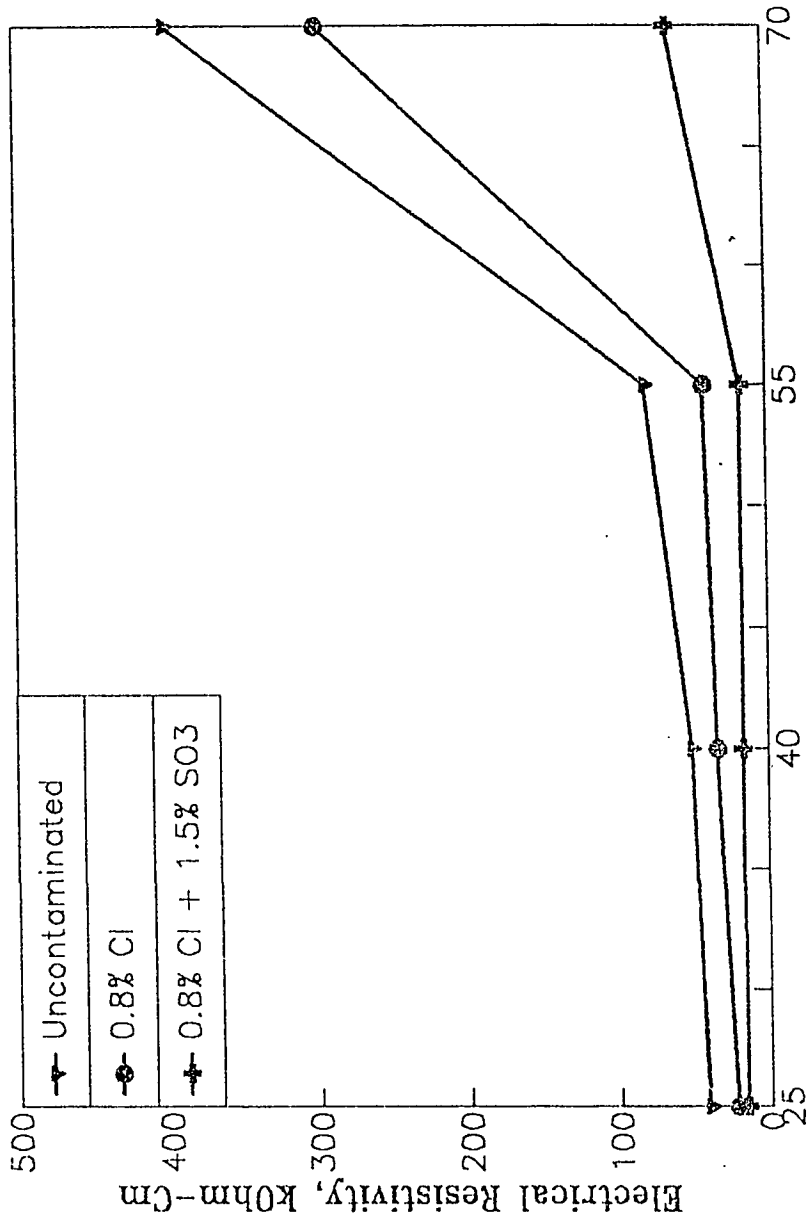

Fig. 4.22 Effect of Temperature and Chloride-Sulfate Contamination on the Electrical Resistivity of Class C FA Cement Concrete Specimens

4.4 EFFECT OF TEMPERATURE AND SALT CONTAMINATION ON ALKALINITY, CHLORIDE AND SULFATE CONTENT

The effect of temperature and salt contamination on the alkalinity, chloride and sulfate content in the plain and blended cements was investigated by contaminating them with (i) 0.8% chlorides and (ii) 0.8% Cl^- + 1.5% SO_3 and exposing them to temperatures of 25, 40, 55 and 70 °C. Uncontaminated cement paste specimens were subjected to similar temperatures and also analyzed to generate control data for comparison. The paste cements were finely ground to pass # 100 sieve, soaked in de ionized water and then analyzed to determine alkalinity, chloride and sulfate concentrations.

4.4.1 Alkalinity

The alkalinity, measured in terms of pH, of the contaminated and uncontaminated ordinary portland cement paste specimens is plotted against exposure temperature in Fig. 4.23. These data indicate higher pH value in contaminated specimens, compared to the uncontaminated specimens. At 25 °C the pH value of uncontaminated, chloride contaminated and chloride-sulfate contaminated specimens was 12.08, 12.28 and 12.33, respectively. The increase in the pH of the contaminated specimens as compared to uncontaminated specimens maybe attributed to the cation associated with the chloride and sulfate ions. The added NaCl reacts with $Ca(OH)_2$ to form Na^+ and OH^- according to the following equations [104].

$$2NaCl + Ca(OH)_2 \rightarrow CaCl_2 + 2Na^+ + 2OH^- \qquad (4.4.1)$$

$$C_3A\ 12H_2O + CaCl_2 \rightarrow C_3ACaCl_2.12H_2O \qquad (4.4.2)$$

A similar mechanism for the reaction of sodium sulfate with the cement hydration products, namely $Ca(OH)_2$ and C_3A thereby liberating Na^+, can be postulated. Therefore, the alkalinity of the specimens contaminated with both chlorides and sulfates

is higher than that in specimens contaminated with chlorides only.

The pH value decreased, in both the contaminated and uncontaminated specimens, when the exposure temperature was increased. The pH value decreased from 12.08 to 11.52, in uncontaminated specimens when the temperature was raised from 25 to 70 °C. In chloride and chloride-sulfate contaminated specimens the drop in the pH value was from 12.26 to 11.54 and from 12.33 to 11.88, respectively. The exact reasons for the reduction in the pH due to increase in the exposure temperature is not very clear. However, the following two possibilities may be considered:

(i) Carbonation i.e. $Ca(OH)_2$ is converted to $CaCO_3$ due to reaction with atmospheric CO_2. This reaction is accelerated at elevated temperatures. Several researchers have indicated the possibility of accelerated carbonation at elevated temperatures of more than 45 °C [105].

(ii) Inhibition of reaction (4.4.1) and (4.4.2), i.e., reaction of calcium chloroaluminate with C_3A is inhibited as a result Na^+ ions are not liberated. However, reduction in the pH value in the uncontaminated specimens indicates that the first mechanism, i.e., carbonation may be more predominant. In contaminated specimens both the mechanisms may be simultaneously occurring.

The variation in the pH values in silica fume cement paste specimens exposed to temperatures in the range of 25-70 °C are plotted in Fig. 4.24. These graphs indicate a trend similar to that of OPC as shown in Fig. 4.23. The pH values for uncontaminated and contaminated specimens at 25 °C were in the range of 11.98 to 12.26. At 70 °C the pH values were in the range of 11.33 to 11.51. The pH values in the silica fume blended cement specimens both uncontaminated and contaminated, were less than the pH values in corresponding plain cement paste specimens. This drop in the pH value in these specimens is attributed to the reaction of silicon dioxide, which constitutes about

95% of silica fume, with the alkali hydroxides and calcium hydroxide. Diamond [106] and Page et al. [107] measured alkali hydroxide concentrations in pore solutions of plain and silica fume blended cements. Reduction in the concentration of cations [Na^+ or K^+] was observed. They also observed that concentration of Ca^{2+} was very low for silica fume blending up to 20%, thereafter an increase in the Ca^{2+} concentration in the 30% silica fume blended cement was attributed due to what is called as common ion effect. At lower replacement levels of up to 20% the concentration of NaOH and KOH was relatively high which inhibits the solubility of $Ca(OH)_2$ crystals.

At higher levels of SF blending, 30% or more the NaOH and KOH concentration drop significantly, thereby allowing $Ca(OH)_2$ crystals to dissolve in pore solution.

The pH values in the contaminated and uncontaminated BFS cement paste specimens are plotted against the exposure temperature in Fig. 4.25. These data show a general trend similar to that shown by silica fume cement paste specimens. The pH values in the contaminated specimens were less than that in uncontaminated specimens. An increase in the exposure temperature resulted in a decrease in the pH value in both uncontaminated and contaminated specimens. Further, the pH values in BFS cements paste specimens were lower than the corresponding ordinary portland cement paste specimens. The pH values at 25 °C were in the range of 11.618 to 11.24 and at 70 °C were in the range of 11.81 to 11.57. The reduction in the pH value between the OPC and BFS cement was on an average 0.5 units, at all temperatures and contamination levels, may be attributed to the fact that BFS cement paste contains only 30% OPC.

The pH values in Class F fly ash blended cement paste specimens (Fig. 4.26) at 25 °C were in the range of 11.5 to 12.06 for uncontaminated and contaminated specimens. At 70 °C exposure these values were in the range of 10.88 to 11.82. An average reduction of 0.68 pH units was observed between these specimens and corresponding OPC. The general trend of increase in the pH in contaminated specimens and its reduction with an increase in the temperature was also observed in these specimens.

Figure 4.27 shows the variation of pH with temperature in Class C fly ash cement paste specimens. These curves also show a trend similar to that shown in Fig. 4.26. The pH values in the uncontaminated and contaminated specimens at 25 °C were in the range of 11.91 to 12.21. At 70 °C these values were in the range of 10.92 to 11.93. An average reduction of 0.33 pH units between these cements and OPC was observed. The reduction in the pH of the fly ash cement specimens, both Class F and Class C fly ash may be attributed to the pozzolanic reaction which consumes the $Ca(OH)_2$. With increasing temperature the pozzolanic reaction is accelerated, thus, further reducing the alkalinity. $Ca(OH)_2$ reduction due to increasing temperature have been confirmed by Shiyuan [99] using XRD and DTA techniques in fly ash blended cement paste specimens as shown in the Fig. 4.16.

Similar results have been reported by Vassie [108] and Byfors et al. [109]. Vassie [108] observed that even when the liquid phase of concrete contained high salt concentrations the maximum pH reduction arising from this effect were only 0.50 pH units and generally pH decreases were substantially less than this. Byfors et al. [109] studied the effect of salt addition of 1% Cl^- as NaCl on the Cl^- and OH^- concentrations. Their results indicated that material additions to cements reduced the OH^- ion content of the pore solution but this was not to a degree that could be considered harmful to the passivity of steel.

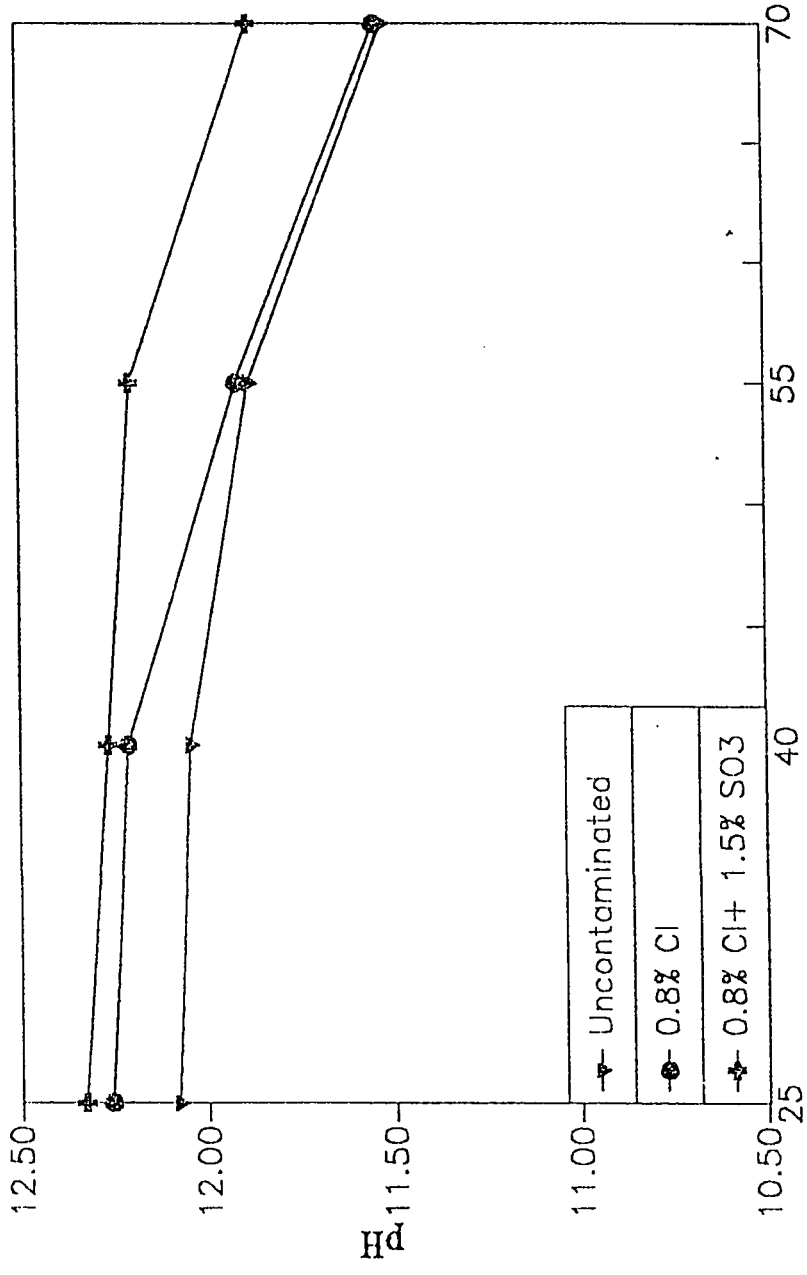

Fig. 4.23 Effect of Temperature and Chloride-Sulfate Contamination of the pH of OPC Paste Specimens

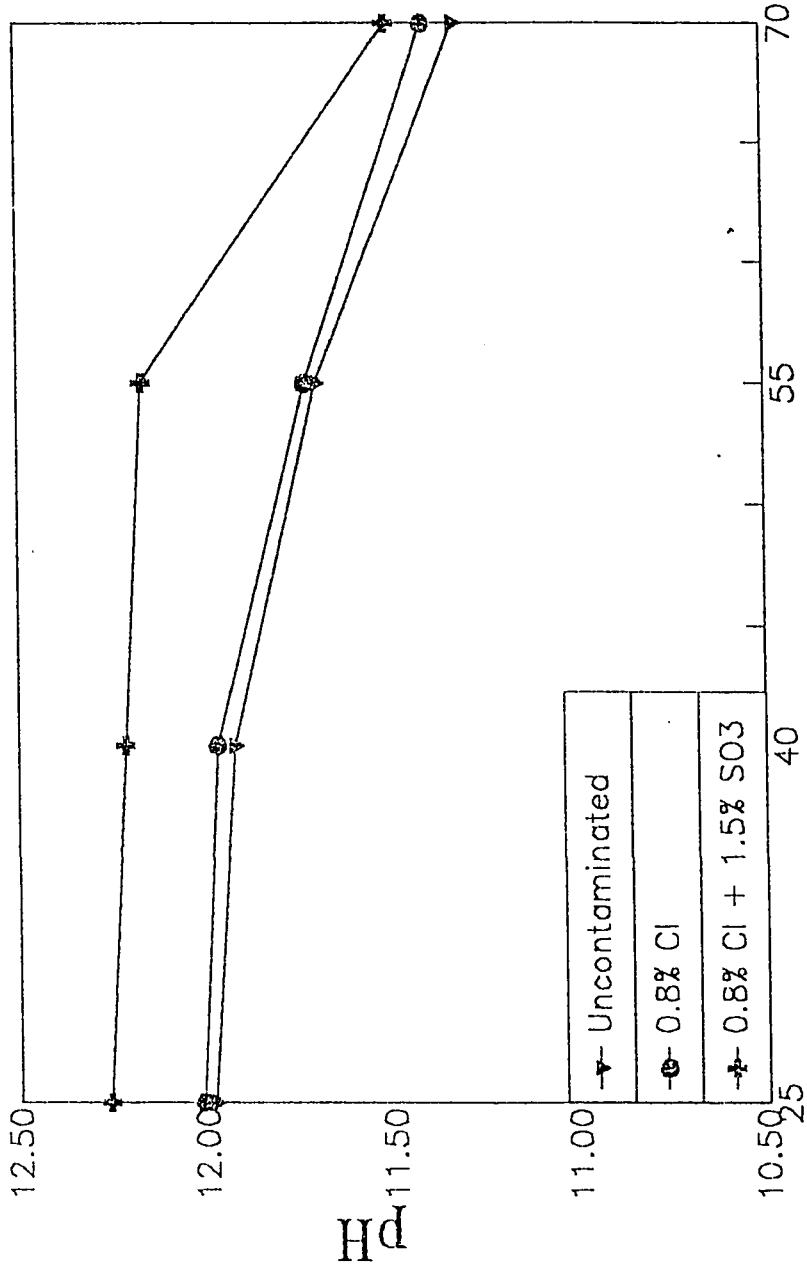

Fig. 4.24 Effect of Temperature and Chloride-Sulfate Contamination on the pH of SF Cement Paste Specimens

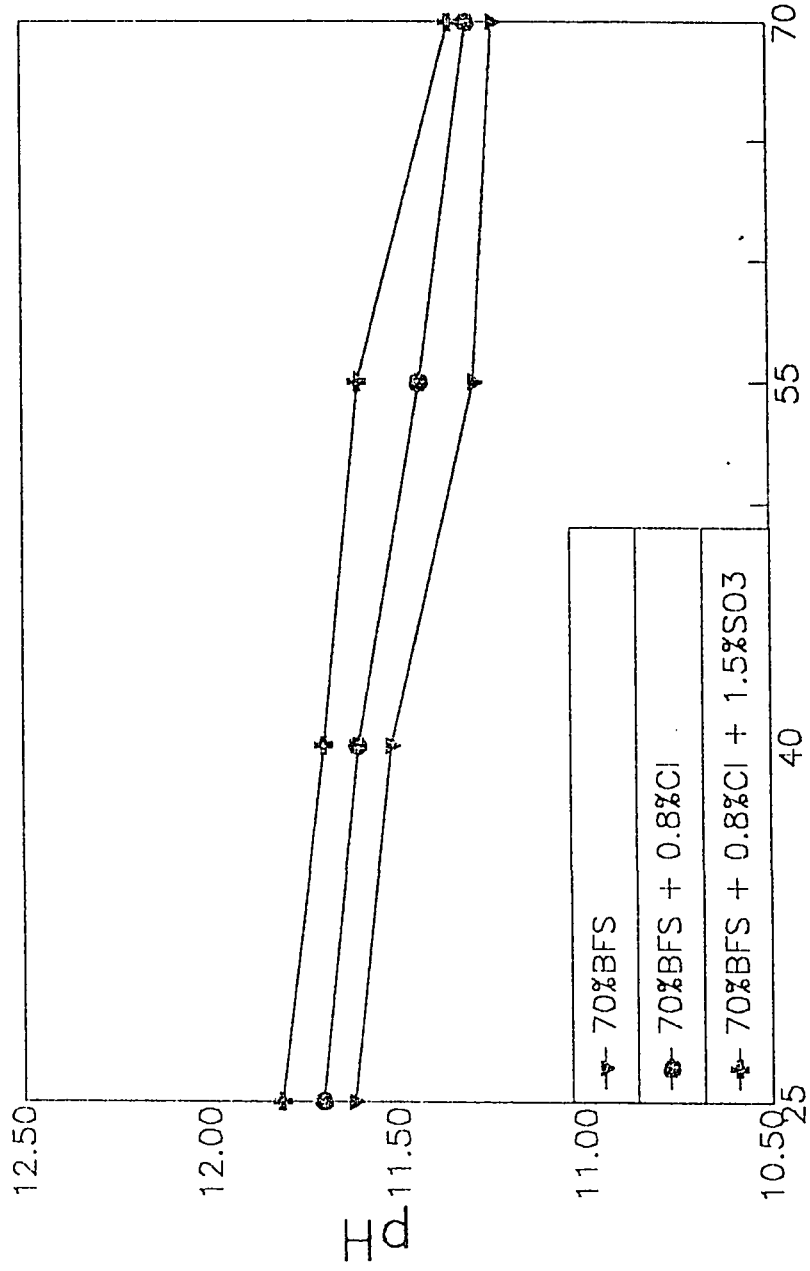

Fig. 4.25 Effect of Temperature and Chloride-Sulfate Contamination on the pH of BFS Cement Paste Specimens

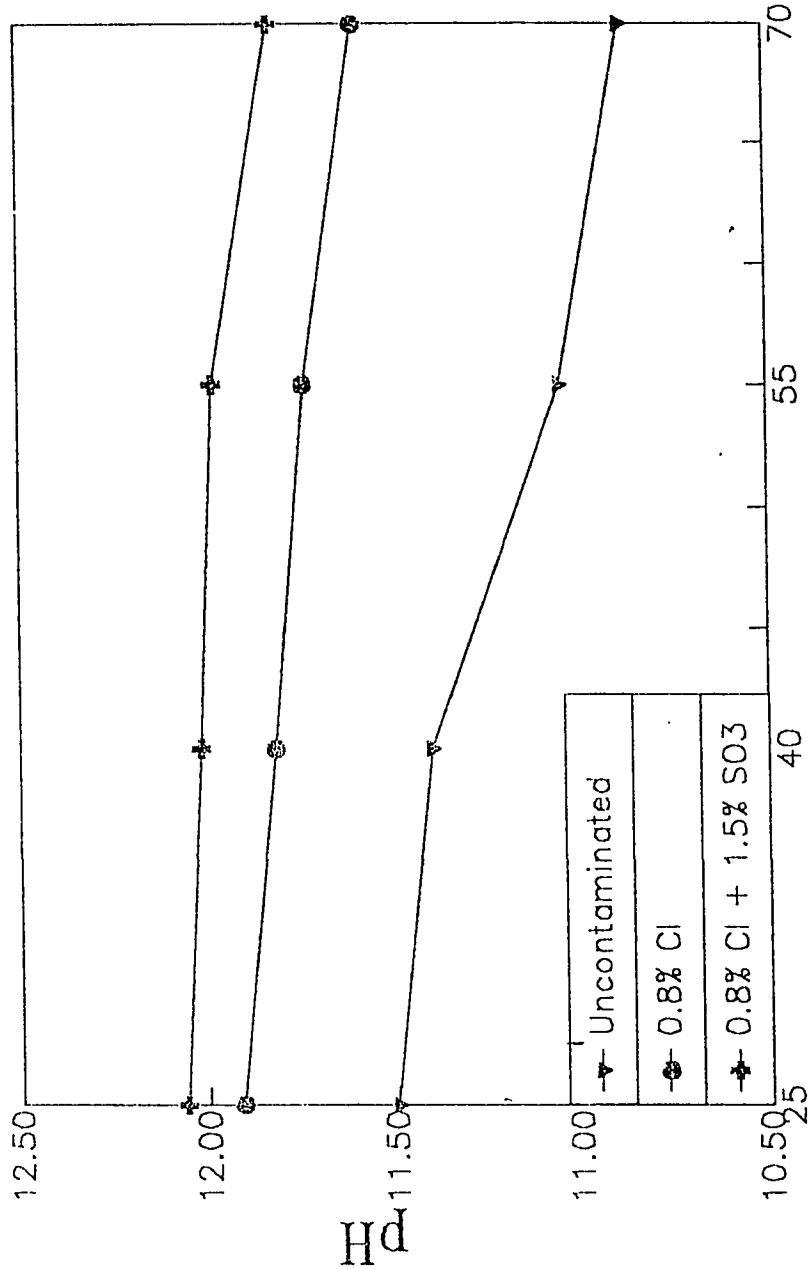

Fig. 4.26 Effect of Temperature and Chloride-Sulfate Contamination on the pH of Class F FA Cement Paste Specimens

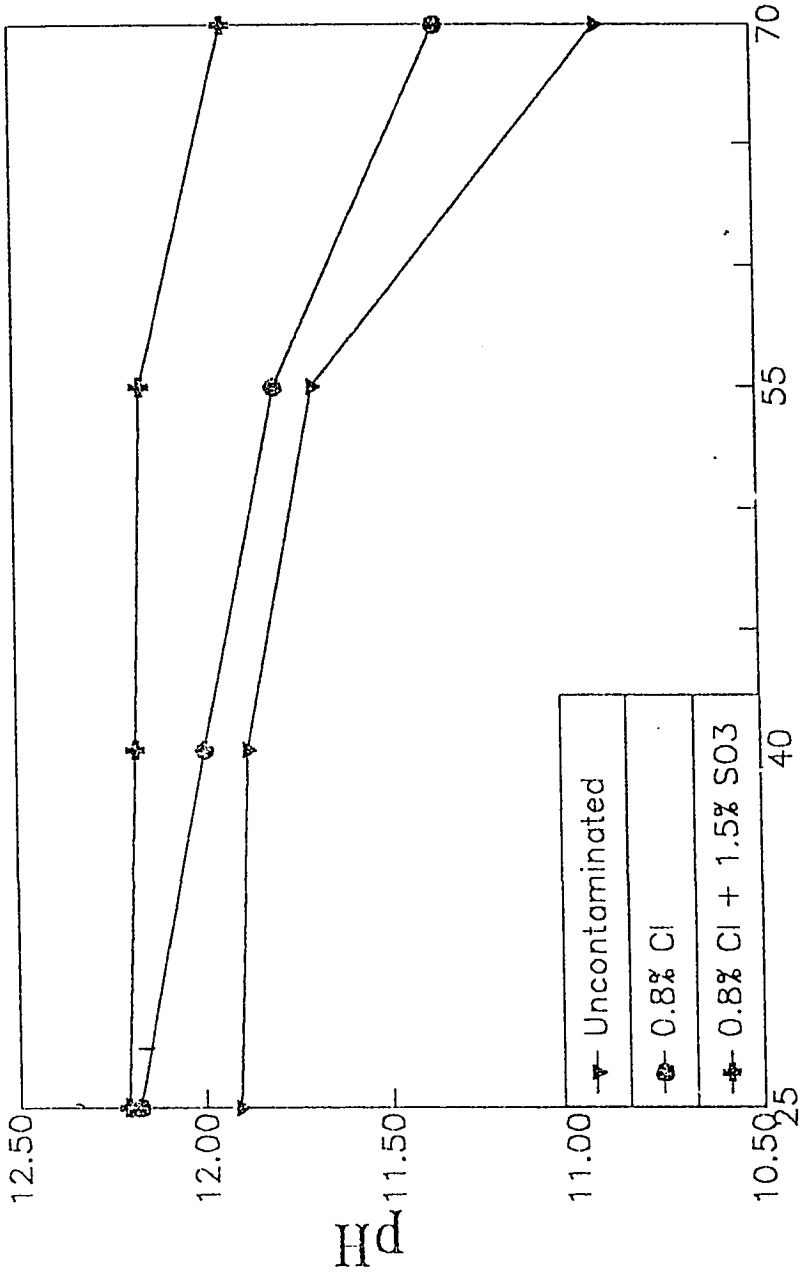

Fig. 4.27 Effect of Temperature and Chloride-Sulfate Contamination on the pH of Class C FA Cement Paste Specimens

4.4.2 Chloride Concentration

The water soluble chloride ion concentrations in the ordinary portland cement paste specimens exposed to 25, 40, 55 and 70 °C temperature are plotted in Fig. 4.28. The chloride ion concentration in specimens contaminated with sulfate-chloride was more than that containing only chlorides at all the temperatures investigated. The chloride ion concentration at 25 °C was 0.017, 0.148, and 0.160% in uncontaminated, chloride contaminated and chloride-sulfate contaminated cement paste specimens. An increase in the water soluble chloride ion concentration with increase in temperature was indicated in all the specimens. The water soluble chloride concentration at 70 °C was 0.027, 0.227 and 0.253% in the uncontaminated and contaminated specimens. The chloride concentration in uncontaminated specimens exposed to 70 °C was 1.3 times that in similar specimens exposed to 25 °C. The chloride concentration in specimens contaminated with chloride salts and exposed to 70 °C was 1.5 times the chloride concentration in similar specimens exposed to 25 °C. These results showing higher water soluble chlorides in specimens subjected to elevated temperatures are in agreement with the data generated by Roberts [26]. He indicated that cements hydrated at elevated temperatures bind lesser chlorides compared to cements which are hydrated at lower temperatures. When the chlorides are added to the cement, they react with tricalcium aluminate (C_3A) forming an insoluble calcium chloroaluminate compound [$3.CaO.Al_2O_3CaCl_2 .10H_2O$] also called Friedel's salt. Thus higher the C_3A, lower will be the unbound chloride and so the corrosion risk. Increase in the quantum of free chloride due to an increase in the exposure temperature, therefore, indicates decomposition of the Friedel's salt, at elevated temperature.

It is also possible that C_3A becomes unstable with increasing temperature [26]. Roberts [26] tested the effect of temperature on the solubility of pure mono calcium chloroaluminate compound and found that the solubility in water and in solutions of calcium sulfate and calcium hydroxide, increases with increasing temperature. The

aforesaid solutions typically simulate concrete pore solutions.

Arya et al [110] while working on methods of determining the free chlorides with OPC mortars also studied the effect of temperature of solvent. They observed that increase in temperature increases the total chlorides passing into solution. They also found that bound chlorides are released at temperatures higher than 50 °C.

Sulfate-chloride bearing pastes show an average increase of about 2.5%, by weight of cement, of free chlorides than when compared to chloride-bearing pastes at all temperatures. Holden et al [3] observed a similar effect of sulfate addition on chloride binding capacity of cements. Three plain cements with C_3A contents of 1.9%, 7.7% and 14.3% were used in their study. Chloride and sulfate additions of 0.4% and 1.5% respectively were made and the specimens were exposed to normal 25 °C temperature. The chloride concentration in the pore solution of specimens contaminated with chloride plus sulfate was more than that in specimens containing only chlorides.

The increase in the quantity of free chlorides in the pore solution due to sodium sulfate addition may be attributable to either an increase in pore solution alkalinity or to the preferential combination of C_3A with sulfate ions in comparison to chloride ions, thereby inhibiting the formation of Friedel's salt. Addition of SO_3 as Na_2SO_4, significantly increases the alkalinity of the pore solution of the hydrated cement paste. The increase in chloride ion concentration in sulfate-chloride bearing pastes at higher temperature, 70 °C per se, may be due to instability of C_3A with temperature rise resulting in the dissolution of bound chlorides in pore water and due to an increase in pore solution alkalinity caused by sulfate addition. The exact mechanisms of formation of Friedel's salt and the factors affecting the chloride binding in cement at various temperatures need further elucidation.

Fig. 4.29 shows the effect of temperature on the water soluble chloride ion concentration in the silica fume cement paste specimens with and without

contamination. Generally, it was observed that an increase in temperature increases the free chlorides. This effect is more pronounced beyond 55 °C. It was also observed that partial cement replacement by silica fume increases the unbound chlorides in pore solution than in the parent cement. There is an average increase of 1% and 3.95% in the unbound chlorides in chloride-bearing and sulfate-chloride bearing silica fume cement paste specimens, respectively, when compared to the ordinary portland cement paste specimens. Increasing the temperature from 25 to 70 °C does not have any effect on the chloride concentration in the uncontaminated silica fume cement paste specimens whereas at 70 °C, an increase of 63.5% (1.6 times) and 78.2% (1.8 times) in the water soluble chloride concentration were observed when compared to chloride bearing and sulfate-chloride bearing silica fume cement paste specimens exposed at 25 °C.

The increase in the chloride concentration in the silica fume cement paste specimens due to increasing temperature particularly beyond 55 °C may be attributed to the decomposition of the Friedel's salt. Page and Vennesland [107] attributed the decomposition to increased solubility of Friedel's salt at reduced pH levels of the pore solution. Hussain [111] based upon XRD and DTA results indicates that silica in the chloride bearing silica fume cement paste may combine with C_3A phase of the cement thereby inhibiting the availability of C_3A for the formation of Friedel's salt.

The results of the present study indicate that at temperatures of 25 °C the unbound chlorides in the plain cements increases with an increase in pore solution alkalinity. The data at ambient/lab temperature show that mechanisms of increase in unbound chlorides due to increase in the pore solution alkalinity is operative not only in plain cements but also in silica fume cements. However, the increase in the unbound or water soluble chlorides in the pore solution due to micro silica blending may be attributable to the increased binding of hydroxyl ions in the paste specimens thereby releasing the chloride ions to balance the cations present in the pore solution.

The inclusion of sulfate as a contaminant in the chloride bearing silica fume cement paste specimen results in an average increase of 6.1% in the chloride concentration. This supports the suggestion that corrosion risks are likely to be significantly increased in circumstances where concrete structures are subject to both chlorides and sulfates, as is commonly the case in the substructures in the coastal areas of the Arabian Gulf.

Fig. 4.30 shows the effect of temperature on chloride ion concentration in BFS cement paste specimens. These curves indicate a trend similar to that exhibited by other cements. The quantum of water soluble chlorides was observed to increase with temperature and incorporation of sulfate ions. The increase in the free chloride concentration is more pronounced at 70 °C. In the contamination free BFS cement, the water soluble chloride concentration is more or less similar to that in the OPC. The chloride concentration in the contaminated BFS cement paste contaminated with chloride and exposed to 70 °C temperature was 0.118% more than that in corresponding OPC paste specimens. In specimens contaminated with chloride-sulfate, this increase was about of 0.162%. A 14.74% increase in the water-soluble chloride concentration in the chloride contaminated specimens was observed when the temperature was increased from 25 to 70 °C. The corresponding increase in the plain cement paste specimens was about 53.38%.

The increase in the water soluble chloride concentration in BFS cement paste specimens contaminated with chlorides and sulfates, was 22.73% when the temperature was raised from 25 to 70 °C. The corresponding increase in the chloride concentration in the OPC paste specimen was 58.13% .

The lower chloride binding of BFS cement pastes contradicts the data cited in the literature. BFS cement was observed to bind more chlorides than OPC [111]. This is probably due to the fact that in BFS cement the chloride binding takes place by mechanisms other than the formation of Friedel's salt and the possibility that slag itself is capable of removing some of the chlorides from the pore solution cannot be ruled

out.

Fig. 4.31 shows the effect of temperature on the chloride ion concentration in Class F fly ash blended cement paste specimens with and without salt contamination. These curves show a trend similar to that indicated by other cements. Further, these data show a lower chloride concentration in all these specimens compared to plain cements. An exception to this trend was indicated in chloride-sulfate contaminated specimens exposed to 70 °C.

The chloride concentration in chloride bearing specimens was on an average 0.024% less than that in the OPC paste specimens. A moderate reduction of 0.003% in the chloride concentration in sulfate-chloride bearing fly ash pastes was observed, as compared to the OPC paste. The chloride ion concentration in the paste specimens contaminated with chloride and sulfate-chloride increased by 68.7% and 82.9%, respectively when the exposure temperature was raised from 25 to 70 °C.

The reduction in the free chloride ion concentration in the fly ash F cement paste specimens compared to OPC paste specimens is attributable to the formation of Friedel's salt. Moreover, fly ash itself may be effective in binding some of the free chlorides. Kawamura et al [112] studied the effect of fly ash addition on the pore solution of cement treated with different levels of Cl^- derived from NaCl and $CaCl_2$. Their results show that in both plain and fly ash cements more Friedel's salt was detected by DTA. These results are in good agreement with the data reported by Page et al [27], Holden et al [3] and Arya et al [28]. A reduction in unbound chlorides in Fly ash was observed due to low CaO content compared to the OPC.

Fig. 4.32 shows the effect of temperature on the chloride concentration in fly ash C blended cement paste specimens. The general trend of increase in the chloride concentration with increasing temperature and sulfate contamination was also observed in these cement paste specimens.

Non-contaminated and chloride-bearing specimens indicated a reduction in free chloride ion concentration as compared to corresponding OPC specimens. An average reduction of 0.015% by weight of cement was observed in chloride-bearing Class C fly ash cement paste. But the addition of sulfates increased the free chlorides by 0.053% in these specimens as compared to OPC pastes at all temperatures. The increase in the water soluble chloride ion concentration in chloride and chloride-sulfate contaminated specimens was 83.1% and 18.34% respectively, when the exposure temperature was increased from 25 to 70 °C.

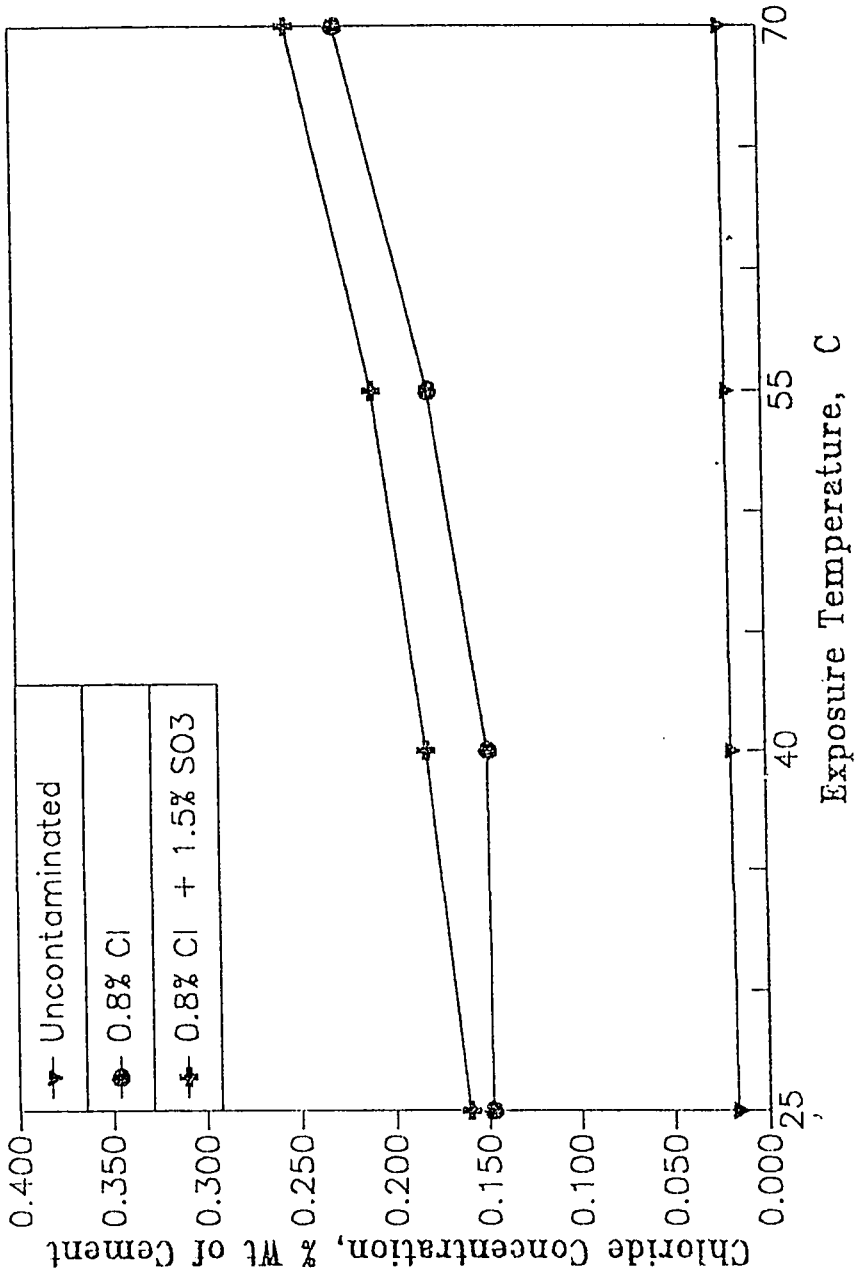

Fig. 4.28 Water Soluble Chlorides in OPC Paste Specimens Exposed to Various Temperatures

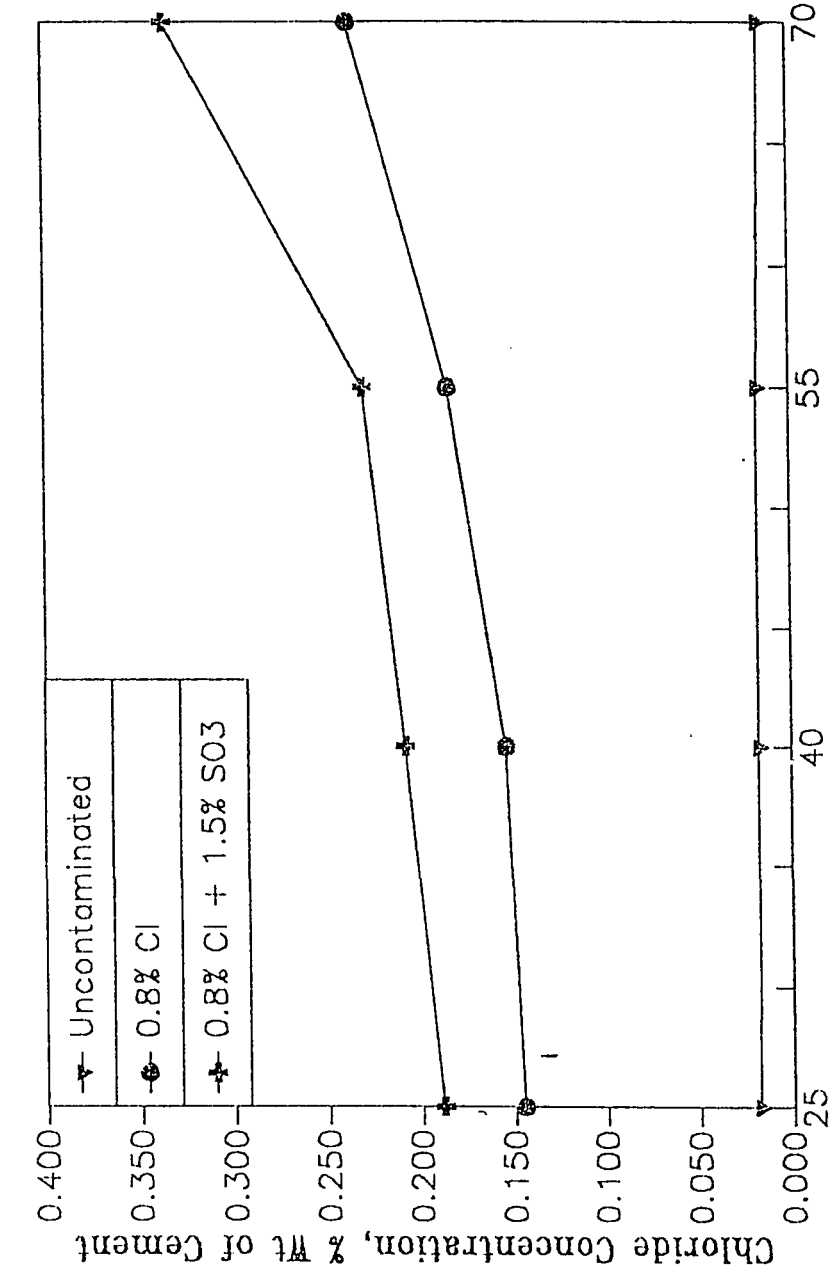

Fig. 4.29 Water Soluble Chlorides in SF Cement Paste Specimens Exposed to Various Temperatures

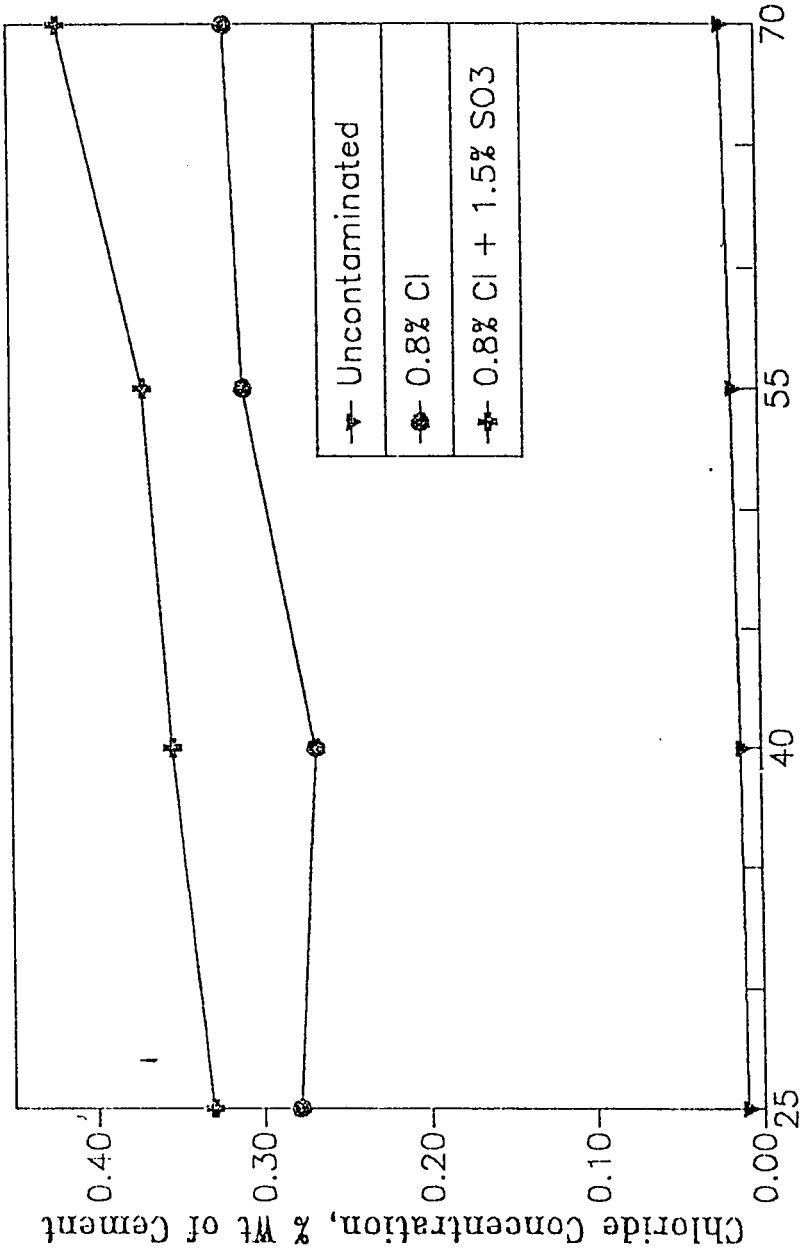

Fig. 4.30 Water Soluble Chlorides in BFS Cement Paste Specimens Exposed to Various Temperatures

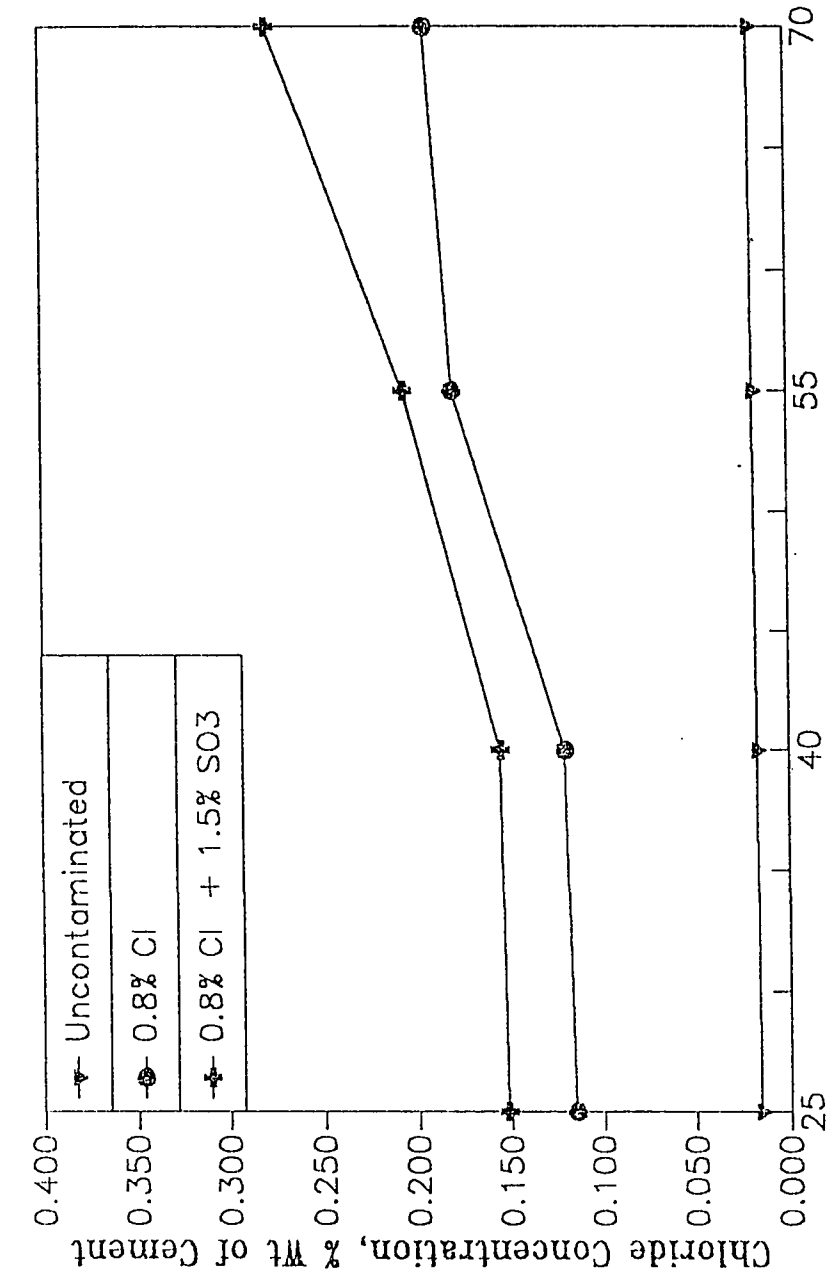

Fig. 4.31 Water Soluble Chlorides in Class F FA Cement Paste Specimens Exposed to Various Temperatures

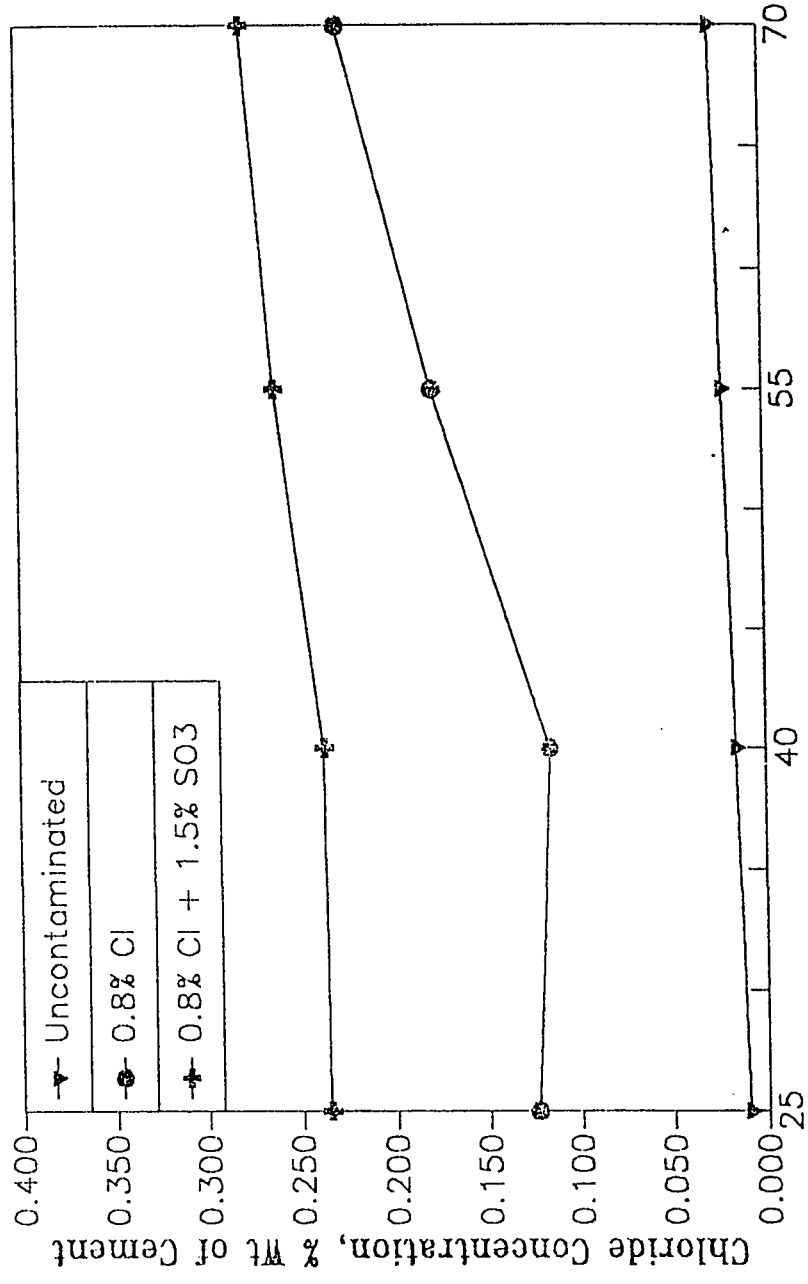

Fig. 4.32 Water Soluble Chlorides in Class C FA Cement Paste Specimens Exposed to Various Temperatures

4.4.3 Cl^-/OH^- Ratio

In spite of their critical importance, chloride concentrations alone do not indicate the corrosion risk. It is now well recognized that depassivation of steel is a function of Cl^-/OH^- ratio in the pore solution rather than the chloride concentration. Hausmann [31] on the basis of mild steel corrosion tests in the concrete simulated artificial $Ca(OH)_2$ solution of pH around 12.5 has proposed a threshold depassivation of Cl^-/OH^- ratio of 0.60.

In a later work, Gouda [33] carried out tests similar to Hausmann's in solutions where maximum NaCl threshold concentrations were evaluated for pH values ranging from 11.8 to 13.95. Diamond [34] has carefully scaled these data and has converted the results into Cl^-/OH^- ratios for easier comparison. These values are given as follows:

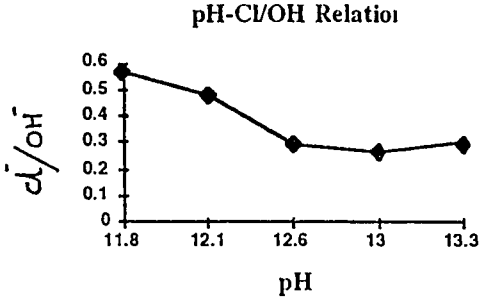

pH	Cl/OH
11.8	0.57
12.1	0.48
12.6	0.29
13.0	0.27
13.3	0.30

The above data suggest that for the actual concrete pore solution which has a pH of 13.3, the critical Cl^-/OH^- ratio is 0.30.

To evaluate the effect of temperature on the Cl^-/OH^- the pH values were converted to OH^- ion concentration by weight of cement. Fig. 4.33 through 4.37 and Tables 4.6 through 4.10 show the effect of temperature on Cl^-/OH^- ratio on various cements.

Fig. 4.33 and Table 4.6 show the effect of temperature on the Cl^-/OH^- ratio in ordinary portland cement paste specimens. The Cl^-/OH^- ratio at 25 °C exposure was more or less similar to that in specimens exposed to 40 °C. However, a steep increase in this value was observed in both the contaminated and uncontaminated specimens beyond 40 °C. Further, at 25 and 40 °C exposure temperatures, the Cl^-/OH^- ratio in both chloride and chloride-sulfate contaminated specimens were more or less the same. However, when the exposure temperature was increased beyond 40 °C, a marked difference between these values was noticeable.

In uncontaminated specimens, the Cl^-/OH^- value at 70 °C was about 4.4 times that at 25 °C. The value of Cl^-/OH^- ratio at 25 and that at 70 °C in chloride and sulfate-chloride contaminated specimens were 8.1 and 4.5 times more than that at 25 °C respectively. The increase in Cl^-/OH^- ratio in chloride contaminated specimens in comparison with those contaminated with chloride-sulfate at 70 °C, per se, may be attributed to the lowering of the OH^- concentration in the former specimens. In the specimens contaminated with chloride and sulfates, both the chloride and OH^- ion concentration are higher than those in specimens contaminated with chlorides alone. Further, the Cl^-/OH^- ion values are higher than the Hausmann's threshold value of 0.6, in specimens contaminated with chloride for exposure temperatures of 55 and 70 °C. Specimens contaminated with chloride and sulfate exhibit a similar higher Cl^-/OH^- value of 0.6 for exposure temperatures of 70 °C. If the Cl^-/OH^- of 0.3, as suggested by Diamond is adopted, contaminated specimens exposed to 55 °C and above form an aggressive environment for reinforcement corrosion.

Fig. 4.34 and Table 4.7 show the Cl^-/OH^- values for contaminated and uncontaminated silica fume cement paste specimens exposed to temperatures in the range of 25-70 °C. The general trend of increase in the Cl^-/OH^- ratio for exposure temperatures of more than 40 °C was observed in chloride contaminated specimens. In sulfate-chloride contaminated specimens, the increase in the Cl^-/OH^- ratio was observed beyond 55 °C temperature. Unlike in the plain cements, the Cl^-/OH^- ratio at 70 °C temperature was observed to be higher in chloride-sulfate contaminated specimens compared to those contaminated with only chloride salts. The Cl^-/OH^- values were more than 0.6 for exposure temperatures of 55 and 70 °C in chloride contaminated specimens and at 70 °C in specimens contaminated with sulfate-chloride salts. The Cl^-/OH^- values in the contaminated specimens were more than 0.30 at all exposure temperatures.

A comparison of data in Figure 4.34 and Table 4.7 with that in Figure 4.33 and Table 4.6 indicates that the Cl^-/OH^- values in silica fume cement paste specimens were higher than those in ordinary portland cement paste specimens. The average increase in the Cl^-/OH^- values was 0.02, 0.39, and 0.582 in uncontaminated, chloride and sulfate-chloride contaminated specimens respectively. The increase in the Cl^-/OH^- ratio in the silica fume cement paste specimens compared to plain paste specimens, at 25 °C temperature has also been reported by several investigators [5,106,111,113].

The Cl^-/OH^- values for blast furnace slag cement paste specimens are plotted against exposure temperature in Figure 4.35 and Table 4.8 shows these values. These curves indicate an increase in the Cl^-/OH^- value with increasing temperature in specimens contaminated with chloride and sulfate-chloride.

The Cl^-/OH^- ratio at 70 °C was 5, 2.8 and 3.6 times that at 25 °C in non-contaminated, chloride and sulfate-chloride contaminated specimens. Compared to plain cements, the average increase in Cl^-/OH^- ratio in the BFS cement was 0.11, 2.11 and 2.47 in non-contaminated, chloride and sulfate-chloride contaminated specimens

respectively. The Cl^-/OH^- ratio were more than 0.6 in the contaminated specimens, at all the temperatures, while they were more than 0.3 in the uncontaminated specimens at 55 and 70 °C exposure. The increased Cl^-/OH^- ratios in BFS cements is indicative of the highly aggressive chemical environment in terms of reinforcement corrosion. These data are in good agreement with that reported by others [3,27], for 25 °C exposure.

The Cl^-/OH^- values were observed to increase with the exposure temperature in fly ash-F cement paste specimens also (Fig. 4.36, Table 4.9). The increase was more apparent for exposure temperatures beyond 40 °C both for uncontaminated and contaminated specimens. The average increase in Cl^-/OH^- values compared to plain cements was 0.313, 0.325 and 0.209 in uncontaminated, chloride and sulfate-chloride contaminated specimens, respectively. The Cl^-/OH^- values in the uncontaminated, chloride, and chloride-sulfate contaminated specimens at 70 °C were 5.2, 3.1 and 3.2 times to those in corresponding specimens cured at 25 °C. The Cl^-/OH^- values were more than 0.6 in chloride and chloride-sulfate contaminated specimens subjected to exposure temperature of more than 55 °C. In uncontaminated specimens, the Cl^-/OH^- value crossed the 0.6 threshold line for exposure temperature of 70 °C. The reduction in the Cl^-/OH^- ratio is attributable to the reduction in the OH^- ion concentration and increase in the chloride ion concentration.

The Cl^-/OH^- values for the contaminated specimens were more than 0.3 for all exposure temperatures. The Cl^-/OH^- values for uncontaminated specimens were more than this threshold value, i.e., 0.3, for exposure temperatures of 55 °C and above. These results are in good agreement with the data reported by Kawamura et al [112], Holden et al [3], Hussain [111] and Al-Amoudi [114] for 25 °C exposure.

Fig. 4.37 and Table 4.10 show the effect of temperature and chloride and chloride-sulfate contamination on the Cl^-/OH^- values in fly ash-C cement paste specimens. A drastic increase in the Cl^-/OH^- value for exposure temperatures greater than 55 °C was

observed in all the specimens. At 70 °C, the Cl^-/OH^- values in the chloride and sulfate-chloride contaminated specimens was 12.1 and 2.26 times that in similar specimens exposed to 25 °C. Also, at 70 °C, the Cl^-/OH^- value in uncontaminated specimens was similar to that in chloride contaminated specimen. The Cl^-/OH^- values were more than 0.6 for exposure temperatures of 55 and 70 °C, for chloride-sulfate, chloride and uncontaminated specimens, respectively. The Cl^-/OH^- value in chloride contaminated specimens were more than 0.3 for exposure temperatures of 40 °C and above. The Cl^-/OH^- values were more than 0.3 in specimens contaminated with chloride-sulfate at all exposure temperatures. In uncontaminated specimens, the Cl^-/OH^- value was more than 0.3 for exposure temperature of 70 °C.

TABLE 4.6 Cl^-/ OH^- Ratio of OPC With and Without Contamination
(Cl^- and OH^- Ion Concentrations are in % by weight of Cement)

	25 °C			40 °C			55 °C			70 °C		
	Cl^-	OH^-	Cl/OH	Cl^-	OH^-	Cl/OH	Cl^-	OH^-	Cl/OH	Cl^-	OH^-	Cl/OH
OPC	0.17	0.409	0.0416	0.019	0.377	0.049	0.019	0.260	0.074	0.021	0.114	0.184
OPC + 0.8% Cl^-	0.148	0.619	0.239	0.149	0.555	0.268	0.179	0.282	0.636	0.227	0.118	1.917
OPC +0.8% Cl^- + 1.5%SO_3	0.160	0.727	0.220	0.182	0.656	0.291	0.209	0.560	0.374	0.253	0.257	0.981

TABLE 4.7 Cl^-/ OH^- Ratio of Silica Fume Blended Cements
(Cl^- and OH^- ion concentrations are in % by weight of Cementiious material)

	25 °C			40 °C			55 °C			70 °C		
	Cl^-	OH^-	Cl /OH	Cl^-	OH^-	Cl /OH	Cl^-	OH^-	Cl /OH	Cl^-	OH^-	Cl /OH
10% SF	0.018	0.325	0.055	0.018	0.283	0.062	0.017	0.171	0.102	0.016	0.073	0.213
10% SF + 0.8% Cl^-	0.145	0.349	0.416	0.154	0.315	0.489	0.184	0.182	1.011	0.237	0.088	2.707
10% SF +0.8%Cl^- + 1.5%SO3	0.180	0.619	0.304	0.208	0.555	0.375	0.230	0.498	0.462	0.335	0.110	3.052

TABLE 4.8 Cl^-/OH^- Ratio of Blast Furnace Slag Blended Cements
(Cl^- and OH^- Ion concentrations are in % by Weight of Cementitious Material)

	25 °C			40 °C			55 °C			70 °C		
	Cl^-	OH^-	Cl/OH	Cl^-	OH^-	Cl/OH	Cl^-	OH^-	Cl/OH	Cl^-	OH^-	Cl/OH
70% BFS	0.01	0.141	0.071	0.012	0.112	0.103	0.016	0.067	0.237	0.021	0.059	0.355
70% BFS + 0.8% Cl^-	0.278	0.171	1.632	0.267	0.137	1.956	0.309	0.094	3.300	0.319	0.069	4.600
70% BFS +0.8%Cl^- + 1.5%SO_3	0.330	0.220	1.503	0.354	0.168	2.104	0.370	0.136	2.727	0.420	0.077	5.430

TABLE 4.9 Cl^-/OH^- Ratio of Class F Fly ash Blended Cements
(Cl^- and OH^- Ion Concentrations are in % by Weight of Cementitious Material)

	25 °C			40 °C			55 °C			70 °C		
	Cl^-	OH^-	Cl/OH	Cl^-	OH^-	Cl/OH	Cl^-	OH^-	Cl/OH	Cl^-	OH^-	Cl/OH
20% FA-F	0.016	0.108	0.149	0.017	0.085	0.199	0.018	0.038	0.477	0.019	0.026	0.774
20% FA-F + 0.8% Cl^-	0.115	0.276	0.416	0.120	0.226	0.531	0.180	0.186	0.966	0.194	.0135	1.433
20% FA-F + 0.8%Cl^- + 1.5% SO_3	0.152	0.391	0.389	0.155	0.352	0.440	0.206	0.325	0.634	0.278	0.225	1.238

TABLE 4.10 Cl^-/ OH^- Ratio of Class C Fly ash Blended Cements
(Cl^- and OH^- Ion Concentrations are in % by Weight of Cementitious Material)

	25 °C			40 °C			55 °C			70 °C		
	Cl^-	OH^-	Cl/OH	Cl^-	OH^-	Cl/OH	Cl^-	OH^-	Cl/OH	Cl^-	OH^-	Cl/OH
20% FA-C	0.010	0.276	0.036	0.016	0.258	0.061	0.216	0.169	0.128	0.026	0.028	0.934
20% FA-C + 0.8% Cl^-	0.124	0.515	0.241	0.116	0.335	0.346	0.178	0.215	0.830	0.227	0.078	2.914
20% FA-C + 0.8%Cl^- + 1.5% SO_3	0.235	0.552	0.426	0.237	0.516	0.460	0.262	0.492	0.533	0.278	0.289	0.963

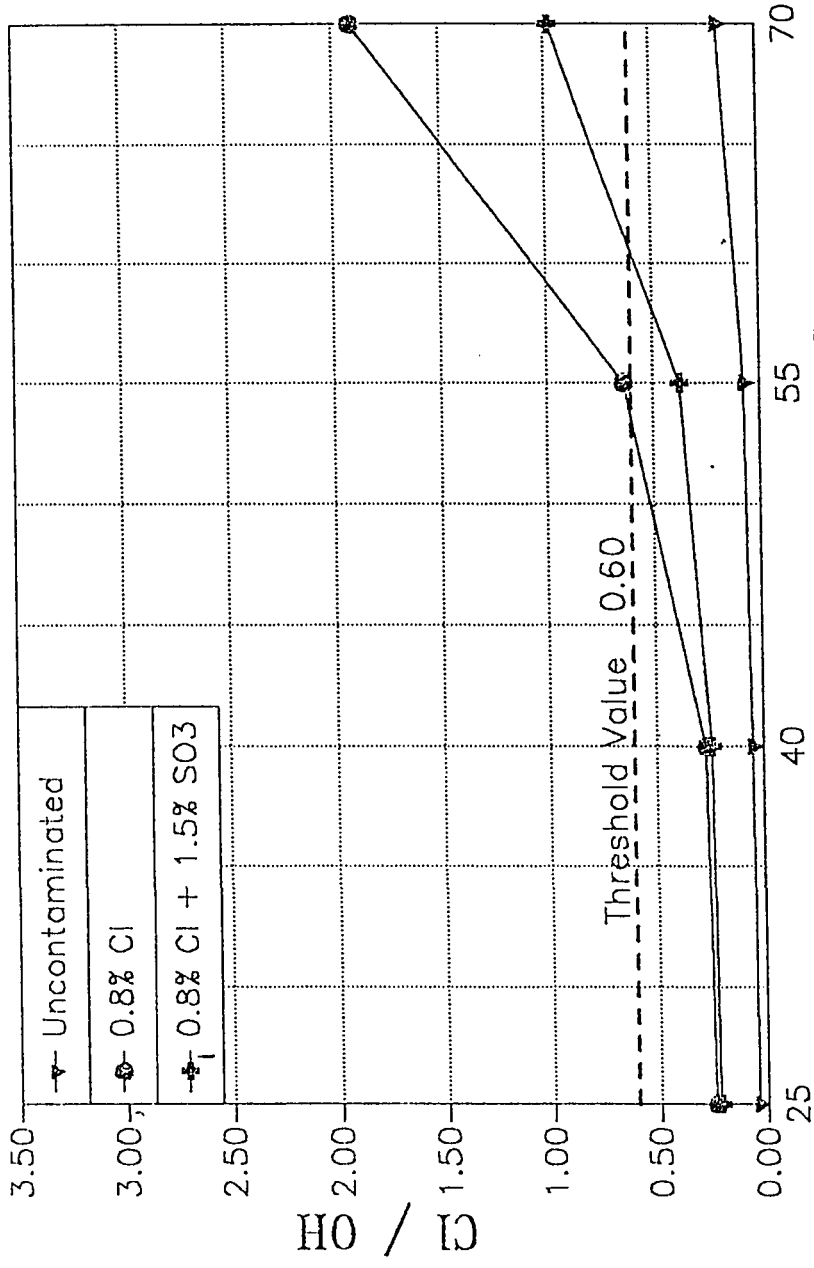

Fig. 4.33 Effect of Temperature on Cl^-/OH^- Ratio in OPC Paste Specimens With and Without Contamination

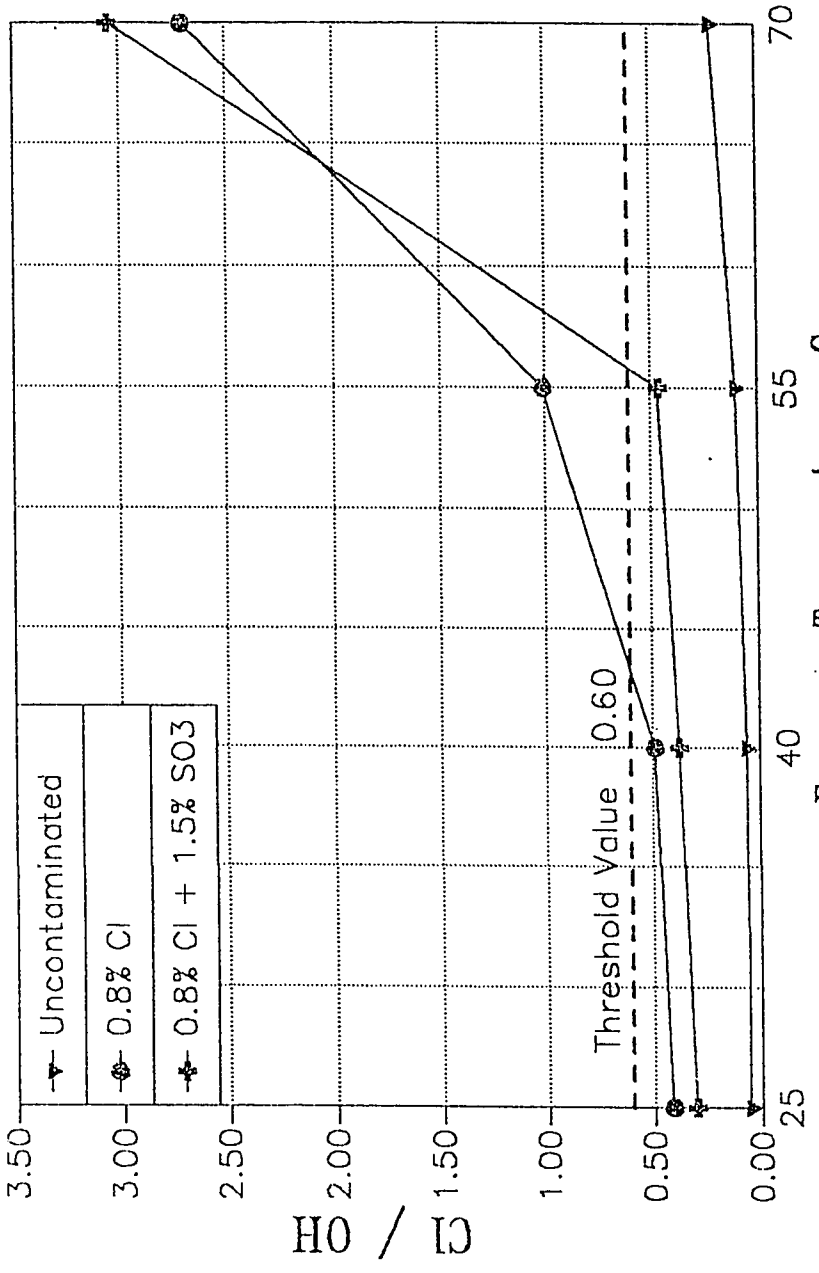

Fig. 4.34 Effect of Temperature on Cl-/OH- Ratio in SF Cement Pastes With and Without Contamination

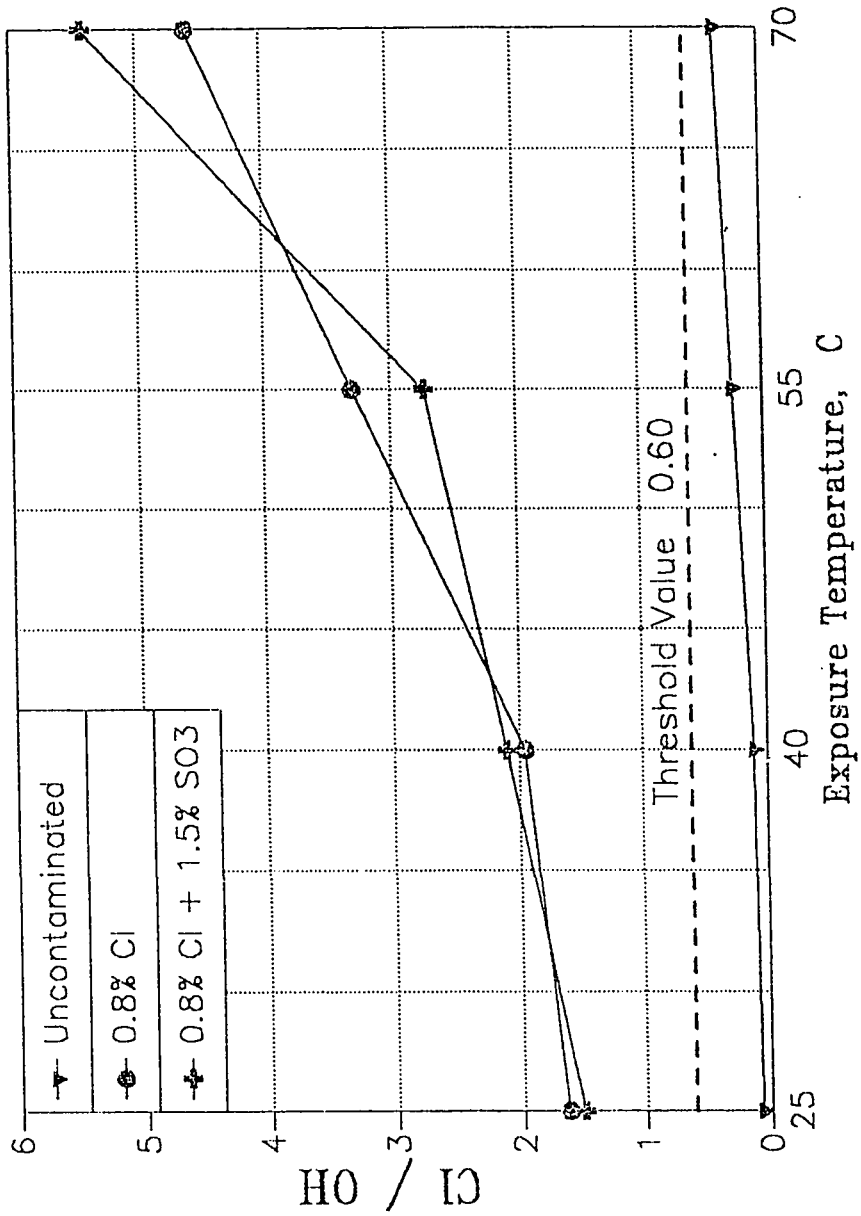

Fig. 4.35 Effect of Temperature on Cl⁻/OH⁻ Ratio in BFS Cement Pastes With and Without Contamination

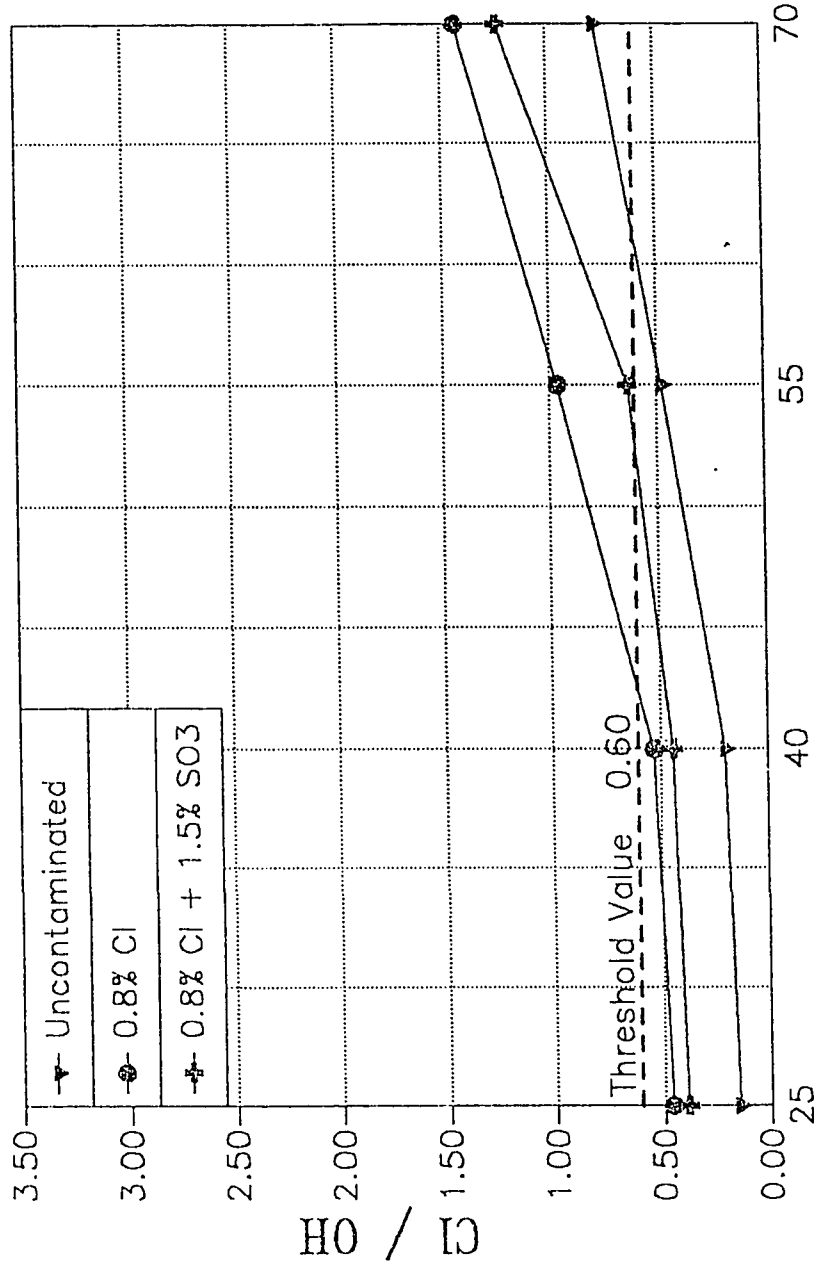

Fig. 4.36 Effect of Temperature on Cl-/OH- Ratio in Class F FA Cement Paste Specimens With and Without Contamination

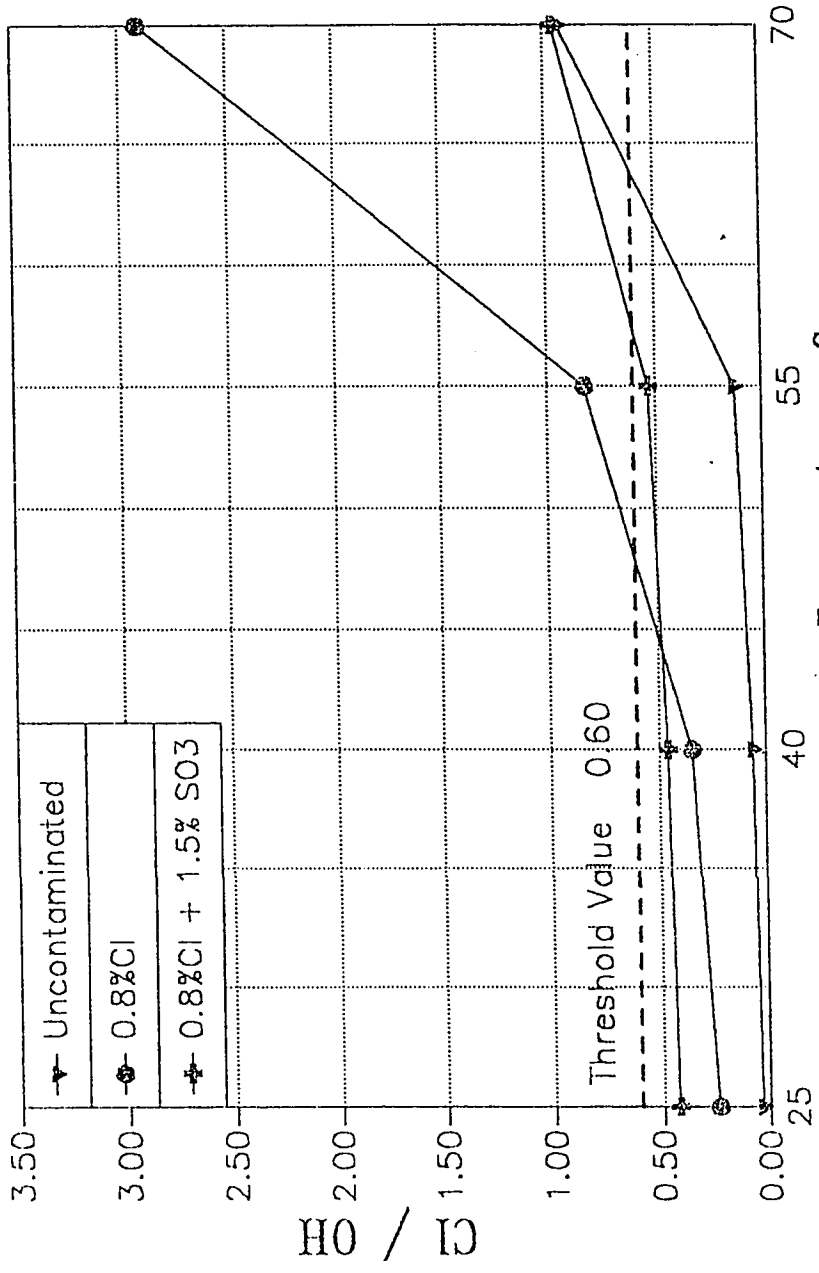

Fig. 4.37 Effect of Temperature on Cl⁻/OH⁻ Ratio in Class C FA Cement Paste Specimens With and Without Contamination

4.4.4 Sulfate Ion Concentration

The effect of temperature on water soluble sulfate concentration in the ordinary portland cement paste specimens are plotted in Figure 4.38. The sulfate concentration in specimens contaminated with chloride-sulfate increased almost linearly with temperature. The sulfate concentration in these specimens at 70 °C exposure were 4.25 times the sulfate concentration at 25 °C. The increase in the sulfate ion concentration was more pronounced beyond 40 °C. The water soluble sulfate ion concentration in silica fume cement paste specimens is plotted against exposure temperature in Fig. 4.39. These data also indicate a significant increase in the sulfate concentration for exposure temperature of more than 40 °C. The sulfate concentration at 55 and 70 °C temperature, however, remains nearly same at 0.63 and 0.61% by weight of cement. These concentrations were nearly three times the concentration at 25 °C. Also, the sulfate concentration in silica fume cement paste specimens were on an average 0.12% (by weight of cement) more than that in OPC.

The sulfate concentration in the blast furnace slag cement paste specimens (Figure 4.40) was also more than that in the plain cement paste specimens. The average increase in the sulfate concentration was about 0.32%. The data in Fig. 4.40 show a trend similar to that indicated by silica fume blended cements. The sulfate ion concentration in the specimens exposed to 70 °C was 4.6 times that in specimens exposed to 25 °C.

The sulfate ion concentration in both Class F fly ash (Fig. 4.41) and Class C fly ash (Fig. 4.42) cement paste specimens increased with exposure temperature. As in other cements, the increase in the sulfate concentration was more significant for temperature beyond 40 °C. The sulfate ion concentration in the specimens exposed to 70 °C was on an average 6.6 times that in specimens exposed to 25 °C.

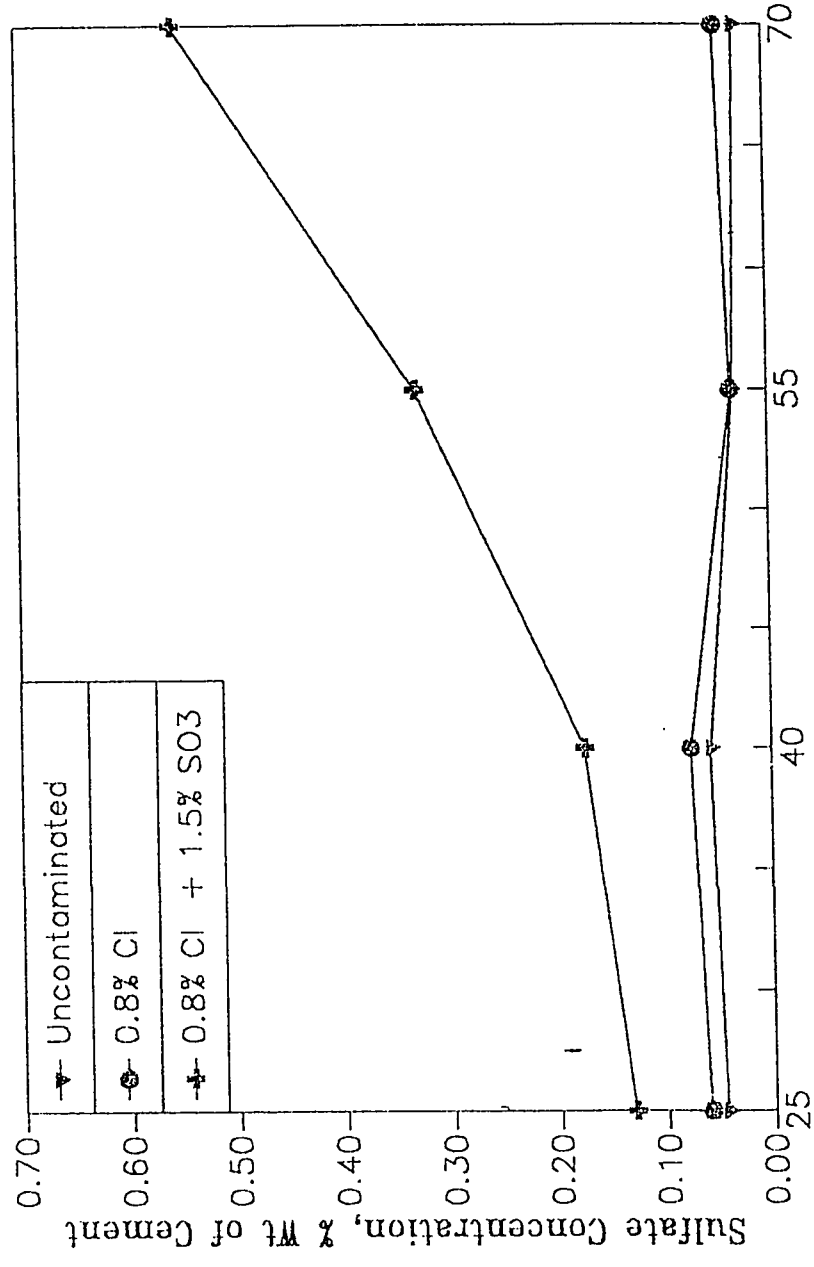

Fig. 4.38 Water Soluble Sulfates in OPC Paste Specimens Exposed To Varying Temperatures.

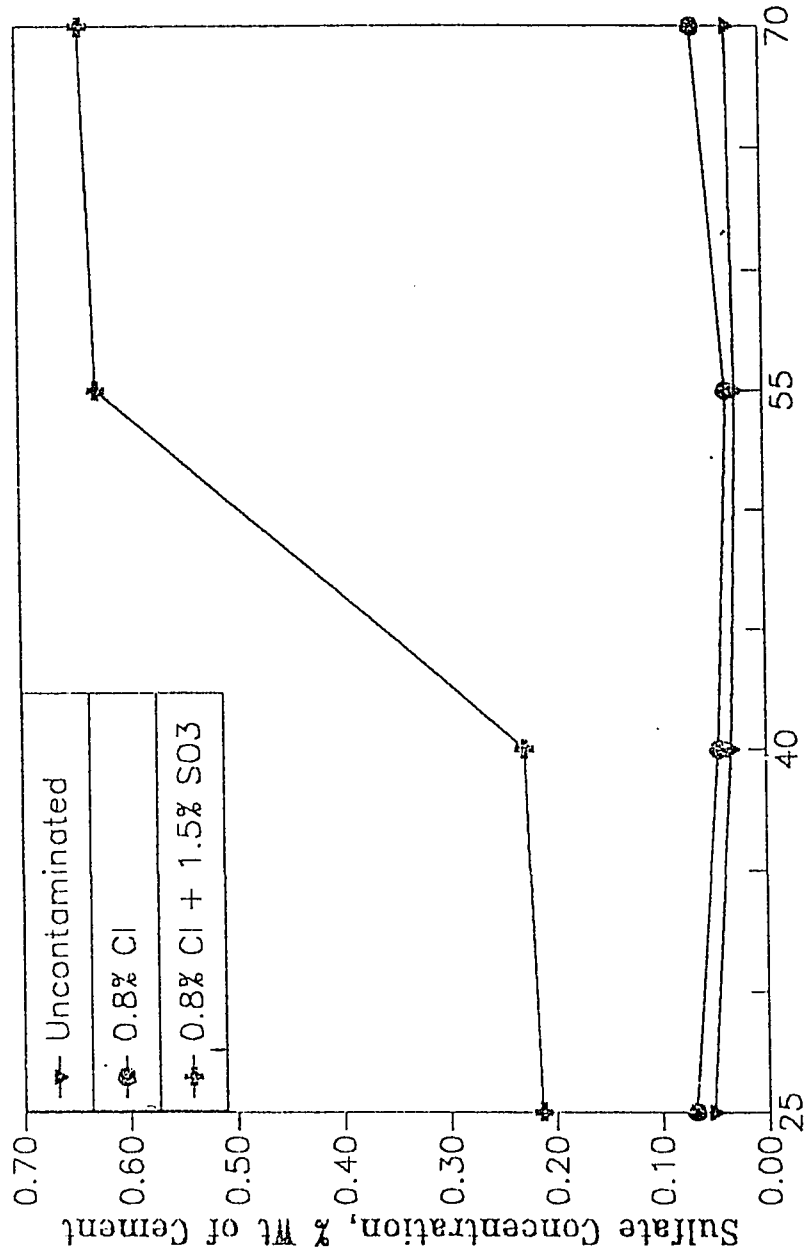

Fig. 4.39 Water Soluble Sulfates in SF Cement Paste Specimens Exposed to Varying Temperatures

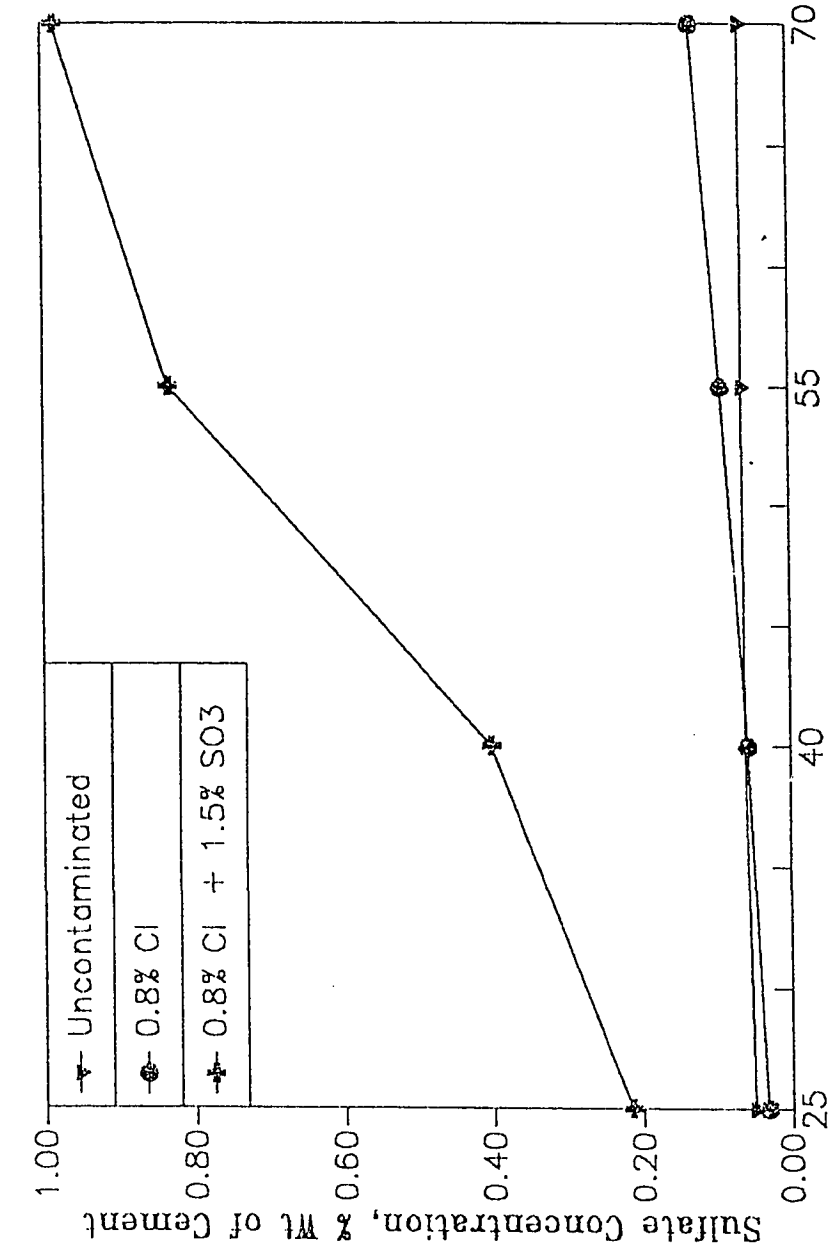

Fig. 4.40 Water Soluble Sulfates in BFS Cement Paste Specimens Exposed to Varying Temperatures

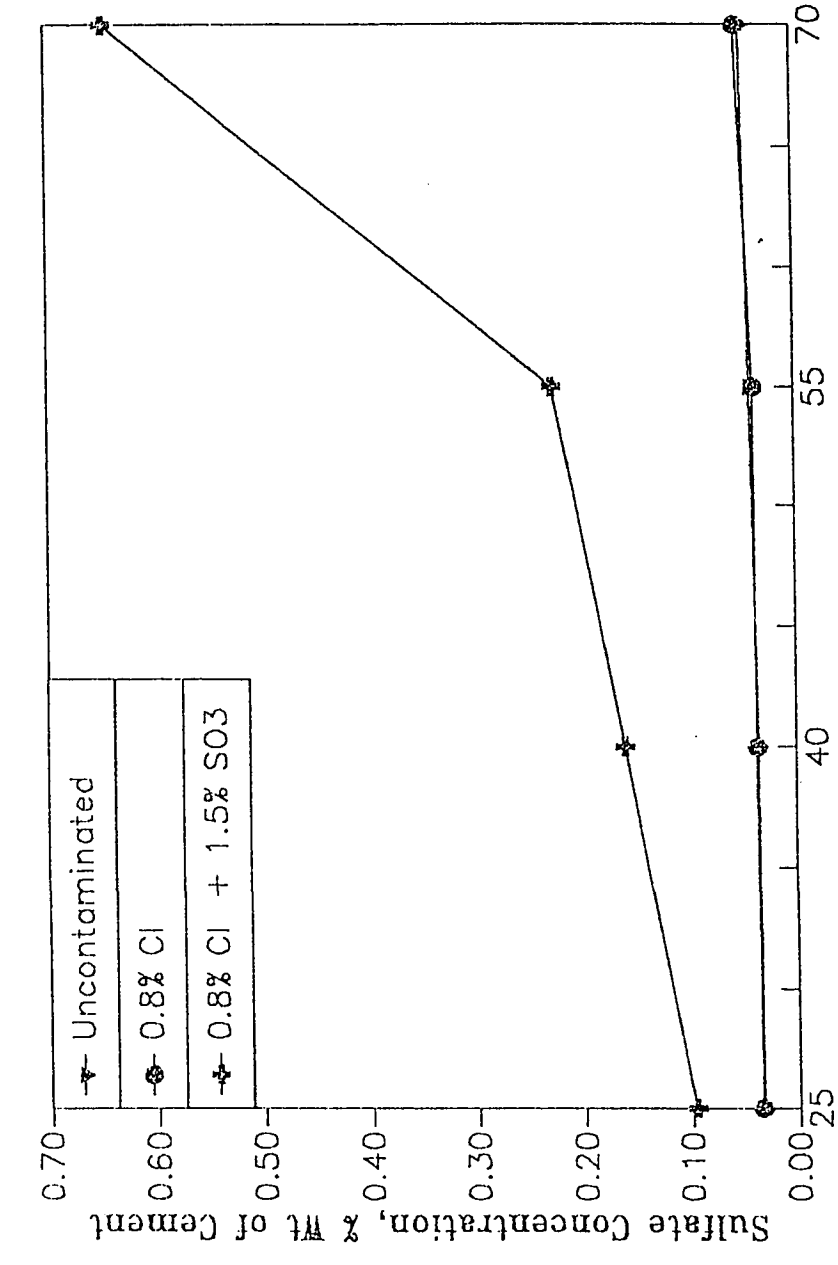

Fig. 4.41 Water Soluble Sulfates in Class F FA Cement Paste Specimens Exposed to Varying Temperatures

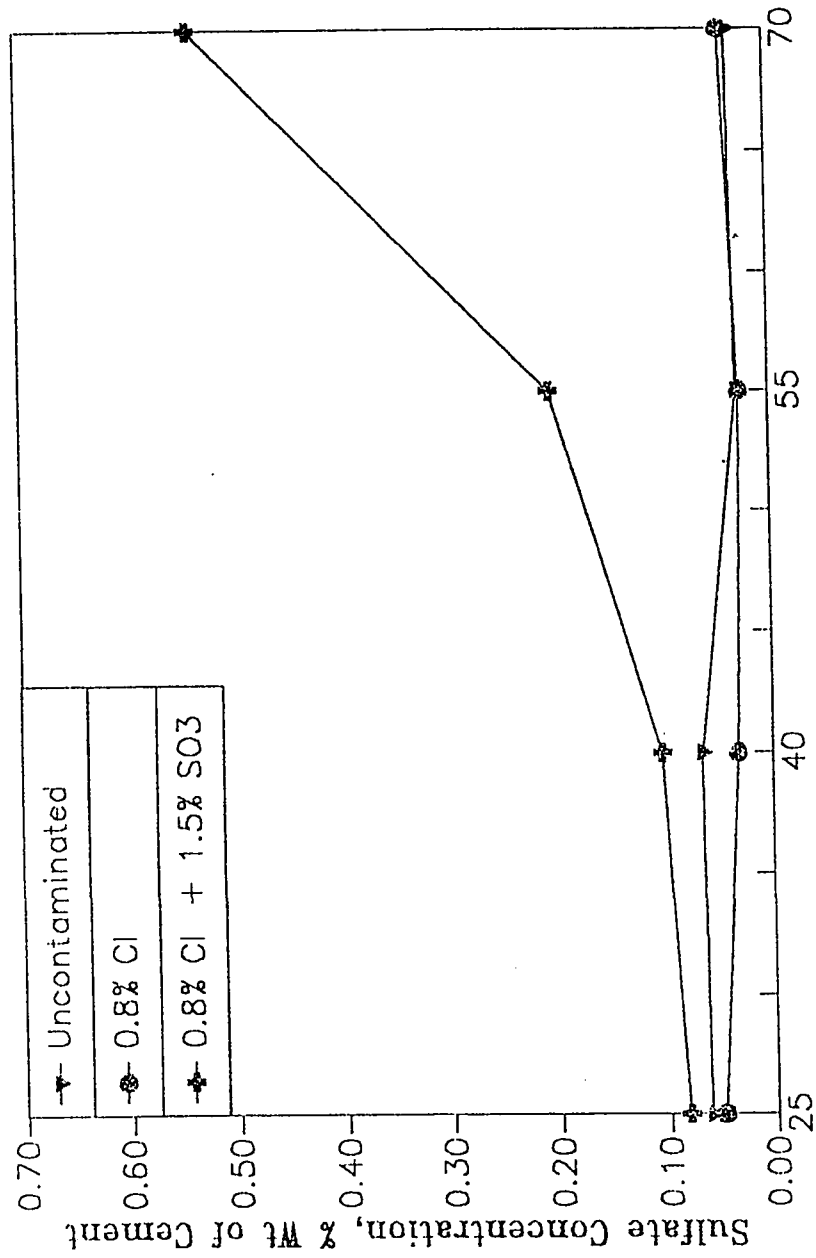

Fig. 4.42 Water Soluble Sulfates in Class C FA Cement Paste Specimens Exposed to Varying Temperatures

The data on sulfate ion concentration in all the cements (Figures 4.38 to 4.42) indicate that a significant quantum approximately 30-80% is liberated for exposure temperatures of more than 40 °C. This increase in the unbound or free sulfate concentration due to elevated temperature has a negative effect on concrete in that it reduces the electrical resistivity of concrete, and also sulfates may react with steel. The increase in the sulfate ion concentration in all the specimens with increase in the temperature indicates that at higher temperatures the reaction between C_3A and SO_4 is inhibited.

4.5 EFFECT OF TEMPERATURE AND SALT CONTAMINATION ON REINFORCEMENT CORROSION IN PLAIN AND BLENDED CEMENT CONCRETES

The effect of salt contamination and temperature on reinforcement corrosion was evaluated by measuring corrosion potentials and corrosion current density at regular intervals. The corrosion potentials were monitored using a high impedance voltmeter and saturated calomel electrode, while the corrosion current density was measured using linear polarization resistance technique using a Potentiostat/Galvanostat. The details of these two test methods of measurements have been discussed in Chapter 3.

4.5.1 Corrosion Potentials

The corrosion potentials for steel in ordinary portland cement concrete specimens are shown in Fig. 4.43 to 4.45. The corrosion potentials of uncontaminated specimens (Fig. 4.43) were less than the ASTM C 876 threshold of -270 mV SCE. Further, the corrosion potentials of steel in specimens exposed to 25 and 40 °C were more or less similar, particularly after about 150 days of exposure. The corrosion potentials of steel in concrete specimens exposed to 55 and 70 °C were more positive than those exposed to 25 and 40 °C.

The corrosion potentials of steel in ordinary portland cement concrete specimen

contaminated with chloride salts and exposed to temperatures in the range of 25 to 70 °C are shown in Fig. 4.44. The corrosion potentials of steel in concrete specimens exposed to 40 °C were less than -270 mV SCE at all the exposure periods. The corrosion potentials of steel specimens exposed to 25, 55 and 70 °C were generally more positive than the threshold potentials. The corrosion potentials of steel in ordinary portland cement concrete specimens contaminated with chloride and sulfate salts and exposed to 25, 40, 55 and 70 °C temperatures are shown in Fig. 4.45. The corrosion potentials of steel in specimens exposed to 25 and 40 °C were more negative than -270 mV SCE. The corrosion potentials of steel in specimens exposed to 55 and 70 °C tend to be more positive than -270 mV SCE. The corrosion potentials of steel in concrete specimens exposed to 70 °C were more positive than those exposed to 55 °C.

The corrosion potentials of steel in silica fume cement concrete specimens are shown in Fig. 4.46 to 4.48. These data show a trend similar to that shown in Fig. 4.43 to 4.45.

The corrosion potentials of steel in Class F fly ash cement in which 20% ASTM C 618 Class F fly ash was replaced with cement, concrete specimens is shown in Figures 4.49 to 4.51. These data also show a trend similar to that in Figures 4.46 to 4.48, except that specimens contaminated with chlorides ions and exposed to 55 °C were more negative than -270 mV SCE after about 225 days of exposure. Similarly, the corrosion potentials of steel in specimens contaminated with chloride and sulfate salts crossed the threshold line after about 50 days of exposure. The corrosion potentials of steel in concrete specimens, contaminated with chloride and chloride plus sulfate salts and exposed to 70 °C were more positive than -270 mV SCE.

The corrosion potentials of steel in Class C fly ash cement, in which 20% cement was replaced with ASTM C618 Class C fly ash, concrete specimens is shown in Fig. 4.52 to 4.54. Fig. 4.52 shows the corrosion potentials of steel in uncontaminated concrete specimens. The corrosion potentials of steel in specimens exposed to all the

temperatures were positive than -270 mV SCE. The potentials of steel in specimens exposed to 40 °C were negative than those exposed to 25 °C. The corrosion potentials of steel in concrete specimens exposed to 55 and 70 °C were more positive than those exposed to 40 and 25 °C. The corrosion potentials of steel in concrete specimens contaminated with chloride salts and exposed to 40 °C were less than -270 mV SCE after about 50 days of exposure. The corrosion potentials of steel in concrete specimens exposed to 25, 55 and 70 °C tend to be more positive than -270 mV SCE, the potentials increasing with increasing temperature.

The corrosion potentials of steel in class C fly ash blended cement concrete specimens contaminated with chloride and sulfate salts are shown in Fig. 4.54. The potentials of steel in concrete specimens exposed 25, 40 and 55 °C are more negative and potentials in specimens exposed to 70 °C remain above the threshold line.

The corrosion potentials of steel in BFS cement concrete specimens are plotted in Fig. 4.55 to 4.57. These curves show a trend more or less similar to that in Fig. 4.52 to 4.54. The corrosion potential data shown in Fig. 4.43 to 4.57 for steel in plain and blended cement concrete specimens indicate the following general trend.

1. The corrosion potentials of steel in all the uncontaminated concrete specimens tend to be more positive than -270 mV SCE.

2. The corrosion potentials of steel in concrete specimens contaminated with chloride ions are more negative than those on steel in uncontaminated concrete specimens.

3. The corrosion potentials of steel in concrete specimens contaminated with chloride and sulfate salts tend to be more negative than -270 mV SCE and more negative than on steel in concrete specimens contaminated with only chloride salts.

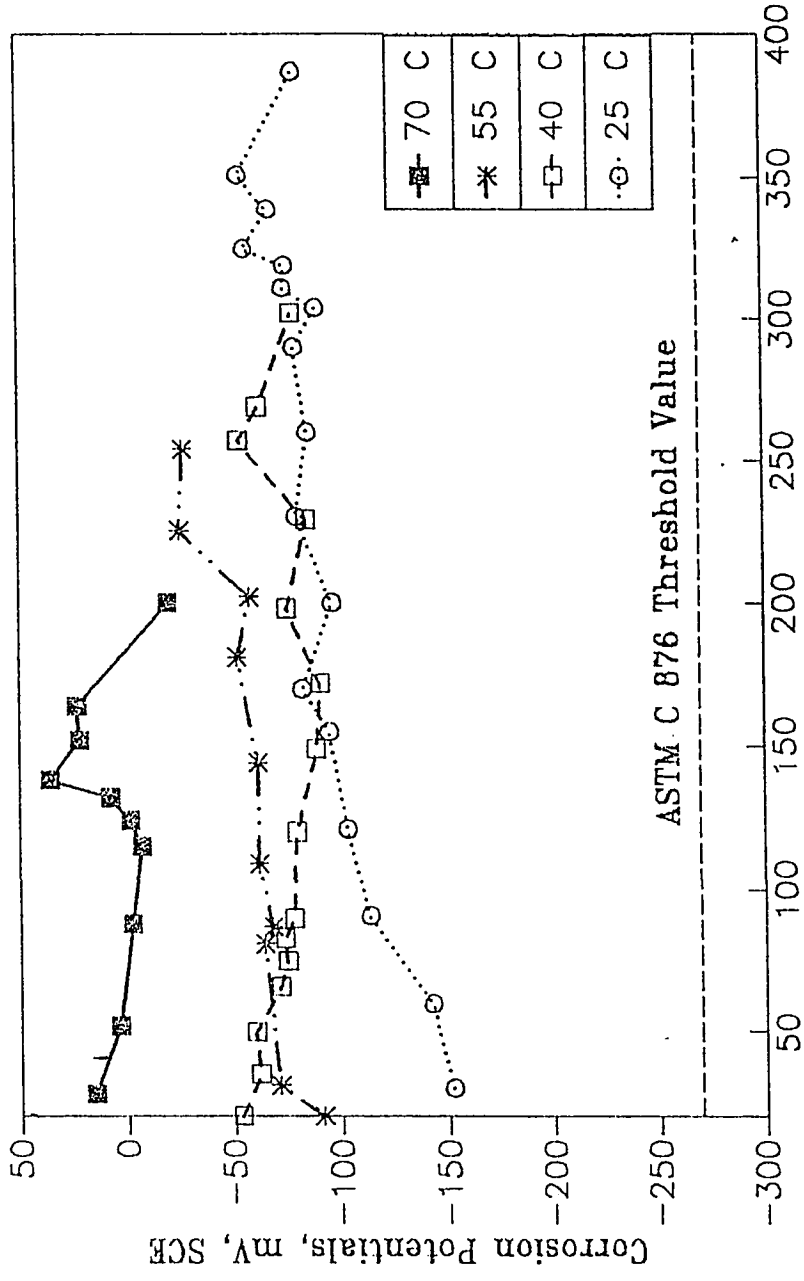

Fig. 4.43 Corrosion Potentials on Steel in OPC Concrete Specimens Exposed to Varying Temperatures

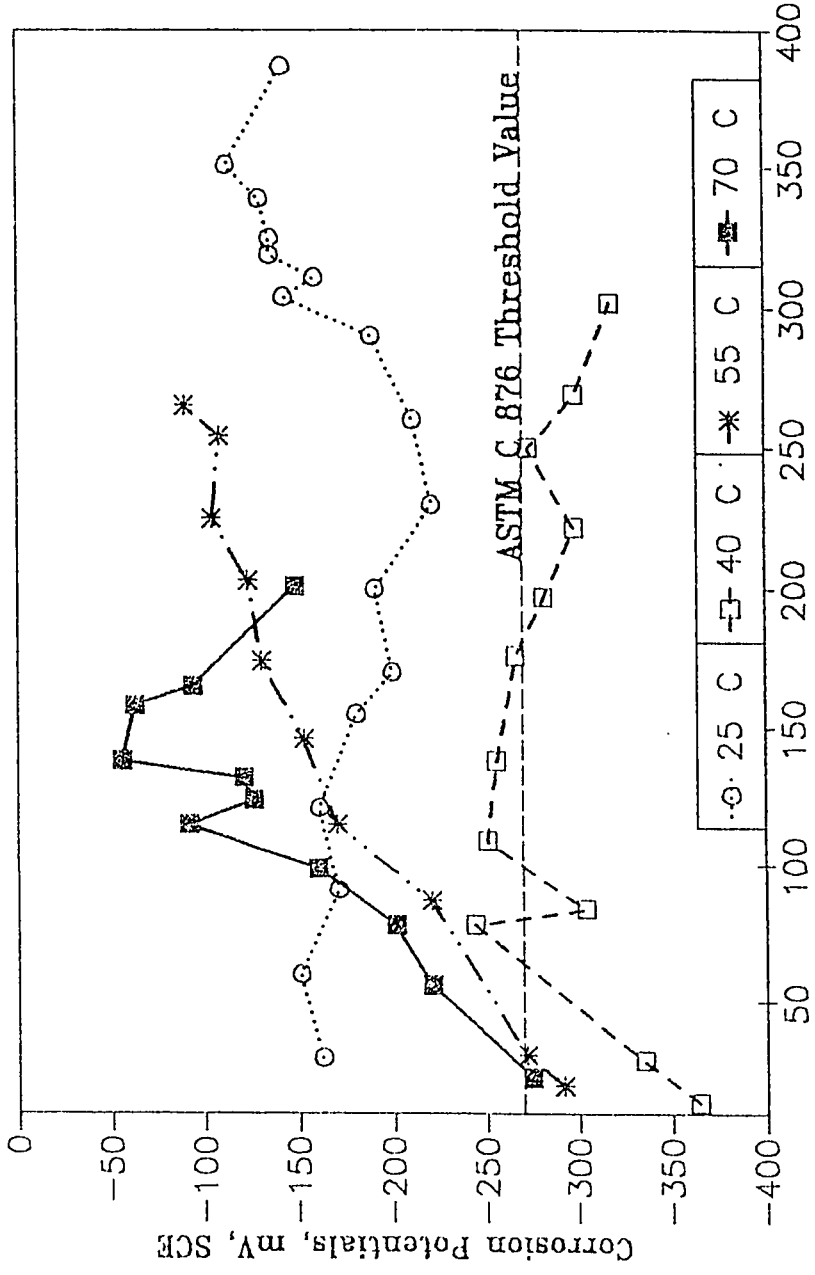

Fig. 4.44 Corrosion Potentials on Steel in OPC Concrete Specimens Contaminated With Chlorides and Exposed to Varying Temperatures

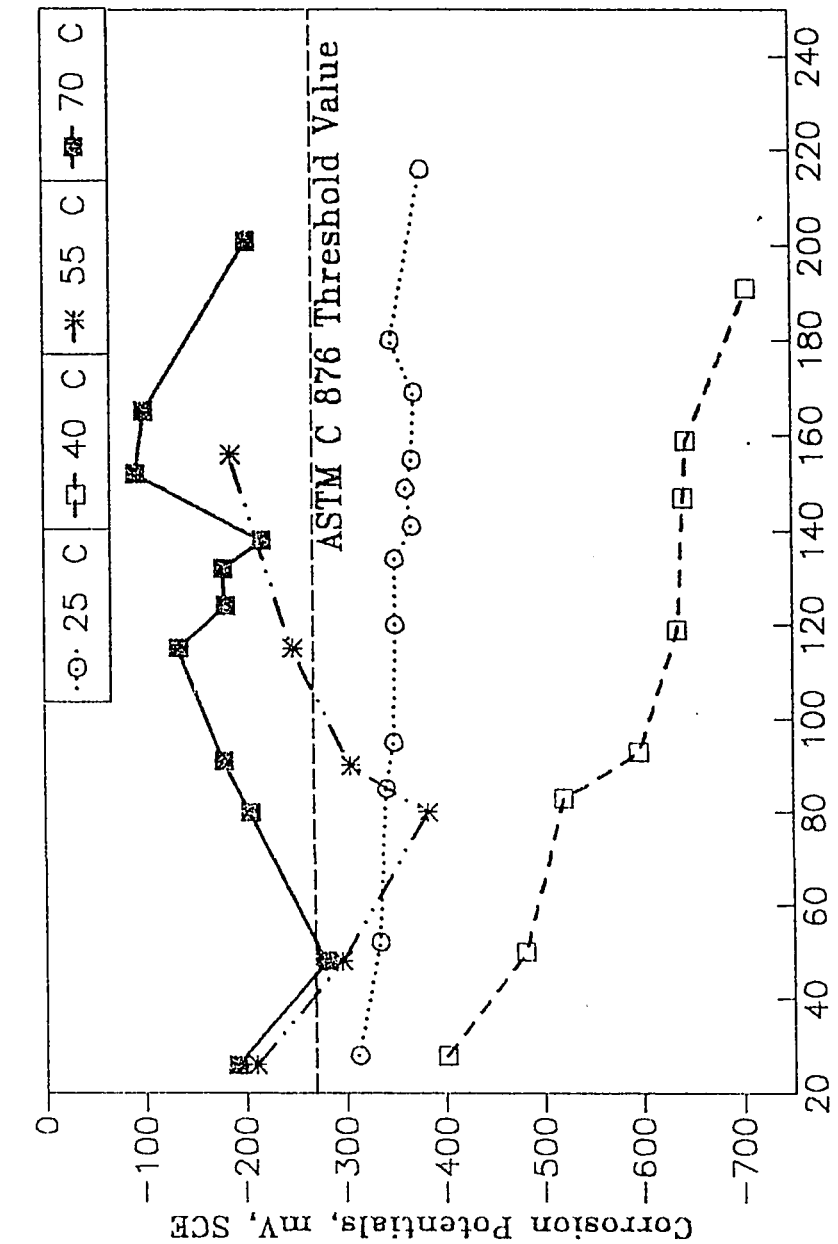

Fig. 4.45 Corrosion Potentials on Steel in OPC Concrete Specimens Contaminated With Chlorides and Sulfates and Exposed to Varying Temperatures

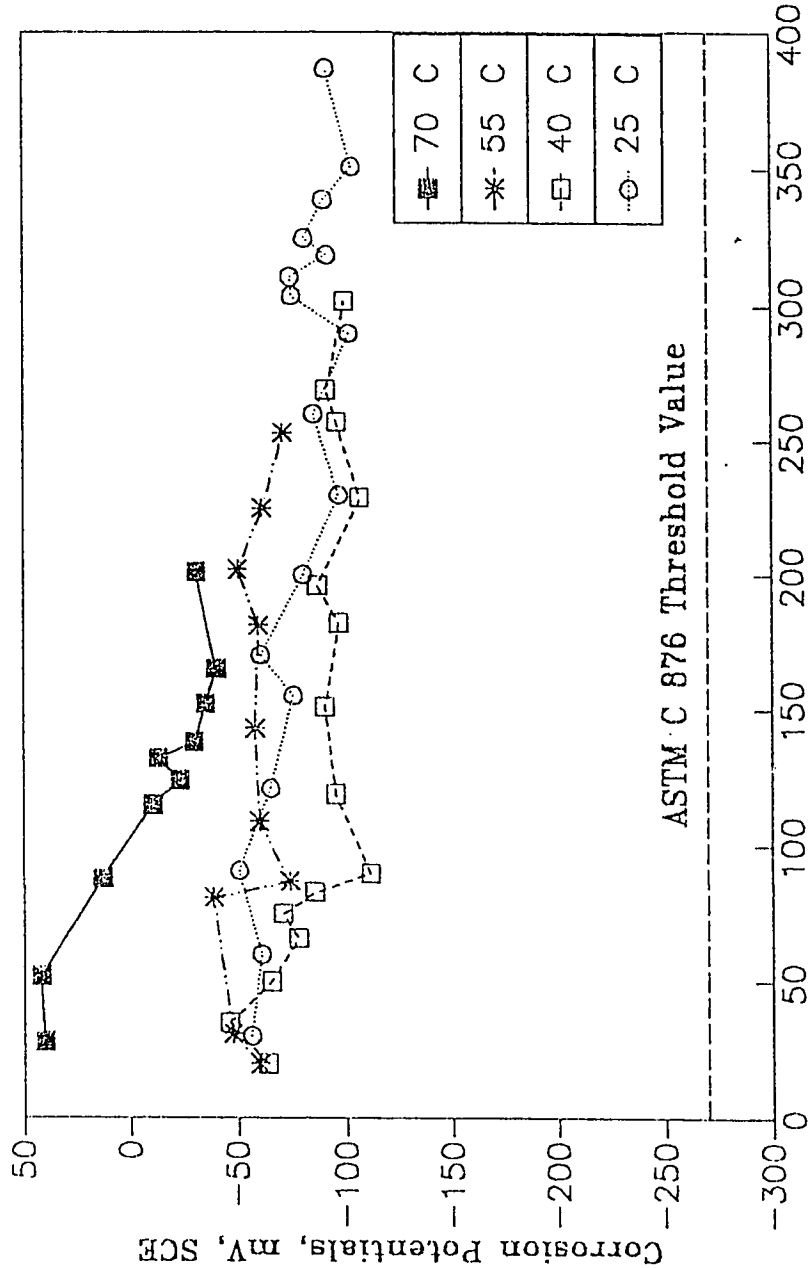

Fig. 4.46 Corrosion Potentials on Steel in SF Cement Concrete Specimens Exposed to Varying Temperatures

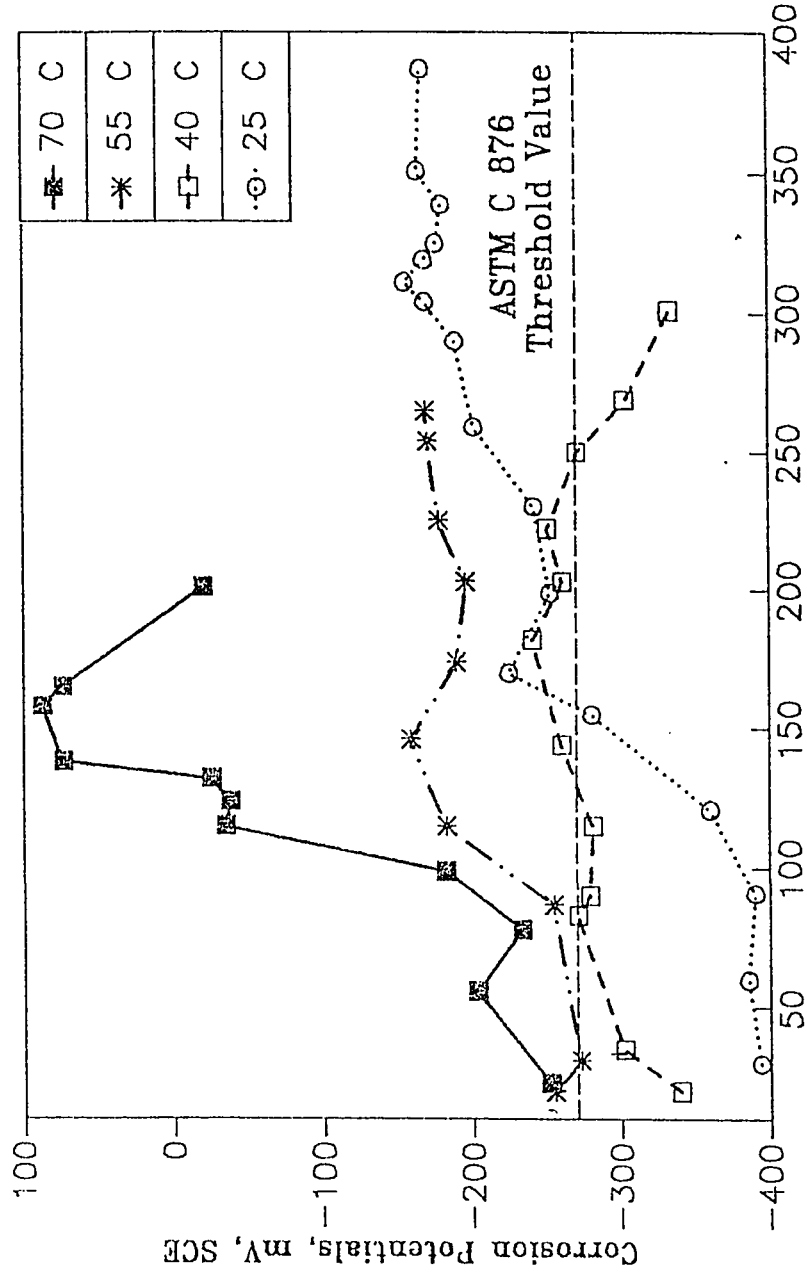

Fig. 4.47 Corrosion Potentials on Steel in SF Cement Concrete Specimens Contaminated With Chlorides and Exposed to Varying Temperatures

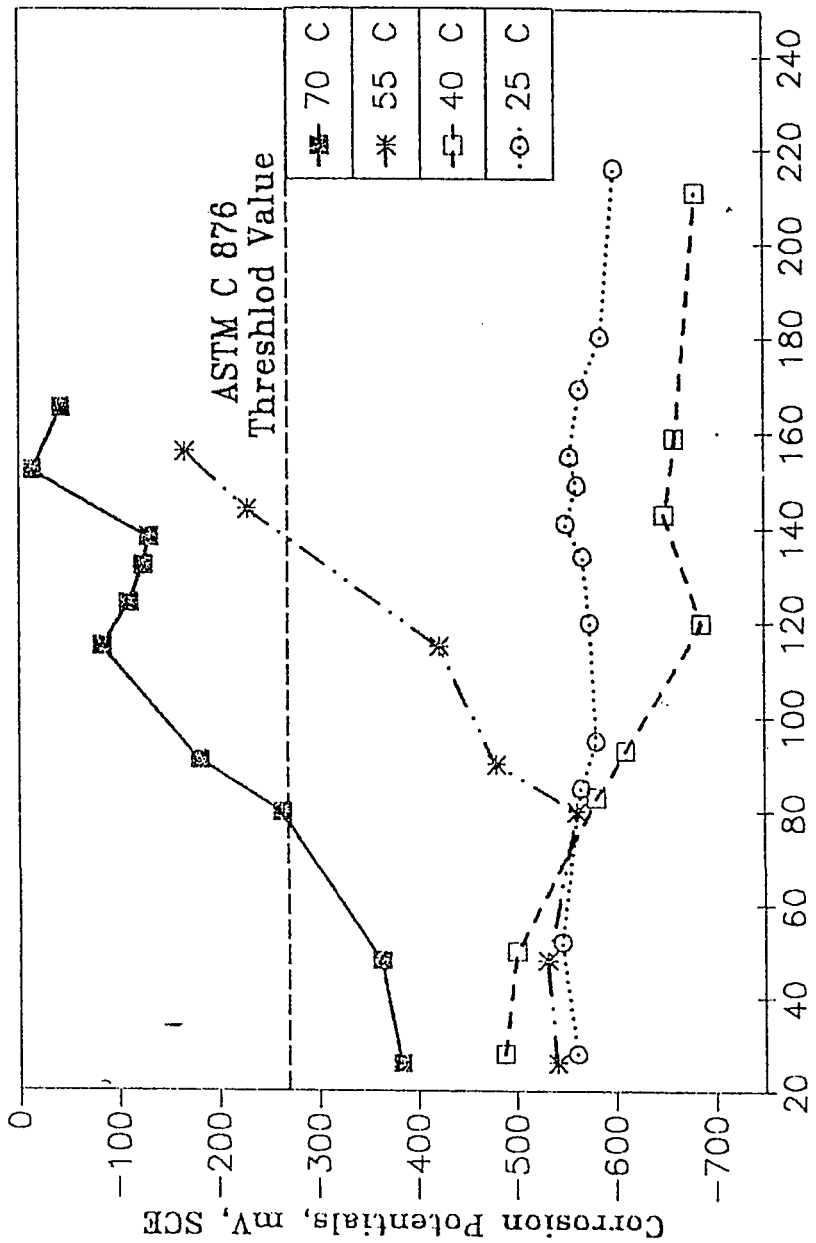

Fig. 4.48 Corrosion Potentials on Steel in SF Cement Concrete Specimens Contaminated With Chlorides and Sulfates and Exposed to Varying Temperatures

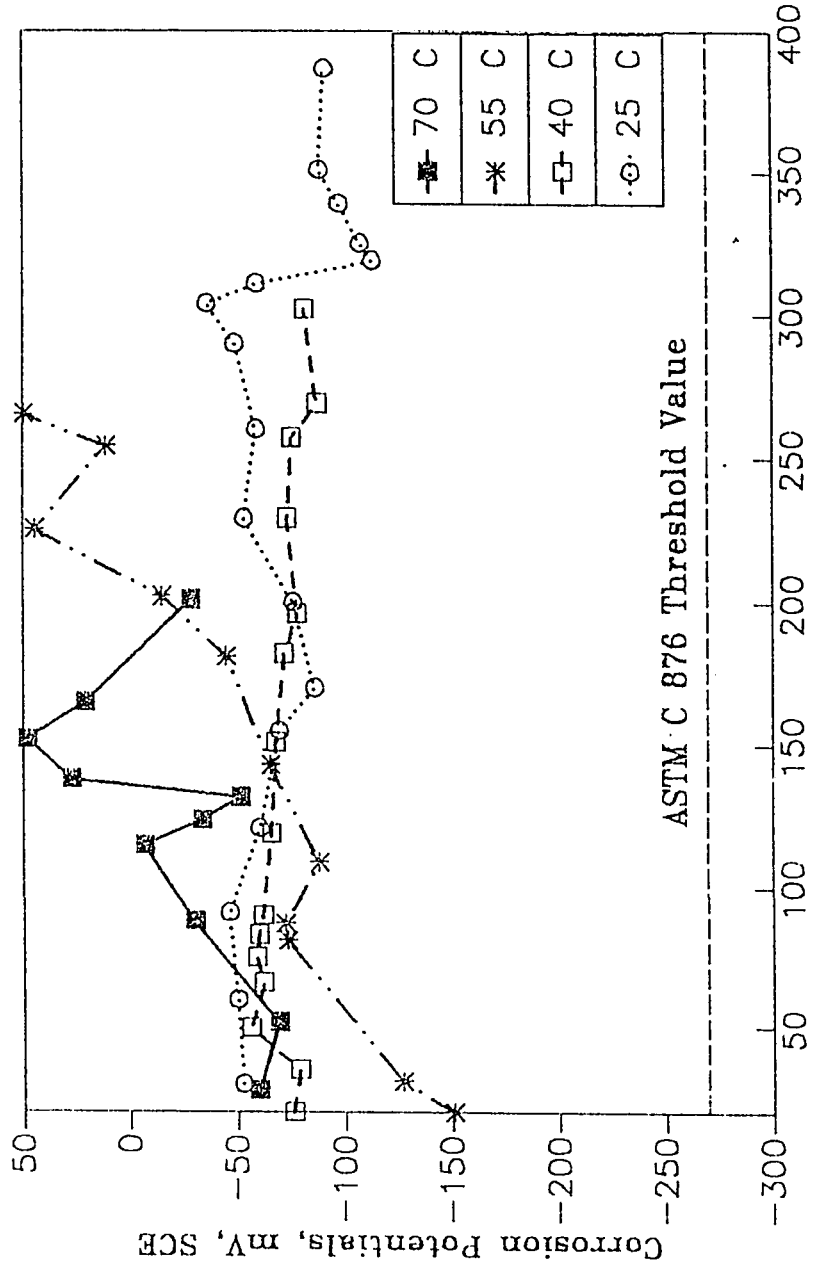

Fig. 4.49 Corrosion Potentials on Steel in Class F FA Cement Concrete Specimens Exposed to Varying Temperatures

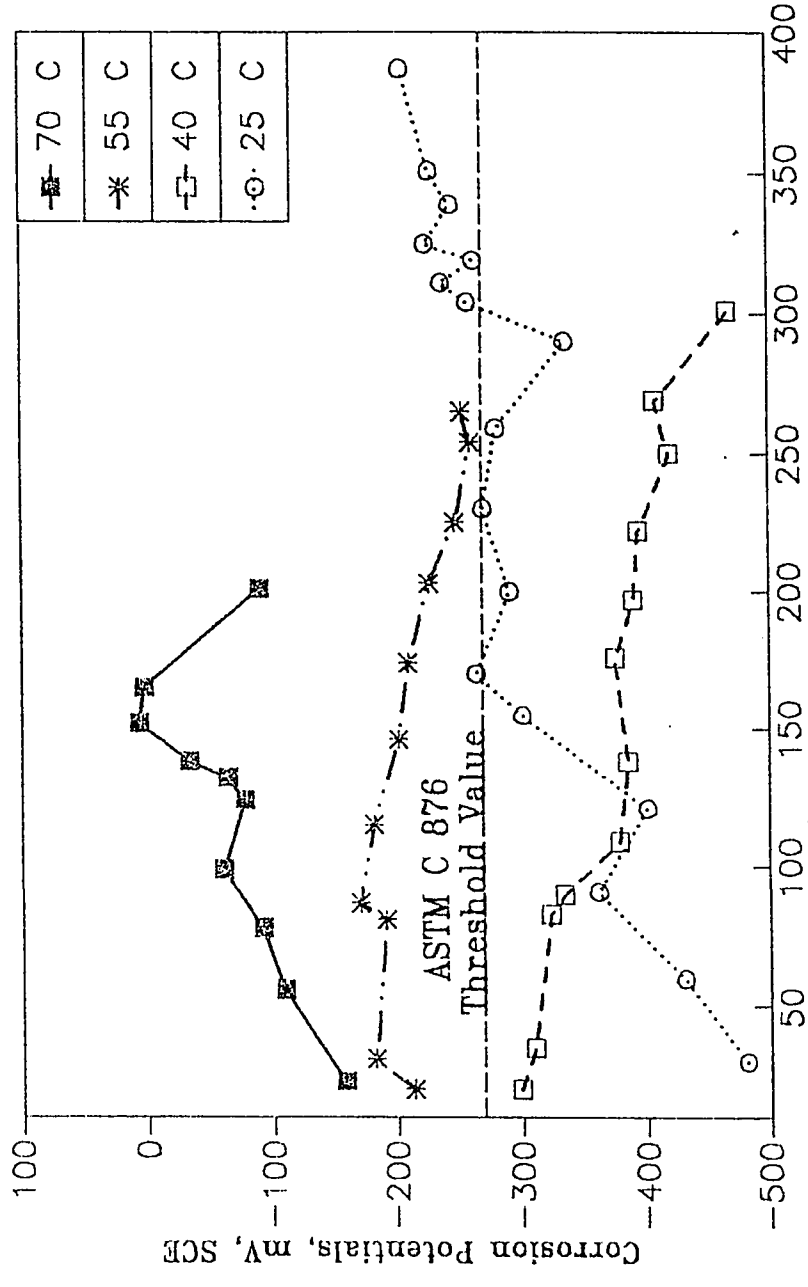

Fig. 4.50 Corrosion Potentials on Steel in Class F FA Concrete Specimens Contaminated With Chlorides and Exposed to Varying Temperatures

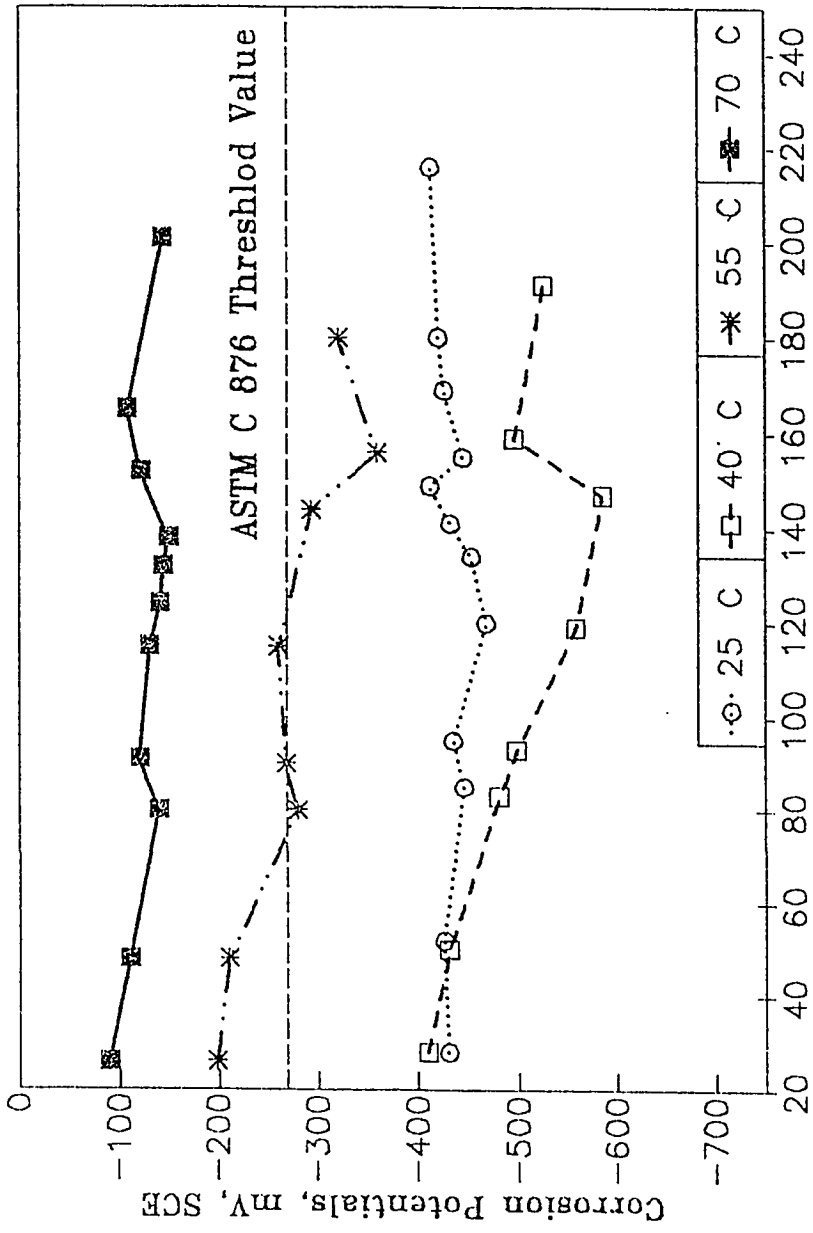

Fig. 4.51 Corrosion Potentials on Steel in Class F FA Concrete Specimens Contaminated With Chlorides and Sulfates and Exposed to Varying Temperatures

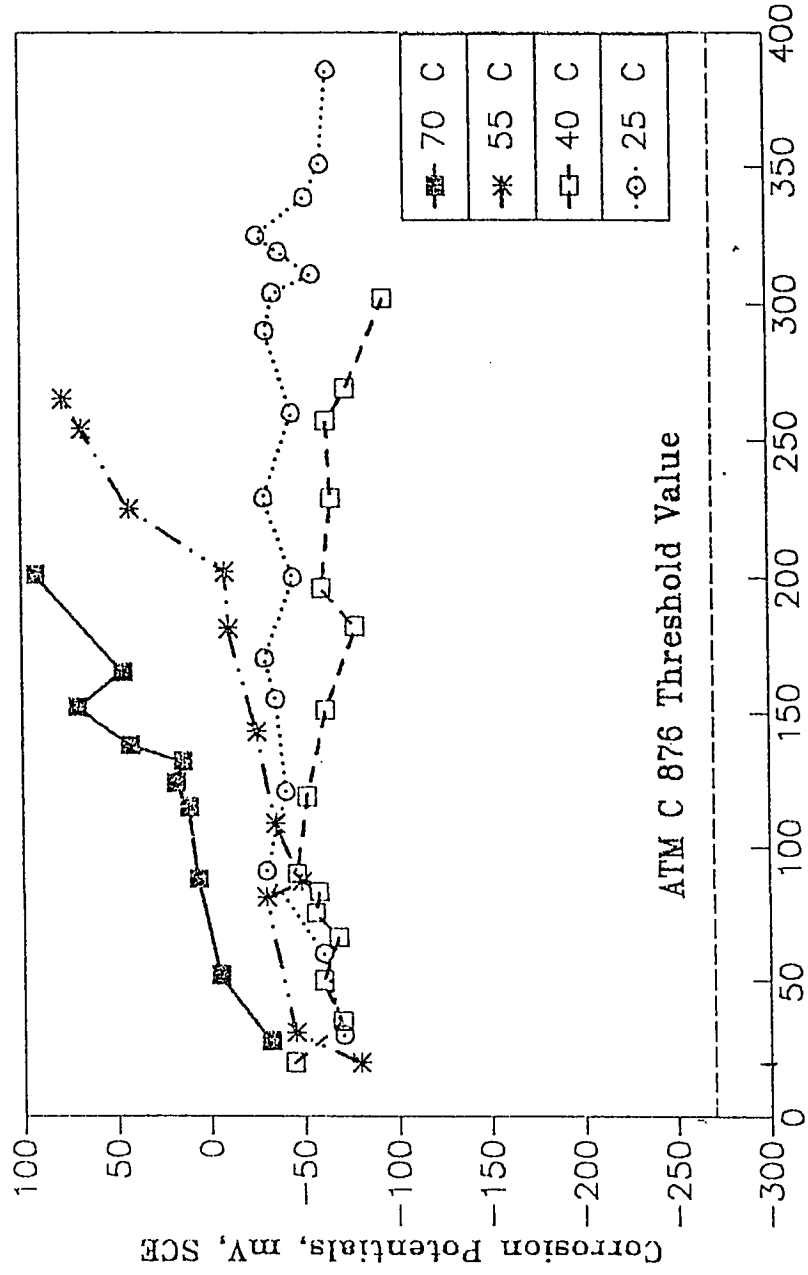

Fig. 4.52 Corrosion Potentials on Steel in Class C FA Cement Concrete Specimens Exposed to Varying Temperatures

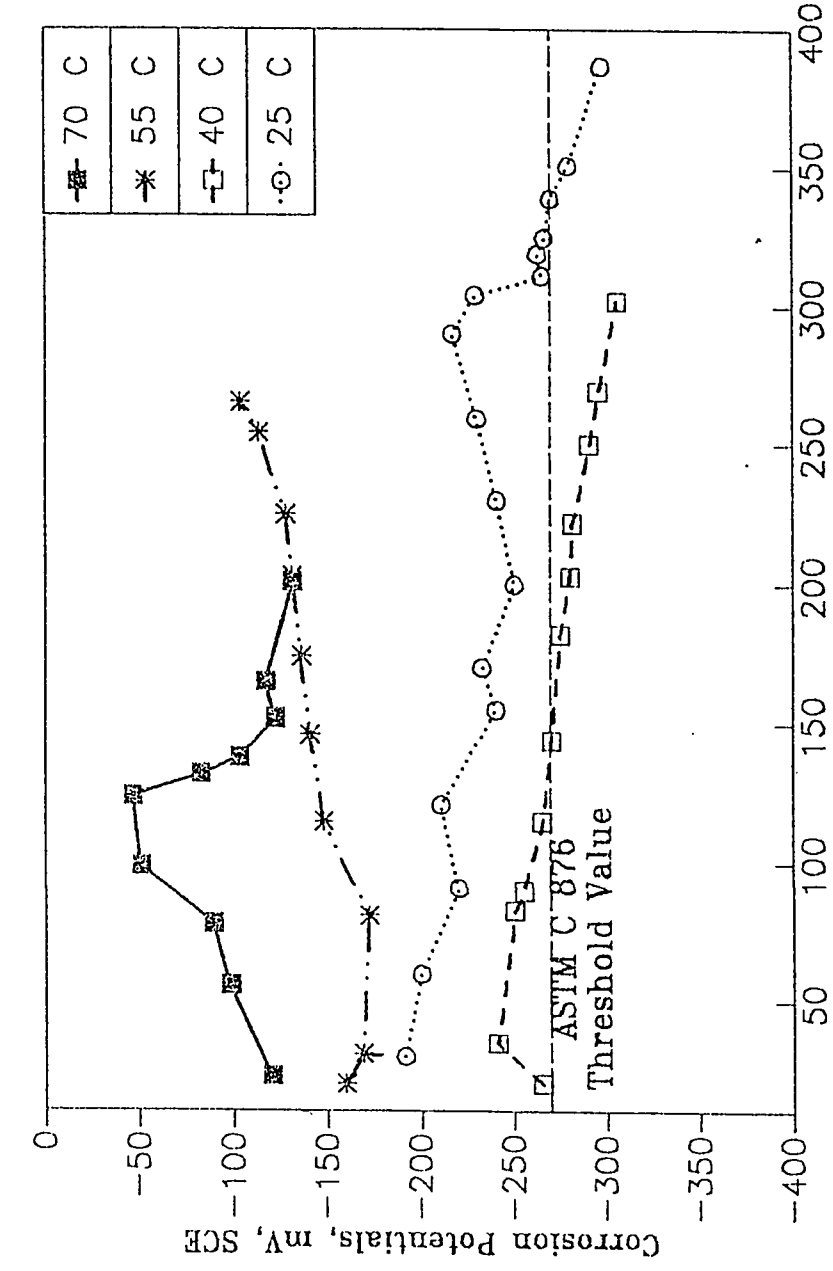

Fig. 4.53 Corrosion Potentials on Steel in Class C FA Concrete Specimens Contaminated With Chlorides and Exposed to Varying Temperatures

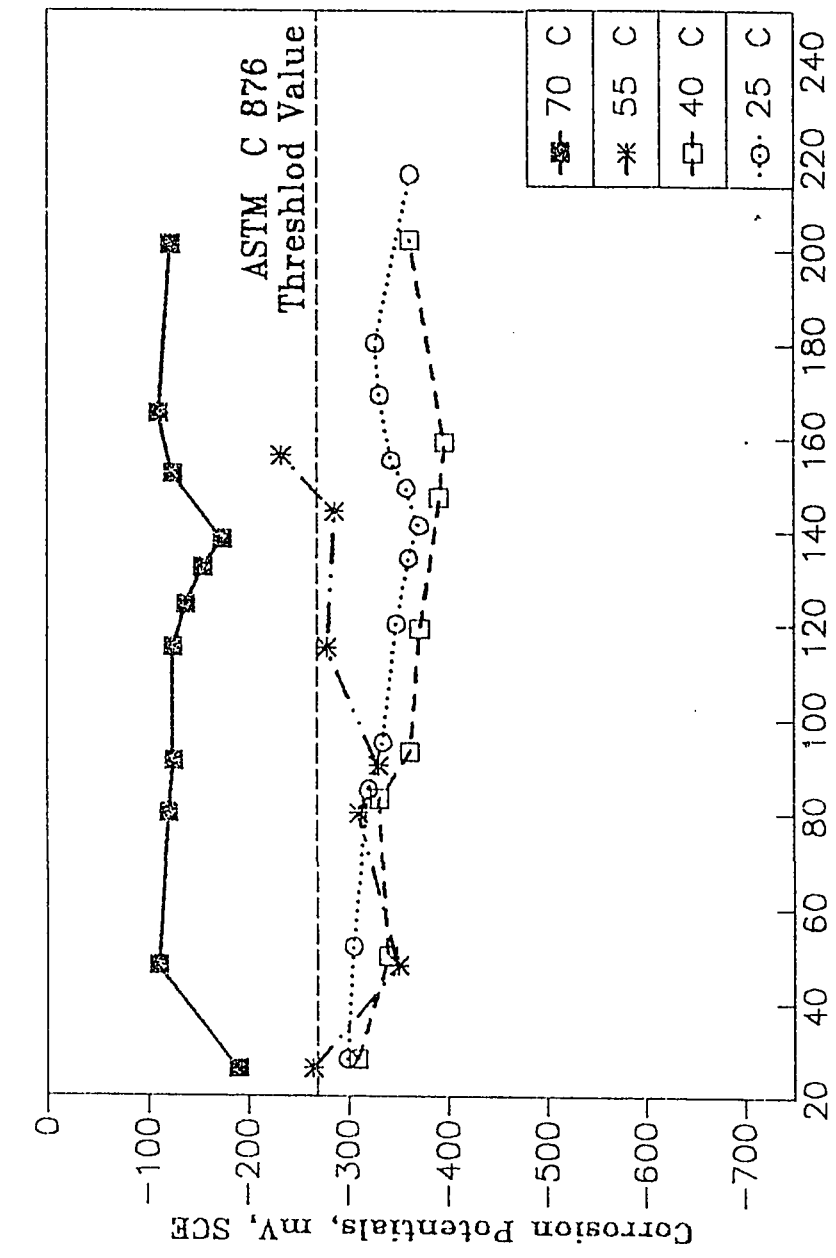

Fig. 4.54 Corrosion Potentials on Steel in Class C FA Concrete Specimens Contaminated With Chlorides and Sulfates and Exposed to Varying Temperatures

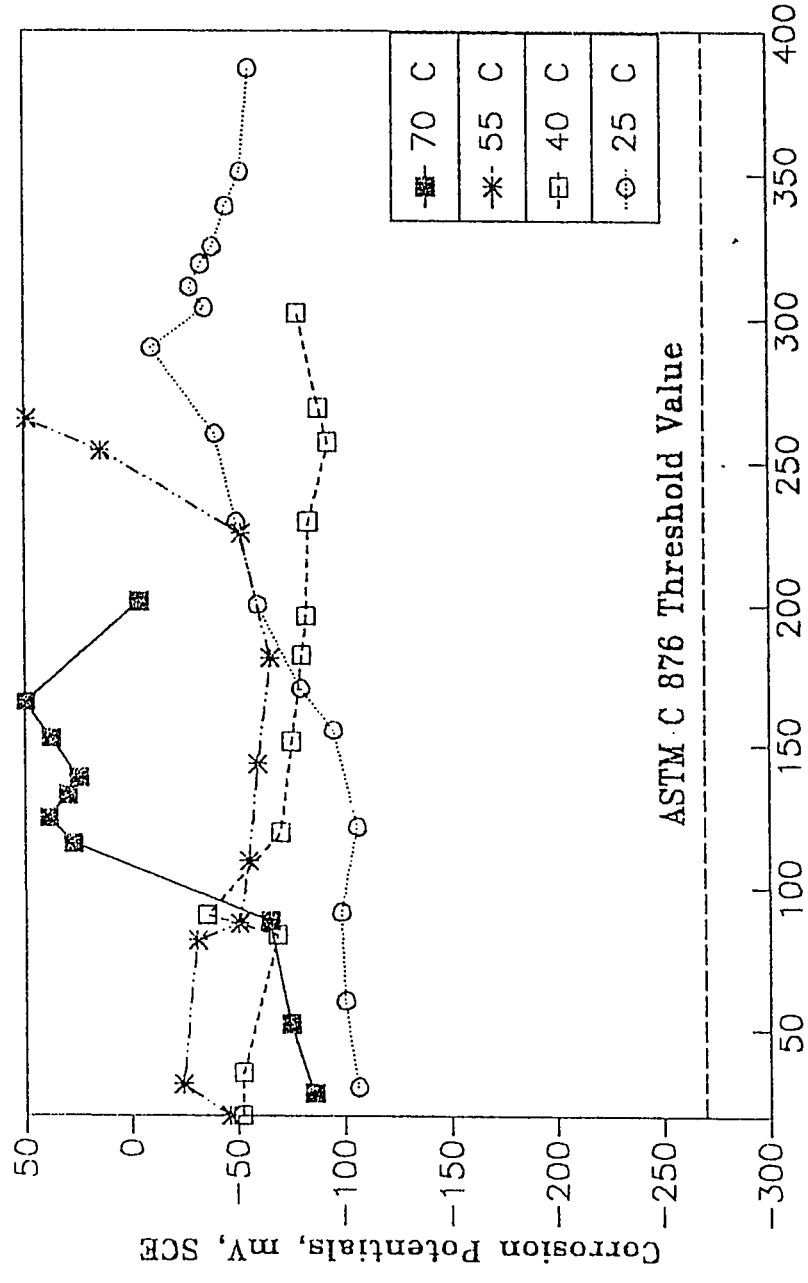

Fig. 4.55 Corrosion Potentials on Steel in BFS Cement Concrete Specimens Exposed to Varying Temperatures

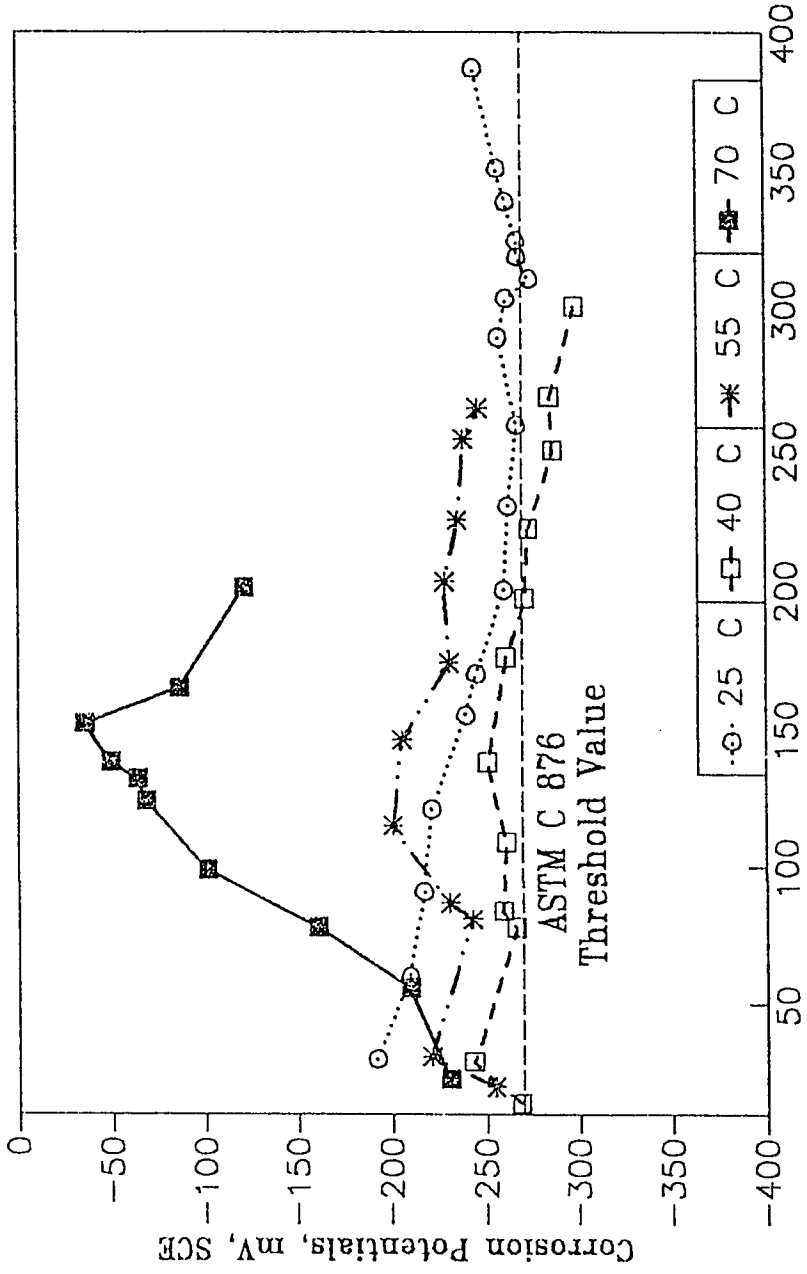

Fig. 4.56 Corrosion Potentials on Steel in BFS Cement Concrete Specimens Contaminated With Chlorides and Exposed to Varying Temperatures

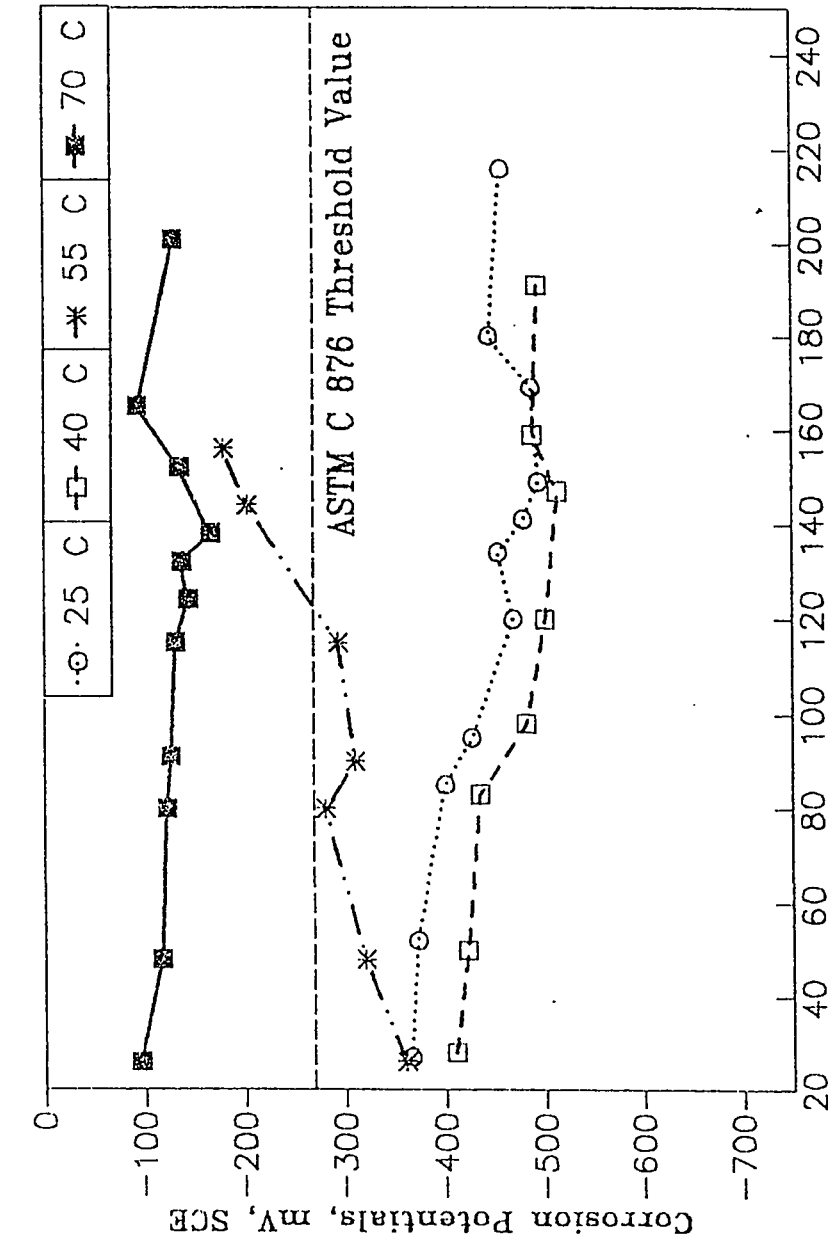

Fig. 4.57 Corrosion Potentials on Steel in BFS Cement Concrete Specimens Contaminated With Chlorides and Sulfates and Exposed to Varying Temperatures

4. The corrosion potentials were more negative in concrete specimens exposed up to 40 °C than in those exposed to 55 and 70 .°C The decrease in the potential values, with increase in the temperature, beyond 55 °C may indicate lower corrosion activity in specimens exposed to elevated temperatures. However, it is also possible that elevated temperature may result in loss of moisture in the pores of concrete. Corrosion potentials in dry concrete tend to be positive. Hanson [56], based on the potential survey of several marine structures indicates that if concrete is allowed to dry out the potentials tend to be more positive. A variation of 180 mV in a similar concrete with varying moisture content was noted. Vassie [115] based on large number of potential surveys states that potential values can be unreliable when concrete is comparatively dry.

4.5.2 Corrosion Current Density

The corrosion current density on steel in ordinary portland cement concrete specimens is plotted against period of exposure to varying temperature conditions in Fig. 4.58 to 4.60. Fig. 4.58 shows the corrosion current density on steel in uncontaminated concrete specimens. These data indicate higher corrosion activity in specimens exposed to 55 and 70 °C temperature as compared to those exposed to 25 and 40 °C. The corrosion current density on steel in concrete specimens exposed to 25 °C was in the range of 0.008 to 0.026 $\mu A/cm^2$, while those exposed to 40 °C were in the range of 0.009 to 0.073 $\mu A/cm^2$. The corrosion current density on steel in concrete specimens exposed to 55 and 70 °C was in the range of 0.009 to 0.38 and 0.027 to 1.05 $\mu A/cm^2$, respectively. The corrosion current density on steel in concrete specimens contaminated with chloride ions are shown in Fig. 4.59. The data indicate an increase in the corrosion activity with increasing period of exposure in all the specimens. Further, the corrosion current density was observed to increase with the

exposure temperature. The corrosion current density, on steel in concrete specimens contaminated with chlorides and sulfates are shown in Fig. 4.60. These data generally show a trend similar to that indicated in specimens contaminated with chloride salts. The corrosion current density in these specimens was, however, more than that in specimens contaminated with chloride salts. For example, after 150 days of exposure the corrosion current density on steel in concrete specimens contaminated with chlorides was 0.097, 0.3302, 0.36024 and 0.6994 $\mu A/cm^2$ for 25, 40, 55, 77 °C exposure (Fig. 4.59), whereas the corrosion current density for steel in concrete specimens contaminated with chloride and sulfate salts was 0.4575, 0.4585, 0.5595, and 0.9233 $\mu A/cm^2$ respectively for the same exposure temperatures (Fig. 4.60).

The corrosion current density on steel in uncontaminated silica fume cement concrete specimens are shown in Fig. 4.61. These data show a trend similar to that shown in Fig. 4.58, except that a slightly higher corrosion activity was observed even at lower temperatures. Fig. 4.62 and 4.63 show the corrosion current density on steel in silica fume blended cement concrete specimens contaminated with chloride and chloride-sulfate respectively. These data indicate a trend similar to that shown in Fig. 4.59 and 4.60. The corrosion current density was observed to increase with exposure temperature and with the addition of sulfate ions to the chloride contaminated concrete.

The corrosion current density on steel in Class F fly ash blended cement concrete specimens is plotted in Fig. 4.64 to 4.66 for uncontaminated, chloride contaminated and chloride plus sulfate contaminated specimens. These data indicate a trend similar to that shown in other cements.

Fig. 4.67 to 4.69 show the corrosion current density on steel in Class C fly ash cement concrete specimens. The corrosion current density on steel in uncontaminated concrete specimens shows a trend similar to that in uncontaminated specimens in other cements. The corrosion current density on steel in chloride contaminated concrete specimens (Fig. 4.68) indicate an almost linear increase in the corrosion current density

with the period of exposure. The corrosion current density also increased with the exposure temperature. The time-corrosion current density curves for steel in chloride-sulfate contaminated concrete (Fig. 4.69) show a similar trend, to that in the other cement concrete specimens.

The variation of corrosion current density on steel in BFS cement concrete specimens with various temperatures and salt contamination is shown in Fig. 4.70 to 4.72. These data show a trend similar to that indicated by other specimens.

To visualize the role of chloride, chloride-sulfate contamination and temperature on reinforcement corrosion the corrosion current density on steel after 150 days of exposure for each cement are plotted in Fig. 4.73 through 4.77. These data generally indicate an increase in the corrosion activity due to (i) increase in temperature, (ii) contamination with chloride ions and (iii) contamination with chloride and sulfate ions. Elevated temperature of 70 °C and chloride-sulfate contamination formed the most aggressive environment as corrosion current density was observed to be the maximum in all the cement concrete specimens at these conditions.

The detrimental effect of temperature on corrosion has been reported by other investigators [115,117,118]. Figure 4.78 shows the effect of temperature on the corrosion of crevice coupons that were mounted on vehicles during a winter season in Winnipeg as quoted in reference 9. The corrosion rates of coupons that were mounted on vehicles and periodically housed in heated garages were approximately three times the corrosion rate of those mounted on vehicles left in the open air or unheated garages. In studies carried out by Benjamin and Sykes [117], pitting corrosion was observed at 40 °C at only 2% NaCl, whereas a 6% NaCl concentration was required for pitting at temperature of 25 °C.

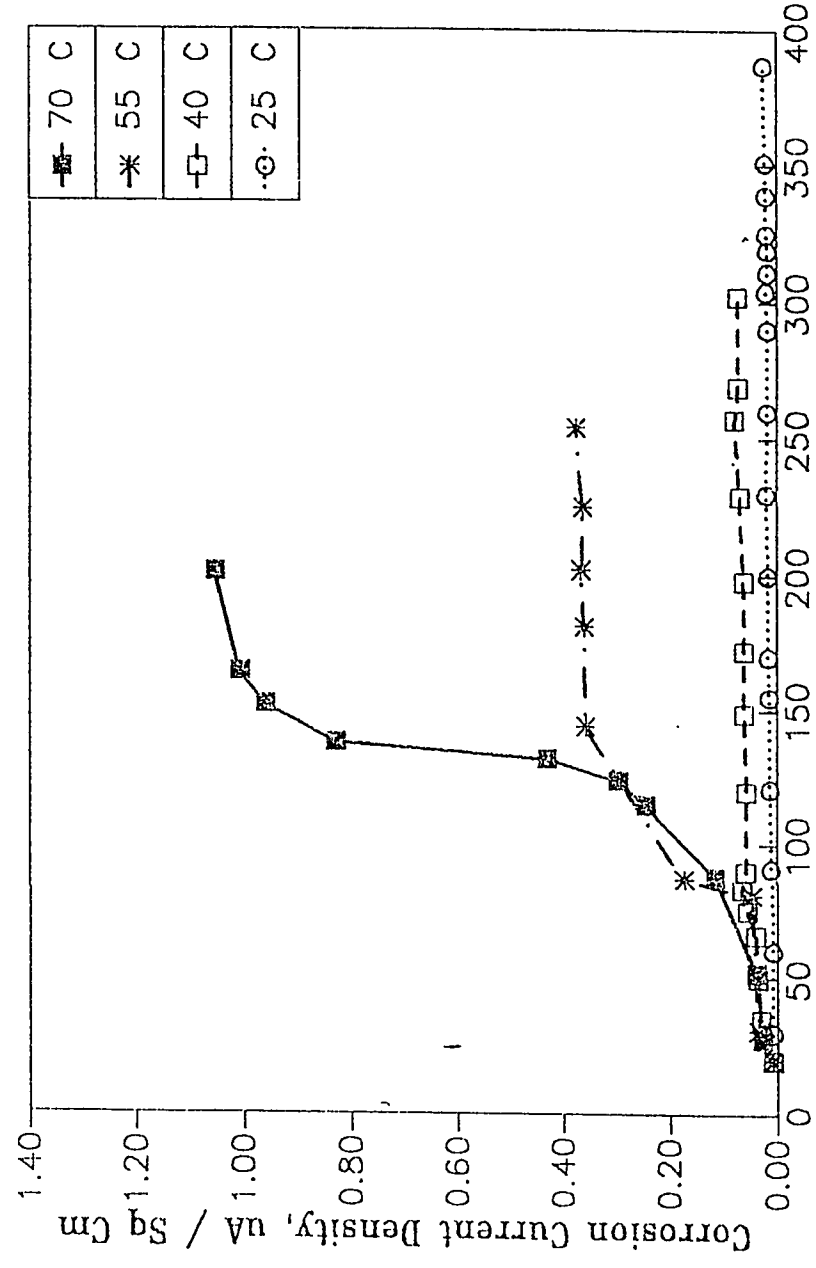

Fig. 4.58 Corrosion Current Density on Steel in OPC Concrete Specimens Exposed to Varying Temperatures

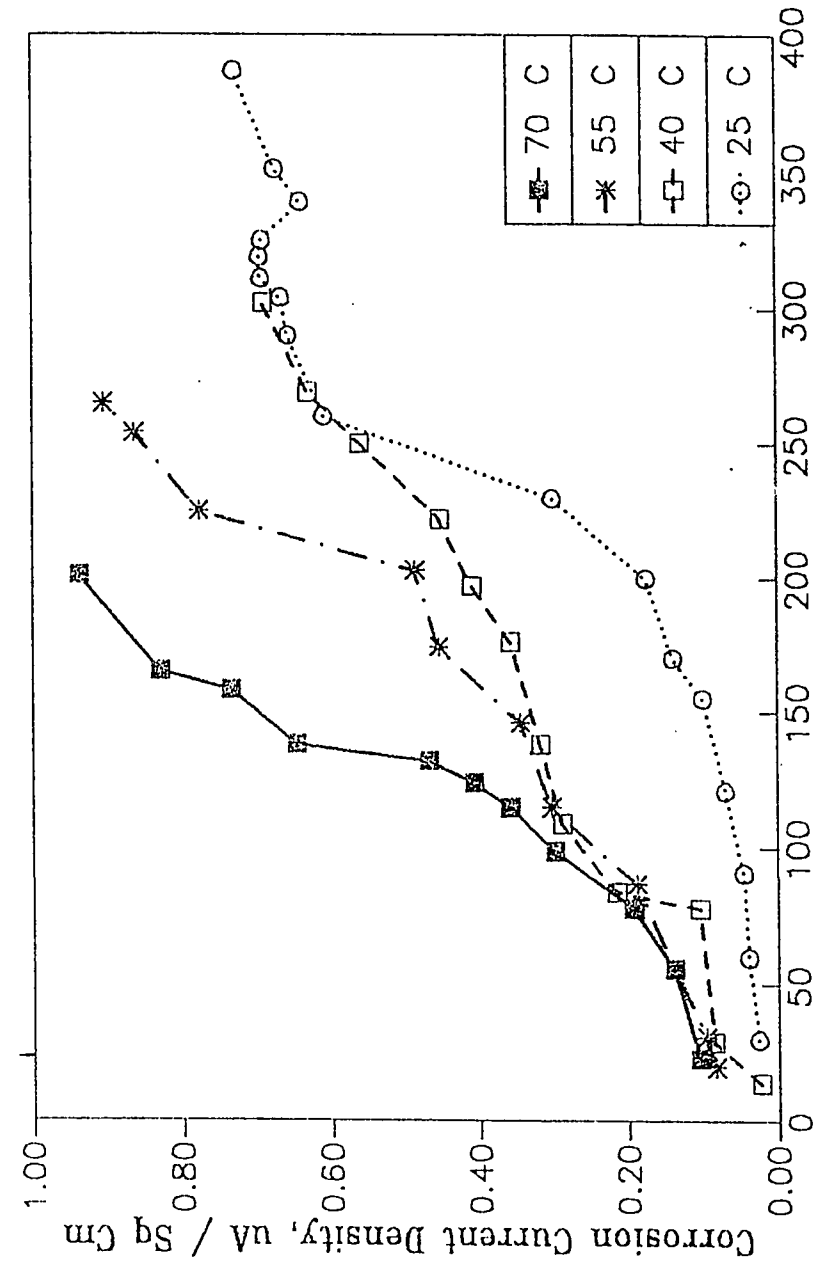

Fig. 4.59 Corrosion Current Density on Steel in OPC Concrete Specimens Contaminated with Chloride and Exposed to Varying Temperatures

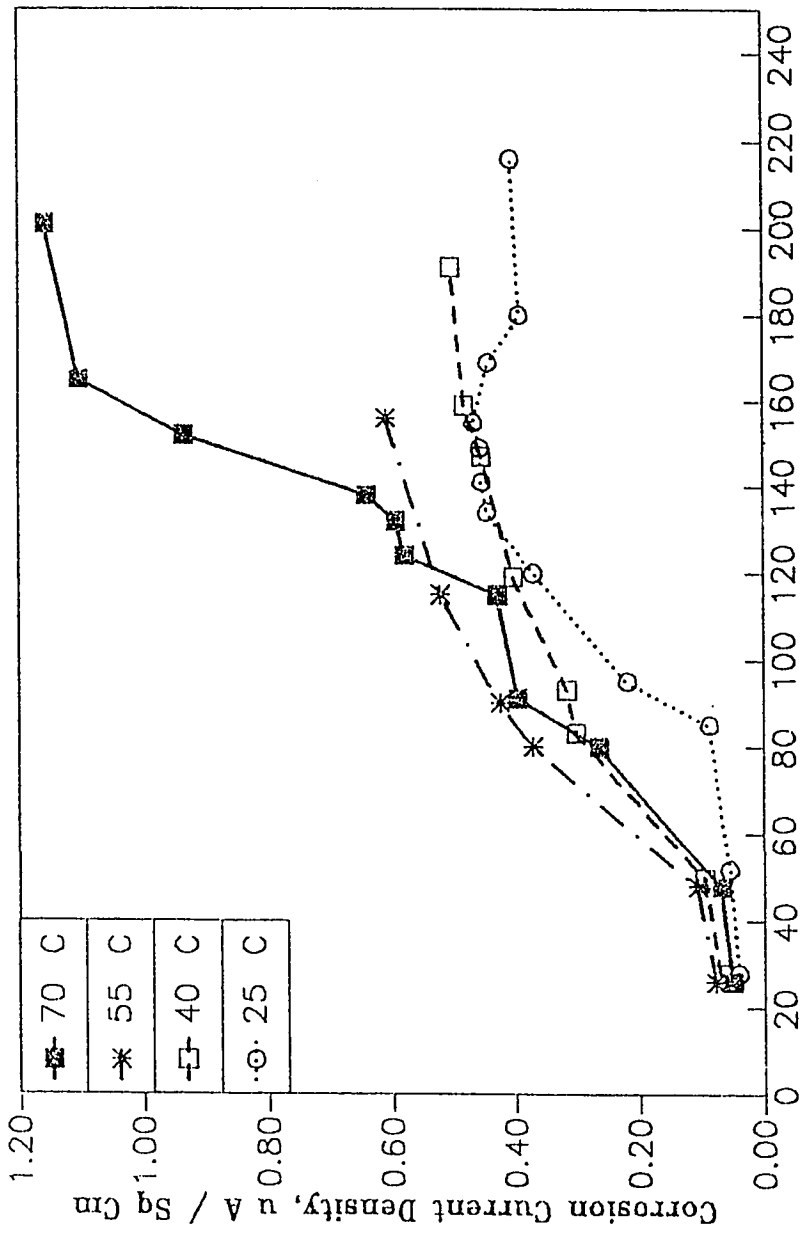

Fig. 4.60 Corrosion Current Density on Steel in OPC Concrete Specimens Contaminated with Chlorides and Sulfates and Exposed to Varying Temperatures

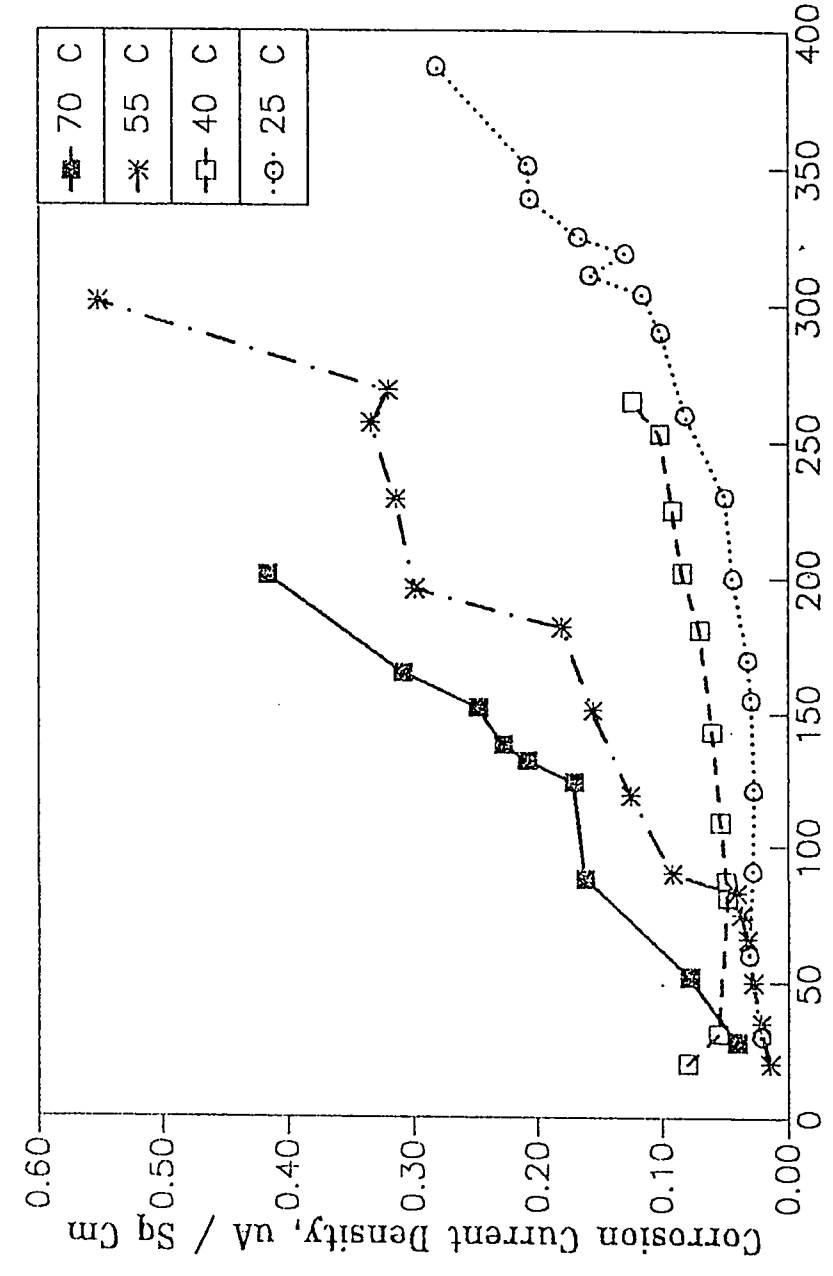

Fig. 4.61 Corrosion Current Density on Steel in SF Cement Concrete Specimens Exposed to Varying Temperatures

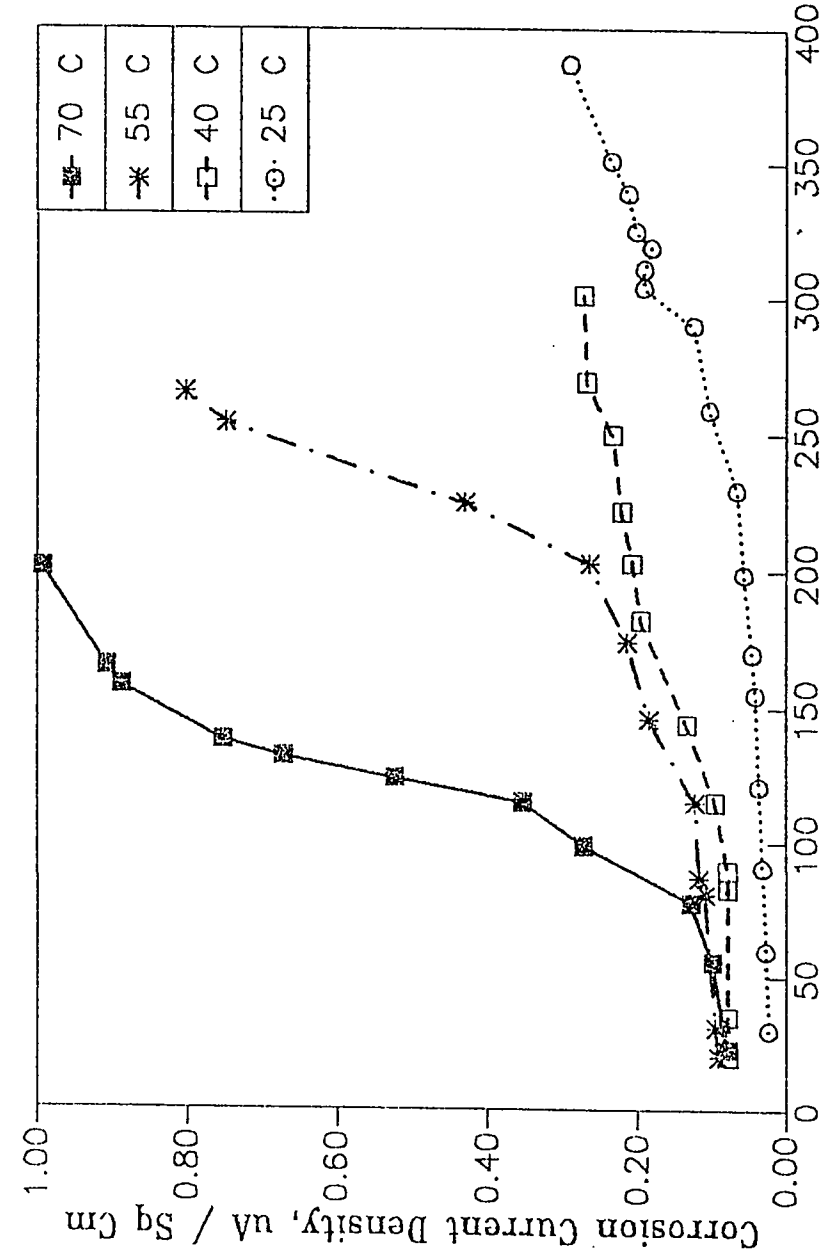

Fig. 4.62 Corrosion Current Density on Steel in SF Cement Concrete Specimens Contaminated with Chloride and Exposed to Varying Temperatures

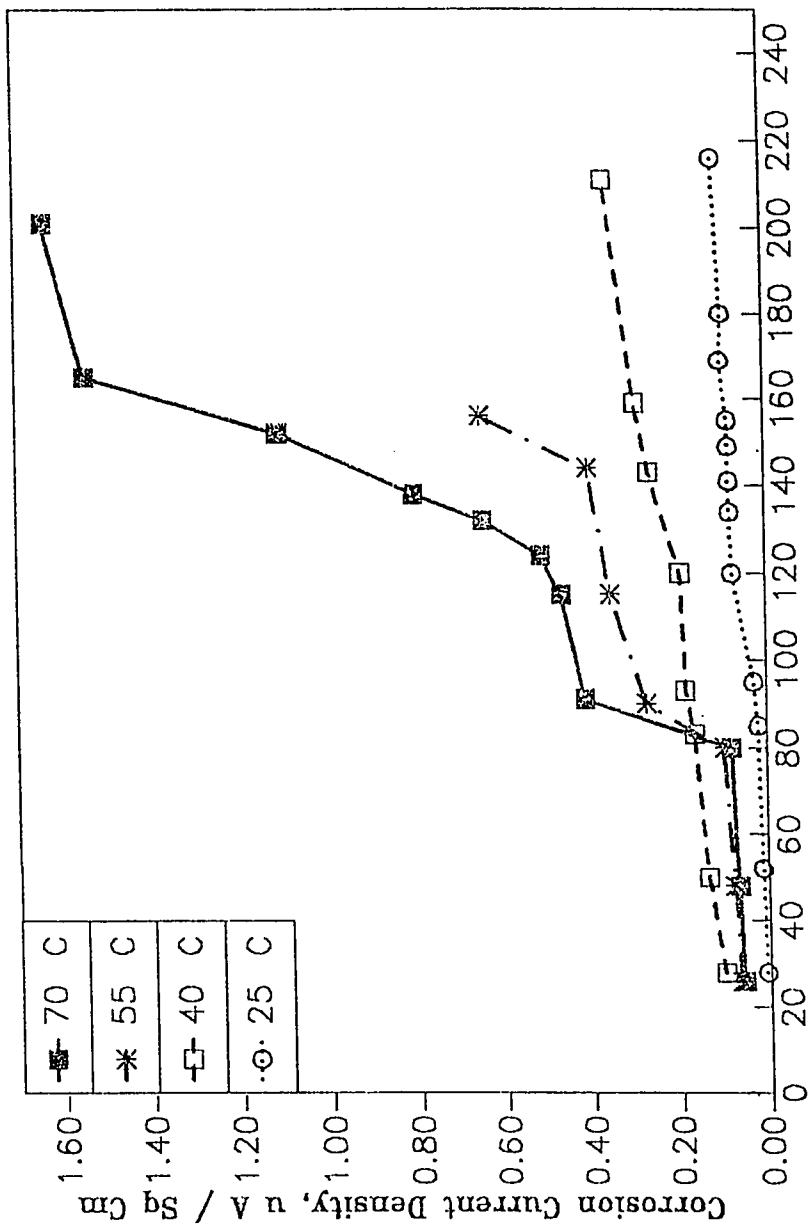

Fig. 4.63 Corrosion Current Density on Steel in SF Cement Concrete Specimens Contaminated with Chlorides and Sulfates and Exposed to Varying Temperatures

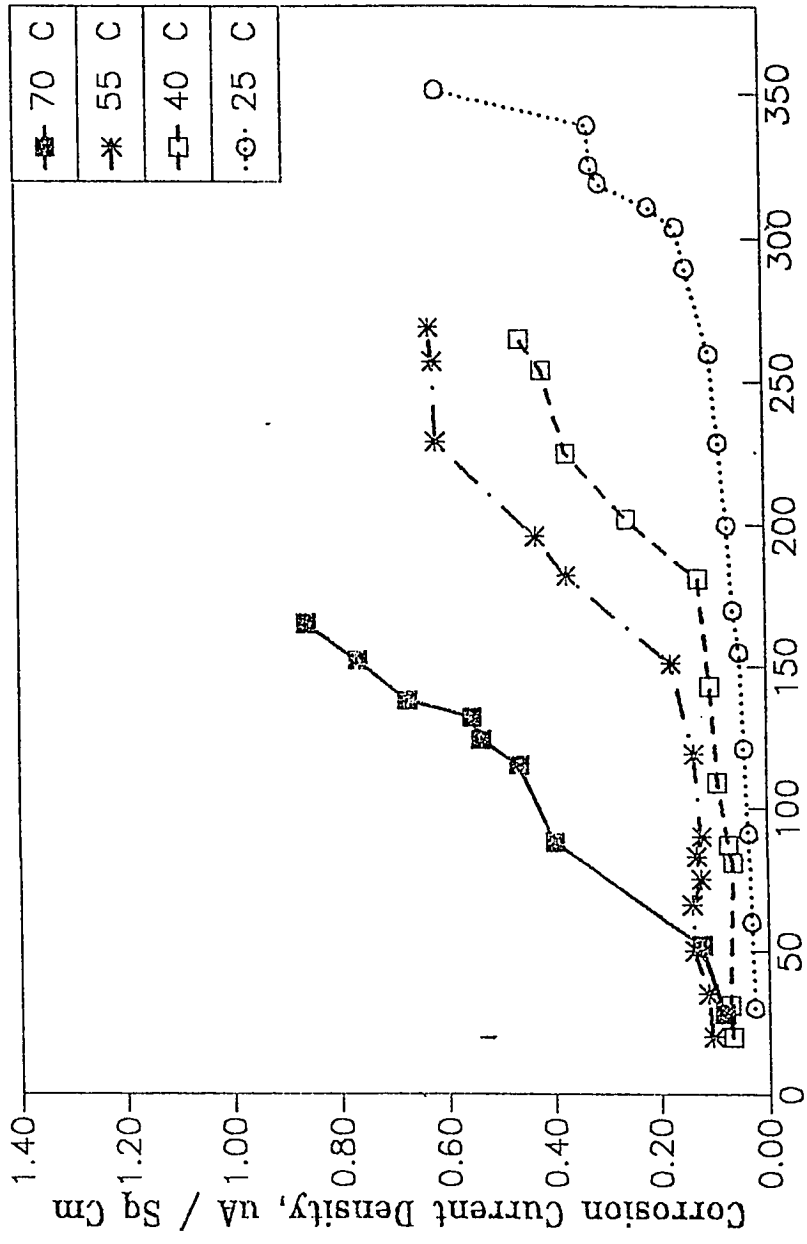

Fig. 4.64 Corrosion Current Density on Steel in Class F FA Cement Concrete Specimens Exposed to Varying Temperatures

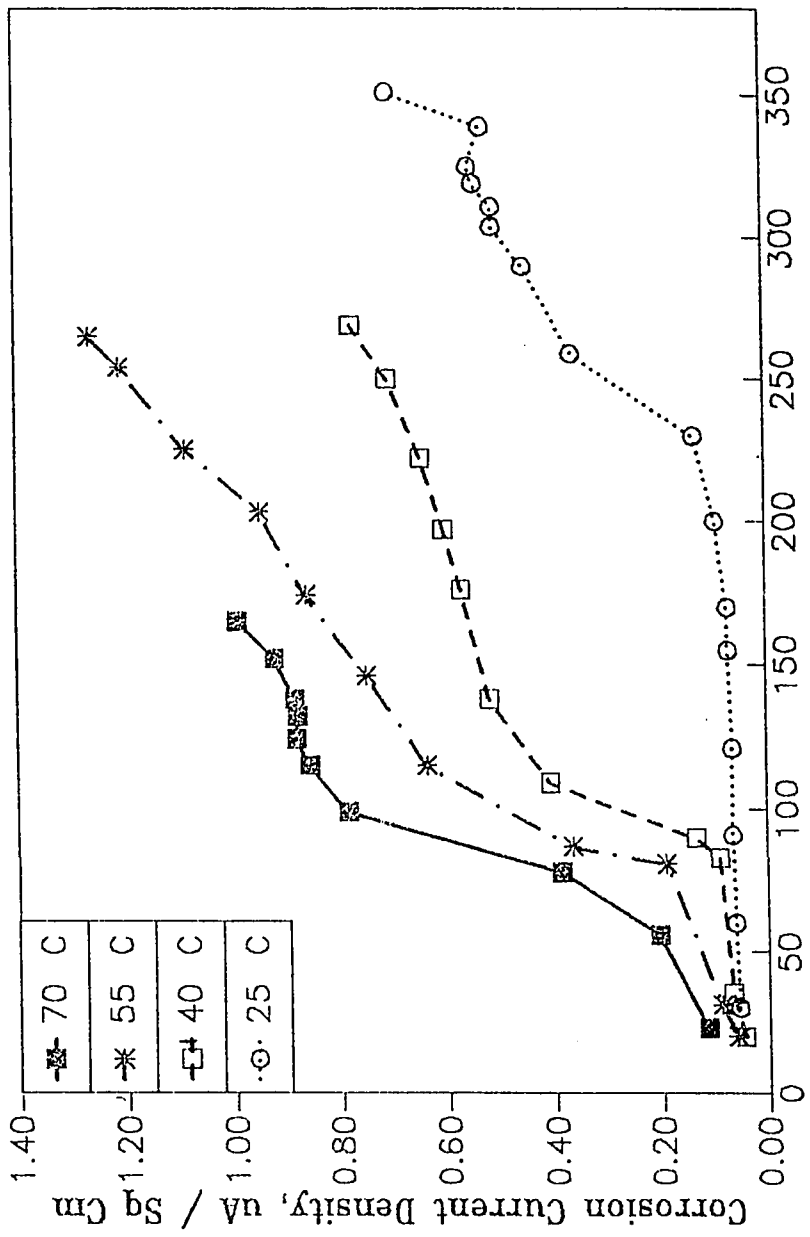

Fig. 4.65 Corrosion Current Density on Steel in Class F FA Cement Concrete Specimens Contaminated with Chloride and Exposed to Varying Temperatures

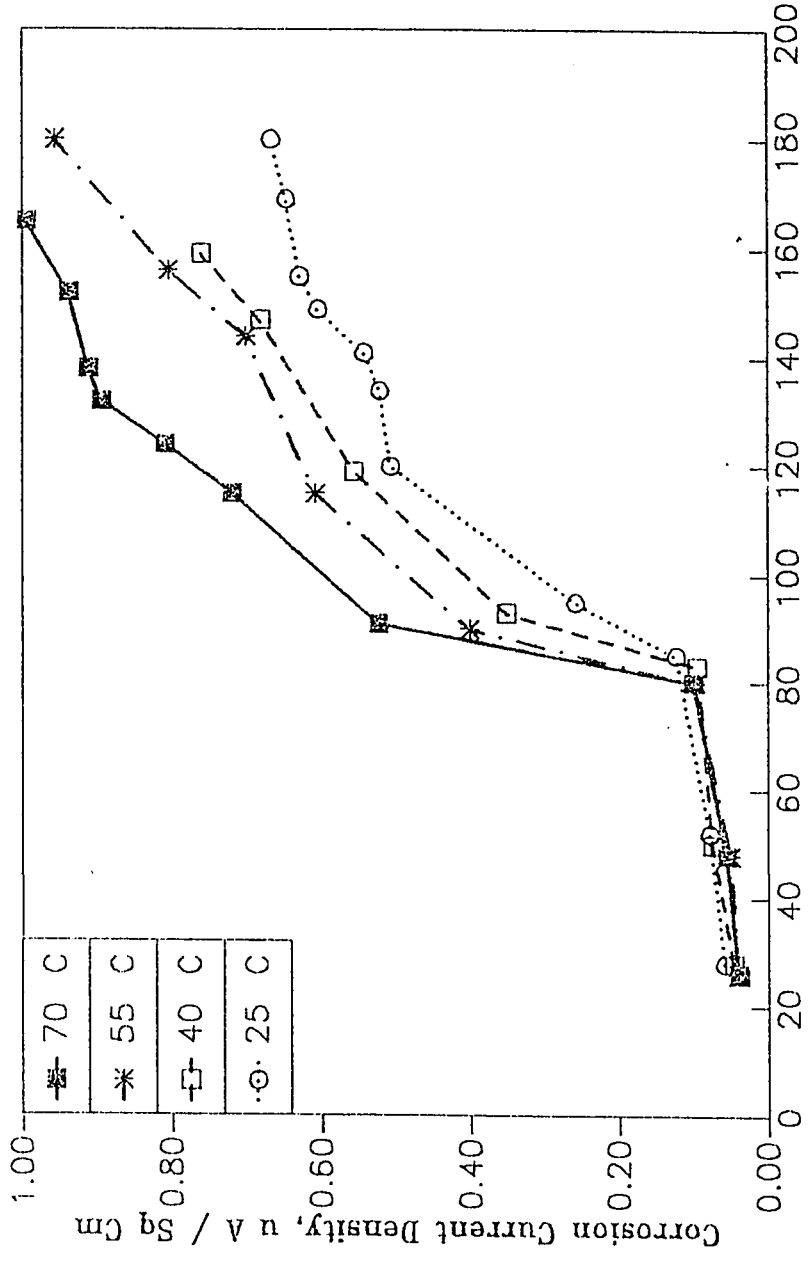

Fig. 4.66 Corrosion Current Density on Steel in Class F FA Cement Concrete Specimens Contaminated with Chlorides and Sulfates and Exposed to Varying Temperatures

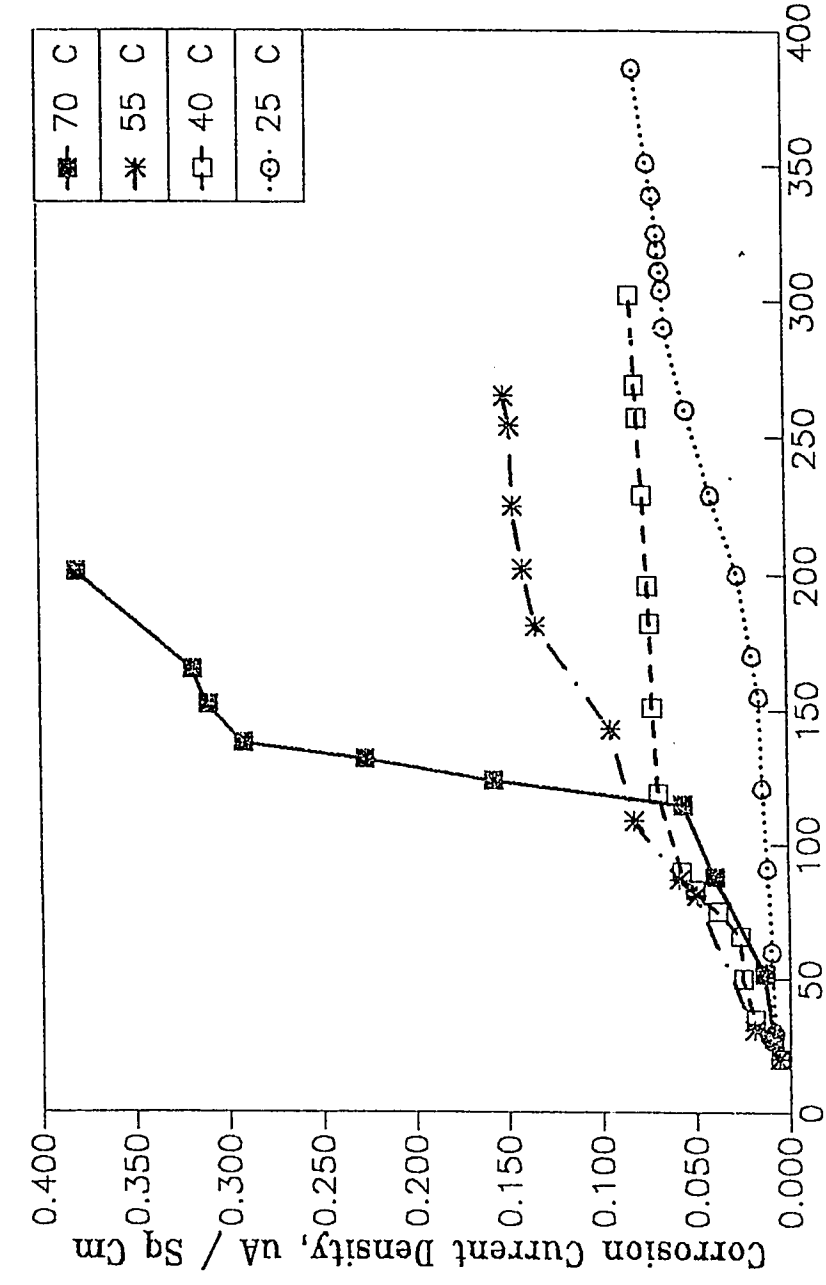

Fig. 4.67 Corrosion Current Density on Steel in Class C FA Cement Concrete Specimens Exposed to Varying Temperatures

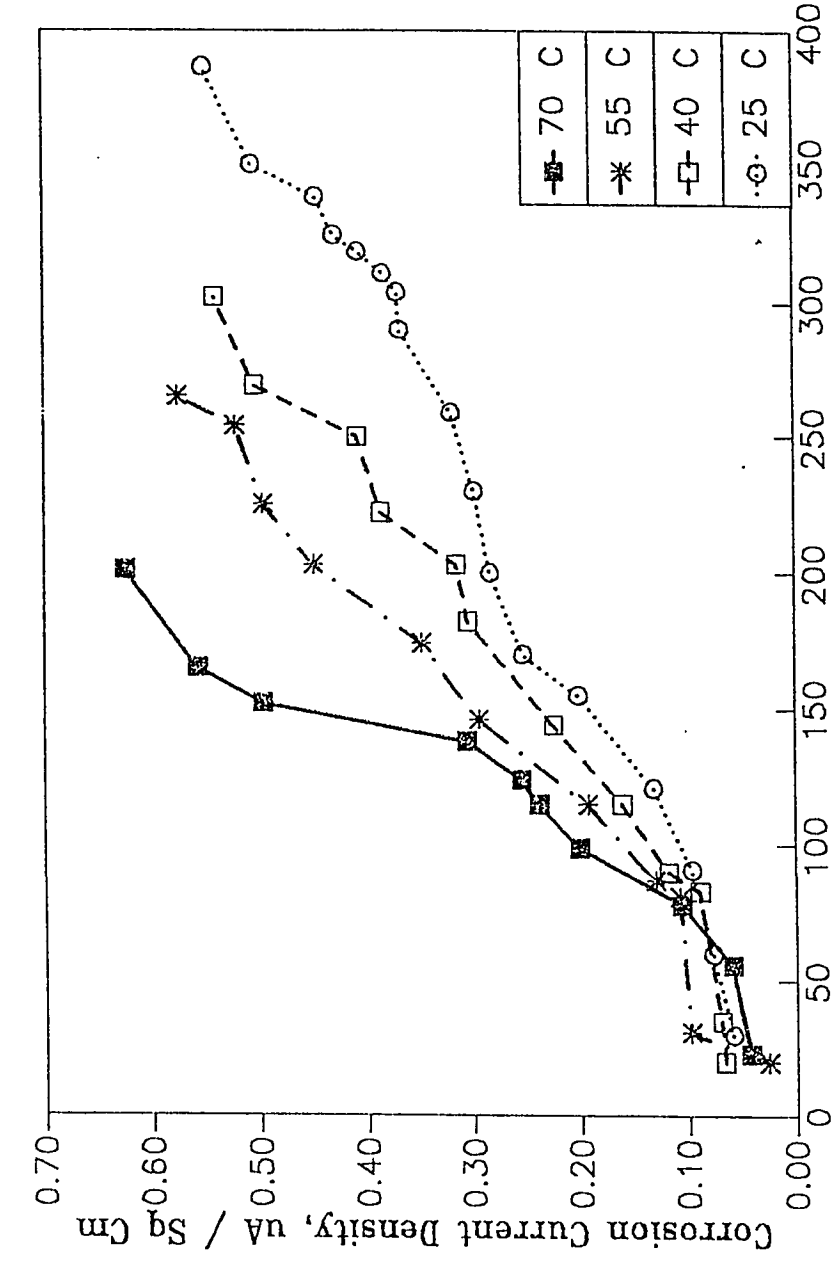

Fig. 4.68 Corrosion Current Density on Steel in Class C FA Cement Concrete Specimens Contaminated with Chloride and Exposed to Varying Temperatures

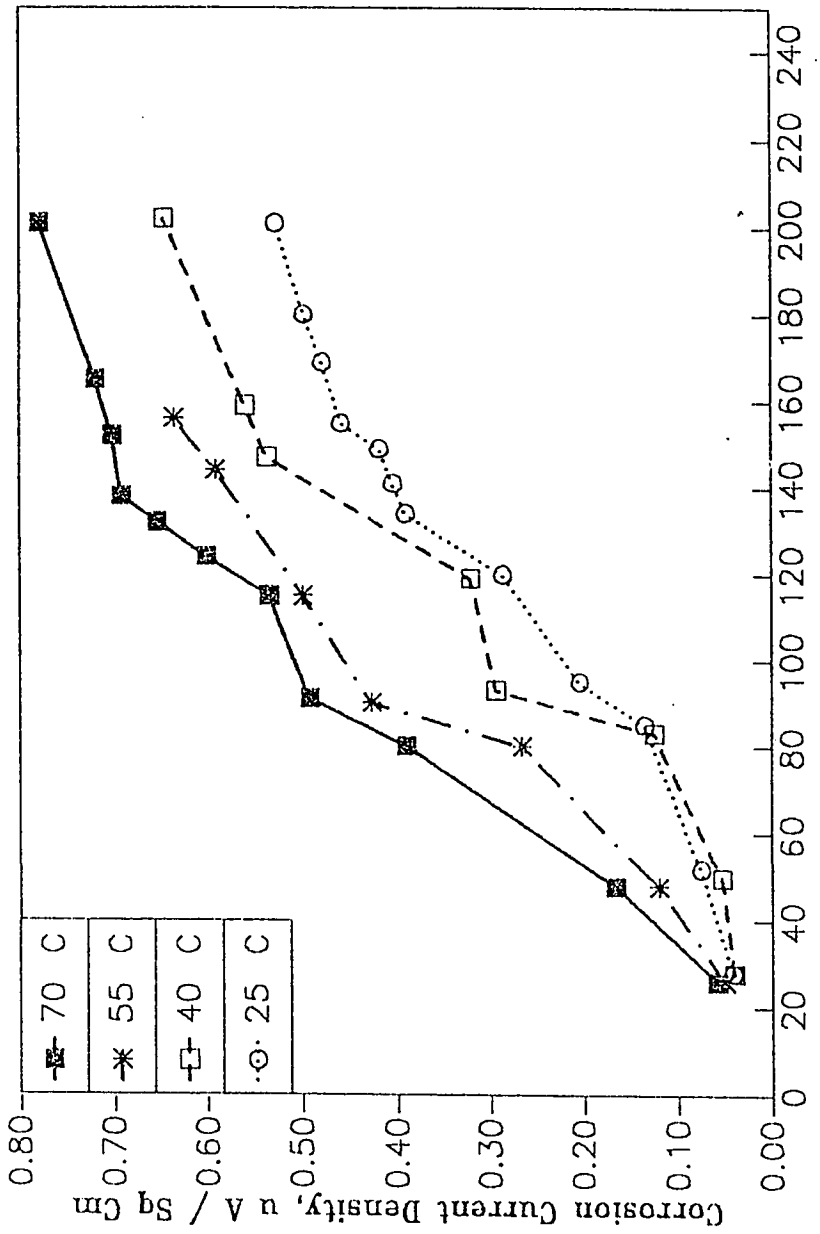

Fig. 4.69 Corrosion Current Density on Steel in Class C FA Cement Concrete Specimens Contaminated with Chlorides and Sulfates and Exposed to Varying Temperatures

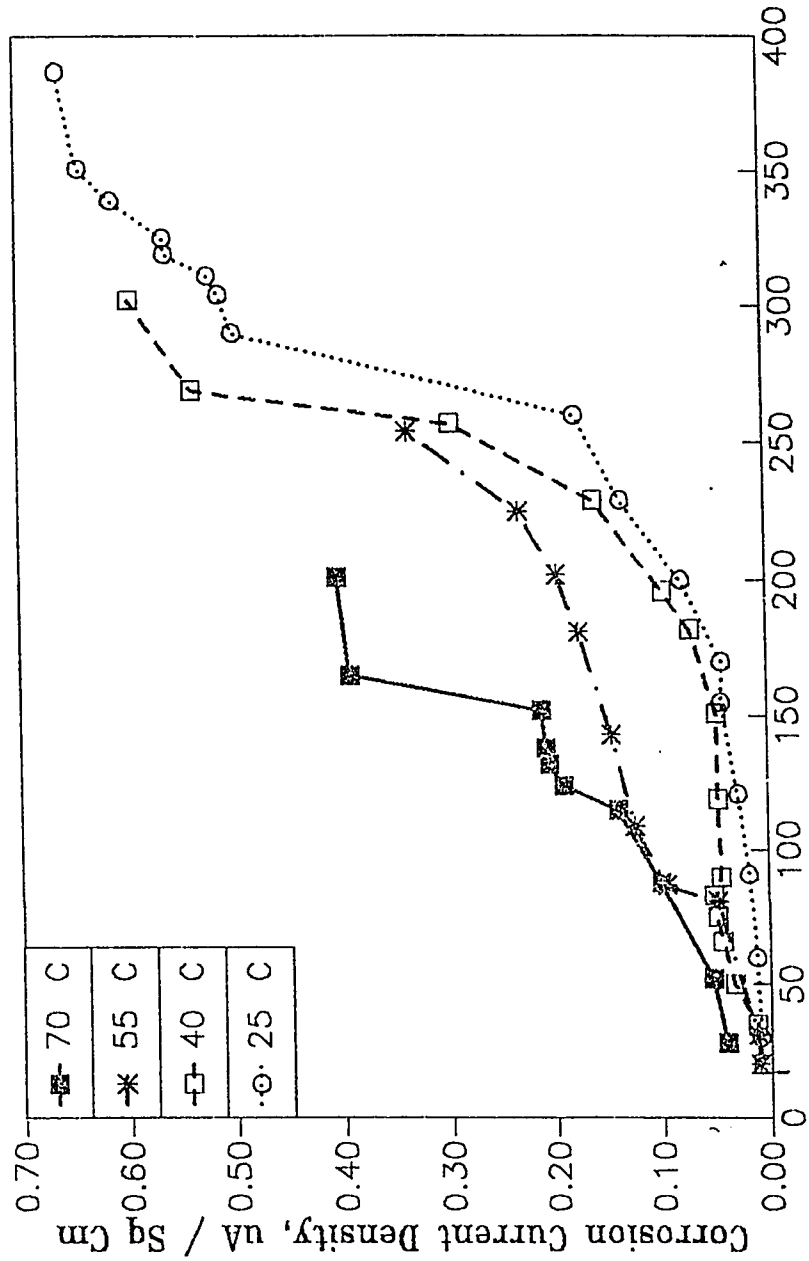

Fig. 4.70 Corrosion Current Density on Steel in BFS Cement Concrete Specimens Exposed to Varying Temperatures

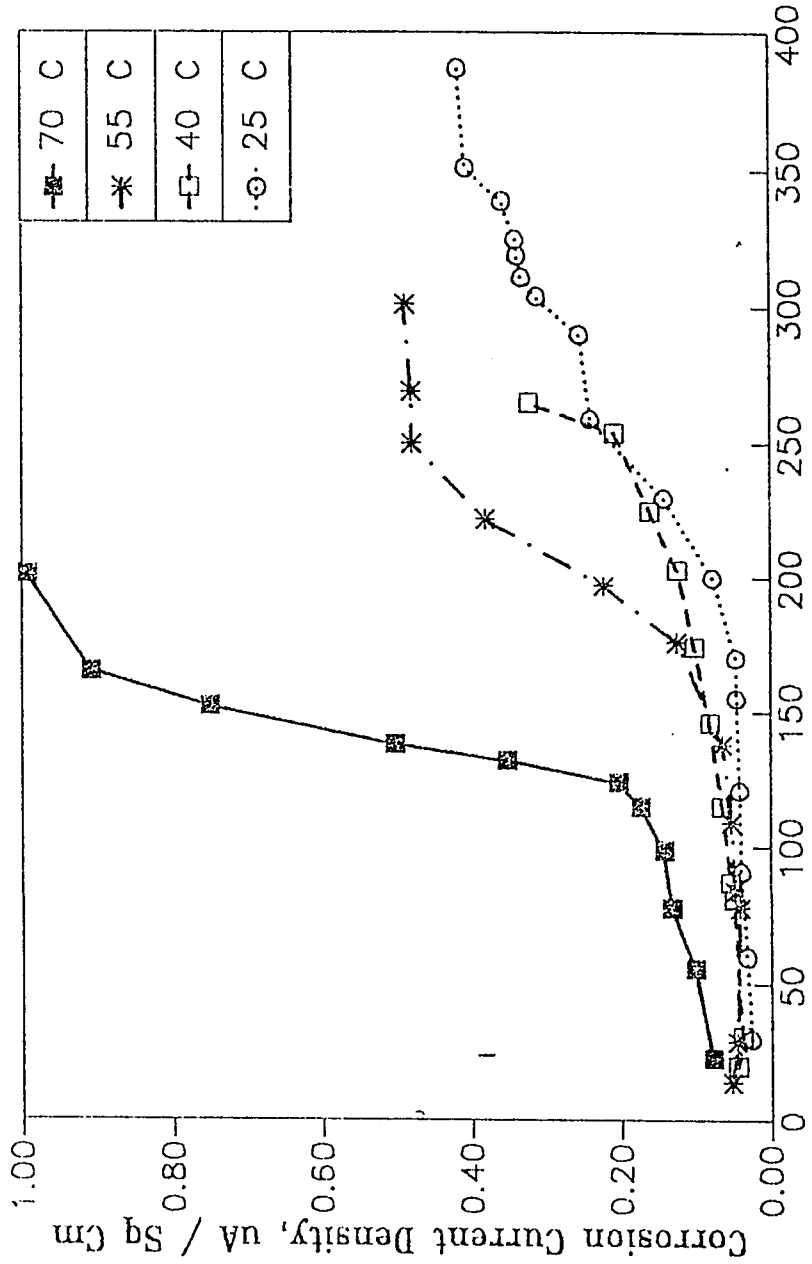

Fig. 4.71 Corrosion Current Density on Steel in BFS Cement Concrete Specimens Contaminated with Chloride and Exposed to Varying Temperatures

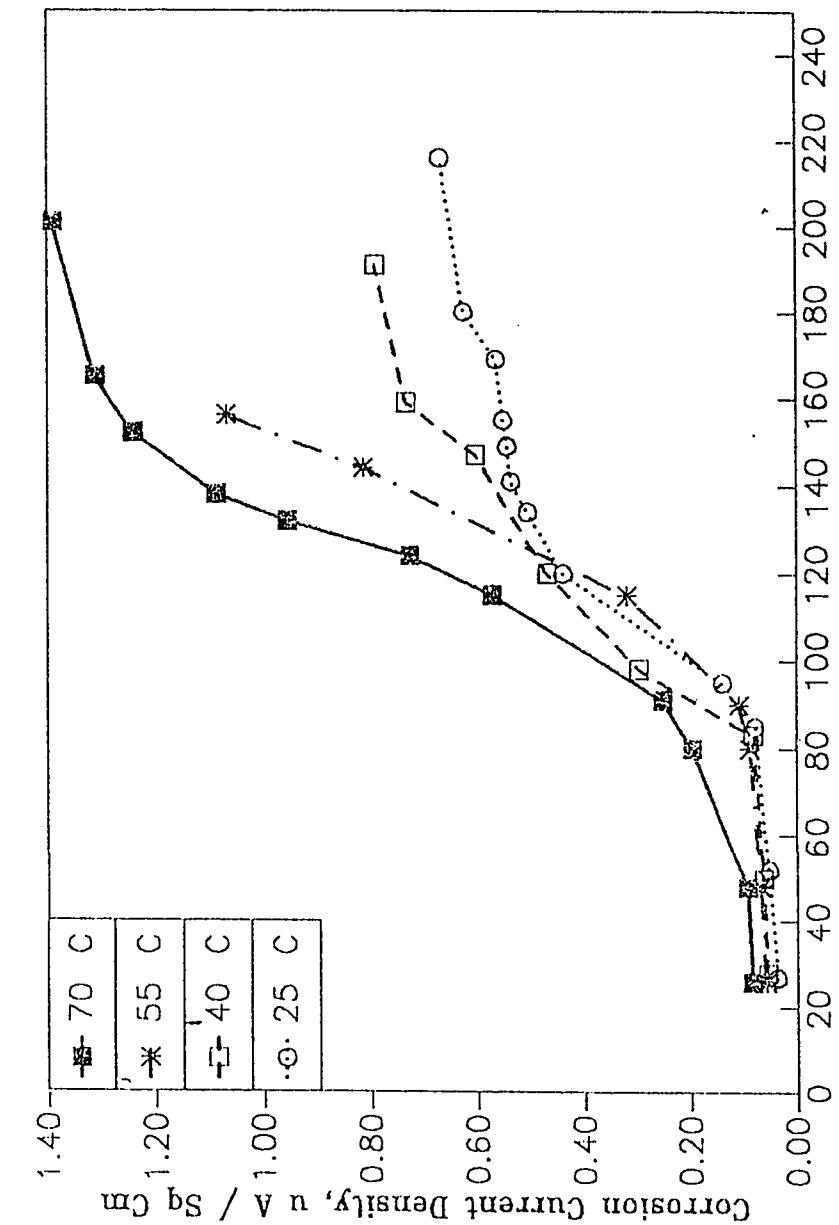

Fig. 4.72 Corrosion Current Density on Steel in BFS Cement Concrete Specimens Contaminated with Chlorides and Sulfates and Exposed to Varying Temperatures

The higher corrosion current density on steel in concrete specimens contaminated with chloride-sulfate salts compared to those contaminated with only chlorides may be attributed to the presence of sulfate salts. The presence of sulfate salts results in a decrease in the electrical resistivity of concrete. Further, it is postulated that sulfate ions react with the steel to accelerate reinforcement corrosion. In the presence of chlorides and sulfates, chlorides are primarily responsible for depassivating the steel, and once the passivity is destroyed, both sulfate and chloride ions react with the steel substrate.

At the anode, iron dissolves into the electrolyte as mentioned below:

$$Fe \rightarrow Fe^{++} + 2e^{-} \qquad (4.5.1)$$

After formation of ferrous ions, both chlorides and sulfate ions react with the it to form ferrous chloride and ferrous sulfate respectively, as shown below:

$$Fe^{++} + 2Cl^{-} \rightarrow Fe\,Cl_2 \qquad (4.5.2)$$

$$Fe^{++} + SO_4^{--} \rightarrow FeSO_4 \qquad (4.5.3)$$

Once ferrous chloride and ferrous sulfates are formed, the presence of moisture and oxygen near the corrosion product/metal interface promotes other types of reactions. Ferrous chloride is gradually converted into iron oxyhydroxide (FeOOH) and hydrochloric acid (HCl) [26].

$$2FeCl_2 + 3H_2O + 1/2O_2 \rightarrow 2FeOOH + 4HCl \qquad (4.5.4)$$

Ferrous sulfate also undergoes similar oxidative hydrolysis reaction with the generation of iron oxyhydroxide and sulfuric acid.

$$2FeSO_4 + 6H_2O + O_2 \rightarrow 4FeOOH + 4H_2SO_4 \qquad (4.5.5)$$

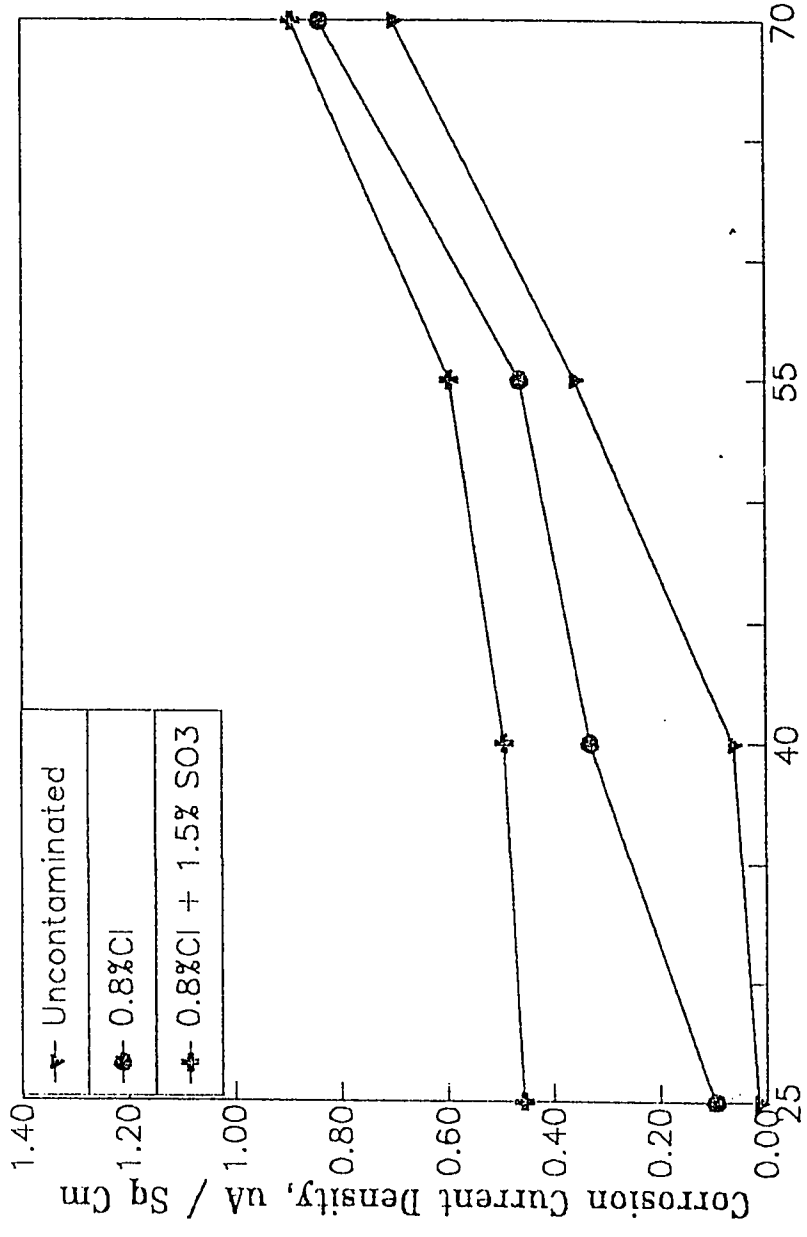

Fig. 4.73 Effect of Temperature on Corrosion Current Density on Steel in OPC Concrete Specimens With and Without Contamination after 150 Days of Exposure

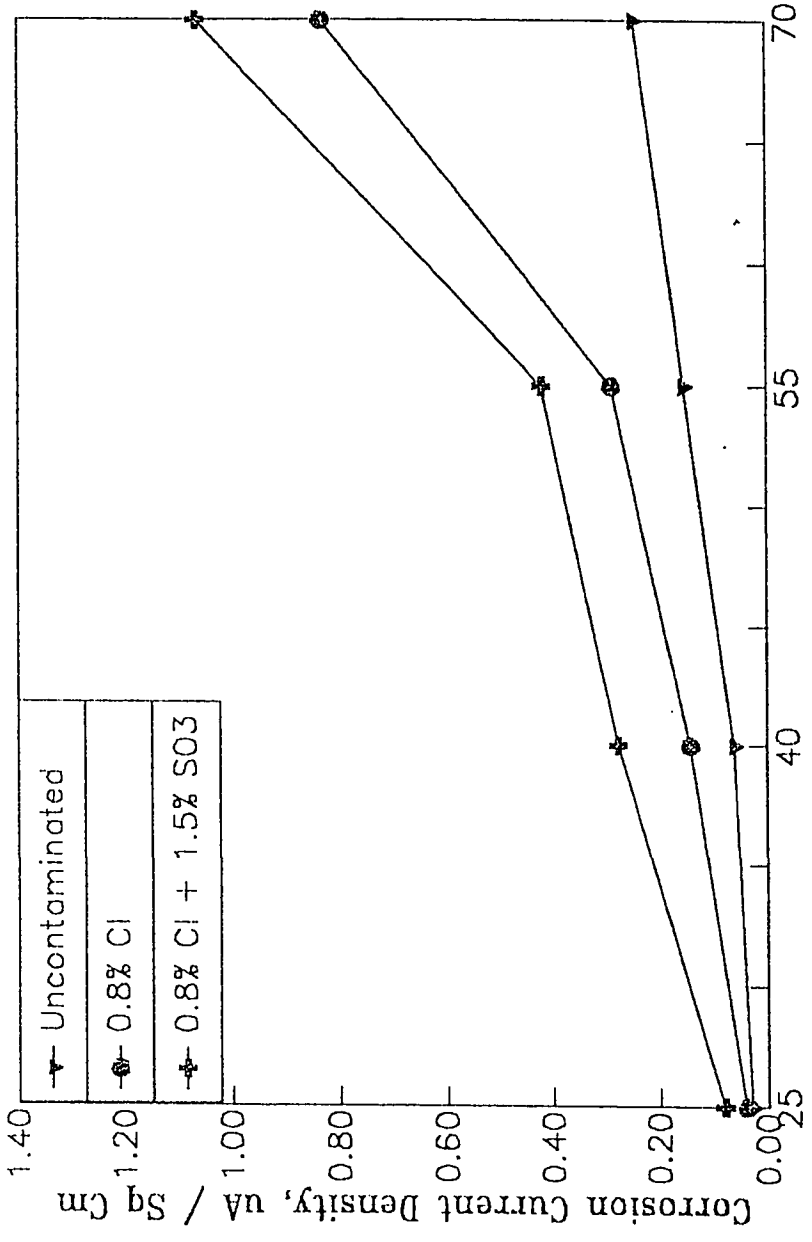

Fig. 4.74 Effect of Temperature on Corrosion Current Density on Steel in SF Cement Concrete Specimens With and Without Contamination after 150 Days of Exposure

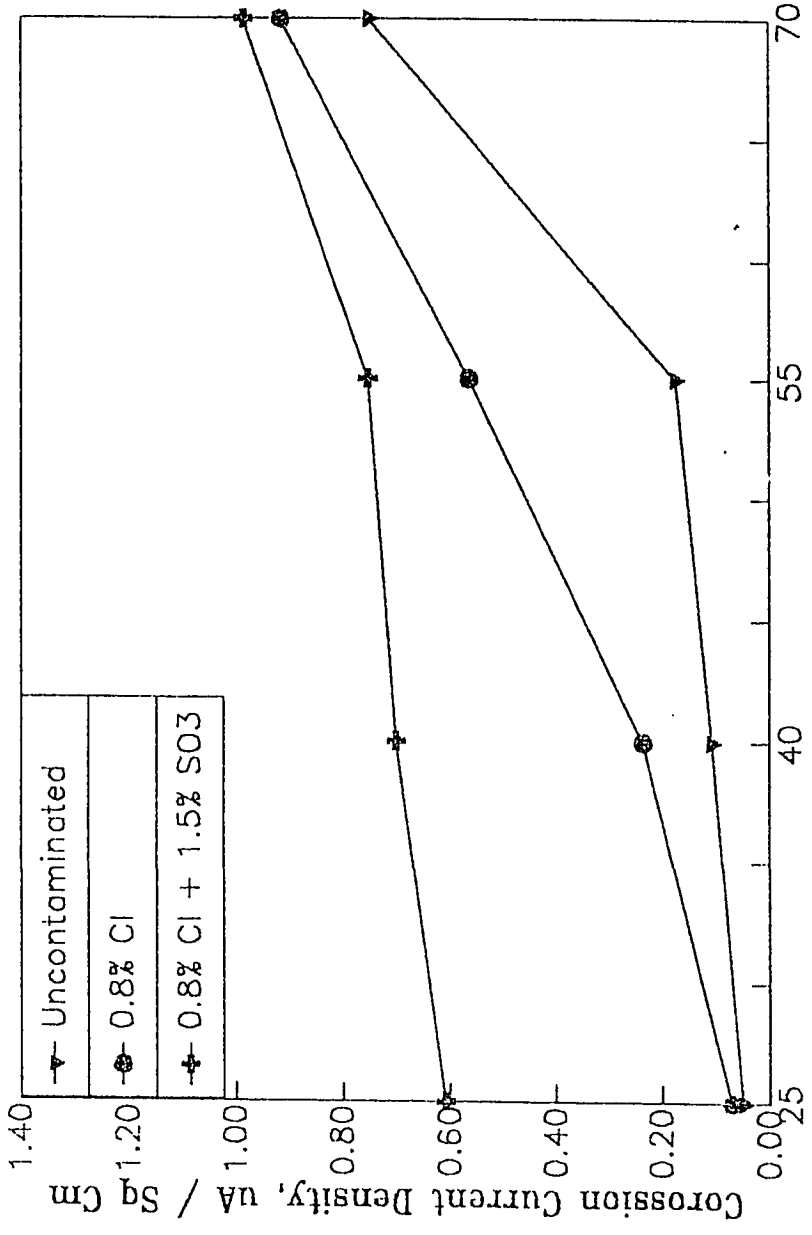

Fig. 4.75 Effect of Temperature on Corrosion Current Density on Steel in Class F FA Cement Concrete Specimens With and Without Contamination after 150 Days of Exposure

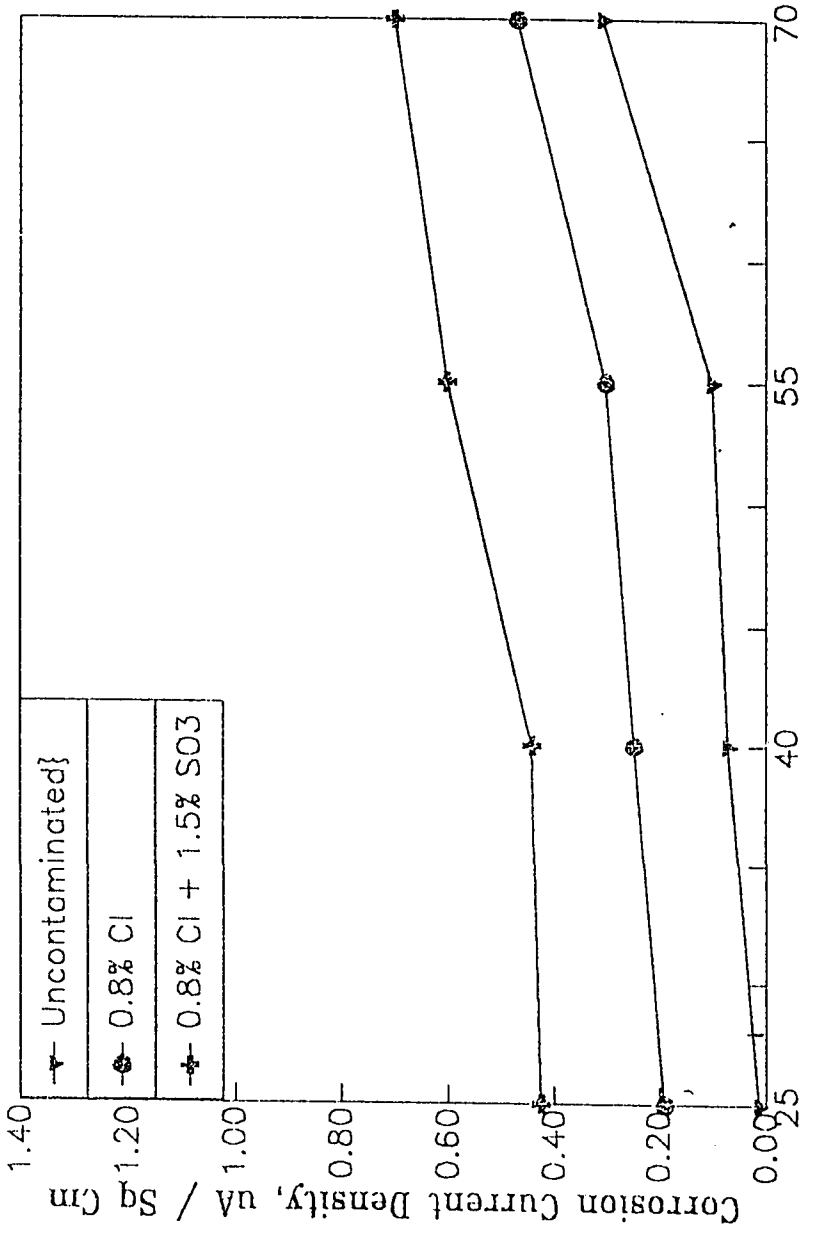

Fig. 4.76 Effect of Temperature on Corrosion Current Density on Steel in Class C FA Cement Concrete Specimens With and Without Contamination after 150 Days of Exposure

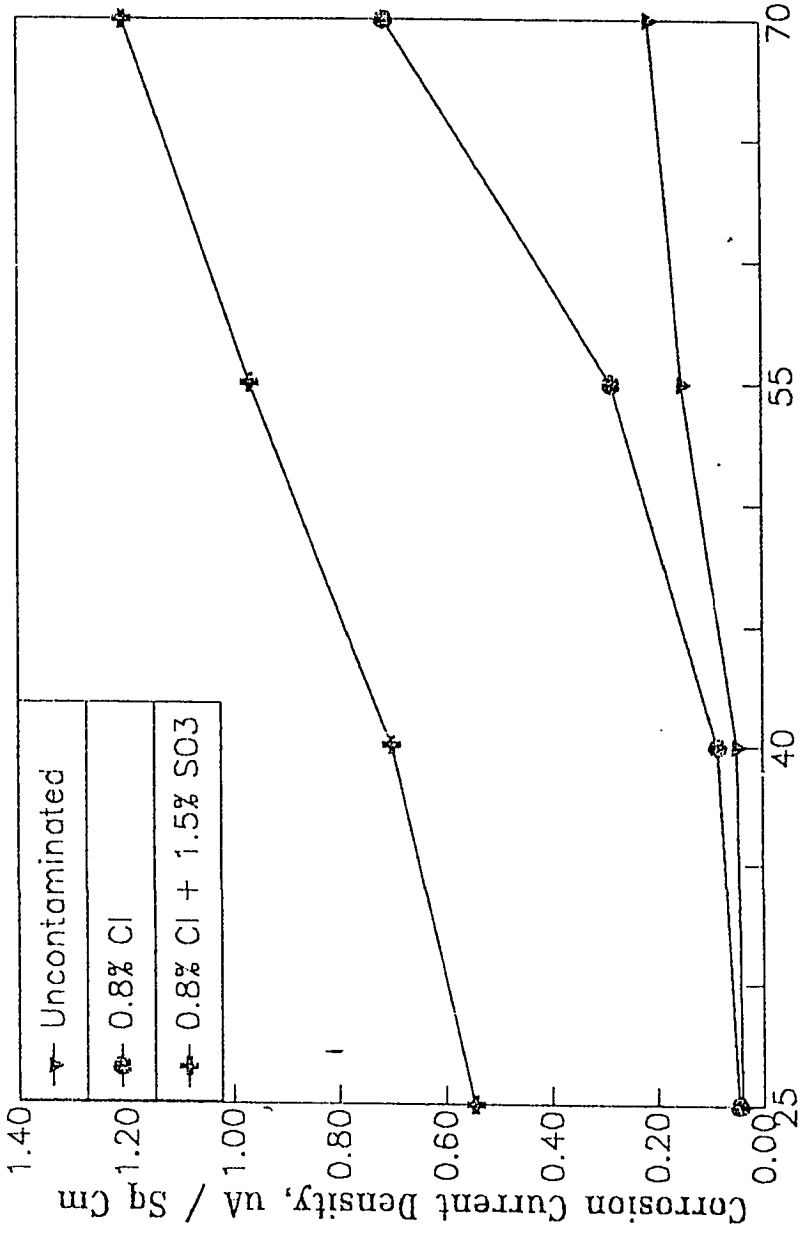

Fig. 4.77 Effect of Temperature on Corrosion Current Density on Steel in BFS Cement Concrete Specimens With and Without Contamination after 150 Days of Exposure

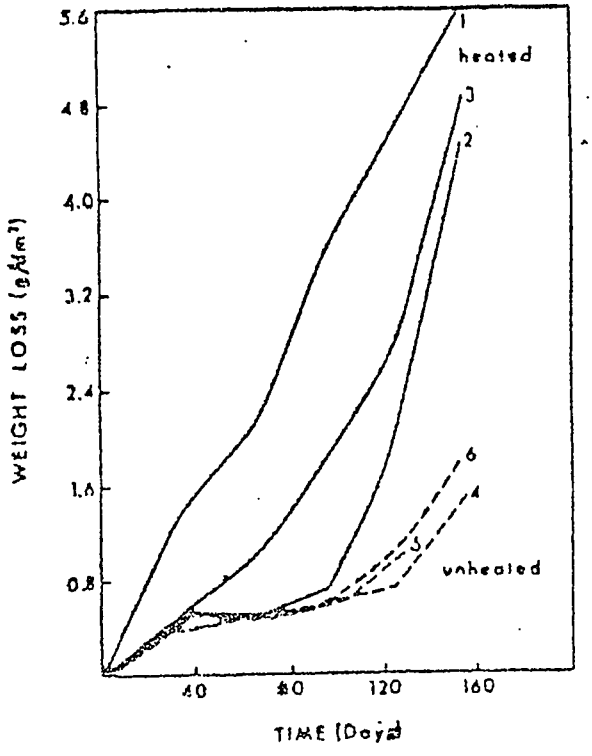

Fig. 4.78 Corrosion Rates of Crevice Specimens Attached to Vehicles Stored in Heated Garages (Continuous Line) Vs Unheated Garages (Discontinuous Line), (as Quoted in Ref. 9)

Both sulfuric acid and hydrochloric acid continue to react with the metal, thus producing more $FeCl_2$ and $FeSO_4$ respectively, and generating H_2SO_4 and HCl (acid generation cycle.

4.5.3 Corrosion Performance of Plain and Blended Cements

The corrosion current density on steel in plain and blended cement concrete contaminated with chloride and sulfates and exposed to 70 °C temperature for 150 days is shown in Table 4.11. Chloride and sulfate contamination of the specimens and 70 °C exposure temperature formed the most aggressive environment and so was selected to evaluate the performance of these plain and blended cements. The performance of blended cements evaluated on the basis of performance of Type I cement is also shown in Table 4.11.

These data indicate that concrete specimens made with class C fly ash had lowest corrosion current density and highest corrosion rating. Andrade et al [116] after 5 years of study, on various blended cement concretes, reported that fly ash was the most impermeable concrete in saline environment.

The higher corrosion activity is observed in blended cements indicates in the presence of salt contamination these cements perform no better than the ordinary portland cements.

TABLE 4.11 Performance of Plain and Blended Cement Concretes with Salt Contamination at 70 °C

Cement Type	Corrosion Current Density	Performance Rating
O P C	0.9	1
Silica Fume	1.05	0.86
Class F Fly ash	0.95	0.95
Class C FA	0.65	1.38
B F S	1.05	0.86

CHAPTER 5
CONCLUSIONS

This research focused on the effect of temperature and salt contamination on various properties affecting the durability of concrete such as compressive strength, pore size distribution, electrical resistivity, pH, chloride concentration, sulfate concentration and reinforcement corrosion. Following conclusions are drawn from this study.

1. The compressive strength in plain and blended cement concrete specimens was observed to decrease with increasing exposure temperature.

2. Addition of chloride and chloride plus sulfate ions to OPC specimens also resulted in a decrease in the compressive strength as compared to non-contaminated specimens.

3. The compressive strength of blended cement concrete specimens contaminated with chlorides and sulfates was generally observed to be higher than that in the uncontaminated specimens. The chloride contaminated specimens indicated higher strength compared to those contaminated with chloride and sulfates.

4. The cumulative pore volume in the OPC paste specimens was observed to increase with increasing exposure temperature. This trend was also observed in the blended cements.

5. A significant increase in the total pore volume was observed as the temperature was increased from 25 to 40 °C in OPC specimens. However, the increase in the total pore volume as the exposure temperature was raised from 55 to 70 °C was negligible.

6. The pore structure in the blended cement paste specimens was much denser

than that in the OPC paste specimens. The pore radii are much smaller than in the OPC paste specimens.

7. At higher temperature, 70 °C, the pore structure in the blended cements was much finer than that at other temperatures.

8. The presence of salts generally increased the cumulative pore volume as compared to non-contaminated specimens. The pore structure in these specimens was much finer than in the uncontaminated specimens.

9. The electrical resistivity of both plain and blended cement concrete specimens was observed to increase with an increase in the exposure temperature. However, the change in the electrical resistivity as the temperature was raised from 25 to 55 °C was not that significant as compared to the tremendous increase noted when the exposure temperature was raised from 55 to 70 °C.

10. The electrical resistivity of plain and blended cement concrete specimens contaminated with chloride salts was lower than the corresponding non-contaminated specimens.

11. The electrical resistivity of plain and blended cement concrete specimens contaminated with both chloride and sulfate salts was also lower than the uncontaminated specimens and those contaminated with only chloride salts.

12. The electrical resistivity of blended cement concrete specimens both uncontaminated and contaminated, was higher than that of the ordinary portland cements at all the exposure temperatures.

13. The drastic reduction in the electrical resistivity in both plain and blended cement concretes, due to chloride and sulfate contamination indicates the chances of corrosion acceleration in structures which are contaminated with these salts.

14. An increase in the exposure temperature resulted in a decrease in the alkalinity, measured in terms of pH, in both plain and blended cement paste specimens.

15. The alkalinity of cement paste specimens contaminated with chloride ions was higher than the uncontaminated specimens at all the exposure temperatures. This increase in the alkalinity may be attributed to the cation effect, i.e. use of NaCl.

16. Similarly, the alkalinity of specimens contaminated with chloride and sulfate salts was much more than that of uncontaminated specimens and those contaminated with chloride salts. This is attributed to the use of NaCl and Na_2SO_4 as the source of chloride and sulfate salts.

17. The alkalinity of blended cements was less than that in the ordinary portland cement paste. This reduction in the pH value in the blended cements compared to ordinary portland cement paste specimens may be attributed to the pozzolanic reaction which removes the $Ca(OH)_2$, thus reducing the basicity.

18. The water-soluble chloride ion concentration in both the plain and blended cement paste specimens was observed to increase with increasing exposure temperature.

19. Addition of sulfates to the chloride contaminated specimens was observed to increase the water-soluble chloride content in both the plain and blended cements. This may be attributed to the preferential reaction of the C_3A in cement with the sulfate ions. At higher temperatures, particularly above 40 °C, the chloride complexing capacity of these cements is reduced.

20. The Cl^-/OH^- ratio was also observed to increase with the exposure temperature. The effect of temperature was more pronounced for exposure temperatures of more than 40 °C.

21. The Cl^-/OH^- ratio in specimens contaminated with chloride and sulfate salts was less than that in specimens contaminated with only chloride salts. This may be attributed to the increased alkalinity in the former specimens due to the addition of NaCl and Na_2SO_4

22. The Cl^-/OH^- values in blended cements, in general, were observed to be more than those in plain cements. This may be attributed to the reduction in alkalinity of these cements, due to pozzolanic reaction.

23. The Cl^-/OH^- values, in general, were more than 0.6 for exposure temperatures of 55 and 70 °C in chloride contaminated specimens and at 70 °C in specimens contaminated with sulfate-chloride salts. The Cl^-/OH^- ratios, in contaminated specimens, were more than 0.30 at all exposure temperatures.

24. The water-soluble sulfate concentration in both the plain and blended cement paste specimens was observed to increase with increasing exposure temperature.

25. A significant increase in the water-soluble sulfate ion concentration was observed for exposure temperature of more than 40 °C.

26. The increase in the sulfate concentration, particularly at higher temperatures, has a negative effect from corrosion view point, in that it not only reduces the electrical resistivity of concrete, but it may also react directly with steel.

27. The corrosion potentials for steel in uncontaminated cement, both plain and blended, concrete specimens indicated passive corrosion at all the exposure temperatures.

28. The data on corrosion potentials for steel in contaminated specimens indicated active corrosion in specimens exposed to 25 and 40 °C temperatures. The corrosion potentials of steel in contaminated specimens exposed to 55 and 70

°C temperature showed more positive values than those exposed to 25 and 40 °C. This behavior may be attributed to the lack of moisture in these specimens due to increase in the exposure temperature.

29. The corrosion potentials of steel in concrete specimens contaminated with chloride and sulfate salts tended to be more negative than those contaminated with only chloride salts. This trend was observed in almost all the cements and at all the exposure temperatures.

30. The corrosion current density on steel in plain and blended cement concrete specimens was observed to increase with exposure temperature.

31. The reinforcement corrosion activity, as measured by the corrosion current density on steel, in both the plain and blended cement concrete specimens was observed to be higher in specimens contaminated with both chloride and sulfate salts as against those contaminated with only chloride salts. This indicates that the presence of both chloride and sulfate ions increases the rate of corrosion.

32. Elevated temperature of 70 °C and chloride-sulfate contamination formed the most aggressive environment as corrosion current density was observed to be the maximum in all the cements at this condition.

33. At 70 °C exposure temperature, and sulfate-chloride contamination, the performance of all the blended cements investigated, except Class C fly ash, was not better than that of plain cements. This indicates that the technological benefit of using supplementary cementing materials like fly ash, silica fume and blast furnace slag can be utilized only when the chloride and/or sulfate contamination contributed by the mix constituents are minimized.

CHAPTER 6

REFERENCES

1. Slater, J. E., *Corrosion of Materials in Association with the Concrete,* ASTM STP- 818, 1993, pp. 6-8.

2. Rasheeduzzafar, Dakhil, F. H., and Al-Qahtani, A. S., "Deterioration of Concrete Structures in the Environment of the Middle East, "*ACI Journal Proceedings*, Jan.-Feb. 1984 , pp. 13-20.

3. Holden, W. R., Page, C. L., and Short, N. R., "The Influence of Chloride and Sulfates on Concrete Durability," *Corrosion of Reinforcement in Concrete Construction*, Alan P Crane Editor, Society of Chemical industry , London, 1983, pp. 143 - 149.

4. Al-Tayyib, A. J., Somuah, S. K., Boah, J. K ., Leblanc, P., and Al-Mana , A. I., "Laboratory Study on the Effect of Sulfate Ions on Rebar Corrosion," *Cement and Concrete Research*, Vol. 18, No 5, Vol. 18, No. 5, 1988, pp. 774-782.

5. Al-Amoudi, O. S. B., *Studies on Soil-Foundation Interaction in the Sabkha Environment of Eastern Province of Saudi Arabia*, Ph.D. Dissertation, Department of Civil Engineering, KFUPM, Dhahran, Saudi Arabia, 1992.

6. Kawamura , K., Sereda, P. J., and Swenson, E. G., *Magazine of Concrete Research*, 17, March 1965.

7. Richard, E. W., David, G. S., "Chloride Diffusion Constant for Concretes," *Structural Materials Proceedings*, San Francisco, Hilton, CA, May 1-5, 1989, pp. 106-115.

8. Mehta, P. K., *Concrete Structure, Properties, and Materials*, Prentice-Hall, Inc., Engle Wood Cliffs, New Jersey, pp. 105-168.

9. Rasheduzzafar, *Advanced Reinforced Aggregates,* class notes of CE 628, Department of Civil Engineering, KFUPM, Dhahran, Saudi Arabia.

10. ACI Committee 201, "Guide to Durable Concrete," *Journal of ACI Proceedings*, Vol. 74, 1977, pp. 573-609.

11. Campbell, A. D., and Ropper., H., *Concrete Structures, Materials, Maintenance and Repair*, Longman Scientific and Technical Publishers, Singapore, 1991.

12. Thompson, D. M., *Problems with concrete*, Bridge Division, Structures Group, Transport and Road Research Laboratory, 1990.

13. Hobbs, D. W., "Expansion of Concrete Due to Alkali Silica Reaction," *The Structural Engineer*, Vol. 62 A, No. 1, Jan. 1984.

14. Cohen, M. D., and Bentur, A.., "Durability of Portland Cement-Silica Fume Pastes in Magnesium Sulfate and Sodium Sulfate Solutions," *ACI Materials Journal*, Vol. 85, No. 3, May-June 1988, pp. 148-157.

15. Kruger, J., "Passivity of Metals- A Materials Science Perspective," *International Materials Review*, 33, 3, 1988, pp. 113-130.

16. Leek D. S., and Poole, A. B., "The Break Down of Passive Film on High Yield Mild-Steel by Chloride Ions," *Third International Symposium on Corrosion of Reinforcement in Concrete Construction*, Page, Treadeway, Bomforth, (Editors), Society of Chemical Industry, UK, 1990, pp. 65-73.

17. Bernard, E., and Verbeck, G. J., "Corrosion of Metals in Concrete-Needed Research," *Corrosion of Metals in Concrete,* ACI SP-49, Detroit, pp. 39-46.

18. Bazant, Z. P., "Physical Model for Steel Corrosion in Concrete Sea Structures-Theory," *Journal of Structural Division, Proc. of ASCE*, Vol. 105, # ST 6, 1979, pp. 1137-1153.

19. Hoar, T. P., Mears, R. B., and Rothwell, G. P., *Corrosion Science*, Vol. 5, 1965, pp. 279.

20. Ogura, K., and Ohama, T., "Pit Formation in the Cathodic Polarization of Passive Iron: II, Effects of Anions," *Corrosion*, Vol. 37, No. 10, October 1981, pp. 572.

21. Uhlig, H. H., *Corrosion and Corrosion Control*, 2nd Ed., John Wiley and Sons, Inc., p. 419, 1971.

22. Ogura, K., and Ohama, T., "Pit Formation in the Cathodic Polarization of Passive Iron: II, Effects of Anions," *Corrosion*, Vol. 37, No. 10, October 1981, pp. 573.

23. Fontana, M. G., and Green, N. D., *Corrosion Engineering*, McGraw Hill, Inc., 1967.

24. Ritter, J. J., and Rodriguez, M. J., "Corrosion Phenomena for Iron Covered With a Cellulose Nitrate Coating," *Corrosion*, Vol. 38, No. 4, April 1982, pp. 223-226.

25. Mehta, P. K., "Effect of Cement Composition on the Corrosion of Reinforcing Steel in Concrete, "*Chloride Corrosion of Steel in Concrete, ASTM STP 629*, 1977, pp. 12-19.

26. Roberts, M. H., "Effects of Calcium Chloride on the Durability of Pre-Tensioned Wire in Prestressed Concrete," *Magazine of Concrete Research*, Vol. 14, No. 42, Nov. 1962, pp. 143-152.

27. Page, C. L., Short, N. R., and Holden, W. R., "The Influence of Different Cements on Chloride Induced Corrosion of Reinforcing Steel," *Cement and*

Concrete Research, Vol. 16, No. 1, 1986, pp. 79-86.

28. Arya, C., Buenfeld, N. R., and Newman, J. B., "Factors Affecting Chloride Binding in Concrete," *Cement and Concrete Research*, Vol. 20, No. 2, 1990, pp. 291-300.

29. ACI 318-85 *Building Code Requirements for Reinforced Concrete*, ACI, Detroit, 1985.

30. BS CP 8110 *Structural Use of Concrete*, British Standards Institute, U K, 1985.

31. Hausmann, D. A., "Steel Corrosion in Concrete. How does it Occur," *Materials Protection*, Vol. 6, No. 11, 1967, pp. 19-23.

32. Lambert, P., Page, C. L., and Short, N. R., "Pore Solution Chemistry of the Hydrated System in Tricalcium Silicate/Sodium Chloride Water," *Cement and Concrete Research*, Vol. 15, No. 4, 1985, pp. 657-680.

33. Gouda, V. K., "Corrosion and Corrosion Inhibition of Reinforcing Steel Immersed in Concrete Solution," *British Corrosion Journal*, Vol. 5, 1970, pp. 657-680.

34. Diamond, S., "Chloride Concentration in Concrete Pore Solution Resulting From Calcium and Sodium Chloride Admixtures," *Cement, Concrete and Aggregates*, Vol. 8, No. 2, Winter 1986, pp. 97-102.

35. Clear, K. C., *Time to Corrosion of Reinforcing Steel in Concrete Slabs*, Report No. FHWA-RD-76-70, Federal Highway Administration, April 1976.

36. Monfore, G. E., and Verbeck, G. J., "Corrosion of Prestressed Wires in Concrete," *ACI Journal, Proceedings*, Vol. 57, No. 5, Nov. 1960, pp. 491-516.

37. "Corrosion of Reinforcement in Concrete," *Materials and Structures*, Vol. 9, No. 51, pp. 187-207.

38. "Spalling Stadium Repaired," *Engineering News Record*, July 8, 1982.

39. Stratful, R. F., "Criteria for Cathodic Protection of Bridge Decks," *Corrosion of Reinforcement in Concrete Construction,* Alan Crane., Ed., Society of Chemical Industry, Ellis Harwood Ltd. London, 1983, pp. 287-331.

40. Treadaway, K. W. J., Page C. L., and Macmillan, G. L., "The Prediction of Reinforcement Corrosion: From Laboratory Studies to Exposure Trials," *Durability of Construction Materials*, J.C. Maso, Editor, Vol. 3, Chapman and Hall, London, 1987, pp. 1323-1329.

41. Al-Amoudi, O. S. B., and Maslehuddin, M., "The Effect of Chloride and Sulfate Ions on Reinforcement Corrosion," *Cement and Concrete Research*, Vol. 23, No. 1993, pp. 139-146.

42. Al-Amoudi, O. S. B., Abduljauwad, S. N., Rasheeduzzafar and Maslehuddin, M., "Effect of Chloride and Sulfate Contamination Ions in Soil on Corrosion of Steel and Concrete," *Transportation Research Record No. 1345*, 1992, pp. 67-73.

43. Mehta, P. K., "Pozzalonic and Cementitious Byproducts in Concrete-Another Look," *ACI SP-114*, Detroit, Vol. 1, 1989, pp. 1-43.

44. Berry, E. E., and Malhotra, V. M., "Fly Ash in Concrete," *Supplementary Cementing Materials for Concrete*, CANMET, SP-8E, Ontario, 1987, pp. 37-163.

45. Douglas, E., "Blast Furnace Slag Cement Mortar and Concrete: Durability Aspects," Chapter 6 of *Supplementary Cementing Materials for Concrete*, CANMET SP 86-8E, 1987, pp. 337-369.

46. Bakker, R. F. M., "La Durabilite des Betons De Ciment de Haunt Fourneau", *Silicates Industries*, 1982-3, pp. 91-95.

47. Markestad, A., "An Investigation of Concrete in Regard to Permeability Problems and Factors Influencing the Results of Permeability Tests," *Sintef Research Report 65A 77077*, NTH, Trondheim, Norway, 1977.

48. Gjorv, O. E., "Durability of Concrete Containing Condensed Silica Fume," *ACI SP-79*, Detroit, 1983, pp. 695-696.

49. Dunstan, E. R., "A Possible Method for Identifying Fly Ashes That Will Improve the Sulfate Resistance of Concrete," *Cement, Concrete and Aggregates,* Vol. 2, No. 1, Summer 1980, pp. 20-30.

50. Mehta, P. K., "Effect of Fly Ash Composition on the Sulfate Resistance of Cement," *ACI Journal Proceedings*, Nov.- Dec. 1986, pp. 994-1000.

51. Crow, R. D., and Dunstan Jr., E. R., "Properties of Fly Ash in Concrete," *Proceedings on Effect of Fly Ash Incorporation in Cement and Concrete*, Materials Research Society, Boston, Massachusetts, Nov. 16-18, 1981.

52. Ramakrishnan, V., Coyle, W. V., Brown, J., Patrick, A. T. P., and Venkataramanujam, P., "Performance Characteristics of Concrete Containing Fly Ash," *Proceedings on Effect of Fly Ash Incorporation in Cement and Concrete*, Materials Research Society, Boston, Massachusetts, Nov. 16-18, 1981.

53. Lea, F. M., *The Chemistry of Cement and Concrete*, 3rd Edition, Chemical Publishing Co., New York, 1971.

54. Bakker, R. F. M., "Permeability of Blended Cement Concrete," *ACI SP-79*, Detroit, pp. 589-605.

55. Mehta, P. K., "Durability of Concrete in Marine Environment," Ibid., pp. 1-20.

56. Roy, D. M., and Idorn, G. M., "Hydration, Structure and Properties of Blast Furnace Slag Cements, Mortars and Concrete," *ACI Journal Proceedings*, Vol. 79, No. 6, Nov.-Dec. 1982, pp. 445-457.

57. Rasheeduzzafar, Dakhil, F. H., Gahtani, A. S., Saddoun S. S., and Bader, M. A., "Influence of Cement Composition on Corrosion of Reinforcement and Sulfate Resistance of Concrete," *ACI Materials Journal*, No. 87, March- April 1990, pp. 114-122.

58. Cohen, D., and Bentur, A., "Durability of Portland Cement-Silica Fume Pastes in Magnesium Sulfate and Sodium Sulfate Solutions," *ACI Materials Journal*, Vol. 85, No. 3, 1973, pp. 1-6.

59. Mehta, P. K., "Mechanisms of Expansion Associated with Ettringite Formation," *Cement and Concrete Research*, Vol. 3, No. 1, 1973, pp. 1-6.

60. Berry, E. E., and Malhotra, V. M. "Fly ash in Concrete," *Supplementary Cementing Materials for Concrete*, CANMET, Publ SP-86, 1987, Chapter 2, pp. 37-163.

61. Vennesland, O., and Gjorv, O. E., " Silica Fume Concrete-Protection Against Corrosion of Embedded Steel," *ACI SP - 91*, Detroit, 1986, pp. 719- 720.

62. Litvan, G. G., and Meyer, A., "Carbonation of Granulated Blast Furnace Slag Cement Concrete During Twenty Years of Field Exposure," ACI SP-91, Detroit, 1986.

63. Gjorv, O. E., "Durability of Concrete Containing Condensed Silica Fume," ACI SP-79, Detroit, 1983, pp. 695-696.

64. Bakker, R. F. M., "On the Causes of Increased Resistance of Concrete Made From BFS to the ASR and Sulfate Corrosion," Ph.D. Dissertation, Faculty of Mining and Metallurgy, R. W. T. H Aachen, Germany, 1980.

65. Getman, F. H., and Daniels, F., *Outlines of Theoretical Chemistry*, John Wiley and Sons, New York, 1941, pp. 662.

66. Berhane, Z., "The Behavior of Concrete in Hot Climates," *Materials and Structures*, 25, 1992, pp. 157-162.

67. *Concrete in Hot Countries*, Published by STUVO, The Dutch Member Group of FIP.

68. Stern, M., and Geary, A. L., "Electrochemical Polarization. 1. A Theoretical Analysis of the Shape of Polarization Curves," *Journal of Electrochemical Society*, Vol. 104, 1957, pp. 56-63.

69. Mansfield, F., "Polarization Resistance Measurements: Experimental Procedure and Evaluation of the Data," *Electrochemical Techniques for Corrosion*, NACE, Houston, 1977, pp. 18-26.

70. Gonzalez, A. J., Feliu, S., Andrade, C., and Rodriguez, I., "On-Site Detection of Corrosion of Reinforced Concrete Structures," *Materials and Structures*, 24, 1991, pp. 346-350.

71. Al-Tayyib, A. J., and Khan, M. S., "Corrosion Rate Measurements of Reinforcing Steel in Concrete by Electrochemical Techniques," *ACI Materials Journal*, May-June 1988.

72. Vogel, I. A., *A text book of Quantitative Inorganic Analysis*, 5th Edition, Revised by Bassett, J., Longman, London, 1985, pp. 754.

73. *Standard Method for the Examination of Water and Waste Water*, 16th Edition, American Public Health Association, Washington, 1985.

74. Brunauer, S., and Kantro, D. L., "The Hydration of Tricalcium Silicate and Dicalcium Silicate from 5 °C to 50 °C ," *Chemistry of Cements* (Taylor, H. F. W., Ed.,) Vol. 1 , Academic Press, London, 1964, pp. 287-309.

75. Klieger, P., "Effect of Mixing and Curing Temperature on Concrete Strength," *ACI Journal Proceedings*, Vol. 22, 1951, pp. 417-432.

76. Price, W. H., "Factors Influencing Concrete Strength," *ACI Journal Proceedings*, Vol. 22, 1951, pp. 417- 432.

77. Verbeck, G. J., and Helmuth, R. H., "Structure and Physical Properties of Cement Paste," *Proceedings of 5th International Symposium on the Chemistry of Cement, Tokyo*, Vol. III, 1968, pp. 1-32.

78. Collerpadi, M., "Pore Structure of Hydrated Calcium Silicate," *Proceedings of International Congress on Colloid and Surface Chemistry*, Prague, Vol. 1, 1973, pp. B25- B49.

79. Desov, A. E., Nekrasov, K. D., and Milovanov A. G., "Cube and Prism Strength of Concrete at Elevated Temperatures," *ACI SP-34*, Detroit, 1970, pp. 423-437.

80. Skalny, J. and Older, I., "Pore Structure of Calcium Silicates," *Cement and Concrete Research*, Vol. 2, No. 4, July-Aug. 1972, pp. 387-400.

81. Chern, J. C., and Chan, Y. W., "Effect of Temperature and Humidity Conditions on the Strength of BFS Cement Concrete," *ACI SP-114*, Detroit, pp. 1377-1398.

82. Hwang, C. L., and Lin, C. Y., "Strength Development of Blended BFS Mortars," *ACI SP-91*, pp. 1323-1340.

83. Yamato, T., Emoto, Y., and Soeda, M., "Strength and Freezing-Thawing Resistance of Concrete Incorporating Condensed Silica Fume," *ACI SP-91*, Detroit, pp. 1095-1118.

84. Ravina, D., "Fly ash Concrete Under Hot Weather Conditions" *Effects of Fly Ash*

Incorporation In Cement and Concrete, Proceedings, Symposium and Annual Meeting of Materials Research Society, November 16-18 ,1981, pp. 172-183.

85. Hughes D. C., "Sulfate Resistance of Fly Ash/OPC Grouts," *Blended Cements in Construction*, Edited by Swamy R.N., Elsevier Applied Science, London, pp. 336-350.

86. Mangat P. S., and El-Khatib, J. M., "Influence of Curing on Pore Structure and Porosity of Blended Cement Concretes," *ACI-SP 132*, Detroit, pp. 813-833.

87. Knut, O. K., Rachel, J. D., Gjorv, O. E., "Pore Structure of Plain Cement Pastes Hydrated at Different Temperatures," *Cement and Concrete Research*, Vol. 20, pp. 927-933.

88. Sellevold, E, J., "Mercury Porosimetry of Hardend Cement Paste Cured or Stored at 97 °C," *Cement and Concrete Research*, Vol. 4, No. 3, May-June, 1974, pp. 399-404.

89. Goto, S., and Roy, D. M., "The Effect of W/C Ratio and Curing Temperature on The Permeability of Hardened Cement Paste," *Cement and Concrete Research*, Vol. 11, No. 4, July-August 1989, pp. 575-579.

90. Villadsen, J., "Hardetemperaturens Indflydelse pa Hardnet Cementpastas Porestruktur," *Laoratoriet for Bygningsmaterialer*, Denmarks Teniske Hojskole, Kobenhavn, 1989.

91. Marsh, B. K., Day, R. L., and Bonner, D. G., "Pore Structure Characteristics Affecting the Permeability of Cement Paste Containing Fly Ash," *Cement and Concrete Research*, Vol. 15 No. 6, November-December 1985, pp. 1027-1038.

92. Mehta, P. K., and Manmohan, D., "Pore Size Distribution and Permeability of Hardened Cement Pastes," *Proceedings, 7th International Congress on the Chemistry of Cement*, Paris, 1980, Vol. II, pp. V II 1-V II 5.

93. Calleja, J., "Durability," *Principal Report VII, 2, 7th International Congress on the Chemistry of Cement*, Paris, 1980.

94. Richartz, W., Zement-Kalk-Gips, 22(10), 1969, pp. 447-456.

95. Regourd, H., Hornain, H., and Montureux, B., "Micro Structure of Concrete in Aggressive Environments ," *Ist International Conference on Durability of Building Materials and Components*, Natural Resources Council Canada, Ottawa, 1978.

96. Midgley, H. G., and Illston, J. M., "The Penetration of Chlorides into Hardened Cement Pastes," *Cement and Concrete Research*, Vol. 14, pp. 546-558.

97. Reinhardt, H. W., and Gaber. K., "From Pore Size Distribution to an Equivalent Pore Size of Cement Mortar," *Materials and Structures*, 1990, 23, pp. 3-15.

98. Page, C. L., Short, N. R., and El-Tarras, A., "Diffusion of Chloride Ions in the Hardened Cement Pastes," *Cement and Concrete Research*, Vol. II 1981, pp. 395-406.

99. Shiyuan, H., "Hydration of Fly Ash Cement and Micro Structure of Fly Ash Cement Pastes," *CBI, Forskning Research Fo 2.81.*

100. Millard, S. G., "Reinforced Concrete Resistivity Measurement Techniques," *Proceedings- Institution of Civil Engineers*, part. 2, 1991.

101. Lewis, D. A., and Copenhagen, W. J., "The Corrosion of Reinforcing Steel in Concrete in Marine Atmospheres," *S.A. Industrial Chemist*, Vol. 11, No. 10 October 1957.

102. Sharp, J. V., Figg, J. W., and Leeming, M. B., "The Assessment of Corrosion of Reinforcement Corrosion in Marine Concrete by Electrochemical and Other Methods," *ASTM STP-109*, Philadelphia.

103. Tashiro, C., and Yoshimoto, T., "Effect of Sodium Compounds on the Strength and Micro-Structural Development of BFS Cement Mortar," *ACI SP-63*, Detroit, pp. 1307-1323.

104. Yonezawa, T., Ashworth, Y., and Procter, R. P. M., "The Mechanisms of Fixing Cl by Cement Hydrates Resulting in the Transformation of NaCl, to NaOH," *Proceedings, 8th International Conference on Alkali Aggregate Reaction*, Tokyo, 1989, pp. 153-160.

105. Evans, U. R., *The corrosion and Oxidation of Metals*, First Supplementary Volume, 1968, Edward Arnold, London.

106. Diamond, S., "Effects of Microsilica on Pore Solution Chemistry of Cement Pastes," *Journal of the American Ceramic Society*, Vol. 66, May 1983, pp. C 82 - C 84.

107. Page, C. L., and Vennesland, O., "Pore Solution Composition and Chloride Binding Capacity of Silica Fume Cement Pastes," *Materials and Structures*, Vol. 16, No. 91, 1983, pp. 19 - 25.

108. Vassie, P. R., *TRRL Laboratory Report*, 1979.

109. Byfors, K., Hanson, C. M., and Tritthart, J., *Cement and Concrete Research*, Vol. 16, No. 5, 1986.

110. Arya, C., Buenfield, N. R., and Newman, J.B., *Cement and Concrete Research*, Vol. 17, p. 907, 1987.

111. Hussain, S. E., *Mechanisms of High Durability Performance of Plain and Blended Cements*, Ph.D. Dissertation, Department of Civil Engineering, King Fahd University of Petroleum and Minerals, Dhahran, Saudi Arabia, August 1991.

112. Kawamura, M., Kayyali, O. A., and Haque, M. N., "Effects of Fly ash on Pore Solution Composition in Calcium and Sodium Chloride Bearing Mortars," *Cement and Concrete Research*, Vol. 18, No. 5, September 1988, pp. 763- 773.

113. Rasheeduzzfar, Dakhil, F. H., Al-Gahtani, A. S., and Saadoun, S. S., "Exposure Site Studies on The Effect of Cement Composition of Corrosion of Reinforcing Steel in Concrete," *Arabian Journal for Science and Engineering,* Vol. 4, No. 2, pp. 235-248.

114. Al-Amoudi, O. S. B., Rasheeduzzafar, and Maslehuddin, M., "Carbonation and Corrosion of Rebars in Salt Contaminated OPC/PFA Concretes," *Cement and Concrete Research,* Vol. 21, No. 1, 1991, pp. 38-50.

115. Vassie, P. R., "A Survey of Site Tests for the Assessment of Corrosion in Reinforced Concrete," *Transport and Road Research Laboratory Report LR 953*, Berkshire.

116. Andrade, C., Alfonso, S., Goni, S., Bade, B., and Gonzalez, J. A., "Five Years Study of Reinforcement Corrosion in Concrete Fabricated with Blended Cements Immersed in Natural Sea-water," *Blended Cements in Construction*, Editor, R.N.Swamy, Elsevier Applied Science, London and New York, pp. 429-441.

117. Benjamin, S. E., and Sykes, J. M., "The Effect of Temperature on the Pitting Corrosion of Iron in OPC Mortars," *3rd International Conference on Deterioration and Repair of Reinforced Concrete in the Arabian Gulf, Bahrain,* 1989, pp. 573-580.

118. "Sun and Salt - The Scourge of Concrete in the Gulf," *Civil Engineer*, 19 June, 1975, pp. 32.